"A Cellular Chronic Fatigue" - Dysregulated Mitochondrial Respiratory Function, Metabolic and Signalling Pathways in ME/CFS and the Identification of Blood Cell-Based Biomarkers of Disease

Submitted by
Daniel Missailidis, Bachelor of Biological Sciences (Advanced, Honours),
2016 La Trobe University

A thesis submitted in total fulfilment
of the requirements for the degree of
Doctor of Philosophy

School of Life Sciences
Department of Physiology, Anatomy and Microbiology
Discipline of Microbiology

College of Science, Health and Engineering

La Trobe University
Victoria
Australia

March, 2021

Table of Contents

List of Figures

List of Tables

List of Abbreviations and Symbols

Abbreviation/Symbol (Alphabetical order)	Full Meaning
4E-BP1	Eukaryotic translation initiation factor 4E-binding protein 1
ACADVL	Very long-chain specific acyl-CoA dehydrogenase
ACC	acetyl-CoA carboxylase
ACOX1	Acyl-CoA oxidase 1
AMPK	AMP-activated protein kinase
ATP	Adenosine triphosphate
AUC	Area under curve (ROC)
BCAA	Branched-chain amino acid
BCAT	Branched-chain amino acid aminotransferase
BCKDH	Branched-chain ketoacid dehydrogenase
BHRF-1	BamHI fragment H rightward open reading frame
CCC	Canadian Consensus Criteria
CCCP	Carbonyl cyanide m-chlorophenyl hydrazone
DMSO	Dimethyl sulphoxide
EBV	Epstein-Barr virus
ECAR	Extracellular acidification rate
ECHS1	Short-chain enoyl-CoA hydratase
ETC	Electron transport chain
ETF	Electron transfer flavoprotein
ETF-QO	Electron transfer flavoprotein-ubiquinone oxidoreductase
FAH	Fumarylacetoacetase
FASN	Fatty acid synthase
FDR	False discovery rate
FRET	Förster resonance energy transfer
GCDH	Glutaryl-CoA dehydrogenase
GLS	Glutaminase
GLUD1	Glutamate dehydrogenase
GO	Gene ontology
GOT2	Aspartate aminotransferase (mitochondrial)
HADH	Hydroxyacyl-CoA dehydrogenase/3-keotacyl-CoA thiolase
HEPES	4-(2-hydroxyethyl)-1-piperazineethanesulphonic acid
IBS	Irritable Bowel Syndrome
IQR	Interquartile range
MAS	Malate-aspartate shuttle
ME/CFS	Myalgic Encephalomyelitis/Chronic Fatigue Syndrome

MMP or Δψm	Mitochondrial membrane potential
MS	Mass spectrometry
NK	Natural killer
NMR	Nuclear magnetic resonance spectroscopy
OCR	Oxygen consumption rate
OXPHOS	Oxidative phosphorylation
PBMC	Peripheral blood mononuclear cell
PBS	Phosphate buffered saline
PDH	Pyruvate dehydrogenase
PEM	Post-exertional malaise
PKN	Protein kinase N
PMF	Proton motive force
POTS	Post-orthostatic tachycardia
PPAR-α	Proliferator-activated receptor-α
PPP	Pentose phosphate pathway
PregS	Pregnenolone sulphate
PVDF	Polyvinylidene difluoride
ROC	Receiver Operating Characteristic
ROS	Reactive oxygen species
SdhB	Succinate dehydrogenase subunit B
SDS	Sodium dodecyl sulphate
SIRT	Sirtuin
SLC25	Solute carrier family 25
SNP	Single nucleotide polymorphism
SREBP-1	Sterol regulatory element-binding protein-1
TCA Cycle	Tricarboxylic acid cycle
TCEP	Tris [2-carboxyethyl] phosphine hydrochloride
TIMM	Translocase of the inner mitochondrial membrane
TOMM	Translocase of the outer mitochondrial membrane
TORC1	Target of Rapamycin Complex 1
TRPM3	Transient receptor potential melastatin 3
Ulk-1	Serine/threonine-protein kinase
VLCFA	Very long-chain fatty acids
α-KG	α-ketoglutarate

Abstract

The lack of objective, timely, and accurate diagnostic criteria or biomarkers for Myalgic Encephalomyelitis/Chronic Fatigue Syndrome (ME/CFS) can leave patients for long periods without a clear diagnosis. Treatment is often based on individual trial and error due to the lack of mechanistic understanding of the disease. It is therefore paramount that fundamental molecular explanations for the underlying pathophysiology of ME/CFS are pursued, as these could contribute towards the development of reliable, faster diagnostics and rational, effective treatments. To address these issues, this PhD project has focused on using stably proliferative and metabolically active cell lines (lymphoblasts) created from ME/CFS patient blood (for the first time) to investigate mitochondrial function, related metabolic or signalling pathways, and potential diagnostic biomarkers. The results show that in ME/CFS lymphoblasts, there is an isolated Complex V inefficiency in ATP synthesis at the final step in mitochondrial oxidative phosphorylation. This is accompanied by multiple homeostatic compensations including increased respiratory capacity, elevated expression of a diverse array of mitochondrial proteins, elevated Target of Rapamycin Complex I (TORC1) activity, and evidence suggesting dysregulated substrate provision towards the TCA cycle and oxidative phosphorylation. Whole-cell proteomics and transcriptomics suggested that in ME/CFS lymphoblasts there is an increased use of alternatives to glycolysis in provisioning the mitochondria with oxidisable substrate. This may represent a homeostatic compensation for the respiratory inefficiency by Complex V. Together, these compensatory changes appear to be sufficient to meet the normal needs of active metabolism despite the inefficiency of ATP synthesis by Complex V. However, this may leave the cells less able to respond to further acute increases in ATP demand despite the elevated respiratory capacity, since the signalling and metabolic pathways involved are already chronically upregulated. If this “cellular chronic fatigue” is present in other cell types, it may contribute to the unexplained fatigue experienced by ME/CFS patients. This is suggested by the fact that all of the mitochondrial abnormalities observed were correlated with the severity of patient symptoms. It was also found that multiple observed abnormalities constituted promising biomarkers, each of them able to distinguish ME/CFS patient and control samples with high reliability, while 100% discriminatory accuracy became possible when using the best combinations of variables available. This project has therefore made significant strides in the mechanistic understanding of ME/CFS and has highlighted promising candidate diagnostic biomarkers.

Statement of Authorship

Except where reference is made in the text of the thesis, this thesis contains no material published elsewhere or extracted in whole or in part from a thesis, this thesis contains no material published elsewhere or extracted in whole or in part from a thesis accepted for the award or any other degree or diploma. No other person's work has been used without due acknowledgement in the main text of the thesis. This thesis has not been submitted for the award of any degree or diploma in any other tertiary institution.

The research undertaken in connection with this thesis was approved as part of two successive projects. First approval by the Australian National University Human Research Ethics Committee (Reference 2015/193) and accepted as an externally approved project by the La Trobe University Human Ethics Committee (26 February 2016). Second approval by the La Trobe University Human Ethics Committee (HEC19316).

This work was supported by an Australian Government Research Training Program Scholarship (Fees Offset) and a La Trobe University Postgraduate Research Scholarship.

Daniel Missailidis Date: 29/03/2021

Acknowledgements

There are many people to thank for the success of this project. I sincerely appreciate the exceptional supervision provided by Dr Sarah Annesley and Prof. Paul Fisher, neither of whom I was ever afraid to approach with the silliest of questions. Sarah and Paul's general patience, optimism, passion and brilliant scientific minds provided a fantastic environment within which to learn and grow, for which I will always be grateful. Huge credit should also go to my family for providing a supportive foundation from which I was able to focus most of my time and energy into the project itself. Especially to mum for her many years of support and patience and particularly during the lengthy consecutive months of thesis and paper writing at home!

I am appreciative of the friendship and assistance provided by other members of the lab. While most of the experiments and data analysis presented herein were performed by myself, the exception is a small subset of experiments presented in Chapter 4 which were generously assisted with by Oana Sanislav (Confirmatory Western blots) and Claire Allan (AMPK activity assay) during periods of restricted laboratory access due to the pandemic. The corresponding methods sections note these contributions. My sincerest gratitude goes out to both Claire and Oana for their assistance and also for being my two teachers on the laboratory side of things.

Monumental thanks go to Susanna Agardy, Associate Prof. Brett Lidbury of the ANU, and the staff at the now closed CFS Discovery Clinic for enabling this work. Susanna in particular has given tremendously of herself despite severe ME/CFS and I will be forever grateful to her. At the clinic, my gratitude goes to Edwina Privitera and Dr Donald P. Lewis for their care of ME/CFS patients despite great challenges, and for mediating our initial access to patients. Dr Lewis passed away during the project on the 29th July 2019 and the research that his clinic has enabled will be testament to an enduring legacy in the ME/CFS community, along with the thousands of patients whose lives he touched.

I also thank Emerge Australia for their efforts in assisting local researchers including myself to share our work with the most important stakeholders: the ME/CFS community. My final and perhaps most crucial acknowledgement goes to the patients, families, carers and funding bodies whose passion, hospitality or generosity made this work possible.

Journal Publications Arising from this Thesis

Missailidis, D., Annesley, S. J. & Fisher, P. R. (2019). Pathological Mechanisms Underlying Myalgic Encephalomyelitis/Chronic Fatigue Syndrome. *Diagnostics (Basel)*, **9**, 3.

Missailidis, D., Annesley, S. J., Allan, C. Y., Sanislav, O., Lidbury, B. A., Lewis, D. P. & Fisher, P. R. (2020). An Isolated Complex V Inefficiency and Dysregulated Mitochondrial Function in Immortalized Lymphocytes from ME/CFS Patients. *Int J Mol Sci,* **21**, 3.

Missailidis, D., Sanislav, O., Allan, C. Y., Annesley, S. J. & Fisher, P. R. (2020). Cell-Based Blood Biomarkers for Myalgic Encephalomyelitis/Chronic Fatigue Syndrome. *Int J Mol Sci*, **21**, 3.

Missailidis, D., O. Sanislav, C. Y. Allan, P. K. Smith, S. J. Annesley and P. R. Fisher (2021). "Dysregulated Provision of Oxidisable Substrates to the Mitochondria in ME/CFS Lymphoblasts." *Int J Mol Sci* **22**(4).

Presentations

Unrest screening at Bio 21 Institute, Melbourne (2nd August, 2018). Expert panellists: Chris Armstrong - biochemistry researcher at University of Melbourne's Bio21 Institute and Melbourne Bioanalytics, **Daniel Missailidis** - PhD researcher at La Trobe University, Dr Don Lewis - Medical Director CFS Discovery, Dr Heidi Nicholl - CEO Emerge Australia, Fiona Marsden - ME patient, MC Owen McKern - broadcaster and Program Manager at PBS 106.7FM. Event organised by #MEAction Network, Melbourne Bioanalytics and Emerge Australia Inc, opened by Adam Bandt MP, Leader of the Australian Greens and Federal Member for Melbourne.

Missailidis, D., Annesley, S. J., Allan, C. Y., Sanislav, O., Lidbury, B. A., Lewis, D. P. & Fisher, P. R. (2018). Dysregulated Mitochondrial Respiratory Function in Immortalised Lymphocytes from ME/CFS Patients. Poster #128. Presented at ComBio 2018 (23rd-26th September 2018), International Convention Centre Sydney, Darling Harbour, Sydney, New South Wales, Australia.

Missailidis, D., Annesley, S. J., Allan, C. Y., Sanislav, O., Lidbury, B. A., Lewis, D. P. & Fisher, P. R. (2018). Dysregulated Mitochondrial Respiratory Function in Immortalised Lymphocytes from ME/CFS Patients. Poster #10. Presented at AussieMit 2018 (29th November-1st December 2018), Bio21 Institute, Melbourne, Victoria, Australia.

Missailidis, D., Annesley, S. J., Allan, C. Y., Sanislav, O., Lidbury, B. A., Lewis, D. P. & Fisher, P. R. (2018). Dysregulated Mitochondrial Respiratory Function in Immortalised Lymphocytes from ME/CFS Patients. Poster and symposium presentations. PAM Research Symposium 2018 (23rd November 2018), La Trobe University, Melbourne, Victoria, Australia. Awarded highly commended presentation and runner-up best presentation.

Missailidis, D., Annesley, S. J., Allan, C. Y., Sanislav, O., Lidbury, B. A., Lewis, D. P. & Fisher, P. R. (2018). Dysregulated Mitochondrial Respiratory Function in Immortalised Lymphocytes from ME/CFS Patients. Poster and symposium presentations. ME/CFS Discovery Research Network scientific meeting 2018 (8th December 2018), La Trobe University, Melbourne, Victoria, Australia.

Missailidis, D., Annesley, S. J., Allan, C. Y., Sanislav, O., Lidbury, B. A., Lewis, D. P. & Fisher, P. R. (2018). Specific mitochondrial respiratory defects and compensatory changes in immortalized ME/CFS patient lymphocytes. Presented at the Emerge Australia International Research Symposium 2019 (March 12th-14th 2019), Novotel Geelong, Geelong, Victoria, Australia. First author, presentation was delivered by P.R. Fisher.

Missailidis, D. Day 1 Conference Report. Presented at the Emerge Australia International Research Symposium 2019 (March 12th-14th 2019), Novotel Geelong, Geelong, Victoria, Australia. 3-day conference held in Geelong, Victoria, Australia which hosted international keynote speakers, guests and delegates to share and discuss their findings with ME/CFS stakeholders and the community. The Day 1 Conference Report was a solo presentation delivered to a large and livestreamed patient audience in order to communicate the key findings shared by researchers on Day 1 of the conference.

Missailidis, D., Annesley, S. J., Allan, C. Y., Sanislav, O., & Fisher, P. R. (2020). Dysregulation of mitochondrial function and fuel preferences in ME/CFS lymphoblasts. Oral presentation delivered virtually due to travel restrictions. IACFS/ME Conference 2020, Stony Brook University, Stony Brook, New York, USA (21st August, 2020).

1.0 An Overview of Prior Evidence for the Molecular Basis of ME/CFS

1.1 Introduction

1.1.1 ME/CFS Background and Diagnosis

Myalgic Encephalomyelitis/Chronic Fatigue Syndrome (ME/CFS) is a chronic, debilitating disease considered amongst the disorders which most adversely affect quality of life (Falk Hvidberg, Brinth et al. 2015). In the EQ-5D-3L (a generic quality of life assessment), scores range from -0.624 to 1.000, with lower values reflecting a more impaired quality of life (Whitehead and Ali 2010). 112 Danish ME/CFS patients had a mean score of 0.47, worse than the lowest score of 0.62 that was obtained from all other conditions assessed in 23,392 individuals, which included schizophrenia, renal failure, multiple sclerosis, lung cancer and stroke (Falk Hvidberg, Brinth et al. 2015).

The characteristic symptoms of ME/CFS are unexplained fatigue lasting more than 6 months, and in the more recent case definitions, post-exertional malaise (PEM) – a delayed, disabling and exacerbated disease state following physical or mental exertion that exceeds a patient-specific threshold (severely affected patients are bed-bound). ME/CFS patients may also exhibit (with varied presentation and severity) many other symptoms, commonly including unrefreshing sleep, fever, muscle weakness, migraine, other flu-like symptoms, cognitive impairment ("brain fog") and sensitivities to a variety of external stimuli that may include light, sound or specific odors and chemicals. These symptoms are often accompanied by comorbidities such as fibromyalgia, bowel disorders, post-orthostatic tachycardia (POTS), and connective tissue disorders. It is estimated that 191,544 (0.76%) people live with ME/CFS in Australia with an annual total cost of $14,499 billion (Johnston, Brenu et al. 2013; Close, Marshall-Gradisnik et al. 2020). Another Australian study found that 78.61% of cases in 535 locally-diagnosed patients were female (Johnston, Staines et al. 2016).

The lack of a clear underlying molecular mechanism or biomarker for ME/CFS has led to the adoption of diagnostic case criteria which are symptom-based and rely on lengthy processes of exclusion of diseases with overlapping symptoms. Case definitions such as the commonly termed Oxford (Sharpe, Archard et al. 1991) or Fukuda (Fukuda, Straus et al.

1994) criteria are most often utilised in the UK and USA respectively, yet may fail to discriminate between generalised chronic fatigue and ME/CFS which specifically also involves PEM. This is important since the inclusion of PEM aids in characterising this disease as a discrete clinical entity. Also in usage are the Canadian Consensus Criteria (Carruthers, Jain et al. 2003) and the International Consensus Criteria (Carruthers, van de Sande et al. 2011) which require PEM for a diagnosis of ME/CFS and therefore may be considered more specific, preferable definitions. While the presence of PEM is an optional component of the Fukuda criteria, PEM is, unfortunately, not required for research participation by all studies using this or other less strict definitions. This is troublesome, since the varied usage of multiple diagnostic case criteria may render comparison between studies difficult depending on how participants were selected. These are factors which may have contributed to inconsistency in much of the ME/CFS literature in the last few decades. The slow diagnostic process is also exacerbated as a problem by the scarcity of expertise regarding ME/CFS clinical practice, which can lead to patients being subjected to unhelpful or longer than necessary diagnostic gauntlets by puzzled clinicians. This in turn delays treatment and may further complicate access to stringently selected populations for research.

With these challenges in mind, the identification of underlying pathological mechanisms and reliable, practicable molecular biomarkers is of paramount importance. Accordingly, the pursuit of a biomarker is perhaps the most commonly recurring theme in modern ME/CFS research. Despite numerous studies reporting results that could constitute potential biomarkers (Myhill, Booth et al. 2009; Booth, Myhill et al. 2012; Myhill, Booth et al. 2013; Armstrong, McGregor et al. 2015; Giloteaux, Goodrich et al. 2016; Naviaux, Naviaux et al. 2016; Yamano, Sugimoto et al. 2016; Germain, Ruppert et al. 2017; Lidbury, Kita et al. 2017; Nacul, Mudie et al. 2018; Esfandyarpour, Kashi et al. 2019; Nacul, de Barros et al. 2019; Almenar-Perez, Sarria et al. 2020), none of these outcomes have yet been validated or implemented as a diagnostic test for ME/CFS. Consequently, this critical need for a robust biomarker remains yet unfulfilled. The elucidation of underlying cytopathological mechanisms is therefore crucial not just to inform the development of rational treatments, but also because molecular abnormalities unique to ME/CFS could constitute biomarkers specific to the disease.

1.1.2 The Diversity of ME/CFS Symptom and Onset Patterns

Not only does ME/CFS affect multiple body systems and organs, but it does so with different and time-varying levels of severity and different patterns of comorbidities in different individuals, thereby producing a highly heterogeneous patient population (Komaroff and Buchwald 1991; Afari and Buchwald 2003; Jason, Corradi et al. 2005; Maclachlan, Watson et al. 2017). This complexity has represented a major challenge to the identification of a sole underlying pathological mechanism. ME/CFS subtype classification to manage this heterogeneity has been previously discussed in the field (Jason, Corradi et al. 2005; Maclachlan, Watson et al. 2017) and attempted by various means. Such proposed methods include: stratification by cytokine co-expression patterns (Russell, Broderick et al. 2016), orthostatic intolerance (Richardson, Lewis et al. 2018) patterns of differential disease-associated gene expression (Kerr, Burke et al. 2008; Kerr, Petty et al. 2008; Zhang, Gough et al. 2010), gene expression profiles concurrent with comorbid POTS (Light, Agarwal et al. 2013), DNA methylation profiles associated with quality of life scores and PEM (de Vega, Erdman et al. 2018), severity and frequency of physical or mental fatigue (Jason, Boulton et al. 2010), irritable bowel syndrome (IBS) comorbidity (Maes, Leunis et al. 2014) and concurrent changes in patient metabolism (Nagy-Szakal, Barupal et al. 2018). Despite this volume of work, none of these methods are widely validated or used, and effective patient classification methods continue to be sought. This issue could be solved by the discovery of robust molecular biomarkers.

Disease onset is generally sudden and often follows an acute “viral-like” illness, yet gradual onset without a history of acute infection has also been observed, albeit less commonly (Komaroff and Buchwald 1991; Buchwald, Ashley et al. 1996). Despite the prevalence of this “post-infectious” mode of onset, it is unlikely that there is a single causative pathogen given the diversity of viral and non-viral pathogens to which different cohorts of ME/CFS patients have been reportedly exposed (Straus, Tosato et al. 1985; Holmes, Kaplan et al. 1988; Buchwald, Ashley et al. 1996; Vernon, Whistler et al. 2006; Zhang, Gough et al. 2010; Halpin, Williams et al. 2017; Proal and Marshall 2018; Shikova, Reshkova et al. 2020). Given the clinical heterogeneity of the patient population, this is unsurprising. It is also likely, given that not all patients experience such an illness prior to disease onset, that the initial pathological insult is not necessarily pathogen-mediated and can otherwise be instigated by any bodily insult of sufficient magnitude.

Damaging bodily insults could elicit a homeostatic response such as the highly conserved cell danger response, which entails a purinergic signalling cascade that is initiated by the damaging release of reactive oxygen species and metabolic intermediates, followed by activation of anti-inflammatory and regenerative pathways (Naviaux 2014). While this and similar proposals suggest an initial, damaging insult which leaves individuals trapped within dysfunctional, alternative homeostatic feedback loops (Craddock, Fritsch et al. 2014; Kashi, Davis et al. 2019), an alternative explanation could involve chronic, ongoing exposure of cells to an antagonist agent. However, chronic pathogen exposure in ME/CFS seems unlikely to be present in the majority of cases, since theories of viral persistence have been investigated over many years and the evidence for chronic viral infection in ME/CFS is collectively inconclusive (Rasa, Nora-Krukle et al. 2018). In any case, variation in the mode of triggering bodily insult, whether acute or ongoing, could contribute to the heterogeneity of ME/CFS symptoms and further emphasizes the importance of identifying causative pathological mechanisms.

Attempts have been made to identify commonality in underlying pathological mechanism despite the diversity of disease onset and presentation of peripheral symptoms. Naturally, this has included the exploration of genetics. However, no substantial evidence for a genetic basis of the disease has yet been confirmed, with only two single nucleotide polymorphisms (SNP) resulting in missense mutations in incompletely characterised genes reported in a genome-wide association study (Schlauch, Khaiboullina et al. 2016). Others have theorised that due to the tendency of ME/CFS to "run in the family", its absence at birth, and historical reports of clustered ME/CFS "outbreaks", there exists an unidentified heritable genetic susceptibility to specific, intersecting trigger circumstances which initiate the onset of disease (Kashi, Davis et al. 2019). It is noteworthy that such an enhanced susceptibility attributed to genetic variation has been reported in similar conditions – such as variation in immune response genes in individuals suffering from chronic Q fever – a distinct chronic illness following *Coxiella burnetii* infection which involves persistent fatigue (Helbig, Heatley et al. 2003; Helbig, Harris et al. 2005). However, since many ME/CFS cases are not associated with any family history or with clustered outbreaks, it is most likely that such theoretical, heritable genetic elements where present would constitute increased risk factors rather than being the underlying mechanism of disease. It is therefore currently unclear whether a specific underlying susceptibility factor is at work in ME/CFS.

The following sections will provide a general overview of relevant evidence for the molecular basis of ME/CFS that has been reported across multiple body systems. More detailed discussion of specific findings is included in subsequent chapters where related to the results therein. In view of the aims and focus of this thesis, this introductory chapter will emphasize mitochondrial dysfunction, metabolic pathways and the little-researched energy stress signalling pathways in ME/CFS. These and subsequent examples pertaining to research of the immune system and gut will also act to draw attention to the prevalence of inconclusive or inconsistent clinical associations in ME/CFS research and the need for new research that tests iterative mechanistic hypotheses in experimental models.

1.2 Energy Metabolism and Mitochondrial Function

1.2.1 Background

The nature of the persistent fatigue and PEM experienced by patients has prompted the investigation of mitochondria and broader cellular metabolism, since defects in either could cause these two key symptoms. In the intervening years since early studies (Behan, More et al. 1991; Barnes, Taylor et al. 1993; McCully, Natelson et al. 1996), mitochondria had been largely neglected in the field until their first re-emergence as an area of interest during the last decade (Myhill, Booth et al. 2009). The research in this area has since generated a basis to support some manner of both mitochondrial and broader metabolic dysfunction in ME/CFS, albeit with many inconsistencies or issues which highlight the importance of re-examining these processes. Owing to the complexity of the many interconnected pathways involved, this section provides an initial, broader introduction to the relevant pathways and ME/CFS literature while subsequent chapters provide additional detail where it is more closely related to the interpretation of specific results.

1.2.2 Snapshot Studies Assessing Energy Metabolism

Evidence supporting dysregulated energy metabolism or mitochondrial function in ME/CFS has been sought across multiple experimental areas. There have been recent studies utilising the metabolomics approach, which captures a quantitative snapshot of steady-state metabolite levels in a sample to infer alterations in the related biochemical pathways. This is typically achieved by either mass spectrometry (MS) or nuclear magnetic resonance (NMR) spectroscopy. Early studies used NMR to measure metabolites within

ME/CFS blood samples and reported decreases in glutamine and ornithine concentrations, suggesting abnormal amino acid metabolism and urea cycle dysregulation (Armstrong, McGregor et al. 2012). A subsequent study utilising MS conversely reported an elevation in ornithine concentration with a decrease in citrulline, but this was also interpreted to involve urea cycle dysregulation (Yamano, Sugimoto et al. 2016). Subsequent work undertaken by the same authors of the early NMR study proposed that impaired glycolytic formation of pyruvate could be providing less downstream, oxidised pyruvate derivatives to be used as substrate for the tricarboxylic acid (TCA) cycle (Armstrong, McGregor et al. 2015). A simplified diagram depicting the most relevant relationships between the various energy stress signalling and metabolic pathways, oxidative phosphorylation (OXPHOS)/electron transport and the TCA cycle is included for the reader's reference for the introductory purposes of Sections 1.2.2-1.2.5 (Figure 1.1).

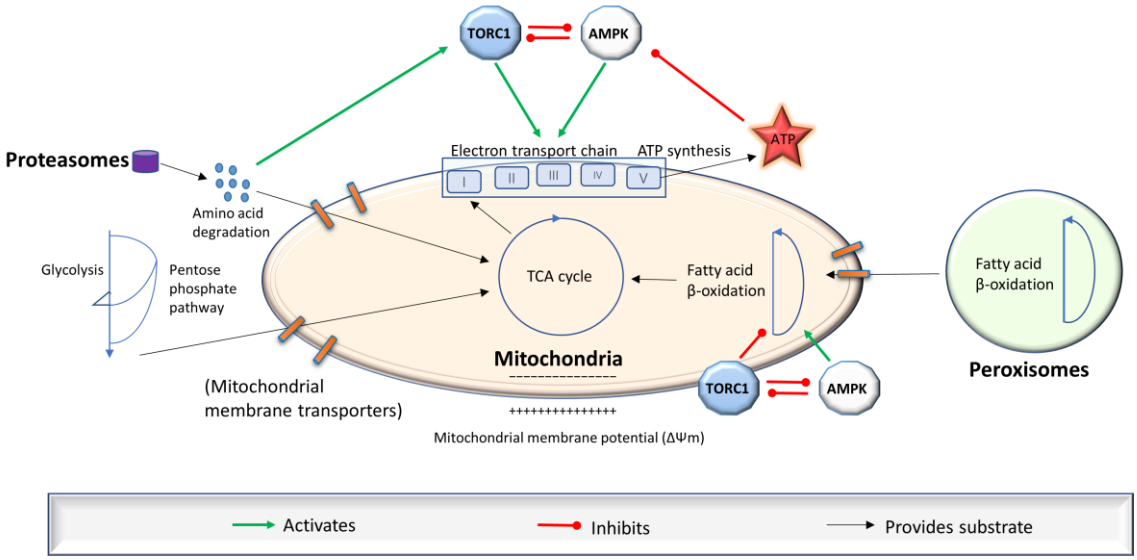

Figure 1.1: Depiction of the relationships between the most relevant signalling, metabolic and mitochondrial pathways involved in cellular energy supply and its study in ME/CFS. ATP is generated by the electron transport chain. ATP synthesis shortfall leads to the activation of the energy-sensing kinase AMPK which stimulates mitochondrial respiratory activity and catabolic pathways in order to return ATP output to adequacy. The various catabolic pathways that provide substrate to the TCA cycle do so from a diverse array of sources such as sugars (glycolysis and the pentose phosphate pathway), amino acids and fatty acids. In turn, the TCA cycle utilises the resulting metabolic intermediates to provide electron donors (reducing equivalents) to the electron transport chain in order to generate the proton-motive force which drives respiratory ATP synthesis. TORC1 is activated by amino acids, reductive stress and processes such as glutamine degradation. It also acts to upregulate cellular energy supply by stimulating mitochondrial biogenesis as part of promoting cell growth.

Work by others suggested that instead of a reduction in glycolytic pyruvate supply, a deficiency in pyruvate dehydrogenase (PDH) function may instead form a bottleneck for the provision of TCA cycle substrate downstream of glycolysis itself, PDH being the enzyme that converts pyruvate into the TCA cycle intermediate acetyl-CoA (Fluge, Mella et al. 2016). These and the previously described differences could be due to differences in techniques (NMR vs MS) and thus the range of detectable molecules. What could be taken from both lines of approach - supported by data from other similar studies (Yamano, Sugimoto et al. 2016; Germain, Ruppert et al. 2017; Nagy-Szakal, Barupal et al. 2018) - is that there may be some manner of TCA cycle disturbance in ME/CFS, perhaps driven by reduced supply of glucose-derived substrate. If the TCA cycle output of oxidative phosphorylation OXPHOS substrate was indeed reduced by a defect in glycolysis (Armstrong, McGregor et al. 2015) or PDH (Fluge, Mella et al. 2016), one might expect disturbances in cellular energy production in ME/CFS cells. There have been several studies which report a reduction of steady-state adenosine triphosphate (ATP) levels (Myhill, Booth et al. 2009; Castro-Marrero, Cordero et al. 2013; Brown, Dibnah et al. 2018), yet other work has instead reported an elevation (Lawson, Hsieh et al. 2016). These reports regarding ATP levels are therefore contradictory. These particular observations were also made using steady-state measurements which do not provide direct information as to the rate of ATP synthesis.

1.2.3 Rate-Based Measurements of Mitochondrial Function and Glycolysis in Cultured Cells

Real-time parameters of aerobic respiration and glycolysis can instead be measured in live cells by extracellular flux assays, which measure oxygen consumption rates (OCR) and extracellular acidification rates (ECAR) using intact cells (to examine respiration and glycolysis, respectively). However, common methods employed by others in the field who have used these techniques bear significant limitations as outlined below.

As noted earlier, glycolytic catabolism of glucose is a major supplier of acetyl-CoA to the TCA cycle, and this can be assayed in intact cells by measuring the rate of acidification of the medium by cells provided with glucose as a substrate. One recent study using natural killer (NK) cells from a small sample of six patients and six healthy controls reported a reduced glycolytic reserve in the ME/CFS cells (Nguyen, Staines et al. 2018). The

glycolytic reserve is a measure of the excess capacity of glycolysis to meet cellular ATP demands when mitochondrial ATP synthesis by oxidative phosphorylation is inhibited. However, this study is clearly limited by sample size. Others reported a reduction in the rate of glycolysis in stimulated and unstimulated T cells (Mandarano, Maya et al. 2019). On the contrary, no evidence of a glycolytic defect was observed by others using heterogenous peripheral blood mononuclear cells (PBMCs) (Tomas, Brown et al. 2017). Reports regarding the rate of aerobic respiration are similarly inconsistent in direction, with reduced (Tomas, Brown et al. 2017) or unchanged rates of respiration (Nguyen, Staines et al. 2018; Mandarano, Maya et al. 2019) being reported. Previous literature regarding respirometry in the ME/CFS field is therefore inconclusive.

Another limitation is that these studies often report individual O_2 consumption and extracellular acidification rates that are either negative or very small positive values, below or only slightly above the background signal, placing them at the threshold of reliable detection. This difficulty arises because *ex vivo* peripheral blood lymphocytes are dying and metabolically inactive (Gardiner and Finlay 2017) and this not only makes metabolic rate assays technically difficult, but it may obscure differences in metabolism that would be apparent in actively metabolising cells. This emphasises the importance of new research examining mitochondrial energy generation and supporting pathways such as glycolysis in metabolically active cells from ME/CFS patients.

1.2.4 Energy Stress Signalling

The homeostatic regulation of cellular energy metabolism is centered on two stress-sensing protein kinases, AMP-activated protein kinase (AMPK) (Hardie and Carling 1997) and target of rapamycin (TOR or, in mammalian cells, mTOR) (Ma and Blenis 2009) which play key, often mutually inhibitory roles. If their activities are chronically dysregulated by metabolic abnormalities or an energy insufficiency in ME/CFS cells, they may be unable to respond to additional energy demand which could contribute to the PEM suffered by patients who undergo exertion. This idea is consistent with reports of AMPK in muscle cells from people with ME/CFS being unresponsive to contraction-induced activation, anticipated to result from ATP depletion (Brown, Jones et al. 2015). Such a theoretical insensitivity could result from AMPK already being in an activated state in these cells, or from AMPK inhibition by chronically hyperactivated TOR complex 1 (TORC1). The latter

is plausible given that both the Complex I inhibitor metformin and the AMPK activator compound 991 elicited activation of AMPK in ME/CFS muscle cells in a subsequent study (Brown, Dibnah et al. 2018). Perhaps the activation signal from the pharmacological agents was sufficiently large as to allow additional activation despite the foregoing constraints. Not only do these possibilities highlight that the role of AMPK in ME/CFS is still incompletely understood, but also that TORC1 activity could be elevated in ME/CFS. Elevated TORC1 activity in ME/CFS cells may be anticipated, since inhibitory phosphorylation of its substrate eukaryotic translation initiation factor 4E-binding protein 1 (4E-BP1) is well understood to selectively activate translation of mitochondrial proteins (Morita, Gravel et al. 2015). This could explain the elevated expression of mitochondrial proteins that was found in studies of patient saliva, PBMCs and platelets (Kaushik, Fear et al. 2005; Vernon, Whistler et al. 2006; Ciregia, Kollipara et al. 2016). Despite these possibilities, TORC1 signalling has not been directly investigated in ME/CFS research until the work undertaken in this thesis.

1.2.5 Fatty Acid and Amino Acid Utilisation

The TCA cycle is provisioned with acetyl-CoA derived from oxidation of glucose/carbohydrate and from fatty acid or amino acid catabolism. While oxidation of carbohydrates may be the default mechanism, the previously mentioned metabolomic studies have proposed that carbohydrate oxidation for energy is reduced in ME/CFS (Armstrong, McGregor et al. 2015; Fluge, Mella et al. 2016; Nagy-Szakal, Barupal et al. 2018). As such, a compensatory elevation of fatty acid β-oxidation or amino acid catabolism could be present in cells from ME/CFS patients.

Fatty acid synthesis and β-oxidation are regulated by both AMPK (Hardie and Pan 2002) and TORC1 (Laplante and Sabatini 2009). AMPK promotes fatty acid β-oxidation when activated by elevated ATP demand while its inactivity favours fatty acid biosynthesis, whereas TORC1 exerts the opposite effects (Hardie and Pan 2002; Laplante and Sabatini 2009). Therefore, one would expect activation of AMPK and TORC1 to mutually inhibit one another, both directly and indirectly, so that in most circumstances, changes in their activity will be in opposite directions. However, both kinases are also regulated by other signals and participate in a complex, reciprocal feedback network (Hindupur, Gonzalez et al. 2015), so that scenarios exist where both are simultaneously activated (Dalle Pezze, Ruf et al. 2016).

Because of the specific mechanisms of regulatory action of these pathways in lipid homeostasis, both AMPK and TORC1 activities could be concurrently elevated in ME/CFS cells and still be accompanied by an increased rate of fatty acid catabolism. This is because activation of TORC1 promotes fatty acid biosynthesis by elevating the expression of gene products including acetyl-CoA carboxylase (ACC) through the upregulation of transcription factors SREBP-1 and SREBP-2 (Horton, Shah et al. 2003). In turn, ACC's promotion of fatty acid biosynthesis results in an accumulation of malonyl CoA which is a potent inhibitor of mitochondrial import of fatty acids for β-oxidation. Upregulated expression of ACC by TORC1 therefore serves a dual purpose in upregulating fatty acid biosynthesis and downregulating β-oxidation. ACC, however, is also a primary regulatory target of AMPK and is inactivated by phosphorylation when AMPK is activated (Winder and Hardie 1996). AMPK and TORC1 therefore exert opposing effects on fatty acid metabolism, AMPK post-translationally and TORC1 transcriptionally (Figure 1.2). Since AMPK inactivates ACC post-translationally, the concurrent activation of AMPK and TORC1, if it did occur in ME/CFS cells, may allow AMPK to constrain the effects of TORC1's upregulation of lipid-biosynthesis and downregulation of β-oxidation.

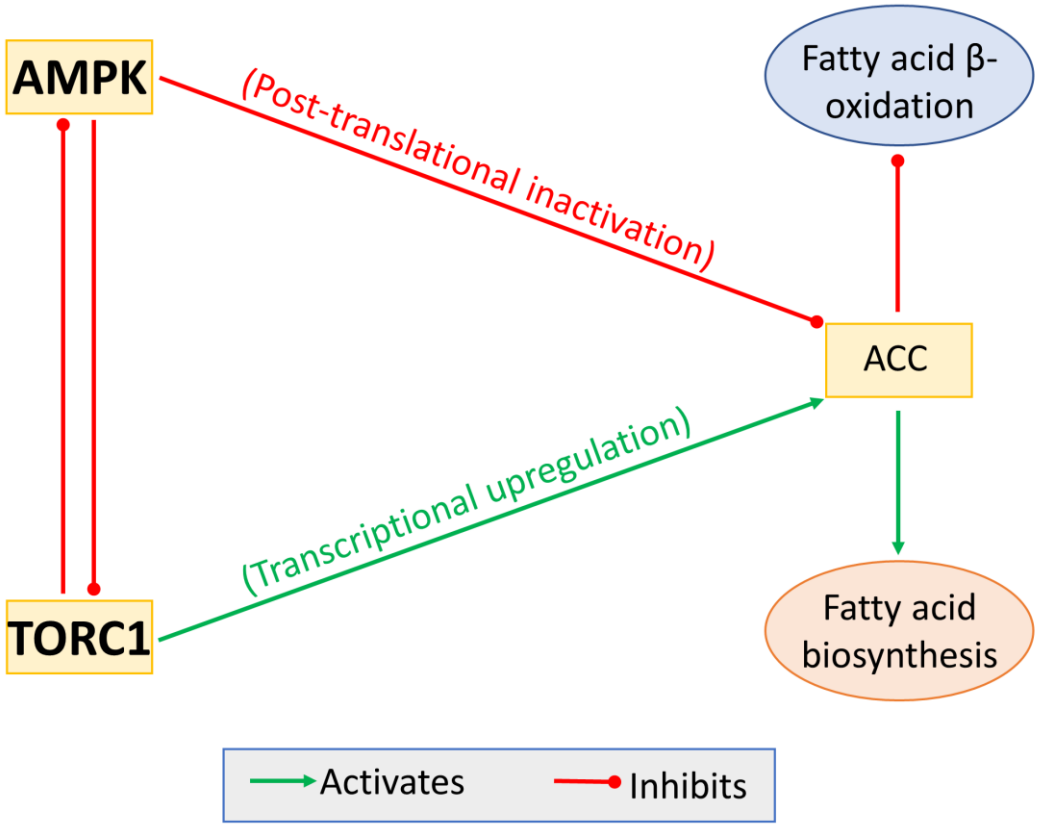

Figure 1.2: ACC controls the balance between fatty acid β-oxidation and biosynthesis and is regulated by both AMPK and TORC1. Through this particular mechanism, AMPK activity stimulates fatty acid β-oxidation and TORC1 stimulates fatty acid biosynthesis.

At the same time, both AMPK and TORC1 directly or indirectly induce the expression of diverse mitochondrial proteins, including those involved in fatty acid β-oxidation. The combined effects could be a steady state in which the cells have increased their use of β-oxidation relative to glycolysis as a supplier of acetyl-CoA to the TCA cycle. If so, this could potentially account for the aforementioned inconsistencies in reports of a glycolytic impairment. Fatty acid oxidation is normally upregulated as a supplementary energy pathway during fasting or exercise as a response to reduced blood glucose concentration (Bartlett and Eaton 2004). An increased reliance on fatty acid oxidation just at rest could therefore also contribute to the inability of people with ME/CFS to meet the elevated energy demands imposed by exertion. However, while prior studies cover some of these aspects individually, these metabolic and signalling pathways and their interconnected relationships have never all been investigated in combination in previous ME/CFS studies.

Amino acid catabolism may also be used as a metabolic alternative to fuel the TCA cycle as a response to insufficient energy generation. Different ME/CFS studies have proposed impaired provision of TCA cycle intermediates accompanied by dysregulation of amino acid metabolism. Two important studies suggest elevated utilisation of glutamate inferred from changes in the levels both of glutamate itself and related metabolites (Armstrong, McGregor et al. 2015; Fluge, Mella et al. 2016). This is important for energy metabolism since glutamate is a source of TCA cycle substrate via its conversion to α-ketoglutarate (α-KG) by multiple enzymes. However, others have reported unchanged glutamate levels and instead propose reduced amino acid catabolism due to reduced levels of flavin adenine dinucleotide, an important cofactor for branched-chain amino acid catabolism which is another source of TCA cycle substrate (Naviaux, Naviaux et al. 2016). The catabolic utilisation of amino acids to assist with generating cellular energy in ME/CFS patients therefore warrants additional investigation.

1.3 Immunity and Inflammation

1.3.1 NK Cell Function

The function of the immune system has been a major focus of much ME/CFS research for many years and thus is important to summarise. Evidence for immune dysfunction in ME/CFS has commonly been sought through studying the functional characteristics of NK

cells, which are cytotoxic immune cells with roles in both the innate and adaptive immune responses. Multiple groups have reported reduced NK cell cytotoxicity or numbers in ME/CFS (Barker, Fujimura et al. 1994; Maher, Klimas et al. 2005; Lorusso, Mikhaylova et al. 2009; Fletcher, Zeng et al. 2010; Marshall-Gradisnik, Huth et al. 2016) or impairing alterations to functional surface markers (Klimas, Salvato et al. 1990; Tirelli, Marotta et al. 1994; Brenu, van Driel et al. 2011). Conversely, other groups have reported increased cytotoxicity. For example, perforin, a glycoprotein used as a functional indicator of NK cell cytotoxicity due to its roles in NK cell mediated lysis (Kawasaki, Shinkai et al. 1990; Osinska, Popko et al. 2014), has been reported as upregulated (Brenu, van Driel et al. 2011), downregulated (Maher, Klimas et al. 2005), or, along with every other assessed parameter of cytotoxicity, unaltered in people with ME/CFS (Theorell, Blomkvist et al. 1999). A recent, comprehensive, large-scale biobank study also found no significant differences in NK cell numbers, subtype composition, or assessed functional parameters (Cliff, King et al. 2019). In summation, NK cells have a long history in the field and continue to remain be studied, but in light of conflicting or inconclusive findings it is still unclear whether specific alterations to NK cells play a role in ME/CFS.

Transient receptor potential melastatin 3 (TRPM3) calcium ion channels have an important role in calcium homeostasis (Grimm, Kraft et al. 2003), and their reduced expression has been reported in a subpopulation of ME/CFS NK cells (Nguyen, Johnston et al. 2017; Cabanas, Muraki et al. 2018; Cabanas, Muraki et al. 2019). The reason for the reduced expression of TRPM3 in these cells is unknown but in other cell types, expression of TRPM3 is repressed by the activity of microRNA-204 (miR-204), encoded by intron 6 of the TRPM3 gene (Cost and Czyzyk-Krzeska 2015). However, miR-204 is not amongst the microRNAs whose expression is reportedly altered in ME/CFS patients (Almenar-Perez, Sanchez-Fito et al. 2019).

Reduced expression of TRPM3 receptors would be expected to cause a reduction in Ca^{2+} responses to pregnenolone sulphate (PregS), a specific activating ligand for TRPM3 channels. However, the opposite was observed when Ca^{2+} levels were assayed by flow cytometry using Indo1, a Ca^{2+}-sensitive fluorescent dye in the TRPM3-depleted NK cells (Nguyen, Johnston et al. 2017). Subsequent studies using whole cell patch clamping, however, have reported loss of PregS-stimulated Ca^{2+} responses (Cabanas, Muraki et al. 2018, Cabanas, Muraki et al. 2019).

1.3.2 Cytokines and Inflammation

System-wide inflammation is theorised to be important in the ME/CFS clinical setting as it has been associated with symptom severity (Komaroff 2017), but the evidence demonstrating a role for abnormalities in proinflammatory cytokines is inconsistent. While there are indeed reports of the elevation of various proinflammatory cytokines in ME/CFS (Brenu, van Driel et al. 2011; Maes, Twisk et al. 2012; Hornig, Montoya et al. 2015; Peterson, Brenu et al. 2015; Russell, Broderick et al. 2016; Milrad, Hall et al. 2017; Montoya, Holmes et al. 2017) these findings contrast with reports of reduced expression of proinflammatory agents such as interleukin-8 or transforming growth factor beta 1 (Tomoda, Joudoi et al. 2005; Fletcher, Zeng et al. 2009). Others have also reviewed evidence for the specific directional shift of individual cytokines as being inconsistent (Mensah, Bansal et al. 2017). One group has reported that a cohort of ME/CFS patients with leaky gut syndrome as a comorbidity may undergo symptom remission when the IgM and IgA immune responses are attenuated by treatment with anti-inflammatory and antioxidant medications (Maes, Coucke et al. 2007; Maes and Leunis 2008). These findings are yet to be validated.

1.3.3 Autoimmunity

Autoimmunity has more recently become an area of interest, albeit with a small number of research-based publications. Autoimmune theories for ME/CFS have been proposed based on early studies using rituximab, a drug used to deplete B cell populations (Fluge and Mella 2009; Fluge, Risa et al. 2015). This was supported by other reports of elevated naïve and transitional B cells in patients (Bradley, Ford et al. 2013). However, a role for such B cell-mediated autoimmunity in the disorder is now challenged by the negative outcome of the more recent rituximab phase III clinical trial (Fluge, Rekeland et al. 2019) which refutes the previous rituximab work. This may also indicate that autoimmunity only presents in a small subset of patients who respond positively to rituximab treatment (Rekeland, Fluge et al. 2018). Other direct lines of evidence for autoimmune behavior in the disorder come from elevated antibodies directed against β adrenergic and muscarinic cholinergic receptors in sera (Loebel, Grabowski et al. 2016), supported by the improvement of symptoms following immunoadsorption removal treatment (Scheibenbogen, Loebel et al. 2018). Others have reported abnormal IgM immune recognition of both microbial and human heat

shock protein 60 in a subset of patients (Elfaitouri, Herrmann et al. 2013) or against phosphatidylinositol (Maes, Mihaylova et al. 2007). There was no evidence of infective pathogen persistence in either study. In view of this body of research, an autoimmune basis for the condition remains possible but currently unidentified.

1.4 Gut Abnormalities

1.4.1 The Gut Microbiota

It is well understood that many ME/CFS patients present with co-occurring gastrointestinal issues. Consequently, a disturbed gut microbiota has been proposed to play a role in ME/CFS (Butt, Dunstan et al. 2001; Sheedy, Wettenhall et al. 2009; Fremont, Coomans et al. 2013; Jackson, Butt et al. 2015; Shukla, Cook et al. 2015; Giloteaux, Goodrich et al. 2016; Armstrong, McGregor et al. 2017). While such reports are numerous, they have been reviewed as collectively inconclusive with contradictory directional changes in specific organisms (Du Preez, Corbitt et al. 2018). While the role of the gut microbiota remains unclear, there are also reports of physiological gut abnormalities such as impaired intestinal motility (Burnet and Chatterton 2004) and elevated intestinal wall permeability (often termed "leaky gut") (Maes, Coucke et al. 2007; Maes and Leunis 2008; Maes, Leunis et al. 2014). Studies have shown that IBS can co-occur with specific other symptoms or abnormalities in different body systems (Aaron, Burke et al. 2000; Nagy-Szakal, Barupal et al. 2018; Tsai, Chen et al. 2019), which has resulted in proposals that ME/CFS patients with IBS might comprise a distinct subtype (Maes, Leunis et al. 2014).

The intestinal microbiota has been proposed to influence (Brown and Clarke 2017; Grainger, Daw et al. 2018) and be influenced by (Nakajima, Vogelzang et al. 2018; Neumann, Blume et al. 2019) the function of the immune system. Associations have also been reported between the gut microbiota and host mitochondrial function and metabolism (Janssen and Kersten 2015; Kaliannan, Wang et al. 2015; Saint-Georges-Chaumet and Edeas 2016; Clark and Mach 2017; Bretin, Gewirtz et al. 2018; Chambers, Preston et al. 2018). It should be noted that this field of study is relatively new, and the relationships drawn between the gut microbiota and other systems are mostly associative or theoretical rather than directly demonstrated.

1.4.2 Intestinal Wall Hyperpermeability in ME/CFS

People with ME/CFS have been reported to present with gut microbiota disturbances concurrent with differences in blood metabolite levels, which has prompted the drawing of associations between the two observations (Sheedy, Wettenhall et al. 2009; Armstrong, McGregor et al. 2017; Nagy-Szakal, Barupal et al. 2018). Sheedy et al., observed increased numbers of Gram-positive intestinal bacteria which produce lactic acid that may lower the gut pH and lead to elevated gut permeability (Henriksson, Tagesson et al. 1988). The translocation of these enteric lactic acid products into the bloodstream could be related to elevated lactate reported in the blood (Rutherford, Manning et al. 2016) and cerebrospinal fluid of ME/CFS patients (Mathew, Mao et al. 2009; Murrough, Mao et al. 2010; Shungu, Weiduschat et al. 2012). However, this contrasts with reports of reduced blood lactate later measured by H-NMR metabolomics in a local Australian cohort more closely resembling the Sheedy *et al.* 2009 cohort (Armstrong, McGregor et al. 2015).

Others have suggested that the immune system and mitochondrial function could be affected by increased translocation of immunogenic bacterial secretions from the gut into the bloodstream, which in ME/CFS could be mediated by intestinal wall hyperpermeability in patients affected with IBS (Maes and Leunis 2008; Maes, Twisk et al. 2012). For example, the generation of excess free radicals which can occur in the mitochondria (Cadenas and Davies 2000), has been proposed to form part of a microbial defense mechanism (Ghosh, Dai et al. 2011; Naviaux 2012; Abuaita, Schultz et al. 2018), with enteric species such as *Escherichia coli* being susceptible to the bactericidal properties of free radical derived reactive nitrogen species (Hurst and Lymar 1997). However, these theories have not been examined experimentally. Theoretical interactions with mitochondrial function in ME/CFS are also challenged by studies reporting mitochondrial abnormalities not selecting cohorts for IBS or leaky gut comorbidity. Since not all ME/CFS patients also experience comorbid IBS, members of these cohorts are likely to have exhibited mitochondrial dysfunction in the absence of these digestive tract problems. Many of these mitochondrial studies also examined *ex vivo* cells in culture medium or isolated mitochondria (Myhill, Booth et al. 2009; Fluge, Mella et al. 2016; Lawson, Hsieh et al. 2016; Tomas, Brown et al. 2017; Mandarano, Maya et al. 2019), which would have separated these samples from the theorised presence of immunogenic bacterial secretions in the blood of patients with comorbid leaky gut syndrome. This body of work therefore comprises yet another inconclusive area of ME/CFS research that relies heavily on speculative clinical associations.

1.5 Summary and Aims

1.5.1 Addressing the Broad Inconclusiveness of Current Literature and the Need for Mechanistic Insight

The earlier sections of this introduction have discussed the prior evidence for molecular abnormalities in ME/CFS patients. Much of the key evidence is summarised in Table 1.1, which while often pointing towards disturbances in the same systems is often inconsistent in the specific abnormalities observed.

Area of study	Brief summary of key reports in ME/CFS
Metabolomics	• Multiple reports of disturbed amino acid metabolism, specific metabolite alterations not always consistent (Armstrong, McGregor et al. 2012; Armstrong, McGregor et al. 2014; Armstrong, McGregor et al. 2015; Fluge, Mella et al. 2016; Yamano, Sugimoto et al. 2016). • Dysregulated lipid metabolism but inconsistent in proposed direction (Armstrong, McGregor et al. 2015; Naviaux, Naviaux et al. 2016; Germain, Ruppert et al. 2017; Nagy-Szakal, Barupal et al. 2018), possible glycolysis impairment (Armstrong, McGregor et al. 2015), possible PDH impairment (Fluge, Mella et al. 2016), urea cycle dysregulation (Armstrong, McGregor et al. 2012; Yamano, Sugimoto et al. 2016).
Mitochondrial function	• Inconsistent: reduced (Myhill, Booth et al. 2009) vs elevated steady-state ATP levels (Castro-Marrero, Cordero et al. 2013; Brown, Jones et al. 2015; Lawson, Hsieh et al. 2016) but resting ATP synthesis rates are normal (Tomas, Brown et al. 2017; Nguyen, Staines et al. 2018).

	• Elevated mitochondrial enzyme expression (Kaushik, Fear et al. 2005; Ciregia, Kollipara et al. 2016).
Muscle energy supply and signalling	• Inconsistent AMPK activity state: Elevated AMPK vs unaltered baseline AMPK activity (Brown, Jones et al. 2015; Rutherford, Manning et al. 2016; Brown, Dibnah et al. 2018). • Reduced glucose or oxygen uptake or mitochondrial biogenesis (Vermeulen and Vermeulen van Eck 2014; Brown, Jones et al. 2015). • Muscle observations are likely confounded by the reduced exercise undertaken by ME/CFS patients since exercise upregulates mitochondrial biogenesis (O'Neill, Maarbjerg et al. 2011).
Natural Killer Cells	• Overall inconsistent evidence – role largely uncertain (Klimas, Salvato et al. 1990; Barker, Fujimura et al. 1994; Tirelli, Marotta et al. 1994; Maher, Klimas et al. 2005; Lorusso, Mikhaylova et al. 2009; Fletcher, Zeng et al. 2010; Brenu, van Driel et al. 2011; Marshall-Gradisnik, Huth et al. 2016).
Calcium signalling	• Evidence for impaired TRPM3 function (Cabanas, Muraki et al. 2018; Cabanas, Muraki et al. 2019).
Inflammation and cytokines	• Highly sought but inconsistent molecular evidence (Blundell, Ray et al. 2015; Mensah, Bansal et al. 2017), yet is likely to play some role based on clinical inflammation and the many reported disturbances in related systems.
Autoimmunity	• Relatively little researched.

	• Role for B cell-mediated autoimmunity challenged by negative outcome of rituximab trial (Fluge, Risa et al. 2015; Rekeland, Fluge et al. 2018; Fluge, Rekeland et al. 2019).
Gut microbiota and physiology	• Largely inconsistent literature (Du Preez, Corbitt et al. 2018). • Effects on other body systems are unproven theoretical associations.

Table 1.1: Brief summary of prior molecular abnormalities reported in ME/CFS.

While so many links between these multiple affected systems have also been proposed by others, each of these phenomena are correlated only in that they have been reported clinically in people with the disorder, often across cohorts diagnosed under different criteria in different countries. The causal relationships between these differences are unknown and cannot be discerned purely on the basis of clinical association. There are many scenarios where more than one of the affected systems may exert pathological effects on another and *vice versa*. This complex and often reciprocal regulatory cross-talk between biological systems makes it difficult to distinguish cause from effect, so there is great need for potential causal relationships underlying the disease to be addressed directly using appropriate experimental models.

1.5.2 Project Aims

As the organelles responsible for most of the cell's energy supply, the mitochondria seem likely to be important in ME/CFS given the hallmark symptoms of PEM and persistent fatigue. Given the critical need for the identification of underlying pathological mechanisms, and the inconsistencies and drawbacks of studies of mitochondrial function and related pathways outlined in Section 1.2, this PhD project was undertaken with the primary aim of assessing mitochondrial function and energy stress signalling in immortalised lymphocytes (termed lymphoblasts) isolated from participant blood.

To assess the potential importance of these key elements of cellular metabolism, it is important to work with metabolically active cells. Just as differences in running speed and

gait cannot be readily compared between sleeping individuals, any differences between patients and healthy controls in mitochondrial function and metabolism are likely to be obscured in quiescent cells. For this and other reasons, I chose in this thesis to work with lymphoblasts isolated from patient PBMCs. These are metabolically active cells which are proliferative and phenotypically stable over many doublings (Sie, Loong et al. 2009; Hernando, Shannon-Lowe et al. 2013). These properties allow not only the assessment of mitochondrial and metabolic functions in a more metabolically active context, but also allow the same samples to be revisited to test additional hypotheses as they arise. This provides the opportunity to continually build a mechanistic model from these very same samples. The same properties cannot be attributed to the cell types employed in any previous ME/CFS research and are necessary to address the current confusion and lack of understanding of ME/CFS disease mechanisms. Lymphoblasts have been used to study mitochondrial function and metabolism in many neurological disorders such as Huntington's Disease, Parkinson's Disease and Amyotrophic Lateral Sclerosis and can reveal differences in metabolism that are not observable in less metabolically active cells such as PBMCs (Sie, Loong et al. 2009; Annesley, Lay et al. 2016; Mejia, Chau et al. 2016; Pansarasa, Bordoni et al. 2018).

The second major aim of this project was to address perhaps the most urgent issue both in the field and facing the patient community, which is the lack of a diagnostic biomarker. Since lymphoblasts and the PBMCs from which they are derived are blood-accessible, any clear, observable changes in these cells between ME/CFS patients and healthy controls have the potential to be investigated as candidate diagnostic blood tests.

2.0 Materials and Methods

2.1 General Procedures

2.1.1 Sterilisation

All glassware, media and tips were sterilised by autoclaving at 100 kPa and 121 °C for 30 min. Unless otherwise stated, sterile distilled water was used as the solvent for all buffers and solutions.

2.1.2 Chemicals

The chemicals used and their suppliers are listed in Appendix 1.

2.1.3 Media and Buffers

The names and composition of media and buffers are listed in Appendix 2.

2.1.4 Commercially Available Assays

Commercially available assay kits are listed with their suppliers in Appendix 3.

2.1.5 Human Lymphocytes and Lymphoblasts

From each human sample, the deidentified participant ID, clinical group, age and gender are listed in Appendix 4.

2.1.6 Growth of Lymphoblast Cell Lines

Lymphoblasts were seeded at concentrations of no less than 2×10^5 cells/mL in T25 flasks in growth medium (Appendix 2), where they were cultured within a humidified 5% CO_2 incubator at 37 °C. The cultures were fed at intervals not exceeding three days by replacing 1/3 of medium with new medium, or split in a 1:3 ratio of cell culture to fresh medium as required. Prior to commencing experiments, lymphoblast cell lines were cultured over as short a time and as few passages as possible. Immortalised lymphoblast cell lines created from healthy donor blood were utilised as internal controls to normalise for variation between experiments where appropriate.

2.1.7 Storage of PBMCs and Lymphoblasts

Confluent cultures were transferred to tubes, harvested by centrifugation, resuspended in storage medium and stored in 250 µL aliquots at −80 °C. PBMCs specifically were stored

in aliquots containing 5×10^6 cells. For the lymphoblasts, dozens of aliquots per individual were stored when the cell lines were initially obtained to allow for ongoing access to proliferative cultures with low passage numbers. Lymphoblasts were removed from storage by thawing in a 37 °C water bath, harvested by centrifugation, resuspended in growth medium, and transferred to a fresh T25 flask.

2.1.8 Viable Cell Counts

Lymphoblast or lymphocyte (PBMC) viable counts for all applications were determined by staining with Trypan Blue prior to hemocytometer cell counting. Trypan Blue-stained cells were counted as dead and unstained intact cells as viable.

For the unimmortalised lymphocyte viability measurements over time, frozen aliquots were thawed in a 37 °C water bath, pelleted at 1000 ×g for 2 min and resuspended in 1 mL complete medium (Appendix 2). The cells were then washed at 1000 ×g for 2 min and resuspended in fresh medium of the same formulation. They were then seeded in a 96-well U-bottom plate at a density of 1×10^6 cells/mL and kept in a humidified 5% CO_2 incubator at 37 °C over the course of the experiment. Each well was mixed gently by pipette before sampling to ensure counting of a homogeneous cell suspension.

2.1.9 Preparation of Epstein-Barr virus (EBV) supernatant stocks

The EBV-producing marmoset B cell line B95.8 (Sigma-Aldrich, St. Louis, MO, USA) was seeded in 10 mL complete medium in a T25 flask (5×10^6 cells) and incubated at 37 ºC with 5% CO_2. After one week, the old medium was removed and replaced with 10 mL fresh growth medium. This process was repeated multiple times until the cell culture had progressed to confluency, at which point flasks were removed from the incubator and incubated at room temperature (RT) overnight with the lids tightly sealed. The next morning, the cell suspension was transferred into a fresh tube, centrifuged at 550 ×g for 10 min, the supernatant (containing EBV) decanted into a new tube to be retained, the cells resuspended in 1 mL medium and transferred to a fresh tube. Following this, the cells were then frozen in liquid nitrogen, rapidly thawed in a 37 ºC water bath, and this freeze-thaw cycle repeated three times. The cells were then centrifuged at 500 ×g for 10 min and the supernatant (containing EBV) retained and pooled with the previously collected supernatant. This larger volume of supernatant was separated into 1 mL aliquots and stored at -80ºC for later use in transfections.

2.2 Participant Cohorts and Creation of Lymphoblast Cell Lines from Isolated PBMCs

2.2.1 Participant Cohort Recruitment, Composition and Subsets

All participants were of European descent and belonged to two groups: ME/CFS patients conforming to the Canadian Consensus Criteria (CCC) (Carruthers, Jain et al. 2003) and healthy controls without any family history of ME/CFS or similar myalgias, with no other known reasons for fatigue, no musculoskeletal disorders, no pregnancy nor cohabiting with ME/CFS patients. ME/CFS severity assessments were conducted using Richardson and Lidbury's Weighted Standing Time (Richardson, Lewis et al. 2018). 15 mL of blood was taken per participant in heparin-treated vacutainer tubes.

Participants were recruited in two stages as part of larger project timelines. The first cohort was recruited between 2016-2017 at CFS Discovery Clinic, Melbourne, Australia, who have a long running specialisation and interest in ME/CFS and almost all of the data reported herein was obtained using only this cohort unless stated otherwise: ME/CFS patients (n = 51, 86% female, median age 50, age range 26–70) and healthy controls (n = 22, 68% female, median age 41, age range 21–58). There was no significant difference between the patient and control groups in either the gender proportions (Fisher's exact test, $p = 0.21$) or age distribution (Fisher's exact test, participants grouped by ages in 5 year increments, $p = 0.19$). Neither gender (ANOVA) nor age (multiple regression) had an effect on any of the parameters of mitochondrial function and Target of Rapamycin Complex 1 (TORC1) signalling reported in later sections ($p > 0.05$).

A randomly selected subset of this cohort was used to determine if the copy numbers of the EBV genome were different in patient and control groups and if they had any effect on the mitochondrial and cell signalling abnormalities that were observed. This subset included 13 ME/CFS patients (85% female, median age 43, age range 26–62) and 15 controls (53% female, median age 41, age range 21–58). Neither the difference in gender proportions (Fisher's exact test $p = 0.11$) nor the distribution of ages (Fisher's exact test, $p = 0.8$ using 15 year bins) was statistically significant. Neither age (multiple regression) nor gender (ANOVA) had any influence on the EBV genome copy number in either patients or controls ($p > 0.05$).

Due to the closure of the CFS Discovery clinic, recruitment of a second group of participants commenced in October 2019, undertaken by trained staff at La Trobe University. Recruitment is ongoing and is part of a larger project initiated late during this PhD project. This second cohort was only utilised and pooled with data from the initial main cohort for a small number of specific experiments (transcriptomics, proteomics, and to assess the effect of freezing time on lymphocyte death rates in Chapter 3). This new, second cohort currently contains 13 new ME/CFS participants (85% female, median age 38, age range 22–70) and 19 new control individuals (42% female, median age 29, age range 19–55). While the age distribution in the new cohort is not significantly different between the patient and control groups (Fisher exact test, $p > 0.1$), the gender proportions are significantly different ($p = 0.02$), yet as demonstrated below this did not affect the results. Details of the combined cohort lymphoblast subsets for proteomics and transcriptomics experiments follow:

1. A randomly selected subset of cell lines from both cohorts was employed for whole-cell proteomics. This subset included 34 ME/CFS patients (88% female, median age 52.5, age range 26–71) and 31 controls (45% female, median age 30, age range 19–58). The difference in gender proportions (Fisher's exact test $p = 0.0004$) and the distribution of ages (Fisher's exact test, $p = 0.000183$ using 15 year bins) were statistically significant. However, there was no significant effect of either age (multiple regression) or gender (ANOVA) on analysed experimental outcomes in either patients or controls ($p > 0.05$).
2. A randomly selected subset of cell lines from both cohorts was employed for whole-cell transcriptomics. This subset included 23 ME/CFS patients (82% female, median age 52, age range 27–71) and 17 controls (59% female, median age 41, age range 21–58). The difference in gender proportions (Fisher's exact test $p = 0.153$) and the distribution of ages (Fisher's exact test, $p = 0.102336$ using 15 year bins) were not statistically significant. There was also no effect of either age (multiple regression) or gender (ANOVA) on analysed experimental outcomes in either patients or controls ($p > 0.05$).

Lymphoblastoid cell lines (lymphoblasts) were generated from the blood of all participants. Multiple assays were conducted on both lymphoblasts and the PBMCs from which they were derived. However, because of limited PBMC supply, subsets were used for the tests using PBMCs:

1. PBMC respirometry assays. The sample selection was determined by the availability of sufficient PBMCs for the experiments. This subcohort included 14 ME/CFS patients (71% female, median age 59, age range 38–71) and nine healthy controls (67% female, median age 41, age range 21–52). The gender proportions were not different (Fisher's exact test $p = 1.0$), but the age distributions were (four control but no ME/CFS individuals under 30; seven ME/CFS individuals over 60; Fisher's exact test $p = 0.013$ using 15-year bins). Neither age (multiple regression) nor gender (ANOVA) had any relationship with the PBMC O_2 consumption rates in either patients or controls ($p > 0.05$).
2. PBMC cell death assays used samples from both cohorts. 35 ME/CFS individuals (89% female, median age 52, age range 26–71) and 14 control individuals (71% female, median age 42, age range 21–58) were used from the first cohort and are included in data presented in Chapter 3 by themselves, since only these individuals had undergone the full set of mitochondrial tests examined therein. Neither the gender proportions (Fisher's exact test $p = 0.15$) nor the age distributions were significantly different (Fisher's exact test $p = 0.13$ using 15-year bins). The second cohort was utilised in its entirety and is included in Chapter 4 alongside data from the first cohort to examine the effect of frozen storage time on cell viability. Neither age (multiple regression) nor gender (ANOVA) had any relationship with the PBMC death rate in either patients or controls in samples from both cohorts ($p > 0.05$).

2.2.2 PBMC Isolation from Whole Blood

Blood samples were diluted 1:1 with RT wash medium (Appendix 2) and 20 mL of this diluted blood was then gently layered onto RT 10 mL Ficoll-Paque. This step was repeated with a second 50 mL tube. The layers were separated by centrifugation at 700 ×g for 40 min and PBMCs present in the resultant buffy coat layer were harvested by pipetting. The cells were pooled into a fresh tube already containing 10 mL wash medium, then topped up to a total volume of 40 ml with wash medium. The PBMCs were then pelleted by centrifugation at 500 ×g for 15 min. The pellet was washed once in 25 ml wash medium, with a final centrifugation at 300 ×g for 10 min to collect the cells. The supernatant was discarded, and the cells resuspended in 5 mL complete medium. The cell density of the suspension was determined by haemocytometer counting with trypan blue staining, and 5

$\times 10^6$ cells were set aside for immortalisation. The excess cells were stored as described in Section 2.1.7.

2.2.3 Immortalisation of PBMCs

For immortalisation, 1 mL culture supernatant from B95.8 cells (Sigma-Aldrich, St. Louis, MO, USA) expressing EBV was added, and 150 µL of the mix was seeded per well in a 96-well U-bottom plate, then incubated for 1 h within a humidified 5% CO_2 incubator at 37 °C. A final concentration of 500 ng/mL Cyclosporin A was then added to each well. Cultures were fed weekly by replacing half of the medium with the same formulation, without disturbing the cells. This process was repeated over a period of approximately three weeks until the cells were confluent and growing rapidly, after which the lymphoblast cultures were processed as described in Section 2.1.6.

2.3 Respirometry and PBMC Rate of Death

2.3.1 Using Seahorse Respirometry to Assess Mitochondrial Function in PBMCs and Lymphoblasts

Oxygen consumption rates (OCR) of 8×10^5 viable PBMCs or lymphoblasts per well were measured using the Seahorse XFe24 Extracellular Flux Analyzer (Agilent, Santa Clara, CA, USA) with Seahorse XFe24 FluxPaks. Immortalised lymphoblasts were cultured in 3 mL growth medium per well in 6-well Costar plates prior to Seahorse experiments while PBMCs were recovered from storage and inoculated immediately.

In order to measure the oxygen consumption rates (OCR in pmol/min) of cells via this method, they must be firmly adhered to and evenly spread across the bottom of the assay wells. The Cell Culture Microplate was therefore prepared to facilitate cell adherence by pipetting a 4.5 µL of a 3:1 mixture of XF Base Medium: Matrigel Matrix into each well and spreading it evenly across the surface under refrigerated conditions. The plate was then left to dry at RT under laminar flow, and 8×10^5 cells/well were later seeded in 525 µL XF base medium containing: 2.5 mM glucose, 1 mM pyruvate, 200 mM L-glutamine and adjusted to pH 7.4. The cells were incubated with these conditions for 1 h at 37 °C prior to the assay.

In order to act as a vehicle for inhibitory compound injection and to facilitate OCR measurements, the sensor cartridge apparatus was rehydrated one day in advance by adding

1 mL XF Calibrant to each well and incubating at 37 ºC until needed. 5 mM drug stocks were prepared beforehand in DMSO and diluted in the same supplemented XF medium that was used to seed the cells prior to injection. Injection port concentrations were 16 µM oligomycin (ATP synthase inhibitor), 9 µM carbonyl cyanide m-chlorophenyl hydrazone (CCCP), an uncoupling protonophore, 50 µM rotenone (Complex I inhibitor) and 11 µM antimycin A (Complex III inhibitor). OCRs were measured prior to (basal OCR) and after successive 75µL injections to final concentrations of 2 µM oligomycin 1 µM CCCP 5 µM rotenone and 1 µM antimycin A.

From the resulting data the OCR associated with respiratory ATP synthesis was determined (oligomycin-sensitive component), the maximum OCR in CCCP-uncoupled mitochondria and the rotenone-sensitive OCR attributable to uncoupled Complex I activity, the antimycin-sensitive Complex II/III activity, the OCR by mitochondrial functions (e.g., protein import) other than ATP synthesis that are mitochondrial membrane potential ($\Delta\psi m$)-driven (so-called ‘proton leak’), non-respiratory oxygen consumption (e.g., by cellular and mitochondrial oxygenases and oxidases), and the respiratory ‘spare-capacity’ (excess capacity of the respiratory electron transport chain that is not being used in basal respiration). A visual depiction of these components is included in Figure 2.1.

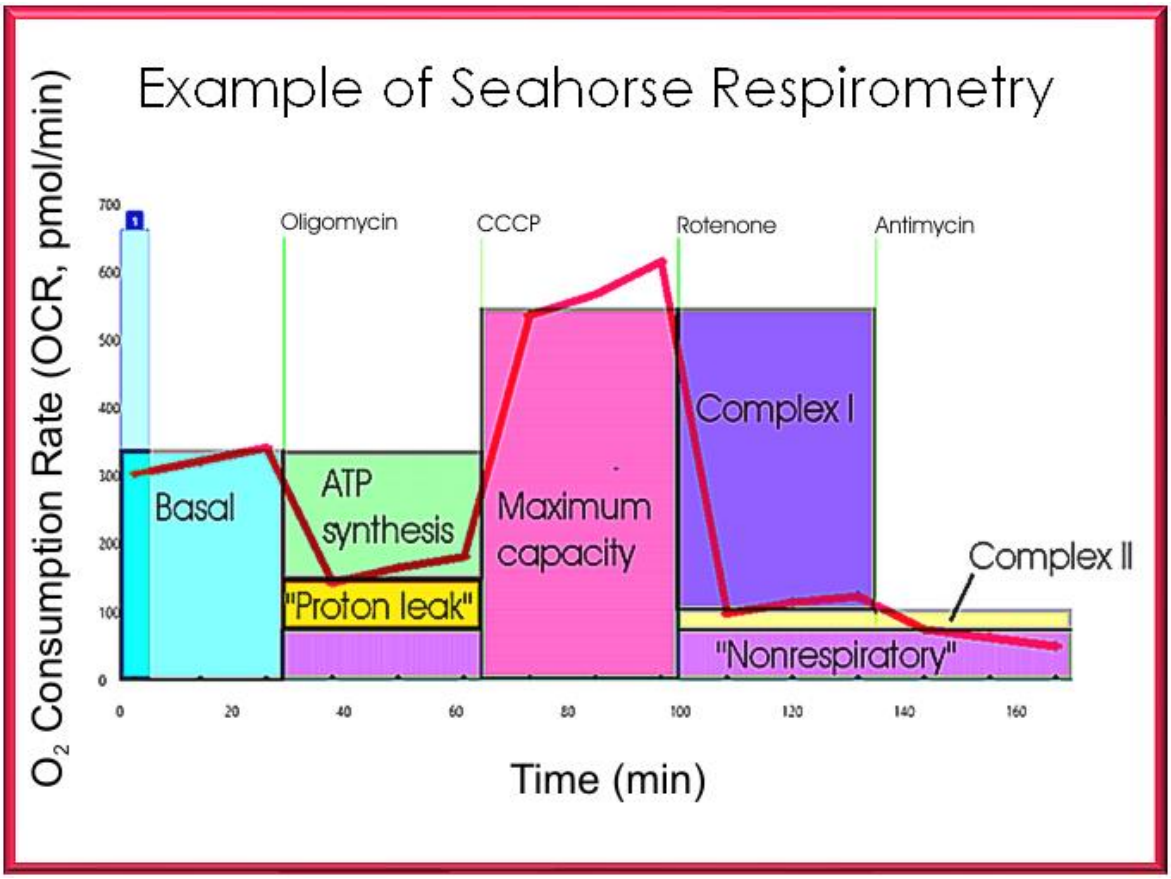

Figure 2.1: Example of Seahorse respirometry. Lymphoblasts (8×10^5 viable cells) were seeded into each of 4 wells in the 24 well plate as described. Four wells without cells were used to measure the background signal which was subtracted from the average signal from the 4 test wells. At each assay time point the medium and drug additions were mixed (3 min), cells rested (2 min) and O_2 consumption rates measured (3 min). The 4 sequential drug additions occurred at the indicated times – oligomycin, CCCP, rotenone and antimycin A. The various respiratory parameters shown were calculated as illustrated from the measured OCRs and the changes in the OCR after each drug addition.

2.3.2 Measuring the Rate of Death of *ex vivo* PBMCs

Frozen PBMC aliquots were thawed in a 37 °C water bath, pelleted at 1000 ×g for 2 min and resuspended in 1 mL complete medium. The cells were then washed at 1000 ×g for 2 min and resuspended again in complete medium. They were then seeded in a 96-well U-bottom plate at a density of 1×10^6 cells/mL and kept in a humidified 5% CO_2 incubator at 37 °C over the course of the experiment. Viable cell counts were carried out every 24 h as described in Section 2.1.8.

2.4 Assessing Other Parameters of Mitochondrial Function, Glycolysis and TORC1 Activity in ME/CFS Lymphoblasts

2.4.1 Steady-State ATP Analysis

Steady-state intracellular ATP concentration was determined by firefly luciferin bioluminescence using the ATP Determination Kit (Invitrogen, Carlsbad, CA, USA). ATP was extracted from lymphoblasts by harvesting 5×10^5 cells at 500 ×g for 5 min, lysing the pellet in 100 µL 1% trichloroacetic acid and incubating for 10 min at RT. 900 µL 20 mM Tricine was then added, the mix centrifuged at 12,000 ×*g* for 2 min and the supernatant transferred to a fresh microcentrifuge tube. Serial dilutions of the 5 mM ATP stock included in the kit were made up with dH_2O according to the following dilution scheme in order to construct a standard curve: 100 µM, 10 µM, 1 µM, 100 nM, 10 nM and 1 nM. The samples, ATP standards, and dH_2O blanks were set up in duplicate tubes, combined with the kit reaction mixture which was set up according to the manufacturer's instructions, and immediately measured in the fluorometer (Modulus, Turner Biosystems, Sunnyvale, CA, USA) using the luminescence module. The luminescence is proportional to the amount of ATP present.

2.4.2 Semi-Quantitative Western Blotting of Oxidative Phosphorylation (OXPHOS) Complex Subunits and Confirmatory Western Blotting for Proteomics

Initial OXPHOS western blotting:

Cells were lysed in loading buffer with a protease inhibitor cocktail (Roche, Penzberg, Germany). A small aliquot of each sample was briefly sonicated and analysed for total protein concentration using a Qubit Protein Assay Kit and Qubit 2.0 Fluorometer (Thermo Fisher Scientific, Waltham, MA, USA) according to the manufacturer's instructions.

The samples were then heated to 90 °C for 10 min and 30 µg of total protein was loaded into each well in 12% sodium dodecyl sulphate (SDS) polyacrylamide gels. After electrophoresis, proteins were transferred onto polyvinylidene difluoride (PVDF) membranes using a Trans Blot Turbo Blotting apparatus (Bio-Rad Laboratories Inc., Hercules, CA, USA) for 30 min at 180 V, 1.0 A, blocked for 1 h with blocking buffer (5% skim milk, TBS buffer) and incubated overnight with primary antibodies (Total OXPHOS human WB antibody cocktail, Abcam, Cambridge, UK) diluted 1:1000 in blocking buffer.

This cocktail is directed against five OXPHOS proteins. Stain-free gel scans were utilised as the internal loading control in combination with an Alexa Fluor 800-labelled secondary antibody for detection (Alexa Fluor 800 goat anti-mouse IgG diluted 1:1000 in TBS). Following incubation with antibodies, the membranes were washed three times with TBS buffer containing 0.5% Tween 20, scanned with a ChemiDoc (Bio-Rad Laboratories Inc., Hercules, CA, USA) and analysed using the Image Lab software (Bio-Rad Laboratories Inc., Hercules, CA, USA). Two arbitrarily selected control cell lines (C105 and C0002) were included in every blot as internal normalisation controls for between-experiment variation. The intensity of individual bands was first normalised to the signal in the corresponding stain free gel track then subsequently normalised to the controls.

Confirmatory western blotting for proteomics:

Samples were lysed, homogenised, quantitated, denatured and loaded as in the previous method. Differences in the apparatus and antibodies used are described as follows. After electrophoresis, proteins were transferred onto PVDF membranes using a Mini gel tank with the Mini Blot module (Thermo Fisher Scientific, Waltham, MA, USA) 60 min at 10 V, 300A, at 4°C and then blocked for 1h with blocking buffer (1% casein, TBST buffer) and incubated overnight with primary antibodies diluted 1:1000 in blocking buffer. The antibodies used were ACO2 (D6D9, Cell Signalling Technology, cat #6571), SdhA (D6J9M, Cell Signalling Technology, cat #11998) and CPTC-MDH1-1. CPTC-MDH1-1 was developed by Clinical Proteomics Technologies for Cancer and obtained from the Developmental Studies Hybridoma Bank, created by the NICHD of the NIH and maintained at The University of Iowa, Department of Biology, Iowa City, IA 52242. Stain-free gel scans were utilised as the internal loading control in combination with an HRP-conjugated secondary antibody for detection (donkey anti-rabbit IgG, cat # A16023, and Goat anti-mouse IgG, cat #31430, Thermo Fisher Scientific, Waltham, MA, USA). Following incubation with antibodies, the membranes were washed three times with TBS buffer containing 0.5% Tween 20, and visualised using a chemiluminescent substrate (Clarity Western ELC substrate, Bio-Rad Laboratories Inc., Hercules, CA, USA) and the Amersham Imager 600 (GE Healthcare Life Sciences, Chicago, IL, USA) and analysed using the Image Lab software (Bio-Rad Laboratories Inc., Hercules, CA, USA). One arbitrarily selected control cell line was included in every blot as internal normalisation control for between-experiment variation. The intensity of individual bands was first normalised to the signal in the corresponding stain free gel track then subsequently

normalised to the controls. Oana Sanislav kindly performed these confirmatory blots due to pandemic-incurred laboratory restrictions.

2.4.3 Assessing Intracellular Reactive Oxygen Species (ROS) Levels

Intracellular ROS levels were determined using the Fluorometric Intracellular ROS Kit (Sigma-Aldrich, St. Louis, MO, USA). An aliquot of 5×10^5 cells was harvested per cell line at 500 ×g for 5 min, resuspended in 360 µL phosphate buffered saline (PBS), and 90 µL loaded into triplicate wells on a 96 well black, clear, flat bottom plate. One hundred microliters of reaction mix prepared according to manufacturer's instructions was added to each well, the plate protected from light and incubated for 1 h at 37 °C with 5% CO_2. The fluorescence was then read at excitation 520 nm emission 605 nm in the Clariostar microplate reader (BMG Labtech, Offenburg, Germany) as a measure of intracellular ROS. C105 was arbitrarily included as an internal normalisation control for between-experiment variation. The fluorescence is proportional to the amount of ROS present.

2.4.4 Whole-Cell Proteome Analysis

Samples of 3×10^6 lymphoblasts in 100 µL PBS were submitted to the La Trobe University Comprehensive Proteomics Platform for whole-cell proteome analysis. The samples were processed as follows:

Each sample was dried using a SpeedVac Concentrator and Savant Refrigerated Vapor trap (Thermo Fisher Scientific, Waltham, MA, USA). Samples were resuspended in 8 M Urea, 100 mM Tris pH = 8.3. 1 µL of tris [2-carboxyethyl] phosphine hydrochloride (TCEP, 200 mM solution in water) and incubated overnight at 21 °C in a ThermoMixer (Eppendorf AG, Hamburg, Germany). Four microliters of 1 M iodoacetamide (IAA in water) was added the following day and incubated in the dark at 21 °C. Next, 500 µL of 50 mM Tris (pH 8.3) and 1 µg trypsin was added to samples and left for 6 h at 37 °C in an incubator. Another 1 µg trypsin was added for double digestion and incubated overnight at 37 °C. The digested samples were purified for mass spectrometry analysis prior to peptide reconstitution and separation using Sep-Pak light C18 cartridges (Waters, Milford, MA, USA) according to manufacturer standard procedures. Data were collected on a Q Exactive HF (Thermo Fisher Scientific, Waltham, MA, USA) in Data Dependent Acquisition mode using m/z 350–1500 as mass spectrometry (MS) scan range at 60,000 resolution, HCD MS/MS spectra were collected for the 15 most intense ions per MS scan at 15,000 resolution with a normalised collision energy of 28% and an isolation window of 1.4 m/z. Dynamic exclusion parameters

were set as follows: exclude isotope on, duration 30 s and peptide match preferred. Other instrument parameters for the Orbitrap were MS maximum injection time 30 ms with AGC target 3 × 106, for a maximum injection time of 25 ms with AGT target of 1 × 105. Raw files consisting of high-resolution MS/MS spectra were processed with MaxQuant version 1.6.1.0 to detect features and identify proteins using the search engine Andromeda. UniProtKB/Swiss-Prot *Homo sapiens* sequence data was used as the database for the search engine. To assess the false discovery rate (FDR) a decoy data set was generated by MaxQuant after reversing the sequence database. Theoretical spectra were generated using the enzyme setting as trypsin and allowing two missed cleavages. The minimum required peptide length used was seven amino acids. Carbamidomethylation of Cys was set as a fixed modification, while N-acetylation of proteins and oxidation of Met were set as variable modifications. Precursor mass tolerance was set to 5 ppm and MS/MS tolerance to 0.05 Da. The "match between runs" option was enabled in MaxQuant to transfer identifications made between runs on the basis of matching precursors with high mass accuracy. PSM and protein identifications were filtered using a target-decoy approach at a false discovery rate (FDR) of 1%.

2.4.5 Assessing Mitochondrial Mass and Membrane Potential

Mitochondrial mass and MMP were assayed using the mitochondrial dyes MitoTracker® Green FM and MitoTracker® Red CMXRos. Both dyes bind specifically to mitochondrial membranes, MitoTracker® Red binding being membrane potential ($\Delta\psi m$)-dependent, while MitoTracker® Green binding was not. Mitotracker Green fluorescence thus measures mitochondrial membrane "mass" and Mitotracker Red fluorescence provides a measurement of $\Delta\psi_m$ when normalised to the Mitotracker Green signal (Pendergrass, Wolf et al. 2004).

Cells (7×10^5) were harvested at 500 ×g for 5 min, and 1×10^5 cells were plated per well into six wells of a 96 well black, clear flat bottom plate. The plate was incubated for 1 h at 37 °C with 5% CO_2. To duplicate wells for each dye treatment, MitoTracker® Green and Red were added to final concentrations of 200 nM, PBS added to background wells and Hoechst 33342 Nuclear Stain was included in every well at a final dilution of 1/2000, for normalising under each treatment condition (excitation 355 nm, emission 455 nm). The plate was then incubated for 1 h at 37 °C and 5% CO_2, the supernatant removed via aspiration and replaced with PBS. Fluorescences were read using the Clariostar microplate reader. Relative mitochondrial mass was determined by background-subtracted

MitoTracker® Green FM fluorescence at excitation 470 nm and emission 515 nm, normalised to the background subtracted signal from the same number of cells of the internal control cell line. The MMP was determined from the background-subtracted MitoTracker® Red CMXRos fluorescence (excitation 570 nm, emission 620 nm) divided by the background-subtracted fluorescence of MitoTracker® Green FM.

2.4.6 DNA Extraction from Lymphoblasts

At least 1×10^6 lymphoblasts were harvested by centrifugation at 500 ×g for 5 min and the pellet lysed in 1 mL DNAzol. This lysate was centrifuged at 10,000 ×g for 10 min to remove debris and the supernatant transferred to a new microcentrifuge tube. 500 µL of 100% ethanol was added to each tube and mixed immediately by inversion. After allowing the DNA to precipitate for 5 min, the DNA was sedimented by centrifugation at maximum speed for 10 min. The supernatant was then carefully removed and replaced with 1 mL 75% ethanol, and washed at top speed for 5 min. The ethanol was again removed carefully and the pellets briefly air-dried. The DNA was then thoroughly resuspended in 50 µL 8 mM NaOH stored at -80 °C until needed and diluted 1/10 prior to use in a qPCR assay.

2.4.7 Assessing Mitochondrial and EBV Genome Copy Number

SYBR green fluorescence was used in qPCR to investigate amplification of fragments of the mitochondrial ND1 and ND4 genes using the primers ND1F (5'cacccaagaacagggtttgt3'), ND1R (5'tggccatgggattgttgttaa3'), MTND4F (5'caacctttcctccgacccc3') and MTND4R (5'ctggataagtggcgttggct3').

To investigate the EBV genome copy number, the following primers were employed to investigate the indicative amplicon *Bam*HI fragment H rightward open reading frame (BHRF-1): BHRF1-F (5' ggagatactgttagccctg3') and BHRF1-R (5' gtgtgttataaatctgttccaag3').

A fragment of the nuclear-encoded mitochondrial gene β2 microglobulin was amplified alongside the investigated genes as an internal control, using the primers B2-MGF (5'cactaggaccttctctgagc3') and B2-MGR (5'ctacagcttgggaattcctgc3'). The reaction mixture (per investigated gene fragment) included 1× SYBR reagent mix for amplicon detection, primers at a concentration of 500 nM, and template DNA constituting 1/10 of the reaction mixture. Negative control wells with no template DNA were included to confirm that no

contamination was present. The Bio-Rad CFX96 qPCR System was used to amplify and detect the fragments of interest using the following thermal cycling scheme:

Cycle	Repeats	Step	Wait	Set temp. (ºC)
1	1	1	3:00	95
2	35	1	0:30	95
		2	0:30	55
		3	0:30	72
3	1	1	3:00	72

The cycle threshold obtained for the target amplicons of interest were subtracted from that of β2-microglobulin to provide normalised measures for the relative genome copy number. Data was collected during step 3 of cycle 2.

2.4.8 Using Respirometry to Investigate Glycolysis

The extracellular acidification rate (ECAR) of live, intact lymphoblasts was measured using a modified glycolytic stress test in the Seahorse XFe24 Extracellular Flux Analyzer with Seahorse XFe24 FluxPaks. Immortalised lymphoblasts were cultured in growth medium in 6-well plates prior to Seahorse experiments.

In order to measure the ECAR of cells using this method, they must be firmly adhered to and evenly spread across the bottom of the assay plate wells. To achieve this, the Cell Culture Microplate was prepared as previously described with a Matrigel coating in the bottom of each well. The plate was then left to dry at RT under laminar flow. Added to each well was 8×10^5 cells in XF base medium containing 200 mM L-glutamine and 5 mM 4-(2-hydroxyethyl)-1-piperazineethanesulphonic acid (HEPES).

The sensor cartridge apparatus was rehydrated one day in advance by adding 1 mL XF Calibrant to each well and incubating at 37 °C until needed. The injection ports of the sensor cartridge apparatus were loaded with the following drugs, in chronological order of four injections to give the indicated final concentrations in the wells: Glucose-10 mM, Oligomycin-2 µM, Rotenone-1 µM and Antimycin A-5 µM (combined injection), 2-Deoxyglucose-50 mM. The treatment with the rotenone/antimycin combination prevented

flow of electrons through the electron transport chain and allowed assessment of its impact on ECAR.

Before and after each successive drug addition, the ECAR was measured over three time points, consisting of a 3 min mix, 2 min wait, and 3 min measurement time. These measurements were subsequently analysed to determine the magnitudes of various parameters of glycolysis based on the targets of each successive drug injection. The difference between the post-glucose ECAR and the post-2-Deoxyglucose ECAR was reflective of glycolytic rate. The difference between the post-oligomycin and post-glucose ECAR indicated the glycolytic reserve. Glycolytic capacity was indicated by the difference between the post-2-Deoxyglucose ECAR and the post-oligomycin ECAR.

2.4.9 Investigating TORC1 Activity by 4E-BP1 Phosphorylation State and TORIN2 Sensitivity

TORC1 activity in ME/CFS lymphoblast lysates was measured using a Time-resolved Förster resonance energy transfer (FRET)-based multiwell plate assay of the phosphorylation state of 4E-BP1, a major TORC-1 substrate (Cisbio Bioassays, Codolet, France). Cells were harvested, resuspended in growth medium at 2×10^6 cells/ml and plated in four replicates at 5×10^4 cells/well in a 96-well plate. Cells were incubated at 5% CO_2/37 °C for 2 h, with two of the replicates subjected to TOR inhibition by 0.5 µM TORIN2. Lysis buffer was added to each well as per manufacturer instructions and the plate mixed on an orbital shaker for 40 min before plating each sample into a 384 well white plate — incorporating various controls and antibody mix (anti-4E-BP1 antibody labelled with d2 acceptor, and anti-phospho-4E-BP1 antibody labelled with Eu3+-cryptate donor) according to manufacturer instructions. After a 2 h incubation at RT the plate was scanned by the Clariostar plate reader and the ratio of the FRET signal from anti-phospho-4-EBP-1 antibody to the donor fluorescence signal from anti-4-EBP-1 antibody was measured according to instructions. C105 cells were included as an internal normalisation control for between-experiment variation.

2.4.10 RNA Extraction from Lymphoblasts

At least 1×10^6 lymphoblasts were harvested by centrifugation at 500 ×g for 5 min and lysed promptly with 1 mL Purezol RNA Isolation Reagent in a microcentrifuge tube. 200 µL chloroform was added to each tube, mixed well and incubated at RT for 15 min. This mixture was centrifuged at 12,000 ×g for 15 min at 4 °C and the colourless, top-layer

aqueous phase transferred to a fresh tube. 500 µL isopropanol was added to each tube and vortexed for 5 seconds, then incubated at RT for 10 min. The supernatant was then carefully discarded following a 12,000 ×g centrifugation for 8 min at 4 °C. The RNA was then washed with 1 mL 75% ethanol at 7500 ×g for 5 min at 4 °C, the supernatant removed and the tube briefly air-dried. The sedimented RNA was then dissolved in 50 µL RNAse-free water. This was then treated with the RQ1 DNAse protocol at working concentrations as specified by the manufacturer, for 60 min at 37 °C before the reaction was terminated by addition of the "stop" solution. RNA was then used for required assays on the same day or stored at -80 °C until used.

2.4.11 Transcriptomics

RNA samples were prepared according to the foregoing protocol and sent to Australian Genome Research Facility (AGRF), Melbourne on dry ice for mRNA sequencing and quantification. This was achieved using the Illumina TruSeq stranded mRNA protocol as per manufacturer instructions (Illumina, Inc. San Diego, California, USA).

2.4.12 Confirmatory qRT-PCR for transcriptomic data

SYBR green fluorescence was used to quantify fragments of transcripts of interest, using the following primers: GLS-Forward (5' GGAAGCCTGCAAAGTAAACCC 3'), GLS-Reverse (5' CCAAAGTGCAGTGCTTCATCC 3') or SdhB-Forward (5' ACTCTAGCTTGCACCCGAAG 3') and SdhB-Reverse (5' GCTGCTTGCCTTCCTGAGAT 3'). A fragment of the transcript encoding histone gene *HIST1H1C* was amplified alongside the investigated genes as an internal loading control (so-called "housekeeping" gene), using the following primers: Forward (5' GCGGCGCAACTCCGAAGAAG 3') and Reverse (5' AGCGGCCTTGGGCTTCACAG 3').

The reaction mixture was prepared according to manufacturer instructions (iTaq Universal One-Step Kit, Bio-Rad Laboratories Inc., Hercules, CA, USA), using primers at a concentration of 500 nM, and sample RNA constituting 1/10 of the reaction mixture. Negative control wells with no sample were included to confirm that no contamination was present. The CFX Connect Real-Time PCR Detection System (Bio-Rad Laboratories Inc., Hercules, CA, USA) was used to amplify and detect the transcript fragments of interest.

The cycle threshold obtained for the target transcript fragments of interest was subtracted from that of HIST1H1C to assess relative quantification.

2.4.13 AMPK Activity assay (ACC1/2 phosphorylation state)

AMPK activity in ME/CFS lymphoblast lysates was measured using a time-resolved FRET-based multiwell plate assay of the phosphorylation state of ACC1/2 (Cisbio Bioassays, Codolet, France). Cells were harvested, resuspended in growth medium at 1.2×10^6 cells/mL and plated in six replicates at 3×10^4 cells/well in a 384-well plate. Cells were incubated at 5% CO_2/37 °C for 4 h, with two of the replicates subjected to AMPK inhibition by 30 µM SBI-0206965 (S7885 Selleckchem, Houston, TX, USA) and two of the replicates subjected to AMPK activation by 30 µM A-769662 (A11071, AdooQ Bioscience, Irvine, CA, USA), the remaining two replicates were treated with an equivalent concentration of DMSO as a control. Lysis buffer was added to each well as per manufacturer instructions and the plate mixed on an orbital shaker for 40 min before plating each sample into a 384 well white plate —incorporating various controls and antibody mix (anti-ACC (Ser79) antibody labelled with d2 acceptor, and anti-Phospho-ACC (Ser79) antibody labelled with Eu3+-cryptate donor) according to manufacturer instructions. After a 24 h incubation at RT the plate was scanned by the Clariostar plate reader and the ratio of the FRET signal from anti-phospho-ACC (Ser79) antibody to the donor fluorescence signal from anti-ACC (Ser79) antibody was measured according to instructions. C105 cells were included as an internal normalisation control for between-experiment variation. Claire Allan kindly performed this assay due to pandemic-incurred laboratory restrictions.

2.4.14 Statistical Analysis

Data was analysed using Microsoft Excel with the Winstat add-in (http://www.winstat.com) or R using the packages R Commander (Fox 2005), REzy (Kanda 2013), Rattle (Williams 2011), pROC (Robin, Turck et al. 2011), edgeR (Robinson, McCarthy et al. 2010; McCarthy, Chen et al. 2012) and stats. Unless otherwise specified, two-sample tests used the Welch t-test. ANOVA and Fisher's exact tests were used as specified and appropriate. The significance of individual coefficients in multiple regression analysis was tested using t-tests.

Proteomics data was analysed employing the software Scaffold (Proteome Software) prior to exporting to Excel for additional analysis. Proteins detected in fewer than 5 samples were

excluded from the analysis. Intensity-based absolute quantitation (iBAQ) abundance values were exported to excel and subsequently normalised to the mean total from 5 healthy controls which were arbitrarily selected for inclusion in each proteomics experiment to control for any inter-experimental variation, with similar outcomes seen from these control cell lines in both experiments.

Transcriptomics data was initially collated by AGRF using the edgeR package for R. For individual transcripts, read counts were normalised to counts per million mapped reads within each respective sample. Data was exported to Excel for subsequent analysis.

PANTHER over-representation tests (Thomas, Campbell et al. 2003; Thomas, Kejariwal et al. 2006; Mi, Dong et al. 2010) were carried out in the early stages of analysis in order to obtain an objective, broad perspective of the data to inform unbiased subsequent analysis of individual, differentially regulated pathways. To facilitate this, genes/proteins were assigned a Q value to correct for multiple comparisons according to the Benjamini–Hochberg method (Benjamini 1995), and separated into two lists: those significantly up- or down-regulated. The up- and down-regulated lists were separately entered into the PANTHER over-representation tool, with binomial tests selected as the statistical test. The list of transcripts or proteins detected in the entire respective experiment was uploaded as the reference list used by PANTHER to determine the number of "expected" pathway hits. From this, PANTHER generated new lists of gene products that were statistically over-represented within the differentially expressed subsets of each experiment. These over-represented gene products were exported to Excel for further assessment, guiding subsequent analysis.

In closer subsequent analysis of individual pathways, detected proteins or transcripts were identified as belonging to a single functional group (e.g., TCA cycle) or respiratory complex using the NCBI gene ontology (GO) annotation database (Harris, Clark et al. 2004) and manually curated for relevance to the group of interest (occasional erroneous inclusions were removed). Using R, the binomial test of proportions was employed to assess whether all detected proteins or transcripts in a single functional group or respiratory complex were together altered in their frequency of up- or down-regulation in the ME/CFS group compared to controls. This test compared two proportions: the number of gene products upregulated and the number downregulated in ME/CFS lymphoblasts. It was expected that the levels of each protein or transcript had an equal probability of being above

or below the control average, so the hypothesised probability was set to 0.5 (equal proportions expected by chance). Two-sided tests were employed for pathways were there was no prior evidence suggesting altered expression in ME/CFS lymphoblasts. For functional groups of proteins where there was prior evidence of upregulation, the alternative hypothesis was applied that the number of upregulated gene products was "greater" than the number downregulated. Single sample *t* tests were also used to assess whether the average fold change in the levels of all detected proteins or transcripts in a single functional group or enzyme complex in the ME/CFS cohort was significantly different from the normalised healthy control mean (in two-sided tests), or significantly greater than the control mean (in one-sided tests) for those functional groups of gene products where there was prior evidence of upregulation.

For the analysis of candidate biomarkers, propensity scores were calculated using logistic regression models in Rattle (Williams 2011). The tested models used data partitioned randomly into a 70% training subset and a 30% test subset. The propensity score represents a probability that the sample in question is from an ME/CFS patient. This score was generated from either single independent variable or multiple variables representing a set of key parameters that were significantly altered in ME/CFS lymphoblasts, the combination varying depending on the biomarker configuration that was modelled and evaluated. The individual variables are summarised as follows:

1. for lymphocyte death rate it was the percentage of dead lymphocytes after 48 h in culture medium.

2. for lymphoblast TORC1 activity, the independent variable was the normalised phosphorylation level of 4E-BP1, a specific cellular substrate of TORC1.

3. for respirometry, the five key parameters used were

    a. the fraction of the basal O_2 consumption rate (OCR) attributable to

        i. ATP synthesis by Complex V and

        ii. the use of the proton gradient in other mitochondrial membrane transport processes (the proton leak),

    b. maximum CCCP-uncoupled OCR,

c. the maximum uncoupled Complex I activity and

d. the nonmitochondrial OCR.

4. The levels of significantly altered gene transcripts present at high levels in the transcriptomic dataset (specific transcripts detailed in Chapter 5 results).

5. The levels of significantly altered proteins present at high levels in the proteomic dataset (Specific proteins detailed in Chapter 5 results).

The measures of respiratory function were also tested in combination with mitochondrial membrane potential measures, as determined by MitoTracker Red and MitoTracker Green fluorescence.

For whole-cell lymphoblast proteomics and transcriptomics, the independent variables differed depending on the specific combination of individual gene products being applied (Refer to Chapter 5 results and discussion). The outcomes of the logistic regression were at first expressed as an error matrix, showing a cross tabulation of the actual source of the sample (ME/CFS or control) and the classification produced by the model. From this, error rates (false positives and false negatives) were calculated.

During the exploration of biomarkers, Receiver Operating Characteristic (ROC) analysis was performed on the propensity scores from the logistic regression models of candidate predictor variables from various assays. In ROC analysis, samples are counted in descending rank order according to the variable being assessed – in this case the propensity scores from the logistic regression. At each possible threshold in the score, samples are classified as "positive" if above threshold and "negative" if below threshold. Thus, a threshold above the highest sample score would result in all samples being classed as "negative" – sensitivity would be zero since no true positives would be detected. However, all true negatives would also be counted (correctly) as "negative" *ie*. there would be no false positives so the specificity would be 1 (100%). Conversely, at the lowest possible threshold for the propensity score, all samples would be classed as "positive", including (erroneously) all true negatives. In this case sensitivity would be 1 (all true positives detected) and specificity would be 0 (no true negatives correctly identified as "negative").

In the ROC curves presented in this thesis, as per convention, the sensitivity (fraction of positives that are correct) is plotted on the Y axis against specificity (fraction of negatives that are correct) on the X axis (with specificity *decreasing* from left to right). The "best" threshold value for the biomarker in question was defined in the ROC analysis as the point on the ROC curve which maximised the sum of the sensitivity and specificity (i.e., minimised the sum of the errors). The AUC (area under the ROC curve) with 95% confidence limits was calculated as an indicator of the usefulness of the biomarker in question in distinguishing ME/CFS from control samples. An AUC of 1.0 would mean that at the "best" threshold value, both sensitivity and specificity are 100%. Confidence limits for the sensitivities (on the vertical axis of ROC curves) were used to plot 95% confidence limits for the ROC curve itself. ROC curve comparisons by the bootstrapping method were performed as described by Robin et al. (2011) using 2000 replicates.

Since ROC analysis depends only on the rank order of observations in the dataset, when there is only a single independent measure being tested, it produces identical results for the raw and for rescaled or transformed data from the corresponding logistic regression analysis. Only the scale changes on which the threshold value itself is measured.

3.0 Dysregulated Mitochondrial Respiratory Function and Signalling in Immortalised ME/CFS Lymphoblasts

3.1 Introduction

3.1.1 Investigating the Mitochondria

A deficiency in the mitochondrial supply of cellular energy could be an explanation for the persistent fatigue, PEM, and other relevant symptoms experienced by ME/CFS patients. Evidence for mitochondrial dysfunction in ME/CFS has been sought in the last decade, but the data have been varied and inconsistent. Reduced mitochondrial biogenesis but not normalised respiratory chain enzyme activities have been reported in the muscle of ME/CFS individuals (Smits, van den Heuvel et al. 2011). Muscle mitochondrial biogenesis is upregulated by exercise (O'Neill, Maarbjerg et al. 2011), so this reduction is likely to be caused by the necessarily reduced exercise that ME/CFS patients can undertake. Mitochondrial respiratory function in ME/CFS neutrophils (Myhill, Booth et al. 2009; Booth, Myhill et al. 2012) and peripheral blood mononuclear cells (PBMCs) is reportedly reduced (Tomas, Brown et al. 2017) or unchanged (Tomas, Lodge et al. 2019), yet the oxidative phosphorylation (OXPHOS) complexes appear normal (Vermeulen, Kurk et al. 2010; Lawson, Hsieh et al. 2016), while the expression of genes encoding mitochondrial proteins in patient saliva, platelets, and lymphocytes is elevated (Kaushik, Fear et al. 2005; Nelson, Ambros et al. 2014; Ciregia, Kollipara et al. 2016). More recently, mitochondrial respiration was found to be unchanged in resting and stimulated $CD4^+$ and $CD8^+$ T cells, with the sole exceptions of a small reduction in the proton leak in resting and ATP synthesis in stimulated $CD8^+$ cells (Mandarano, Maya et al. 2019). These latter results could be a legacy of multiple comparisons being made in very small samples.

Differences between patient and control serum and urine metabolomes have been attributed to reduced provision of acetyl-CoA to the TCA cycle caused by a defect in glycolysis (Armstrong, McGregor et al. 2015) or by a defect in pyruvate dehydrogenase (PDH) (Fluge, Mella et al. 2016). While inconsistent, both proposals draw attention to a potential role in ME/CFS for impaired provision of reducing equivalents to mitochondrial OXPHOS by the TCA cycle. Despite their shared conviction that ME/CFS cells have fundamental problems in energy metabolism, the conflicting reports on the nature of these problems highlighted

the need to reexamine the issue of mitochondrial function and its regulation in ME/CFS cells.

A key regulator of mitochondrial function is TORC1 which regulates cell growth and energetics in a variety of cellular stress-sensing pathways (Loewith and Hall 2011). This pathway upregulates the expression of nuclear-encoded mitochondrial proteins (Cunningham, Rodgers et al. 2007), among which are subunits of the OXPHOS complexes (Morita, Gravel et al. 2015). Despite this connection, and the important roles of TORC1 within a complex regulatory network which responds to intracellular stressors including energy supply, dysregulation of this signalling pathway has not yet been investigated in ME/CFS cells.

3.1.2 Project Strategy and Overview of Findings

To clarify the roles of aberrant mitochondrial function and TORC1 signalling in ME/CFS, parameters of mitochondrial function in immortalised lymphocytes (termed lymphoblasts) from patient blood were compared with those from healthy age- and gender-matched controls. Mitochondrial function in ME/CFS lymphoblasts was indeed abnormal, with an isolated Complex V inefficiency accompanied by elevated capacity of Complexes I to IV, decreased membrane potential, upregulation of TORC1 activity and elevated expression of diverse mitochondrial proteins including OXPHOS complexes, TCA cycle enzymes, and mitochondrial small molecule import machinery. Despite these abnormalities, the rates of glycolysis and steady state ATP levels in the ME/CFS cells were normal. This pattern of changes in mitochondrial function in ME/CFS lymphoblasts was distinct from what our laboratory previously observed using the same approach to other neurological conditions. An example is the mitochondrial hyperactivity, normal membrane potential and elevated steady state ATP levels our group reported previously in lymphoblasts from patients with Parkinson's disease (Annesley, Lay et al. 2016) or fragile X-associated tremor/ataxia syndrome (Loesch, Annesley et al. 2017). The observations presented in this chapter suggest a model of mitochondrial dysfunction in ME/CFS lymphoblasts involving a primary deficiency in Complex V function, combined with homeostatic, compensatory upregulation of TORC1 activity and mitochondrial protein expression. Subsets of the information contained within this chapter have been published in research articles (Missailidis, Annesley et al. 2020; Missailidis, Sanislav et al. 2021).

3.2 Results

3.2.1 Ex Vivo Lymphocytes Are Metabolically Quiescent and Those from ME/CFS Patients Die More Rapidly than Controls

Whereas mitochondrial protein expression is elevated in ME/CFS saliva, lymphocytes and platelets (Kaushik, Fear et al. 2005; Vernon, Whistler et al. 2006; Ciregia, Kollipara et al. 2016), physiological measures of respiratory function and capacity in ME/CFS lymphocyte mitochondria are reportedly reduced (Myhill, Booth et al. 2009; Tomas, Brown et al. 2017). A possible explanation is that the *ex vivo* ME/CFS lymphocytes are more deeply quiescent (metabolism more suppressed) than control cells. This was investigated by comparing respiration rates in immortalised lymphocytes (lymphoblasts) from ME/CFS patients and controls with those of lymphocytes from a random subset (determined by limited lymphocyte supply) of the same participant cohort. Although the ME/CFS lymphocytes appeared to have slightly smaller respiration rates than controls, the difference was not significant. However, the basal respiration rates in both patient and control lymphocytes were two orders of magnitude lower than in the immortalised cells, approaching the lower limits of detectability in the instrument (Figure 3.1A), as in previously reported experiments with this cell type (Tomas, Brown et al. 2017). This confirmed that *ex vivo* lymphocytes from both patients and controls are in a deep state of physiological quiescence and so perhaps not representative of metabolically active cells *in vivo*.

Another potential contributor to the reported reduction in mitochondrial activity in ME/CFS lymphocytes compared to controls, is an increased death rate in ME/CFS lymphocytes compared to controls. The viability over time of ME/CFS lymphocytes versus healthy controls was therefore assessed (Figure 3.1B). In multiple log-linear regression analysis, the intercepts (which in the log-linear regression corresponds to an incubation time of 1 h) and the difference between them were not statistically significant. Although an extrapolation, this suggests that in both ME/CFS and control samples the fraction of dead cells at the start of the incubation was small and was similar in the two groups. However, the death rate over time was significant in both ME/CFS and control samples and was dramatically higher in the ME/CFS lymphocytes than in the controls.

Importantly, these *ex vivo* lymphocytes are already dying before measurements of basal OCR have begun. Most protocols for Seahorse respirometry involve incubating the cells *in situ* in the assay plates overnight prior to assay. During this time many cells will have died, more of them in ME/CFS samples than in controls. This suggests that previously reported reductions in ME/CFS lymphocyte mitochondrial function might have resulted from a higher fraction of dying (ie: metabolically suppressed) or dead cells in the assayed population. If it reflects the *in vivo* life span of unactivated lymphocytes, this result would also suggest that the turnover of unactivated lymphocytes in ME/CFS patients may be elevated.

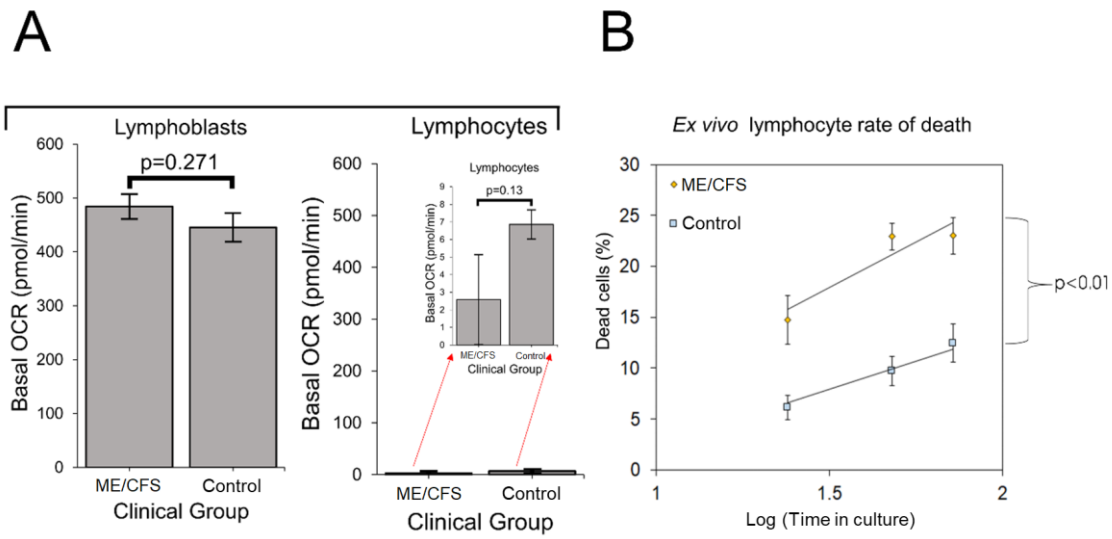

Figure 3.1: *Ex vivo* lymphocytes are metabolically quiescent and Myalgic Encephalomyelitis/Chronic Fatigue Syndrome (ME/CFS) lymphocytes die more rapidly. Error bars are standard errors of the mean. (**A**) Basal oxygen consumption rates (OCR) were measured in lymphoblasts and lymphocytes from ME/CFS and control individuals. Lymphoblasts: each ME/CFS (n = 50) and control (n = 22) cell line was assayed over four replicates in at least three independent experiments. Lymphocytes: each ME/CFS (n = 14) and control (n = 9) cell line was assayed over four replicates once due to limited supply. The red arrows point to the same data magnified with a smaller Y axis scale. The low basal OCRs for lymphocytes match those previously reported (Tomas, Brown et al. 2017). (**B**) ME/CFS lymphocytes die more rapidly than healthy controls. Lymphocytes stored for the same duration as the respirometry tests from both ME/CFS patients (n = 35) and healthy controls (n = 14) were seeded at a density of 1×10^6 viable cells/mL in RPMI 1640 with 10% serum, and kept in a humidified 5% CO_2 incubator at 37 ^oC during the experiment. Each point represents the mean percentage of dead cells at the corresponding time point for *ex vivo* lymphocytes from ME/CFS patients and healthy controls. Stepwise multiple regression analysis was performed with dummy variables allowing both slopes and intercepts to differ between groups, with removal of least significant regression variables until only significant coefficients

remained. The difference in the slopes (death rates) of the log-linear regressions between the ME/CFS and control group was statistically significant (*t* test).

3.2.2 Using Lymphoblasts to Investigate Mitochondrial Function in ME/CFS

The foregoing results suggest that lymphoblastoid cell lines (lymphoblasts) may better reflect the function of actively metabolising cells, including activated leukocytes such as may be involved in inflammatory processes in ME/CFS patients. Lymphoblasts were therefore used in the remainder of this study to investigate mitochondrial function in ME/CFS cells. Creation of the lymphoblasts involves immortalisation by EBV infection and integration of the EBV genome into the lymphocyte genome. To check for possible effects of EBV on the mitochondrial and cellular stress signalling parameters which were measured, EBV genome copy numbers were assayed (by qPCR) and no significant difference between ME/CFS and control lymphoblasts was found (Figure 3.2). Furthermore, there was no relationship between the EBV genome copy number and the mitochondrial and cell stress-signalling parameters that were measured in either the patient or the control group (Pearson, Spearman rank, and Kendall's tau correlation coefficients, $p > 0.05$ in all cases).

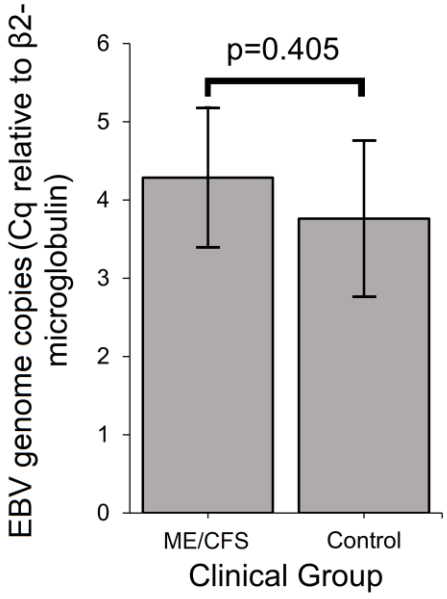

Figure 3.2: The genome copy number of the indicative EBV gene *BHRF-1* is unchanged between ME/CFS and control lymphoblasts. Genome copy numbers (qPCR for the EBV gene *BHRF-1* relative to nuclear β-microglobulin gene) are unchanged in ME/CFS lymphoblasts (independent *t*-test, $p > 0.05$). Each ME/CFS (n = 13) and control cell line (n = 15) was assayed by qPCR in multiple independent experiments. Error bars represent 95% confidence intervals.

3.2.3 ATP Synthesis by Complex V Is Inefficient in ME/CFS Lymphoblasts

In ME/CFS lymphoblasts, basal respiration was slightly elevated and the rate of O_2 consumption by ATP synthesis (oligomycin-sensitive component of basal respiration) slightly depressed, but neither change was statistically significant. However, as a proportion of the basal OCR, the rate of ATP synthesis by Complex V was significantly reduced (by about 15% relative to controls) in ME/CFS lymphoblasts, indicating an inefficiency in respiratory ATP synthesis (Figure 3.3A).

Since the absolute rate of ATP synthesis was not significantly altered, despite its inefficiency, it was anticipated that resting ME/CFS cells homeostatically maintain normal ATP levels. To verify this, whole cell ATP levels were assayed and no difference was observed between ME/CFS and control lymphoblasts (Figure 3.3B).

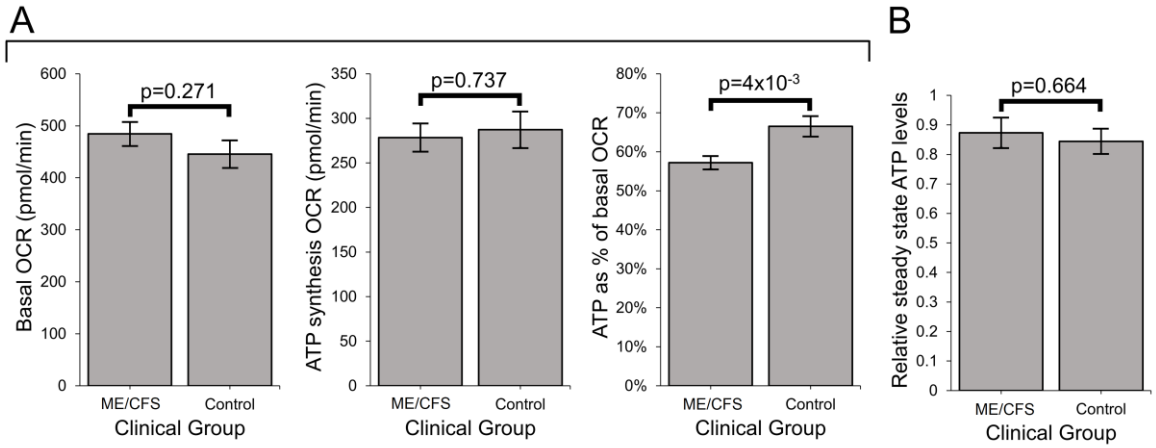

Figure 3.3: ATP synthesis by Complex V is inefficient in ME/CFS lymphoblasts. Error bars are standard errors of the mean. (**A**) Basal OCR and OCR by ATP synthesis were unchanged while OCR by ATP synthesis as a % of basal OCR was reduced in ME/CFS lymphoblasts (independent t-test). Each ME/CFS (n = 50) and control (n = 22) cell line was assayed over four replicates in at least three independent experiments. (**B**) Intracellular ATP concentration (relative background-subtracted luciferase luminescence) is unchanged in ME/CFS lymphoblasts (independent t-test). Each ME/CFS (n = 49) and control (n = 22) cell line was assayed in duplicate within each of at least three independent experiments. Data is normalised to an internal control cell line (C101).

3.2.4 ME/CFS Lymphoblasts Exhibit Elevated Respiratory Capacity, Activity and Expression of OXPHOS Complexes that, Except for Complex V, Are Functionally Normal

To achieve normal ATP synthesis rates and steady state levels, ME/CFS lymphoblasts may compensate for the reduced efficiency of respiratory ATP synthesis by upregulating their capacity for respiratory electron transport. This was likely to be the case given the increased maximum OCR of the CCCP-uncoupled mitochondria and the main contributor to this, uncoupled O_2 consumption by Complex I (rotenone-sensitive) as well as the spare respiratory capacity not utilised by basal respiration (Figure 3.4A). This elevated respiratory capacity in ME/CFS mitochondria implies an increase in the expression, import or activity of the proteins in these complexes and in the supporting pathways. To determine if this was the case, semiquantitative Western blotting was undertaken using crude lysates from ME/CFS and control lymphoblasts to assay the relative expression levels of indicative subunits of each of the five mitochondrial respiratory complexes. Significant increases in the levels of Complex I, II, and IV subunits were found by this semiquantitative Western blotting (Figure 3.4B). Smaller increases in the levels of subunits in the other complexes (III, V) were not statistically significant (Figure 3.4C).

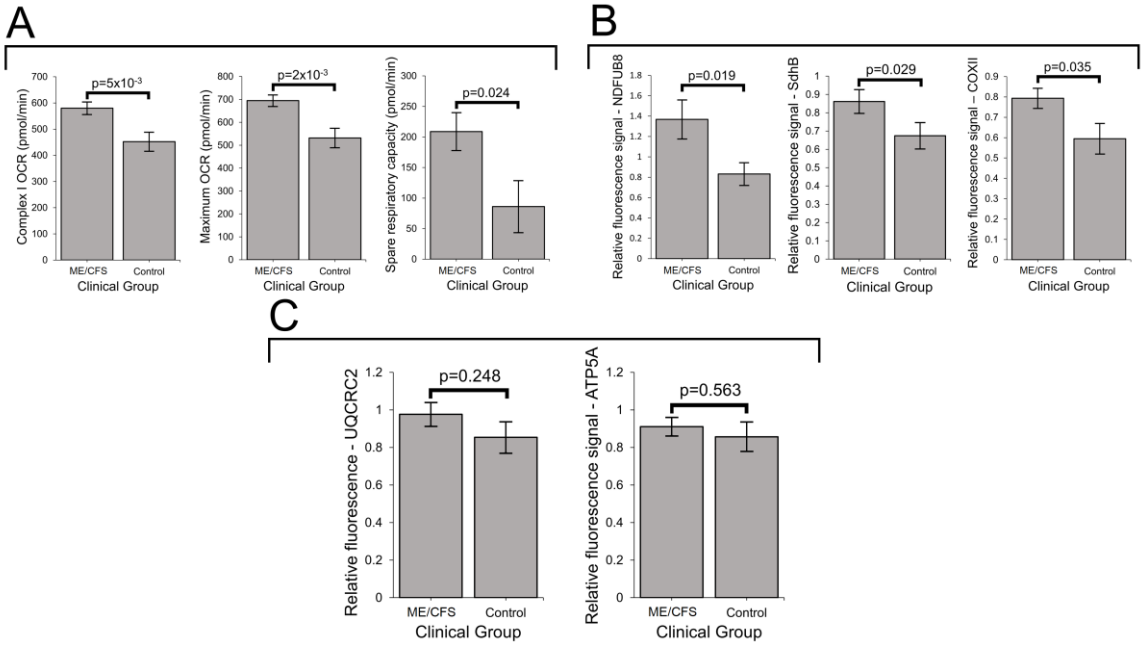

Figure 3.4: ME/CFS lymphoblasts exhibit elevated respiratory capacity and expression of oxidative phosphorylation (OXPHOS) complexes as assessed by respirometry and western blotting. Error bars are standard errors of the mean. (**A**) Complex I OCR, maximum OCR and spare respiratory capacity are elevated in ME/CFS lymphoblasts (independent t-test). The OCR was

measured in lymphoblasts from ME/CFS and control individuals by the Seahorse XFe24 Extracellular Flux Analyzer. Each ME/CFS (n = 50) and control (n = 22) cell line was assayed over four replicates in each of at least three independent experiments. (**B**) Relative expression levels of Complex I subunit NDUFB8, Complex II subunit SdhB and Complex IV subunit COXII were elevated in semiquantitative Western blots (independent t-test). Each ME/CFS (n = 48) and control (n = 17) cell line was assayed in at least three independent experiments. (**C**) Complex III subunit UQCRC2 and Complex V subunit ATP5A expression was elevated but not significantly in semiquantitative western blots (independent t-test). Each ME/CFS (n = 48) and control (n = 17) cell line was assayed in at least three independent experiments and means ±SEM were calculated (bar graphs). Western blot data is expressed in relative terms as each experiment was normalised to internal loading controls. Western blots were carried out by Oana Sanislav.

These results as a whole suggest that in ME/CFS cells the expression of the respiratory complexes is homeostatically increased to compensate for inefficient ATP synthesis. To test this hypothesis further, whole-cell proteomics analysis of 31 control and 34 patient lymphoblast cell lines was conducted. The expression of subunits of each of the 5 respiratory complexes was elevated in ME/CFS lymphoblasts in the proteomics analysis (Table 3.1).

	Number of subunits	**Number of subunits detected***	**Fraction fold change >1 in ME/CFS proteomes**	**Binomial test *p***	**Mean fold change (± standard error)**	**Single sample *t* test *p***
Complex I	44	23	17/23	0.01734	1.20±0.05	3.44×10^{-4}
Complex II	4	2	2/2	NA	1.08±0.03	NA
Complex III	10	6	6/6	0.1563	1.22±0.03	7.69×10^{-4}
Complex IV	19	10	7/10	0.1719	1.07±0.04	0.07
Complex V	22	22	18/22	2.17×10^{-3}	1.11±0.02	1.18×10^{-4}
All Complexes	99	63	50/63	1.51×10^{-6}	1.14±0.02	1.21×10^{-8}

Table 3.1: **Expression of OXPHOS complex subunits is elevated in whole cell proteomes from ME/CFS patients (n = 34) compared to healthy controls (n = 31).** Each cell line was sampled once, or twice for a subset of healthy controls arbitrarily selected to act as an internal control between experiments in the proteomics work. Fold-change refers to the mean abundance of a given protein in the ME/CFS group divided by the mean abundance in the control group. Binomial tests were employed to assess fraction upregulated with H_o set to 0.5. Single sample *t* tests were employed to assess magnitude of upregulation with H_o as mean fold change $\leq$1 and H_1 as mean fold change >1 (Western blot and respirometry results led to the *a priori* hypothesis that upregulation would be observed).

In subsets where the total number of detected proteins is small, the power of the binomial test to detect departures from expected proportions is limited. Single sample *t*-tests were also employed, instead to assess the magnitude of difference in the mean fold change from the normalised healthy control average. Although the small number of Complex II subunits did not allow for sufficient statistical power in either kind of test, the trend for Complex II is consistent with the significant increase detected by Western blotting (including the specific subunit assessed there, succinate dehydrogenase subunit B (SdhB). Together, these results show that the levels of the key mitochondrial OXPHOS proteins are elevated in ME/CFS cells, thereby confirming elevated complex expression as an explanation for the increased maximum OCR in Seahorse respirometry assays.

This data is also in agreement with Complex-specific parameters in the respirometry assays. In keeping with the elevated oxygen consumption by Complex I, 23 of the 44 Complex I subunits were detected and most exhibited increases in their levels in ME/CFS cells compared to the controls (Table 3.1), significantly more than would be expected by chance. The average expression of these Complex I subunits in ME/CFS cells was significantly higher than in the controls (1.19 fold, $p = 3.4 \times 10^{-4}$). Elevated expression of Complex V, specifically, could also be expected in an "attempt" by the cell to offset the inefficiency in respiratory ATP synthesis. Indeed, 18 of the detected Complex V subunits were upregulated, also a significantly higher fraction than would be expected by chance (Table 3.1). Average expression levels were also significantly elevated for the subunits of Complex V (1.1 fold, $p = 3.0 \times 10^{-3}$). Taking into account this ~10% higher expression of Complex V subunits, the relative efficiency of Complex V in the ME/CFS cells is even lower than measured directly by respirometry — almost 25% lower than the controls.

While this elevation in protein-level expression was confirmed in both the whole-cell proteomes and Western blots, investigation of OXPHOS complex subunit expression via whole cell transcriptomics[1] revealed largely reduced expression at the RNA level in the ME/CFS lymphoblasts (Table 3.2). Thus, significant downregulation of Complexes I, III, IV, and V was detected while Complex II subunit transcripts were elevated in their magnitude of expression ($p = 0.019$, *t* test). This suggested that the upregulation of

[1] The broader conclusions of this experiment (pertaining to other pathways) are detailed in Chapter 4.

OXPHOS complexes in ME/CFS lymphoblasts is being stimulated specifically at the translational level. The sole exception is Complex II which functions as a key rate-limiting enzyme in the TCA cycle and makes only a relatively small contribution to oxygen consumption (approx. 5% of the maximum OCR in lymphoblasts) as part of OXPHOS. The departure of its transcriptional regulation pattern from that of the other complexes suggests that regulation of Complex II expression is more tightly coupled to that of other TCA cycle enzymes (which were later found to trend upwards at the transcriptional level and are also upregulated at the translational level in Section 3.2.7). This is not unexpected given that regulation of Complex II expression has been long understood as being separate from the closely-coordinated expression and assembly of the other four OXPHOS complexes (Rutter, Winge et al. 2010).

	Number of subunits	**Number of subunits detected**	**Fraction fold change < 1 in ME/CFS**	**Fraction fold change > 1 in ME/CFS**	**Binomial test *p***	**Mean fold change (± SEM)**	**Single sample *t* test *p***
Complex I	44	39	37	2	2.84×10^{-9}	0.811± 0.03	2.63×10^{-8}
Complex II	4	4	0	4	0.125	1.116± 0.03	0.0243
Complex III	10	9	8	1	0.039	0.820± 0.03	6.31×10^{-4}
Complex IV	19	19	16	3	0.0044	0.833± 0.03	8.41×10^{-6}
Complex V	22	18	17	1	0.00015	0.797± 0.04	2.25×10^{-5}
All Complexes	99	89	78	11	1.37×10^{-13}	0.828± 0.02	$<2.2\times10^{-16}$

Table 3.2: Expression of transcripts encoding subunits of OXPHOS complexes I, III, IV, V is reduced while that of Complex II transcripts is elevated in whole cell transcriptomes from ME/CFS patients (n = 23) compared to healthy controls (n = 17). Each cell line was sampled once in an RNA sequencing transcriptomics experiment. Mean fold change in the ME/CFS group was calculated versus the control group average. Binomial tests were employed to assess fraction differentially regulated with H_o set to 0.5. Single sample *t* tests were employed to assess magnitude of differential expression with H_o being fold change = 1.

Electron flow from Complex I through Complexes III and IV is the major contributor to respiratory electron transport, the contribution from Complex II in these cells being very small (Annesley, Lay et al. 2016). Having observed that Complex V was functioning

inefficiently, contributing a smaller fraction to the basal respiration rate in ME/CFS lymphoblasts than in control cells, it was determined whether the flow of electrons from Complexes I through Complexes III, and IV was functionally normal.

In contrast with the reduced fractional contribution of Complex V to basal respiration, it was found that the fractional O_2 consumption by uncoupled electron flow from Complex I through Complexes III and IV to molecular oxygen was unchanged in the ME/CFS cells (Figure 3.5). Thus, electron transport is functionally normal in ME/CFS lymphoblasts and the defect in oxidative phosphorylation is isolated to ATP synthesis by Complex V. This can be concluded since a defective Complex I, III, or IV would result in the electron flow through these complexes contributing proportionately less to total OCR, even if compensatory upregulation of expression were to bring respiration rates back to normal or even higher than normal absolute levels. Electron transport in the ME/CFS lymphoblasts is thus functionally normal, but elevated in capacity because of elevated levels of expression of the respiratory complex proteins involved.

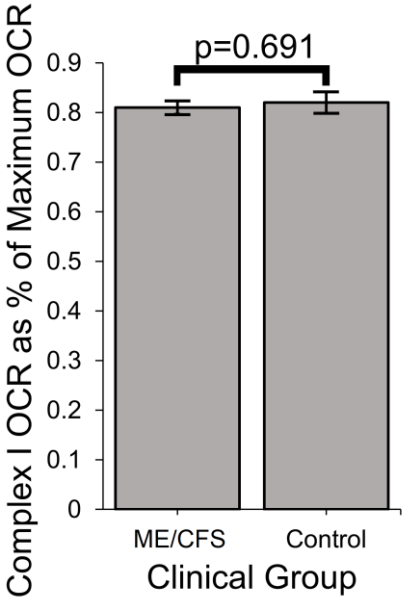

Figure 3.5: Complex I OCR as a percentage of the uncoupled maximum OCR was unchanged in ME/CFS lymphoblasts (independent t-test). The OCR was measured in lymphoblasts from ME/CFS and control individuals by the Seahorse XFe24 Extracellular Flux Analyzer. Each ME/CFS (n = 50) and control (n = 22) cell line was assayed over four replicates in at least three independent experiments and means were calculated. Error bars are standard errors of the mean.

Another indicator of abnormalities in electron transport is the level of reactive oxygen species (ROS). ROS are produced by electron "leakage" to molecular oxygen at the point

where electrons are normally passed to Complex III from either Complex I or II. ROS production can be increased either by an increased flux of electrons through the electron transport chain or by a "downstream" blockage that diverts the electron flow. The levels of intracellular ROS were therefore measured in patient and control lymphoblasts with no difference observed in the ME/CFS cells when compared with controls (Figure 3.6A). This is consistent with the insignificant changes in basal respiration rate and also suggests that the electron transport chain (ETC) is functionally normal.

A compensatory elevation of respiratory enzyme levels and uncoupled activity of mitochondrial respiratory complexes suggests that ME/CFS mitochondria should exhibit increased capacity for proton motive force (PMF)-driven transport processes in the mitochondrial membrane that support and maintain mitochondrial biogenesis or function. Most mitochondrial membrane transporters in the inner mitochondrial membrane belong to the Solute Carrier family 25 (SLC25) family. Expression levels of the majority of them were significantly upregulated in the whole cell proteomes of ME/CFS lymphoblasts, while remaining unchanged at the transcriptional level (Table 3.3). Like the OXPHOS complexes, the SLC25 transporters are thus upregulated translationally in ME/CFS cells. Since many SLC25-mediated transport processes are driven by the PMF (Ruprecht and Kunji 2020), their elevated activity should result in an increased "proton leak" (depletion of the PMF by mitochondrial transport processes other than ATP synthesis by Complex V) in ME/CFS mitochondria. As predicted, the proton leak was significantly elevated as a proportion of the basal metabolic rate (Figure 3.6B) in ME/CFS lymphoblasts when compared with controls. These results also suggest that pathways providing the mitochondria with alternative oxidisable substrates are upregulated in ME/CFS cells, consistent with the dysregulation of catabolism inferred from metabolomic studies (Armstrong, McGregor et al. 2015; Fluge, Mella et al. 2016).

Unlike the SLC25 transporters, expression levels of the TIMM, TOMM and SAMM mitochondrial protein import complexes were unchanged at the protein level, while in the whole cell transcriptomes their levels were reduced. This suggests two things - firstly that the reduced transcript levels for TIMM, TOMM and SAMM subunits must be offset by higher translation rates, in order to maintain unchanged levels of the proteins in the proteome and secondly that the mitochondrial protein import machinery is not rate-limiting for mitochondrial activity in lymphoblasts.

Group	Number detected	Number reduced fold change	Number elevated fold change	Binomial test *p*	Mean fold change (± standard error)	Single sample *t* test *p*
Proteomes (CFS n = 34, Control n = 31)						
SLC25 family	11	2/11	9/11	0.033	1.33±0.14	0.016
Protein import complex subunits	11	7/11	4/11	0.8867	1.00±0.04	0.805
Transcriptomes (CFS n = 23, Control n = 17)						
SLC25 family	40	21/40	19/40	0.875	1.011	0.628
Protein import complex subunits	25	20/25	5/25	0.004	0.884	3.29×10^{-5}

Table 3.3: Expression of mitochondrial transporters was investigated in the whole cell proteomes and transcriptomes of ME/CFS lymphoblasts compared to healthy controls. RNA sequencing transcriptomics experiment: ME/CFS n = 23, control n = 17. Mass spectrometry proteomics experiment: ME/CFS n = 34, control n = 31. Each cell line was sampled once, or twice for a subset of healthy controls arbitrarily selected to act as an internal control between experiments in the proteomics work. The levels of the SLC25 family of transporters were elevated in the proteomes but not in the transcriptomes. The levels of mitochondrial protein transporter complexes (TIMM, TOMM and SAMM) were significantly reduced in the transcriptomes but not in the proteomes. Fold-change refers to the mean abundance of a given gene product in the CFS group compared with the mean abundance in the control group. Binomial test of fraction differentially regulated with H_o set to 0.5. Single sample *t* test of magnitude of upregulation with H_o as mean fold change ≤ 1 and H_1 as mean fold change >1 in proteomics (upregulation expected *a priori* by elevated mitochondrial protein expression and elevated proton leak). Single sample *t* tests were employed to assess magnitude of differential expression in the transcriptomics with H_o being fold change = 1.

The foregoing data shows that mitochondrial respiratory capacity in ME/CFS lymphoblasts is upregulated, perhaps in response to inefficient ATP synthesis by Complex V. This is coupled with increased depletion of energy by transport processes which were hypothesised to include those that provide alternative sources of oxidisable substrate to the mitochondria. It was therefore expected that the rates of nonmitochondrial catabolic processes that provide

these substrates would also be increased. The respirometry data supports such a possible shift in metabolism as the "nonmitochondrial" OCR, an indicator of nonmitochondrial catabolic rate, was significantly elevated in ME/CFS lymphoblasts (Figure 3.6B).

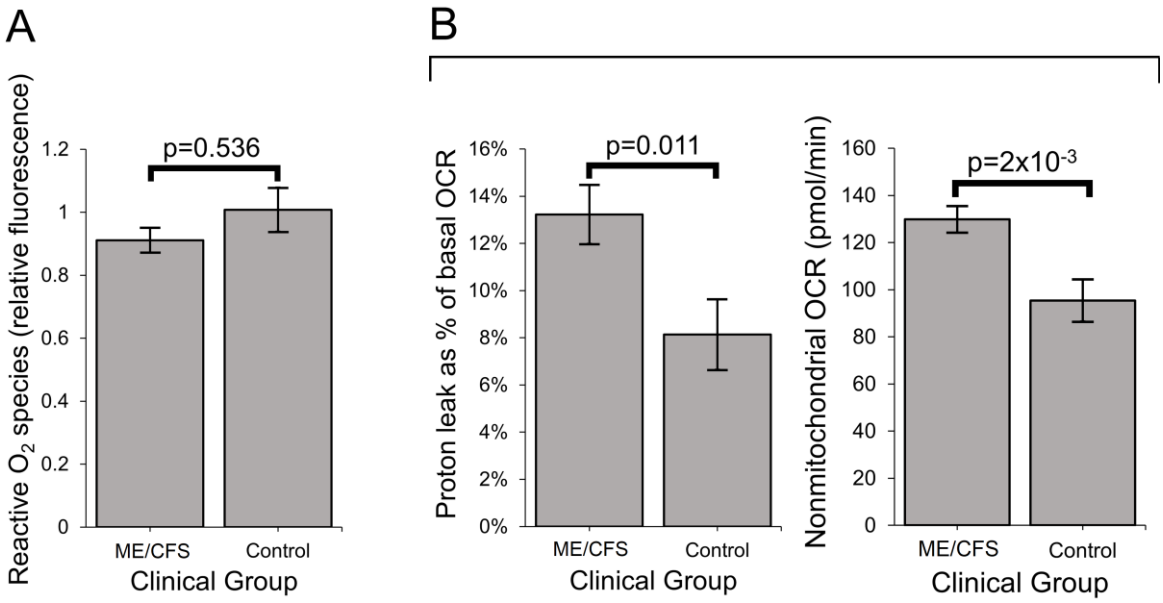

Figure 3.6: (**A**) Intracellular ROS levels (relative background-subtracted Deep Red fluorescence) are unchanged in ME/CFS lymphoblasts (independent *t*-test). Each ME/CFS (n = 49) and control (n = 22) cell line was assayed in duplicate within each of at least three independent experiments. (**B**) Proton leak as % of basal OCR and the **(C)** nonmitochondrial OCR are elevated in ME/CFS lymphoblasts (independent *t*-test). Each ME/CFS (n = 50) and control (n = 22) cell line was assayed over four replicates per experiment in at least three independent experiments.

3.2.5 Respiratory Abnormalities in ME/CFS Lymphoblasts Are Correlated with Disease Severity

In view of the foregoing functional abnormalities in ME/CFS mitochondria, the key elevated respiratory parameters were tested for correlation with disease severity (Figure 3.7) as assessed by the Richardson and Lidbury Weighted Standing Test (Richardson, Lewis et al. 2018). It was found that all were correlated with the clinical outcomes. This strengthens the proposal that the mitochondrial abnormalities observed here are clinically relevant, and also the likelihood that these observations could be fruitfully investigated as biomarkers of disease.

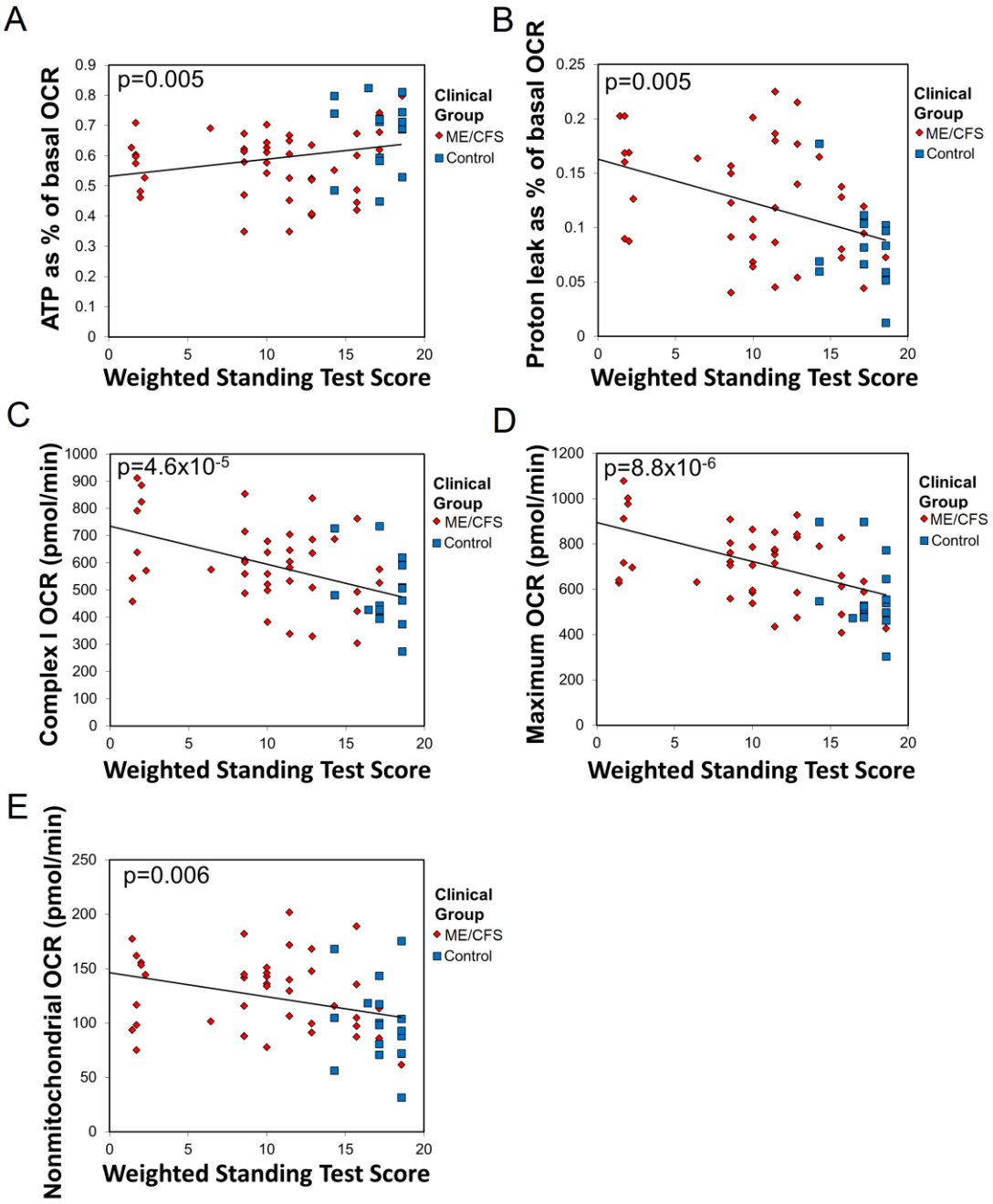

Figure 3.7: The respiratory shift in ME/CFS lymphoblasts is correlated with disease severity. (**A**) ATP synthesis as a percentage of basal respiration and (**B**) the elevated proton leak, (**C**) maximum OCR, (**D**) nonmitochondrial OCR and (**E**) Complex I OCRs correlate with Weighted Standing Test score, a measure of disease severity in which lower values indicate more severe clinical presentation (Pearson correlation with indicated significance) (ME/CFS *n* = 45, control *n* = 17). Patients whose illness was so severe as to preclude them taking the test were not included. Lines fitted by linear least squares. Outliers falling outside 95% confidence limits were excluded.

3.2.6 Mitochondrial Genome Copy Number and Mass per Cell Are Unchanged in ME/CFS Lymphoblasts, but Mitochondrial Membrane Potential Is Lowered

Mitochondrial mass as a measure refers to total inner mitochondrial membrane within the cell's dynamic network of mitochondria (Bereiter-Hahn and Voth 1994), whilst membrane potential is the charge gradient across the inner mitochondrial membrane—which constitutes part of the total PMF, driving ATP synthesis by Complex V (ATP synthase). Since the expression of mitochondrial proteins is upregulated in ME/CFS lymphoblasts, it was possible that this would be reflected in an increase in the total cellular mitochondrial content. To assess this, both the mitochondrial genome content relative to the nuclear genome, as well as the mitochondrial membrane "mass" per cell were assayed and no differences were observed between ME/CFS and control lymphoblasts (Figure 3.8A). Thus, the higher levels of OXPHOS complexes in ME/CFS cells are expressed from unchanged numbers of copies of the mitochondrial genome and accommodated in the same total amount of mitochondrial membrane per cell. This suggests that the ME/CFS mitochondria contain a higher concentration of mitochondrial respiratory proteins than the control mitochondria.

The inefficiency of ATP synthesis by Complex V means that basal respiration rates by ME/CFS lymphoblast mitochondria would also be reduced, were it not for the compensatory upregulation of their respiratory complex levels. This allows them to maintain normal ATP synthesis rates and, as observed, is accompanied by increased respiratory capacity of the electron transport chain (mostly Complex I activity), supported by an increased use of the proton gradient to drive mitochondrial membrane transport processes (the aforementioned "proton leak"). These changes could result in a reduction of the steady state mitochondrial membrane potential, because of elevated "consumption" by the "proton leak". To test the hypothesis that the $\Delta\psi_m$ was reduced in ME/CFS lymphoblasts, Mitotracker Red fluorescence was measured, whose binding to the mitochondrial membrane is $\Delta\psi_m$-dependent. This was normalised to the mitochondrial membrane "mass" (measured by MitoTracker® Green fluorescence) and an internal control cell line to determine the relative $\Delta\psi_m$. It was found that the Mitotracker Red fluorescence

and the mitochondrial membrane potential ($\Delta\psi_m$) were reduced (p = 0.02) in ME/CFS lymphoblasts (Figure 3.8B). Similar findings were recently reported from $CD4^+$ and $CD8^+$ T-cells taken from ME/CFS patients (Mandarano, Maya et al. 2019).

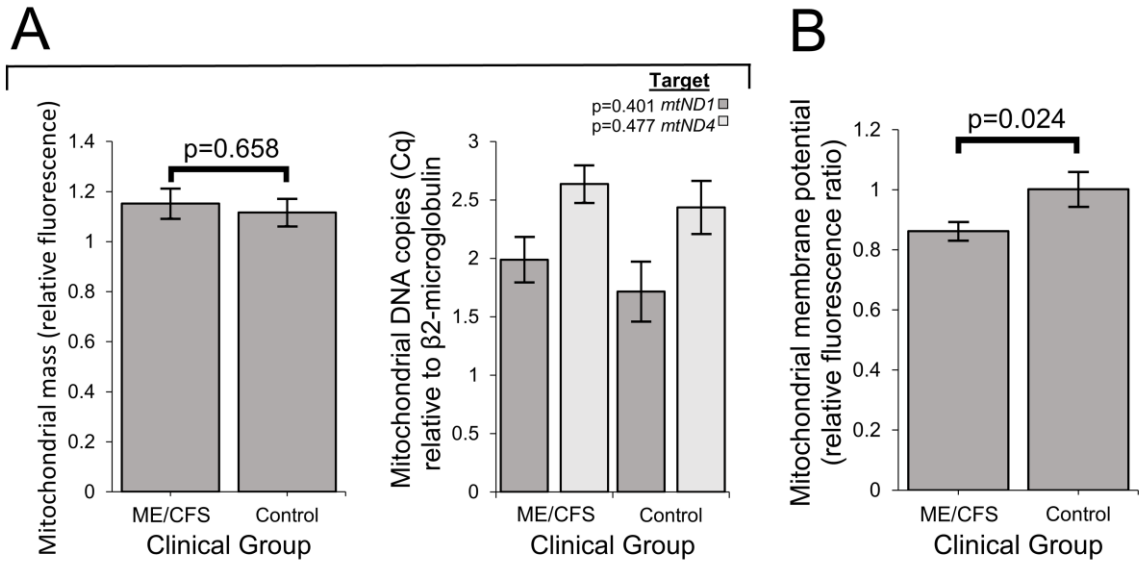

Figure 3.8: Mitochondrial genome copy number and mass per cell are unchanged in ME/CFS lymphoblasts, but mitochondrial membrane potential is lowered. Error bars represent standard errors of the mean. (**A**) Mitochondrial mass (background-subtracted MitoTracker® Green fluorescence normalised to internal control cell line C105) and genome copy number (qPCR of two mitochondrial genes, mtND1 and mtND4, relative to nuclear β-microglobulin gene) are unchanged in ME/CFS lymphoblasts (independent *t*-test). Each ME/CFS (*n* = 50) and control cell line (*n* = 22) was assayed in duplicate within each of at least three independent experiments. (**B**) Mitochondrial membrane potential is significantly reduced in ME/CFS lymphoblasts (independent *t*-test). The relative mitochondrial membrane potential ($\Delta\psi_m$) was measured in lymphoblasts from ME/CFS and control individuals (ratio of MitoTracker® Red CMXRos ($\Delta\psi$m-dependent) to MitoTracker® Green (mitochondrial mass-dependent) fluorescence, normalised to internal control cell line C105). Each ME/CFS (*n* = 50) and control (*n* = 22) cell line was assayed in duplicate within each of at least three independent experiments.

3.2.7 Levels of Enzymes Involved in the TCA Cycle Are Elevated in ME/CFS Lymphoblasts

The elevated respiratory capacity and expression of nutrient transporters indicates that mitochondrial pathways providing OXPHOS with oxidisable substrates may be similarly dysregulated. As previously mentioned, metabolomic studies by others together suggest

dysregulated provision of pyruvate-derived acetyl-CoA to the TCA cycle itself (Armstrong, McGregor et al. 2015; Fluge, Mella et al. 2016; Yamano, Sugimoto et al. 2016). As a major provider of OXPHOS substrates and as a mitochondrial convergence point for many related metabolic pathways, the TCA cycle was therefore an important candidate to examine. Expression of TCA cycle enzymes was examined in both the whole-cell proteomes and transcriptomes.

The results showed that the expression of TCA cycle enzymes was elevated in the proteomes of ME/CFS lymphoblasts while unchanged in the transcriptomes (Table 3.4). 18 of 19 detected proteins involved in the TCA cycle were more abundant in the ME/CFS proteomes (binomial test, $p = 3.8 \times 10^{-5}$). The mean expression level of TCA cycle proteins in ME/CFS lymphoblasts was 17 $\pm$ 4% higher than in the control cells (*t* test, $p = 1.0 \times 10^{-4}$).

Dataset	Number detected	Number with reduced levels	Number with elevated levels	Binomial test *p* value	Mean fold change (± Std. error)	Single sample *t* test *p* value
TCA Cycle enzymes (proteomes)	19	1	18	3.82×10^{-5}	1.17±0.04	1.03×10^{-4}
TCA Cycle transcripts	21	7	14	0.189	1.03±0.02	0.171

Table 3.4: The expression level of TCA cycle enzymes is elevated in ME/CFS lymphoblasts proteomes but unchanged in the transcriptomes. RNA sequencing transcriptomics experiment: ME/CFS n = 23, control n = 17. Mass spectrometry proteomics experiment: ME/CFS n = 34, control n = 31. Each cell line was sampled once, or twice for a subset of healthy controls arbitrarily selected to act as an internal control between experiments in the proteomics work. Error bars represent standard error of the mean. ME/CFS n = 34, control n = 31. Each cell line was sampled once, or twice for a subset of healthy controls arbitrarily selected to act as an internal control between experiments in the mass spectrometry proteomics work. 19 TCA cycle enzymes were detected within the whole cell proteomes of ME/CFS and control lymphoblasts. Fold-change refers to the mean abundance of a given protein in the ME/CFS group divided by the mean abundance in the control group. The fraction of detected enzymes that were upregulated (binomial test with H_o set to 0.5) and the average extent of the upregulation (single sample *t* test with H_o $m \leq 1$ and H_1 $m > 1$) were statistically significant.

Elevated TCA cycle enzyme expression taken together with the elevated respiratory capacity suggests that ME/CFS lymphoblasts have an increased ability to utilise TCA cycle outputs to drive oxidative phosphorylation at rates faster than would otherwise have been the case. This could reflect part of the compensatory mechanism working to offset the respiratory ATP synthesis inefficiency in ME/CFS lymphoblasts. It may also suggest upregulation of metabolic pathways providing substrate to the TCA cycle (and thereby to OXPHOS), a proposal strengthened by the elevated nonmitochondrial OCR, elevated proton leak and elevated expression of SLC25 family transporters. This would imply a broad shift in the cell's metabolism, which is likely to be driven by dysregulation of the signalling pathways which sense and regulate cellular energy supply.

3.2.8 TORC1 Is Chronically Hyperactivated in ME/CFS Lymphoblasts

Any compensatory action to bring ATP levels back to normal in ME/CFS lymphoblasts despite Complex V's inefficiency is likely to be driven by the signalling networks that sense and homeostatically respond to diverse cellular stresses (Zong, Ren et al. 2002; Reznick and Shulman 2006; Carling, Mayer et al. 2011; Hardie 2011; Hindupur, Gonzalez et al. 2015; Dalle Pezze, Ruf et al. 2016). A central element in these pathways, interconnected with the others, is the protein kinase, TORC1 (Target of Rapamycin Complex I), which coordinates the translational upregulation of major functional groups of proteins, including nuclear-encoded mitochondrial proteins. I therefore measured TORC1 activity in ME/CFS and control lymphoblasts by assaying the phosphorylation state of one of its key substrates, 4E-BP1 (eukaryotic translation initiation factor 4E-Binding Protein 1) (Ma and Blenis 2009). 4E-BPs are phosphorylated by TORC1, whose catalytic subunit is mTOR (mechanistic Target of Rapamycin). Together with S6 kinase (S6K), 4E-BP1 mediates the roles of TORC1 in regulating translation in the cytosol of mRNAs encoding major functional groups of proteins (Dowling, Topisirovic et al. 2010; Hsieh, Costa et al. 2010; She, Halilovic et al. 2010). As one of the key substrates of TORC1 involved in regulating protein synthesis, 4E-BP1 phosphorylation is often used as a marker of TORC1 activity (Qin, Jiang et al. 2016).

The results showed that 4E-BP1 phosphorylation levels were significantly elevated in ME/CFS lymphoblasts and were accompanied by a correspondingly increased response to the mTOR inhibitor, Torin2 (Figure 3.9A). Using subsequently obtained proteomics data, the expression of proteins selected using the Gene Ontology (GO) term TORC1 signal

transduction was significantly upregulated in magnitude (*t* test) (Figure 3.9B). Of the 4 proteins involved, all 4 were upregulated. With such a small sample, the binomial test has insufficient power to reach significance at 0.05 – even this most extreme of all possible results has a probability of occurrence of 0.065 (Figure 3.9B). Given its role in translational upregulation of nuclear-encoded mitochondrial proteins, the steady-state elevation of TORC1 activity and signalling pathway expression provides a particularly likely explanation of the upregulated translation of OXPHOS complexes (Tables 3.1 and 3.2) and other mitochondrial proteins.

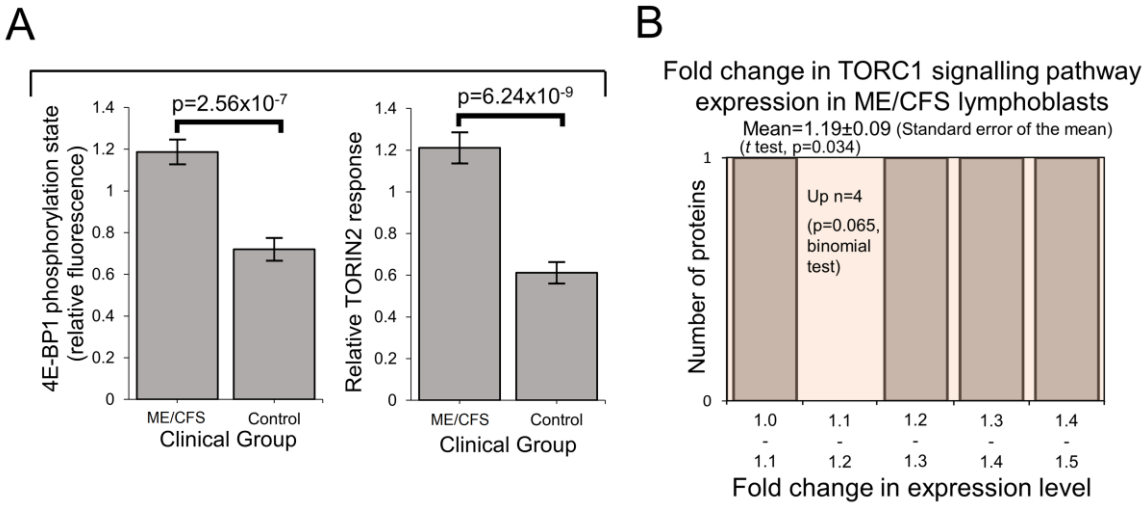

Figure 3.9: TORC1 (Target of Rapamycin Complex I) is chronically hyperactivated in ME/CFS lymphoblasts. Error bars represent standard errors of the mean. (**A**) TORC1 activity and response to Torin2 inhibition is elevated in ME/CFS lymphoblasts (independent t-test). Each ME/CFS (n = 45) and control (n = 22) cell line was assayed over at least three independent experiments. Data is expressed in relative terms as each experiment is normalised to an internal control cell line (C105). (**B**) Four proteins involved in TORC1 signal transduction were detected within the whole cell proteomes of ME/CFS (n = 34) and control (n = 31) lymphoblasts. Each cell line was sampled once, or twice for a subset of healthy controls arbitrarily selected to act as an internal control between experiments in the mass spectrometry proteomics work. Fold-change refers to the mean abundance of a given protein in the CFS group divided by the mean abundance in the control group. The frequency of proteins that were upregulated (4/4) was not significant due to the small number of detected proteins (binomial test with H_o set to 0.5) but the average magnitude of the upregulation (single sample *t* test with H_o $m \leq 1$ and H_1 $m > 1$) was statistically significant.

3.3 Discussion

3.3.1 Previous Studies of Mitochondrial Respiratory Function in ME/CFS

Previous steady state measurements and metabolic flux measurements of mitochondrial respiratory function in ME/CFS lymphocytes have suggested that in ME/CFS cells there is either a generalised reduction (Myhill, Booth et al. 2009; Booth, Myhill et al. 2012; Tomas, Brown et al. 2017) or little change (Mandarano, Maya et al. 2019; Tomas, Lodge et al. 2019) in mitochondrial activity and respiratory capacity. However, functionally normal OXPHOS Complex I to IV activity has also been reported in ME/CFS lymphocytes (Lawson, Hsieh et al. 2016; Tomas, Brown et al. 2019), while the expression of mitochondrial proteins is upregulated in patient saliva, platelets and lymphocytes (Kaushik, Fear et al. 2005; Vernon, Whistler et al. 2006; Ciregia, Kollipara et al. 2016). Elevated nonmitochondrial ATP production has also been reported in ME/CFS lymphocytes (Lawson, Hsieh et al. 2016).

In the work presented in this chapter, these inconsistencies have been resolved by revisiting the issue of mitochondrial function and capacity in immortalised lymphocytes (lymphoblastoid cell lines or lymphoblasts). Although *ex vivo* lymphocyte populations are well suited for rapid characterisation of relatively stable molecular features, such as the patterns of cell surface antigens they express, they may be less well suited to studying rapidly labile processes such as metabolism, mitochondrial function or intracellular signalling activities. As was shown here, unactivated, *ex vivo* lymphocytes are metabolically quiescent and dying (Section 3.2.1). A difference between patient and control groups in the depth of this quiescence and/or the extent of cell death may thus explain the previously reported reduction in mitochondrial activities in ME/CFS lymphocytes.

3.3.2 Elevated PBMC Death and the Utility of Lymphoblasts

The results in Section 3.2.1 showed that not only were PBMCs quiescent, but the fraction of dead cells after 1–3 days incubation in culture medium was dramatically greater for ME/CFS lymphocytes than for control lymphocytes. It is likely that in some previous studies, the ME/CFS lymphocytes assayed for mitochondrial activity included a higher proportion of dead cells than did the controls. Tomas et al. (2017) found no significant difference in the viability of fresh and frozen PBMCs and no difference between ME/CFS

and control samples (Tomas, Brown et al. 2017), a result that accords with the regression analysis of the death rates of PBMCs in culture (Figure 3.1). However, these authors followed the common procedure in their Seahorse assays of incubating the cells overnight *in situ* in the assay plates before the respirometry measurements were done. Although they did not detect significant differences between frozen and fresh PBMCs in the Trypan Blue staining *before* overnight incubation and assay, they did observe consistently significant reductions in respiration of frozen compared to fresh cells, again *after* overnight incubation in assay medium. The results shown in Figure 3.1 suggest that by this time there may have been a significant fraction of dead cells both in their control and ME/CFS samples and that this fraction may have been higher in the ME/CFS samples. The greater mortality rates for ME/CFS lymphocytes are not surprising given that pharmacological inhibition of mitochondrial respiration, including Complex V impairment, has long been known to result in apoptotic cell death in *ex vivo* lymphoid cells (Wolvetang, Johnson et al. 1994).

Another recent study examined mitochondrial respiratory function in resting and stimulated $CD4^+$ and $CD8^+$ T-cells from ME/CFS subjects and controls (Mandarano, Maya et al. 2019). The only significant differences found were small reductions in the ME/CFS $CD8^+$ lymphocytes in the proton leak in resting and ATP synthesis in stimulated cells. Surprisingly however, the overnight stimulation (with anti-CD3/anti-CD28 beads plus IL2) made almost no difference to mitochondrial respiratory function in these cells. This suggests that under the conditions used, the mitochondria in these cells were still quiescent after the overnight activation stimulus.

By contrast, the lymphoblastoid cell lines (LCLs or lymphoblasts) used in this work are metabolically active lymphoid cells that may better represent activated lymphocytes, which drive inflammation *in vivo* (Ransohoff, Schafer et al. 2015). The use of cultured lymphoblasts in this way as models not only of metabolically active lymphoid but other cell types, both in health and disease, has been reviewed in detail previously (Sie, Loong et al. 2009; Hussain and Mulherkar 2012). Because the viral genome exists in multiple copies as a circular episome in the latent state in infected cells, it does not disrupt the genome, but affects gene expression patterns in favour of proliferation, as does B cell activation by other means. Lymphoblasts have thus been used both in genetic and genomic studies, including the well-known 1000 Genomes Project (Genomes Project, Auton et al. 2015). They have also been used, as here, in functional studies of diverse, complex diseases, including autism,

schizophrenia, Alzheimer's, and Parkinson's disease (Sie, Loong et al. 2009; Annesley, Lay et al. 2016). Whereas PBMCs, used *ex vivo* in some other ME/CFS studies, are a complex mixture of cell types, EBV-mediated immortalisation and culture selects B cells from this population, because the EBV receptors are expressed in B cells. It has been reported previously that the cell type composition of PBMCs from ME/CFS patients is different from healthy controls (Cortes Rivera, Mastronardi et al. 2019) and such differences could also contribute to observed functional differences in the mixed populations in *ex vivo* PBMCs. The lymphoblast cell lines used here were not clonal, but as a result of the selective nature of EBV infection, they can be expected to be more homogeneous in cell type than the PBMCs from which they were selected.

As EBV-infected B cells begin to proliferate, around 250 genes become hypomethylated (Hernando, Shannon-Lowe et al. 2013). Many of these genes already exhibit low levels of methylation and high levels of expression in resting B cells, while many others exhibit hypomethylation and overexpression during B cell proliferation. They fall into 6 major GO categories—immune response, homophilic cell adhesion, humoral immune response, B cell receptor signalling pathway, inflammatory response and chemotaxis genes. In the whole cell proteomes of lymphoblasts from both healthy and ME/CFS individuals, it was observed that the expression of many B-cell specific proteins was not significantly different in ME/CFS and control cell lines. The overall pattern of expression is consistent with lymphoblasts having had their normal B cell transcription and proliferation program activated by the virus (Hernando, Shannon-Lowe et al. 2013). Importantly, this phenotype is stable through up to 180 cell doublings, unlike other *in vitro* methods of B cell activation (such as antigen stimulation) which induce similar changes in gene expression that increase and decline over only a few days and culminate in cell death.

Like primary cell cultures of other cell types such as myoblasts (which die after a few doublings) or fibroblasts (which progressively enter senescence between *ca* 30-60 doublings), lymphoblasts eventually die off after approximately 160–180 doublings (Sie, Loong et al. 2009). Thereafter, the original lymphoblast population may be replaced by cells bearing mutational changes in the genome that support ongoing proliferation. At this point, the cells may no longer be representative of activated forms of the B lymphocytes from which they were derived. In the work described here, none of the lymphoblast cultures

were allowed to proceed through more than a handful of cell doublings before storage or use in experiments.

During their more limited life spans, primary cell lines like myoblasts and fibroblasts undergo a progressive process called replicative senescence as part of which their relevant phenotypic and molecular features may change (Bigot, Jacquemin et al. 2008). Fibroblast and myoblast gene expression programs are also tightly regulated by contact inhibition so that their phenotypes can be dramatically affected by their density in culture (Huttenlocher, Lakonishok et al. 1998). Furthermore, their life span and phenotypes may be affected by the age of the donor from whose tissues they were derived. These various sources of phenotypic differences can be disentangled but this requires care, appropriate controls and may need larger samples or more experiments to account for the additional variables. Provided long periods of culture approaching their replicative life span limits are avoided, lymphoblasts do not present these problems. They are not contact-inhibited and their metabolic phenotypes are stable in culture and storage, depending only, as was shown here for ME/CFS and previously for Parkinson's disease (Annesley, Lay et al. 2016), on the disease state, not the gender or age of the person from whom they were isolated. Despite these advantages, it will be important in future work to determine whether the mitochondrial and cell signalling anomalies in ME/CFS lymphoblasts are also observed in other cell types.

3.3.3 A Complex V Inefficiency

The results of this work show that ME/CFS lymphoblasts exhibit an isolated Complex V inefficiency that is accompanied by upregulation of mitochondrial protein expression, including mitochondrial respiratory complexes and enzymes involved in the TCA cycle. These findings confirm that these ME/CFS cells do indeed exhibit a mitochondrial deficiency in ATP generation, but reveal that, in lymphoblasts at least, this specifically involves Complex V rather than a generalised reduction in all mitochondrial functions. This profile of mitochondrial dysfunction in intact ME/CFS lymphoblasts is distinct from the mitochondrial hyperactivity which other members of our group previously found in Parkinson's disease lymphoblasts (Annesley, Lay et al. 2016), so cannot be a simple reflection of neuroinflammatory processes believed to occur in both diseases.

What might cause such a mitochondrial Complex V inefficiency? Three possibilities are: a mutation affecting one of the Complex V subunits or assembly proteins, an elevation of the relative use of the PMF for other purposes ("proton leak") making less available for ATP synthesis, or a dysregulation of Complex V itself. A mutational defect in Complex V seems unlikely in view of the failure of previous investigations to uncover any single nucleotide polymorphisms in Complex V genes that associate with the disease state (Billing-Ross, Germain et al. 2016; Schlauch, Khaiboullina et al. 2016). The second possibility, that Complex V is inefficient in these ME/CFS cells because of the elevated use of the PMF by other processes, is suggested by the elevated proton leak observed in ME/CFS lymphoblasts (Figure 3.6B). However, the ME/CFS mitochondria have excess unused respiratory capacity and respiratory complex levels (Section 3.2.4). These would indicate that the electron transport capacity in ME/CFS lymphoblasts is more than sufficient to allow Complex V to operate at normal efficiency. Dysregulatory inhibition of Complex V is the third possibility. It is known that mitochondrial ATP synthase activity can be regulated by a variety of proteins, small molecules and signalling pathways, some of them by acting through Complex V's own inhibitory subunit AIF1 (Campanella, Seraphim et al. 2009; Garcia-Bermudez and Cuezva 2016). These possible causes for Complex V inefficiency in ME/CFS lymphoblast mitochondria should be investigated in future work.

3.3.4 EBV-Mediated Immortalisation

It was possible that the dysregulation of Complex V and mitochondrial function in ME/CFS lymphoblasts arises because they respond differently to EBV infection than do control lymphoblasts. However the result in Section 3.2.2 showed that the EBV genome copy number did not differ between the participant groups and, in any case, had no effect on any of my assays. Furthermore, the elevated expression of OXPHOS complex subunits (also prominently Complexes 1 and 5) and proteins in substrate-providing pathways (such as the TCA cycle) was later replicated in unimmortalised lymphocyte proteomes, by Sweetman *et al*. (Sweetman, Kleffmann et al. 2020). This confirms that elevated respiratory capacity and upregulation of substrate-providing mitochondrial pathways exhibited by ME/CFS lymphoblasts occurs independently of immortalisation. Nevertheless, it is possible that in ME/CFS lymphoblasts, EBV reactivates more readily to enter the lytic cycle and this in turn affects aspects of mitochondrial function. This idea, if true, would raise the possibility that EBV may also reactivate more readily in infected ME/CFS B-cells *in vivo*. Despite the

appeal of this hypothesis, the profile of mitochondrial changes observed here is not consistent with the reported effects of EBV on mitochondria in the lytic cycle. These include *decreases* in ROS production, mitochondrial membrane potential, expression of mitochondrial proteins, and mitochondrial biogenesis (Anand and Tikoo 2013; Gilardini Montani, Santarelli et al. 2019). Although decreased mitochondrial membrane potential was observed in ME/CFS lymphoblasts (Figure 3.8B), there was no change in ROS levels, no change in mitochondrial mass or genome copy number and an elevation, not a reduction, in expression of mitochondrial proteins. There does not appear to be any evidence that EBV causes an isolated inefficiency in Complex V coupled with an elevated proton leak and an increase in maximum OCR and Complex I activity. Instead of EBV reactivation causing mitochondrial dysfunction in ME/CFS lymphoblasts, it is also possible that the reverse occurs—namely that mitochondrial dysfunction causes the virus to be more readily reactivated. This possibility is suggested by the fact that EBV is reactivated by cellular stress and could potentially contribute to the post-exertional malaise that characterises ME/CFS. The interactions between EBV and mitochondrial function in B-cells and lymphoblasts from ME/CFS patients are clearly worth pursuing in future work.

3.3.5 Elevated Respiratory Capacity in ME/CFS Lymphoblasts

The elevated maximum respiratory capacity, mitochondrial Complex I activity, and proton leak seen in ME/CFS lymphoblasts are consistent with the higher mitochondrial protein expression also observed in these cells, as assayed using both semiquantitative Western blots and whole cell proteomics. Consistent with this, it was reported previously that the expression of genes encoding mitochondrial proteins is upregulated in ME/CFS saliva, lymphocytes, and platelets (Kaushik, Fear et al. 2005; Vernon, Whistler et al. 2006; Ciregia, Kollipara et al. 2016). Together the results shown here suggest a model in which the Complex V defect is likely a proximal activator of compensatory upregulation of expression of mitochondrial proteins.

The increased expression of diverse mitochondrial proteins in ME/CFS observed both here and others (Kaushik, Fear et al. 2005; Ciregia, Kollipara et al. 2016; Lawson, Hsieh et al. 2016; Sweetman, Kleffmann et al. 2020) suggests the possibility that mitochondrial biogenesis more broadly is activated in these cells. However, it was found that the mitochondrial membrane "mass" per cell (Mitotracker Green fluorescence) and the copy number of the mitochondrial genome relative to the nuclear genome were unchanged in the

ME/CFS lymphoblasts (Figure 3.8A). Accordingly, the mitochondria in these cells appear to have higher concentrations of mitochondrial respiratory proteins and catabolic enzymes.

3.3.6 TORC1 Hyperactivity and Regulation of Mitochondrial Protein Expression

One of the key upstream regulators of mitochondrial protein expression is TOR Complex I (TORC1 whose catalytic subunit is mTOR, the mechanistic Target of Rapamycin). It was found that TORC1 activity is elevated in ME/CFS lymphoblasts (Figure 3.9A). The expression of mitochondrial enzymes involved in electron transport is known to be upregulated by TORC1 via selective activation of translation via inhibitory phosphorylation of the TORC1 target 4E-BP1 (Morita, Gravel et al. 2015). In addition to its actions on the translation of nuclear-encoded mitochondrial proteins, TORC1 upregulates the expression of transcription factors PGC-1α (transcriptionally via Yin Yang 1) and TFAM (translationally), which respectively induce the transcription of nuclear and mitochondrial genes encoding mitochondrial proteins (Cunningham, Rodgers et al. 2007). Most notable amongst the mitochondrial proteins whose translation is upregulated by TORC1 are nuclear-encoded subunits of Complexes I and V (Morita, Gravel et al. 2015), the two respiratory complexes whose expression were found to be the most evidently elevated in the whole cell proteomes of ME/CFS lymphoblasts.

While TORC1 activity was elevated, it is not the only cellular stress sensing protein that regulates expression of proteins involved in cellular metabolism and mitochondrial function. It acts in concert with AMPK as part of a complex stress-sensing network (Zong, Ren et al. 2002; Dalle Pezze, Ruf et al. 2016). AMPK is activated by a variety of cellular stressors including ATP insufficiency, elevated cytosolic Ca^{2+} concentrations and oxidative stress (Hawley, Pan et al. 2005; Woods, Dickerson et al. 2005). As the primary ATP sensor (Hardie and Carling 1997), AMPK is implicated in mitochondrial disease (Bokko, Francione et al. 2007), and activates a variety of catabolic pathways that provide alternative oxidisable substrates to the mitochondria—including amino acids or fatty acids (Hardie and Pan 2002). In ME/CFS lymphoblasts, with their chronically inefficient ATP synthesis and elevated nonmitochondrial OCR, it is therefore possible that AMPK could be chronically activated and participate in the upregulation of mitochondrial respiratory capacity that was observed.

AMPK activity in muscle cells cultured from CFS patients (Fukuda criteria) is reportedly unresponsive to electrical pulse-induced contraction in vitro, but not because AMPK itself is unresponsive to activation by either a mitochondrial Complex I inhibitor (metformin) or a direct AMPK activator (compound 991) (Brown, Jones et al. 2015; Brown, Dibnah et al. 2018). The authors suggested that the unresponsiveness of CFS cells to additional energy demands thus seems to lie elsewhere. One possibility is the chronically elevated TORC1 activity, since TORC1 is an inhibitor of upstream pathways that activate AMPK. In any case, this highlights the value of measuring the activities of AMPK and TORC1 in parallel in ME/CFS cells, which has not yet been undertaken by others.

3.4 Conclusions

3.4.1 A Metabolic Switch

ME/CFS lymphoblasts exhibit inefficient ATP synthesis by Complex V that, among other abnormalities, is accompanied by upregulated respiratory capacity, TCA cycle enzyme and mitochondrial nutrient transporter expression, as well as elevated nonmitochondrial catabolic rate. This suggests that ME/CFS lymphoblasts abnormally utilise catabolic pathways that provide oxidisable substrates to the mitochondria to assist with satisfying resting energy demands moreso than lymphoblasts from healthy controls. These observations are in agreeance with the previous metabolomic studies suggesting a similar switch in metabolism (Armstrong, McGregor et al. 2015; Fluge, Mella et al. 2016). This prompted me to explore further in the next chapter how ME/CFS lymphoblasts may shift their metabolism to meet their energy demands in spite of an inefficient Complex V. Alongside my investigation of this metabolic shift, I also investigated the activity of AMPK in ME/CFS lymphoblasts in the following chapter given its potential involvement.

3.4.2 A "Cellular Chronic Fatigue"

A compensatory elevation of respiratory capacity and expected shift in metabolism would appear to be sufficient to meet the energy needs of ME/CFS lymphoblasts, given that steady state ATP levels and absolute ATP synthesis rates were both close to normal in these cells. However, these changes may leave the cells less able to respond to further acute increases in ATP demand despite the elevated respiratory capacity, since the signalling and metabolic pathways involved are already chronically upregulated. If this "cellular chronic fatigue" is

present in other cell types, it may contribute to the unexplained fatigue experienced by ME/CFS patients, as suggested by the fact that all of the respiratory abnormalities observed were correlated with the severity of patient symptoms measured by the Weighted Standing Time. These correlations also suggest that the mitochondrial abnormalities found are of clinical relevance to the underlying cytopathological mechanisms and have the potential to be investigated as biomarkers of disease. Accordingly, the value of these abnormalities as biomarkers is revisited in-depth in Chapter 5.

4.0 Dysregulation of Pathways Providing Oxidisable Substrate to the Mitochondria

4.1 Introduction

4.1.1 Supply of Oxidisable Substrate to the Mitochondria in ME/CFS

In the previous chapter, inefficient ATP synthesis by Complex V in ME/CFS lymphoblasts was observed. OXPHOS is the primary source of cellular ATP and is driven by the flow of electrons through Complexes I-IV, which mediates the pumping of protons out into the mitochondrial intermembrane space. This generates the electrochemical gradient utilised by Complex V to phosphorylate ADP to ATP. The electrons necessary for this process are deposited into the electron transport chain by the reduced intermediates, NADH and $FADH_2$. The provision of these electron donors to the OXPHOS complexes is therefore critical for ATP synthesis by aerobic respiration. The principal mitochondrial source of reduced NADH and $FADH_2$ is the TCA cycle, which is supplied with metabolic intermediates at multiple entry points by a variety of nutrient metabolism pathways. The TCA cycle is thus a mitochondrial junction point for the participation of diverse fuel sources in respiration, including carbohydrates, fatty acids and amino acids (Figure 4.1).

In accordance with suspicions of insufficient cellular energy supply, the study of metabolism and pathways supplying the mitochondria with substrate in ME/CFS has increased in the last decade. Through the use of techniques such as nuclear magnetic resonance (NMR) or mass spectroscopy, quantitative snapshots of the metabolites present within a sample (commonly blood or urine) can be obtained. The relative levels of metabolites in patients versus controls can be subsequently used to infer which metabolic pathways may be upregulated, downregulated or bypassed. Metabolomic studies have been adopted by an increasing number of research groups in the ME/CFS field. Much of this work has discussed potential dysregulation of glycolysis in ME/CFS. Glycolysis mediates the multi-step conversion of glucose to pyruvate, which can be converted by pyruvate dehydrogenase (PDH) to acetyl-CoA, a major TCA cycle substrate.

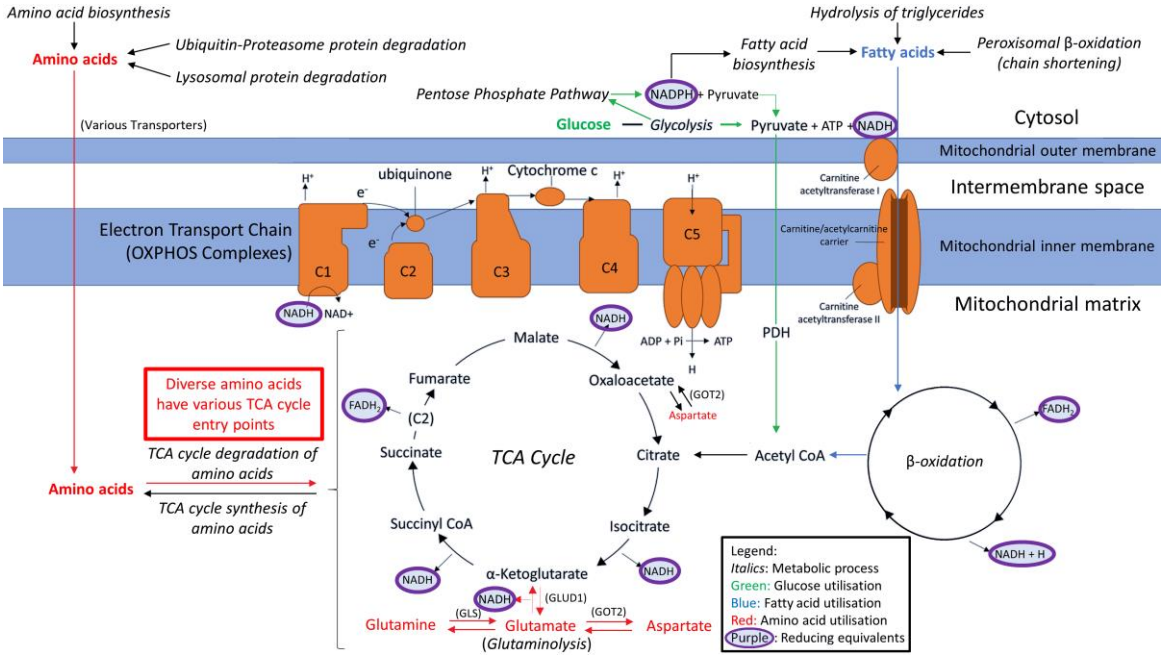

Figure 4.1: Simplified depiction of oxidisable substrate provision and usage by the mitochondria. The generalised "flow" of substrate molecules derived from glucose, fatty acids or amino acids is represented by arrows colour-coded green, blue and red, respectively. Reducing equivalents are denoted by purple outlines. Processes are italicised. Glucose may be catabolised by glycolysis in order to provision the mitochondria with pyruvate, converted by pyruvate dehydrogenase (PDH) to acetyl-CoA for entry into the TCA cycle. Fatty acid β-oxidation also provides acetyl-CoA for the TCA cycle, instead by the catabolism of lipids rather than carbohydrates. The means by which amino acids may be similarly utilised are diverse and are described as appropriate throughout the text, however highlighted glutamine usage has been highlighted in this figure due to its importance. Glutamine may be converted to glutamate by glutaminase. Glutamate may be converted to α-KG by glutamate dehydrogenase (GLUD1) for entry into the TCA cycle, or to aspartate by mitochondrial aspartate aminotransferase (GOT2) which is utilised in cellular redox balancing and TCA cycle anaplerosis, thereby providing both reducing equivalents for OXPHOS and intermediates for the TCA cycle. Reducing equivalents resultant from these various processes can deposit electrons into the electron transport chain to facilitate generation of the proton-motive force which drives ATP synthesis.

Armstrong *et al.* utilised ^{1}H-NMR to assess the levels of metabolites in the serum and urine of ME/CFS patients compared to healthy controls (Armstrong, McGregor et al. 2012; Armstrong, McGregor et al. 2015). Their results suggested an inhibition of glycolysis, which is consistent with a report by others using ME/CFS plasma, indicating that utilisation

of glycolytic pyruvate by the TCA cycle is reduced (Yamano, Sugimoto et al. 2016). However, others using serum have proposed that impaired provision of glucose-derived acetyl-CoA towards the TCA cycle is instead caused by an impairment of PDH function downstream of glycolysis, rather than an impairment of glycolysis itself (Fluge, Mella et al. 2016). Other studies have instead employed Seahorse respirometry to investigate real-time parameters of respiration and glycolysis in live cells from ME/CFS patients compared with healthy controls. While the rate of glycolysis was found to be reduced in ME/CFS $CD4^+$ and $CD8^+$ T-cells (Mandarano, Maya et al. 2019), no change was observed in ME/CFS PBMCs or skeletal muscle cells (Tomas, Brown et al. 2017; Tomas, Elson et al. 2020). Overall, the role of glycolysis in ME/CFS is unclear and would benefit from continued investigation.

In view of the inconsistent evidence for a specific glycolytic defect, the consideration of other processes involved in carbohydrate utilisation is also warranted. Others have reported reductions in the levels of 5/7 subgroups of metabolites involved in carbohydrate metabolism (including the disaccharide sucrose) in ME/CFS plasma samples versus those of healthy controls (Germain, Barupal et al. 2020). A reduction in the plasma levels of disaccharides in the energy-deficient context of ME/CFS could reflect broadly increased carbohydrate catabolism to satisfy elevated cellular glucose usage. If the rate of glycolysis itself was unaffected or impaired, glucose could instead be depleted by increased usage of the pentose phosphate pathway (PPP). The PPP branches from glycolysis by the irreversible dehydrogenation of glucose-6-phosphate and involves the ATP-neutral synthesis of products crucial in cellular redox balancing and biosynthetic pathways (Horecker 2002). Importantly, PPP products such as pyruvate can also be utilised to generate ATP, providing oxidisable substrates to the mitochondria. Indeed, the same authors who observed reduced plasma disaccharides in ME/CFS have previously suggested that the PPP may be dysregulated in ME/CFS (Germain, Ruppert et al. 2017). This pathway should therefore also be examined more closely.

4.1.2 Alternative Sources of Oxidisable Substrate than Carbohydrates

Amino acids may be metabolised to feed into the TCA cycle as sources of oxidisable substrate for respiration, or to participate in the replenishment of other metabolic intermediates. Glutamate is the metabolic product of multiple amino acids, prominent among which is glutamine (Krebs 1935; Tapiero, Mathe et al. 2002). The conversion of

glutamine to glutamate by glutaminase (GLS) (Krebs 1935) and subsequent conversion to the TCA cycle intermediate α-ketoglutarate (α-KG) by glutamate dehydrogenase (GLUD1) is an important mechanism through which the TCA cycle can utilise amino acids to assist with driving mitochondrial energy production (Owen, Kalhan et al. 2002). This reaction simultaneously reduces NAD^+ to NADH, and so doubles as another direct means of replenishing reducing equivalents for OXPHOS. The functions of GLS and GLUD1 in tandem are therefore important for both direct mitochondrial NADH replenishment and as a major route of amino acid entry into the TCA cycle. This mechanism is regulated according to cellular energy demand, with GLUD1 activity mainly controlled allosterically - negatively by GTP and positively by ADP (Mastorodemos, Zaganas et al. 2005).

Cells may also utilise glutamate to both replenish reducing equivalents inside the mitochondria and assist in TCA cycle intermediate replenishment through participation in the malate-aspartate shuttle (MAS) (Owen, Kalhan et al. 2002; Abrego, Gunda et al. 2017). Here, glutamate and oxaloacetate are converted to aspartate and α-KG by mitochondrial aspartate aminotransferase (GOT2) (Figure 4.1). Aspartate is then transported out of the mitochondria and participates in the remainder of the cycle, which regenerates a) cytosolic NAD^+ from NADH, to be again reduced in catabolic nonmitochondrial processes such as glycolysis or peroxisomal β-oxidation and b) mitochondrial NADH for OXPHOS through malate dehydrogenase in the TCA cycle. Glutamate therefore acts not only as a direct source of amino acid-derived NADH and TCA cycle substrate through the earlier described GLUD1 route, but also does so by provisioning the GOT/MAS route.

The aforementioned studies using serum by Fluge *et al.* and Armstrong *et al*. also suggested that catabolism of amino acids to feed the TCA cycle is more heavily utilised in ME/CFS patients, albeit by different means (Armstrong, McGregor et al. 2015; Fluge, Mella et al. 2016). Armstrong *et al*. propose elevated glutamate usage by the mitochondria, specifically via the deamination of glutamate to aspartate as indicated by reduced glutamate and elevated aspartate levels (GOT2 route). By contrast, Fluge *et al.* observed reductions in the levels of both glutamine and glutamate but also in the levels of aspartate, which may instead suggest increased glutamate degradation through the GLUD1 route, rather than through GOT2 as suggested by Armstrong *et al*. However, perhaps in contradiction to this, Fluge *et al.* also reported elevated Sirtuin 4 (SIRT4) mRNA expression in ME/CFS PBMCs and SIRT4 is known to suppress GLUD1 activity (Haigis, Mostoslavsky et al. 2006). In spite

of some inconsistent details, these studies highlight dysregulated amino acid metabolism as an important area of exploration which should be pursued further in ME/CFS, especially in a metabolically active cellular context.

The potential for abnormal utilisation of alternative sources of oxidisable substrate has arisen clearly in the work presented in this thesis, having demonstrated inefficient ATP synthesis by Complex V accompanied by a compensatory elevation of respiratory capacity and elevated expression of mitochondrial transporters and TCA cycle enzymes in ME/CFS lymphoblasts (Chapter 3). Fatty acid β-oxidation is the breakdown of fatty acids to acetyl-CoA for the TCA cycle while also replenishing reducing equivalents and could be one such dysregulated process in ME/CFS lymphoblasts. While discussed in multiple metabolomic studies, lipid metabolism in general in ME/CFS research is also a point of uncertainty which requires reexamination. Naviaux *et al.* first reported that ceramide levels were decreased in ME/CFS patients, while Nagy-Szakal *et al.* subsequently did not observe a consistent decrease, and most recently Germain *et al.* reported an increase in ceramide levels (Naviaux, Naviaux et al. 2016; Nagy-Szakal, Barupal et al. 2018; Germain, Barupal et al. 2020). Another discrepancy is that the reduced FAD levels reported by Naviaux *et al.* and reduced carnitines reported by Nagy-Szakal *et al.* are interpreted as likely to hinder fatty acid β-oxidation, while increased levels of the compound hexanoylglutamine reported by Germain *et al.* are suggested to instead indicate an upregulation of fatty acid β-oxidation in ME/CFS patients (Naviaux, Naviaux et al. 2016; Nagy-Szakal, Barupal et al. 2018; Germain, Barupal et al. 2020). Germain *et al.* reported differences between two of their own studies, attributing these to differences in sample collection and handling (Germain, Ruppert et al. 2018; Germain, Barupal et al. 2020). This highlights the value of building and revisiting disease models in stably proliferative cell culture systems which are less affected by these sample collection issues and more readily reproducible.

Fatty acid β-oxidation is stimulated by AMP-activated protein kinase (AMPK) activity, one of the master regulators of energy metabolism in the cell (Hardie and Pan 2002). Abnormal elevation of AMPK activity could explain the reported elevation of short-chain fatty acid levels in ME/CFS patients (Armstrong, McGregor et al. 2017). Elevated levels of phosphorylated (activated) AMPK were observed by Mensah *et al.* in particular subpopulations of B cells whose frequency in the B cell population was elevated in ME/CFS samples (Mensah, Armstrong et al. 2018). However, others have reported that the

AMPK activation state was not significantly different between cultured muscle cells from ME/CFS patients (Fukuda criteria) and healthy controls (Brown, Jones et al. 2015). Additional study is therefore warranted to clarify the role of AMPK in ME/CFS.

4.1.3 Investigating Fuel Source Preference in ME/CFS Lymphoblasts

Amidst the findings presented in Chapter 3 (inefficient ATP synthesis, elevated respiratory capacity, nonmitochondrial catabolism, and increased expression of mitochondrial solute carriers and TCA cycle enzymes in ME/CFS lymphoblasts), it became clear that the utilisation of other pathways providing substrates to the mitochondria was also likely to be dysregulated in these cells. Combined transcriptomics and proteomics were subsequently embarked upon with the aims of identifying pathways which are dysregulated in ME/CFS lymphoblasts with greater clarity across both levels of regulation. Customised Seahorse experiments designed to measure real-time rates of glycolysis were also undertaken using lymphoblasts. AMPK activity in ME/CFS lymphoblasts was also measured. The resulting observations suggest that while glycolysis is unchanged, there is an elevated usage by ME/CFS cells of the PPP, fatty acid β-oxidation, and of the degradative mitochondrial pathways for specific amino acids. Together these results seem to reflect a shift towards fatty acid and amino acid catabolism as preferred sources of oxidisable substrate for the mitochondria in ME/CFS lymphoblasts. Subsets of the information contained within this chapter have been published in research articles (Missailidis, Annesley et al. 2020; Missailidis, Sanislav et al. 2021).

4.2 Results

4.2.1 Global Changes in ME/CFS Lymphoblast Transcriptomes and Proteomes

Up- and down-regulated lists of genes and proteins from both the proteomics and transcriptomics experiments were determined by applying the Benjamini-Hochberg step-up correction for multiple comparisons (with $Q < 0.05$) to the significance probabilities from *t* tests in the proteomics or F tests in the transcriptomics (Benjamini 1995). The numbers of differentially expressed vs unchanged gene products detected in ME/CFS lymphoblasts across both types of experiment are shown in Figure 4.2. Comparing the

whole cell proteomes of ME/CFS and healthy control lymphoblasts revealed 218 upregulated, 41 downregulated, and 2861 proteins whose levels were unchanged. The expression of significantly more proteins was upregulated than downregulated (binomial test). Conversely, the transcriptomics revealed 843 transcripts upregulated, 1409 downregulated, and 11,128 unchanged – significantly more downregulated than upregulated (binomial test, null hypothesis – equal up- and down-regulated proportions).

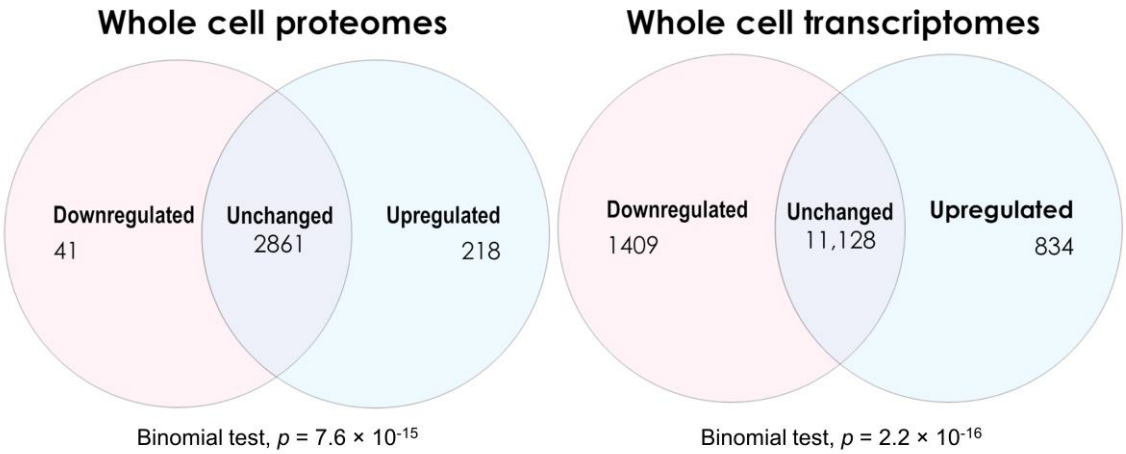

Figure 4.2: Venn diagrams depicting the numbers of differentially expressed gene products in ME/CFS lymphoblasts within the whole-cell proteomics and transcriptomics experiments. Two-sided binomial tests were undertaken with H_o set to $p = 0.5$ to assess whether the differentially expressed fractions significantly departed from proportions expected by chance. Resulting significance probabilities (p) are indicated.

To obtain a broad perspective of pathway-level changes to guide subsequent analysis, the PANTHER over-representation tool (Thomas, Campbell et al. 2003; Thomas, Kejariwal et al. 2006; Mi, Dong et al. 2010) was employed to analyse outcomes from both the whole-cell transcriptomics and proteomics experiments. The entire list of detected genes or proteins from the respective experiment type was used as the "reference" list for comparison by PANTHER against the "input" lists of differentially expressed genes and proteins ($Q < 0.05$). This produced a readout of pathways which are over-represented in the differentially-expressed fractions of both datasets. The over-representation analysis applied a binomial test of the hypothesis that more genes or proteins in a given pathway are present in the respective "input" list than would be expected by chance, using their occurrence in the "reference" list as the expected proportion eg. if genes or proteins in a particular pathway represent 10% of all that were detected in the experiment, they are expected to also make up 10% of the significantly dysregulated genes/proteins. Finding them in a

significantly elevated fraction of the dysregulated lists would indicate that the pathway is dysregulated.

The resulting global pathway-level analysis has been included in Appendix Tables A5.1-A6.2 and is summarised briefly throughout this Section. Since the focus of this analysis was to investigate the metabolic provision of oxidisable substrates to the mitochondria, Table 4.1 highlights the PANTHER analysis of these particular metabolic and mitochondrial pathways of interest - carbohydrate metabolism, TCA cycle and respiration, other mitochondrial pathways, lipid metabolism, β-oxidation, amino acid metabolism, protein degradation, substrate transport and metabolism more broadly. The relevant pathways were subsequently revisited in-depth (see later).

4.2.1.1 Transcriptomes

With additional correction for multiple comparisons (number of pathways) by a false discovery rate (FDR) cutoff of 0.05, 123 pathways were still statistically over-represented in the genes downregulated in ME/CFS lymphoblast transcriptomes (Appendix Table A5.1), while no pathways were over-represented in the upregulated genes. Table 4.1 shows pathways of particular interest that were dysregulated in the proteomics and/or transcriptomics, while Appendix Table A5.1 shows the full list of pathways significantly downregulated at the transcript level. The results show that pathway expression at the transcript-level, including those involved in mitochondrial respiration is broadly reduced in ME/CFS lymphoblasts. This contrasts starkly with the elevated protein expression and function data both for the mitochondrial functions investigated in Chapter 3 and the broader metabolic functions investigated in this chapter.

Nevertheless, 834 individual transcripts were significantly upregulated ($Q < 0.05$). The possibility was considered that FDR correction of the PANTHER pathway analysis of the up-regulated transcript list was overly conservative. To identify which pathways might indeed show evidence of upregulation, the analysis was repeated with FDR correction excluded in the PANTHER analysis to identify candidate pathways. Of the resultant 51 pathways over-represented in this upregulated fraction (binomial test, P value < 0.05), most pertain to innate immune system activation or the import and intracellular transport of small molecules (Appendix Table A5.2). The latter could indicate homeostatic upregulation of

the uptake of vitamins, sugars, amino acids or other small molecules important for sustaining cellular metabolism from the surrounding medium.

Reactome pathway	Category	Dataset	Altered fraction	Fold - enriched	Binomial test P-value
Gluconeogenesis (R-HSA-70263)	Carbohydrate metabolism	Proteomics	Upregulated	3.81	0.022
Pentose phosphate pathway (R-HSA-71336)	Carbohydrate metabolism	Proteomics	Upregulated	4.52	0.03
The citric acid (TCA) cycle and respiratory electron transport (R-HSA-1428517)	TCA cycle and respiration	Proteomics	Upregulated	1.89	0.027
Formation of ATP by chemiosmotic coupling (R-HSA-163210)	TCA cycle and respiration	Proteomics	Upregulated	4.52	0.03
Respiratory electron transport, ATP synthesis by chemiosmotic coupling, and heat production by uncoupling proteins. (R-HSA-163200)	TCA cycle and respiration	Transcriptomics	Downregulated	3.59	1.33×10^{-11}
Respiratory electron transport (R-HSA-611105)	TCA cycle and respiration	Transcriptomics	Downregulated	3.69	2.14×10^{-10}
The citric acid (TCA) cycle and respiratory electron transport (R-HSA-1428517)	TCA cycle and respiration	Transcriptomics	Downregulated	2.83	1.95×10^{-9}

Complex I biogenesis (R-HSA-6799198)	TCA cycle and respiration	Transcriptomics	Downregulated	4.19	7.59×10^{-8}
Beta oxidation of lauroyl-CoA to decanoyl-CoA-CoA (R-HSA-77310)	Lipid metabolism	Proteomics	Upregulated	13.57	0.0015
Beta oxidation of hexanoyl-CoA to butanoyl-CoA (R-HSA-77350)	Lipid metabolism	Proteomics	Upregulated	10.85	0.0028
Beta oxidation of octanoyl-CoA to hexanoyl-CoA (R-HSA-77348)	Lipid metabolism	Proteomics	Upregulated	10.85	0.0028
Beta oxidation of decanoyl-CoA to octanoyl-CoA-CoA (R-HSA-77346)	Lipid metabolism	Proteomics	Upregulated	10.85	0.0028
Mitochondrial fatty acid beta-oxidation of unsaturated fatty acids (R-HSA-77288)	Lipid metabolism	Proteomics	Upregulated	10.85	0.0028
Fatty acid metabolism (R-HSA-8978868)	Lipid metabolism	Proteomics	Upregulated	2.87	0.0029
Acyl chain remodeling of CL (R-HSA-1482798)	Lipid metabolism	Proteomics	Upregulated	18.09	0.0057

Beta oxidation of myristoyl-CoA to lauroyl-CoA (R-HSA-77285)	Lipid metabolism	Proteomics	Upregulated	18.09	0.0057
Mitochondrial Fatty Acid Beta-Oxidation (R-HSA-77289)	Lipid metabolism	Proteomics	Upregulated	5.51	3.32×10^{-4}
Beta oxidation of palmitoyl-CoA to myristoyl-CoA (R-HSA-77305)	Lipid metabolism	Proteomics	Upregulated	18.09	6.64×10^{-4}
mitochondrial fatty acid beta-oxidation of saturated fatty acids (R-HSA-77286)	Lipid metabolism	Proteomics	Upregulated	10.34	6.72×10^{-4}
NR1H2 & NR1H3 regulate gene expression linked to triglyceride lipolysis in adipose (R-HSA-9031528)	Lipid metabolism	Transcriptomics	Upregulated	7.47	0.03
Regulation of cholesterol biosynthesis by SREBP (SREBF) (R-HSA-1655829)	Lipid metabolism	Transcriptomics	Upregulated	2.3	0.026

Regulation of lipid metabolism by PPARalpha (R-HSA-400206)	Lipid metabolism	Transcriptomics	Upregulated	1.87	0.031
Phenylalanine and tyrosine metabolism (R-HSA-8963691)	Amino acid metabolism	Proteomics	Upregulated	7.24	0.032
Glutamate Neurotransmitter Release Cycle (R-HSA-210500)	Amino acid metabolism	Proteomics	Upregulated	13.57	0.0015
Neurotransmitter release cycle (R-HSA-112310)	Amino acid metabolism	Proteomics	Upregulated	6.03	0.014
Metabolism of amino acids and derivatives (R-HSA-71291)	Amino acid metabolism	Proteomics	Upregulated	1.64	0.021
Aspartate and asparagine metabolism (R-HSA-8963693)	Amino acid metabolism	Proteomics	Upregulated	7.24	0.032
Lysine catabolism (R-HSA-71064)	Amino acid metabolism	Proteomics	Upregulated	6.03	0.044
Metabolism of amino acids and derivatives (R-HSA-71291)	Amino acid metabolism	Transcriptomics	Downregulated	3.13	2.06×10^{-20}

Response of EIF2AK4 (GCN2) to amino acid deficiency (R-HSA-9633012)	Amino acid metabolism	Transcriptomics	Downregulated	5.85	6.10×10^{-26}
Ubiquitin-dependent degradation of Cyclin D (R-HSA-75815)	Protein degradation	Transcriptomics	Downregulated	2.93	2.75×10^{-4}
Autodegradation of the E3 ubiquitin ligase COP1 (R-HSA-349425)	Protein degradation	Transcriptomics	Downregulated	2.93	2.75×10^{-4}
Vpu mediated degradation of CD4 (R-HSA-180534)	Protein degradation	Transcriptomics	Downregulated	2.93	2.75×10^{-4}
Ubiquitin Mediated Degradation of Phosphorylated Cdc25A (R-HSA-69601)	Protein degradation	Transcriptomics	Downregulated	2.93	2.75×10^{-4}
Degradation of GLI2 by the proteasome (R-HSA-5610783)	Protein degradation	Transcriptomics	Downregulated	2.79	2.98×10^{-4}
GLI3 is processed to GLI3R by the proteasome (R-HSA-5610785)	Protein degradation	Transcriptomics	Downregulated	2.79	2.98×10^{-4}

Degradation of GLI1 by the proteasome (R-HSA-5610780)	Protein degradation	Transcriptomics	Downregulated	2.75	3.60×10^{-4}
Processing of SMDT1 (R-HSA-8949664)	Other mitochondrial	Proteomics	Upregulated	6.78	0.01
Release of apoptotic factors from the mitochondria (R-HSA-111457)	Other mitochondrial	Proteomics	Upregulated	12.06	0.012
Mitochondrial biogenesis (R-HSA-1592230)	Other mitochondrial	Proteomics	Upregulated	2.81	0.013
Transcriptional activation of mitochondrial biogenesis (R-HSA-2151201)	Other mitochondrial	Proteomics	Upregulated	3.45	0.03
Mitochondrial translation initiation (R-HSA-5368286)	Other mitochondrial	Transcriptomics	Downregulated	3.37	1.80×10^{-8}
Mitochondrial translation termination (R-HSA-5419276)	Other mitochondrial	Transcriptomics	Downregulated	3.37	1.80×10^{-8}
Mitochondrial translation (R-HSA-5368287)	Other mitochondrial	Transcriptomics	Downregulated	3.26	2.23×10^{-8}

Mitochondrial protein import (R-HSA-1268020)	Other mitochondrial	Transcriptomics	Downregulated	2.64	3.73×10^{-4}
Mitochondrial translation elongation (R-HSA-5389840)	Other mitochondrial	Transcriptomics	Downregulated	3.48	5.03×10^{-9}
Mitochondrial calcium ion transport (R-HSA-8949215)	Other mitochondrial	Proteomics	Upregulated	6.96	8.53×10^{-4}
Transport of nucleotide sugars (R-HSA-727802)	Transport of substrate molecules	Transcriptomics	Upregulated	4.98	0.023
SLC transporter disorders (R-HSA-5619102)	Transport of substrate molecules	Transcriptomics	Upregulated	2.03	0.048
Transport of small molecules (R-HSA-382551)	Transport of substrate molecules	Transcriptomics	Upregulated	1.35	0.037
Signalling by Leptin (R-HSA-2586552)	Metabolism	Proteomics	Upregulated	9.05	0.021
Diseases of metabolism (R-HSA-5668914)	Metabolism	Proteomics	Upregulated	3.02	0.045
Metabolism (R-HSA-1430728)	Metabolism	Proteomics	Upregulated	1.51	2.12×10^{-4}
Activation of gene expression by SREBF (SREBP) (R-HSA-2426168)	Metabolism	Transcriptomics	Upregulated	2.3	0.049

Metabolism (R-HSA-1430728)	Metabolism	Transcriptomics	Downregulated	1.43	3.80×10^{-8}

Table 4.1: Significantly altered mitochondrial, substrate-providing and related metabolic pathways of interest as indicated by PANTHER gene expression analysis of both the proteomic and transcriptomic datasets. "Reactome Pathway" was set as the level of biological granularity. Pathways were categorised and colour-coded by areas of most interest to this investigation as follows: green for carbohydrate metabolism, purple for the TCA cycle and respiration, blue for lipid metabolism, red for amino acid metabolism, yellow for protein degradation, cyan for other mitochondrial, and grey for transport of substrate molecules. Unshaded entries correspond to pathways too broad in scope to categorise into narrow functional roles pertaining to specific processes.

In view of a prior report of elevated SIRT4 mRNA expression in ME/CFS PBMCs (Fluge, Mella et al. 2016), I also examined whether expression of any of the sirtuins was altered. In ME/CFS lymphoblasts the expression levels of SIRT4 as well as SIRT1, SIRT5 and SIRT7 were not significantly changed, while SIRT2 was significantly upregulated and SIRT3 and SIRT6 were downregulated (Appendix Table A6.1). The sirtuins were not detected in the proteomics analysis, so it is unclear whether the levels of any sirtuin proteins are altered in ME/CFS lymphoblasts.

It has also been reported that compared to controls, ME/CFS PBMCs exhibit different proportions of immune cell subtypes as detected by flow cytometry of CD cell surface markers (Curriu, Carrillo et al. 2013; Hardcastle, Brenu et al. 2015). The data was therefore also examined for differential expression of CD cell-surface markers and it was found that CD19, CD47, CD52 and CD79A were significantly downregulated while only CD164 was significantly upregulated in ME/CFS lymphoblasts (Appendix Table A6.1). Although all of these are expressed in activated B cells, none are markers for specific subsets of B cells (Allman and Pillai 2008), the immune cell type that is specifically infected by EBV during immortalisation. None of them were differentially expressed in the whole cell proteomes (see below).

4.2.1.2 Proteomes

Similar analysis of differential pathway expression in the whole-cell proteomes showed results that were highly distinct from the transcriptomes. While the lists of up- and down-regulated proteins were also conservatively selected using the $Q < 0.05$ method, additional FDR correction of the pathway over-representation tests was excluded in the proteomic pathway analysis. This was done as the additional FDR correction at the pathway level was found to be overly conservative and obscured true positives which were separately confirmed by closer analysis of individual pathways, and in the case of OXPHOS proteins also by prior multi-pronged tests of activity and expression. These true-positive pathways satisfied a $p < 0.05$ threshold for the binomial test of over-representation when the pathway FDR was not used. This analysis identified 77 pathways over-represented in the significantly upregulated fraction of proteins (Appendix Table A5.3), while 13 pathways were over-represented in the downregulated fraction (Appendix Table A5.4).

Of the downregulated fraction, most of the 13 pathways were represented by very few detected proteins or proteins that were significantly downregulated or were pathway hits irrelevant in the context of lymphoid cells (such as meiosis). The most significantly affected pathway with both tissue-specific relevance and a greater number of downregulated proteins was the activation of protein kinase Ns (PKNs) by RHO GTPases (Reactome pathway R-HSA-5625740). This could suggest reduced activation of PKNs in ME/CFS lymphoblasts. The various PKNs, while involved in signal transduction related to many processes such as cell migration and cytoskeleton assembly, also play roles in transcriptional activation which have been most clearly observed in cardiac tissue (Morissette, Sah et al. 2000). If fulfilling similar roles in lymphoid cells, reduced PKN activities could be a contributor to the largely reduced transcript-level expression apparent in ME/CFS lymphoblasts.

By contrast, the 77 pathways over-represented in the upregulated protein fraction included functional categories which were altered significantly in much higher numbers than pathways in the downregulated fraction and were more informative in their biological context (Appendix Table A5.3). Most strikingly, 9/20 of the most significantly upregulated pathways pertained directly to fatty acid β-oxidation (Table 4.1, Appendix Table A5.3). This strongly suggests an upregulation of fatty acid β-oxidation in ME/CFS lymphoblasts.

Another seven out of twenty of the most significantly upregulated pathways pertained to activation of both the innate and adaptive immune responses (Appendix Table A5.3) as was also evident in the transcriptomes, together suggesting elevated immune activation in ME/CFS lymphoblasts. Of several CD antigens detected in the proteomics, most trended upwards, although only the expression of CD226, CD48 and CD70 were individually altered significantly (upregulated) in ME/CFS lymphoblasts (Appendix Table A6.2). None of these were differentially expressed in transcriptomes of ME/CFS lymphoblasts, none are markers of specific B cell subsets (Allman and Pillai 2008) but all are expressed on proliferating, activated B cells. CD70 expression is a marker of highly activated lymphocytes (Israel, Gulley et al. 2005), and its higher expression in ME/CFS lymphoblasts is thus in keeping with the (presumably compensatory) general hyperactivation of metabolism in these cells.

Also prominent among the list of significantly upregulated pathways were mitochondrial biogenesis (R-HSA-1592230), the TCA cycle and respiratory electron transport (R-HSA-1428517) and other mitochondrial proteins (Table 4.1, Appendix Table A5.3). This was as expected, given the elevated respiratory capacity (elevated expression of OXPHOS complex subunits) and TCA cycle enzyme expression. The PPP was also found to be over-represented in this analysis (Table 4.1, Appendix Table A5.3), in line with a metabolic shift suggested by the foregoing results (Chapter 3) and by others (Germain, Ruppert et al. 2017). At least 5 of the over-represented pathways were reflective of abnormal amino acid metabolism or degradation (Table 4.1, Appendix Table A5.3), which implied dysregulated amino acid usage by ME/CFS lymphoblasts, also in agreement with the previous results (Chapter 3) and those reported by others (Armstrong, McGregor et al. 2015; Fluge, Mella et al. 2016).

Upregulation of OXPHOS subunits at the protein level was previously verified by Western blotting in Chapter 3. Additional Western blots and qRT-PCR experiments were also undertaken to further verify the outcomes of the proteomic and transcriptomic experiments. Using Western blotting, both ACO2 and SDHA showed the same absence of altered expression as is present in the proteomics dataset, while elevated levels of MDH1 in the proteomes were also confirmed (Appendix Figures A7.1A and A7.2). At the transcript level, the directional trends of *SDHB, GLS, NDUFB1* and *NDUFB10* normalised to the

histone gene *HIST1H1C* were confirmed in all four cases between qRT-PCR experiments and the transcriptomic dataset (Appendix Figure A7.1B).

Based on the results presented in Chapter 3, it was proposed that ATP synthesis by Complex V was inefficient in ME/CFS lymphoblasts, and that this is accompanied by compensatory upregulation of mitochondrial protein expression and likely by the dysregulation of substrate-providing pathways. Elevated usage of such pathways would act to supply the upregulated TCA cycle and respiratory electron transport complexes with substrate at faster rates. The analysis at the global proteome level presented here is consistent with these conclusions and strongly suggests the upregulation of alternatives such as fatty acid β-oxidation, the PPP and amino acid catabolism in order to provide ME/CFS lymphoblast mitochondria with oxidisable substrate. The broad trends apparent in whole-cell transcriptomics also indicate that elevated levels of the proteins in such pathways could occur as a result of upregulation specifically at the translational level. These observations were used as a basis to guide the subsequent, closer analysis of specific pathways of interest to understand how provision of mitochondrial substrates could be dysregulated in ME/CFS lymphoblasts in more detail.

4.2.2 Glycolytic Rate and Gene Expression are Unchanged in ME/CFS Lymphoblasts and PPP Enzyme Expression is Elevated

The elevated non-mitochondrial catabolic rate in ME/CFS lymphoblasts and the ability of activated lymphoid cells to switch between preferential utilisation of either glucose or fatty acids together first prompted the examination of glycolysis in detail, being one of the potentially dysregulated substrate-providing pathways. To examine glycolytic function in intact ME/CFS lymphoblasts, a customised Seahorse assay was implemented to assess real-time glycolytic production of lactate by live cells by measuring the extracellular acidification rate (ECAR) of the medium. The results revealed no difference between ME/CFS and control cells in glycolytic rate, reserve or capacity (Figure 4.3A). In keeping with the unchanged rate of glycolysis, expression of the two key rate-controlling enzymes of glycolysis – phosphofructokinase and hexokinase - was unchanged from that of controls (Figure 4.3A). Indeed, the levels of all detected glycolytic enzymes (including subunits and isoenzymes: 16 proteins) were also found to be unchanged as a whole in the ME/CFS lymphoblast proteomes ($p > 0.05$, *t* test and binomial test) (Figure 4.3B). This contrasts

with slightly elevated levels of mRNAs encoding these enzymes which were observed in the whole-cell transcriptomes (Figure 4.3C). Here, 14/21 detected transcripts favoured upregulation with mean levels 10 ± 4% higher than controls (*t* test, p = 0.0247), 6 of which encoded isoenzymes or subunits of phosphofructokinase and hexokinase. It has been shown by others that the accumulation of untranslated mRNAs encoding glycolytic enzymes can occur when lymphoid cells are in a metabolic state favouring fatty acid β-oxidation rather than glycolysis (Ricciardi, Manfrini et al. 2018). If ME/CFS lymphoblasts do indeed favour fatty acid β-oxidation instead of glycolysis, this would be consistent with the pattern of expression observed here.

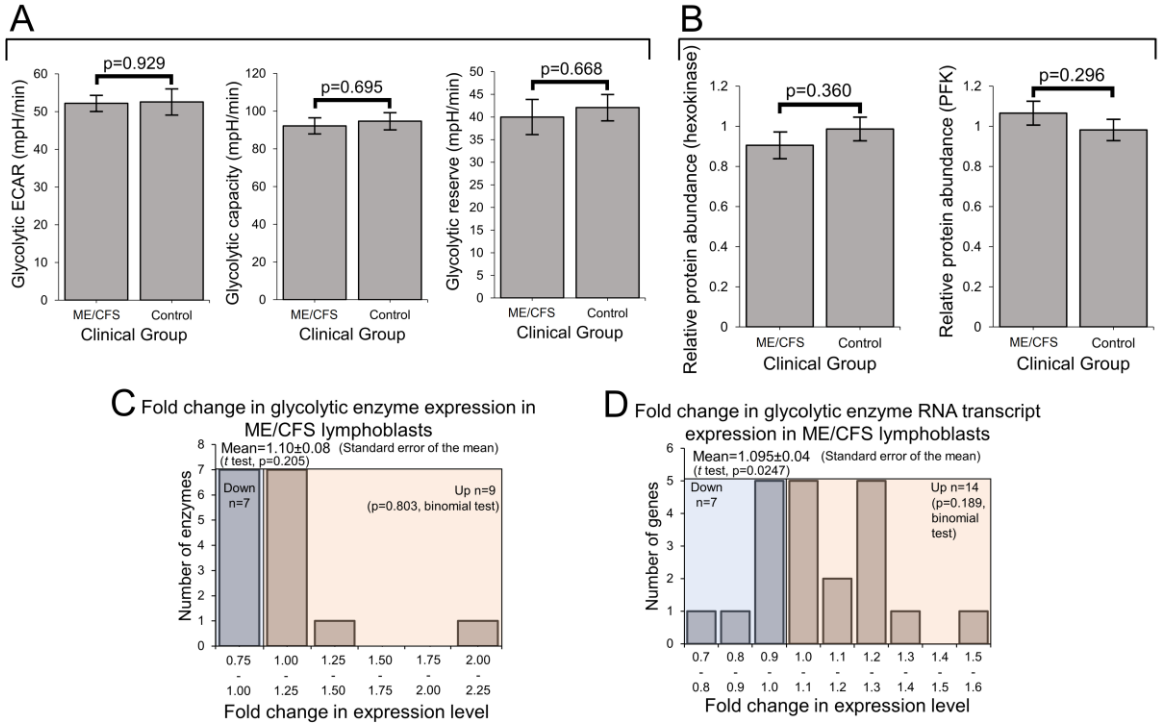

Figure 4.3: The rate of glycolysis is unaffected in ME/CFS lymphoblasts. Error bars represent standard error of the mean. (**A**) Glycolytic rate, capacity and reserve are unchanged in ME/CFS lymphoblasts (independent t-test). The ECAR was measured in lymphoblasts from ME/CFS and control individuals by the Seahorse XFe24 Extracellular Flux Analyzer. Each ME/CFS (n = 23) and control (n = 16) cell line was assayed over four replicates in at least three independent experiments. (**B**) The expression level of hexokinase and phosphofructokinase is unchanged in whole cell mass spectrometry proteomics experiments (independent t-test). Mean fold changes were calculated using the iBAQ fold-change per individual sample for each isoenzyme (none of which were statistically significant on their own, threshold p < 0.05). Each cell line was sampled once, or twice for a subset of healthy controls arbitrarily selected to act as an internal control between experiments in the proteomics work. Mass spectrometry proteomics experiment: ME/CFS n = 34, control n = 31. (**C**) 16 glycolytic enzymes were detected within the whole-cell proteomes of lymphoblasts from

ME/CFS and control lymphoblasts. Fold-change refers to the mean abundance of a given protein in the CFS group divided by the mean abundance in the control group. There was no significant difference in the differentially expressed proportions of detected glycolytic enzymes (binomial test with H_o set to 0.5) or the magnitude of expression (single sample *t* test with H_o m = 1) between ME/CFS and controls. (**D**) 21 RNA transcripts encoding glycolytic enzymes were detected by RNA sequencing within the whole-cell transcriptomes of ME/CFS and control lymphoblasts. Mean fold-change was calculated for the ME/CFS group versus the control average for each transcript. The proportion of detected transcripts that were upregulated (binomial test with H_o set to 0.5) was not significant while the average extent of the upregulation (single sample *t* test with H_o m = 1) was statistically significant. Each cell line was sampled once. mRNA transcript abundance refers to the read count. RNA sequencing transcriptomics experiment: ME/CFS n = 23, control n = 17.

Glucose tracer experiments by others have shown that when B cells switch their metabolism in favour of fatty acid β-oxidation instead of towards glycolysis, glucose is utilised at the same overall rates, but instead by the PPP (Waters, Ahsan et al. 2018; Weisel, Mullett et al. 2020). In ME/CFS research, reports of reduced glucose (Armstrong, McGregor et al. 2015) and disaccharides (Germain, Barupal et al. 2020) in patient blood could reflect elevated utilisation of the PPP if the rate of glycolysis is indeed unchanged in patient cells as has been observed here in the lymphoblasts. In any case, compensatory provision of additional pyruvate is one means by which the PPP may be utilised to support respiration as a source of oxidisable substrate in ME/CFS lymphoblast mitochondria whose mitochondrial ATP synthesis is inefficient. PPP enzymes were also significantly over-represented among the upregulated fraction of proteins across the entire proteomics experiment (Appendix Table A5.3). This was confirmed by selecting all PPP enzymes that were detected in the proteome and examining their expression levels in the lymphoblast proteomes and transcriptomes. With mean levels 20 ± 9% higher than controls (*t* test, p = 0.034) (Figure 4.4A), PPP enzymes were significantly upregulated in the proteomes of ME/CFS lymphoblasts, while their expression was not significantly altered at the transcriptional level (Figure 4.4B). Importantly, Glucose-6-phosphate 1-dehydrogenase (G6PD), the enzyme catalysing the first and rate-limiting step of the oxidative arm of the PPP (Benatti, Morelli et al. 1978), was significantly elevated on its own by 43 ± 10% in the proteomes of ME/CFS lymphoblasts versus healthy controls ($p = 5.5 \times 10^{-4}$) (Figure 4.4C). This suggests that the PPP is indeed upregulated as an alternative means of glucose utilisation to glycolysis in ME/CFS lymphoblasts.

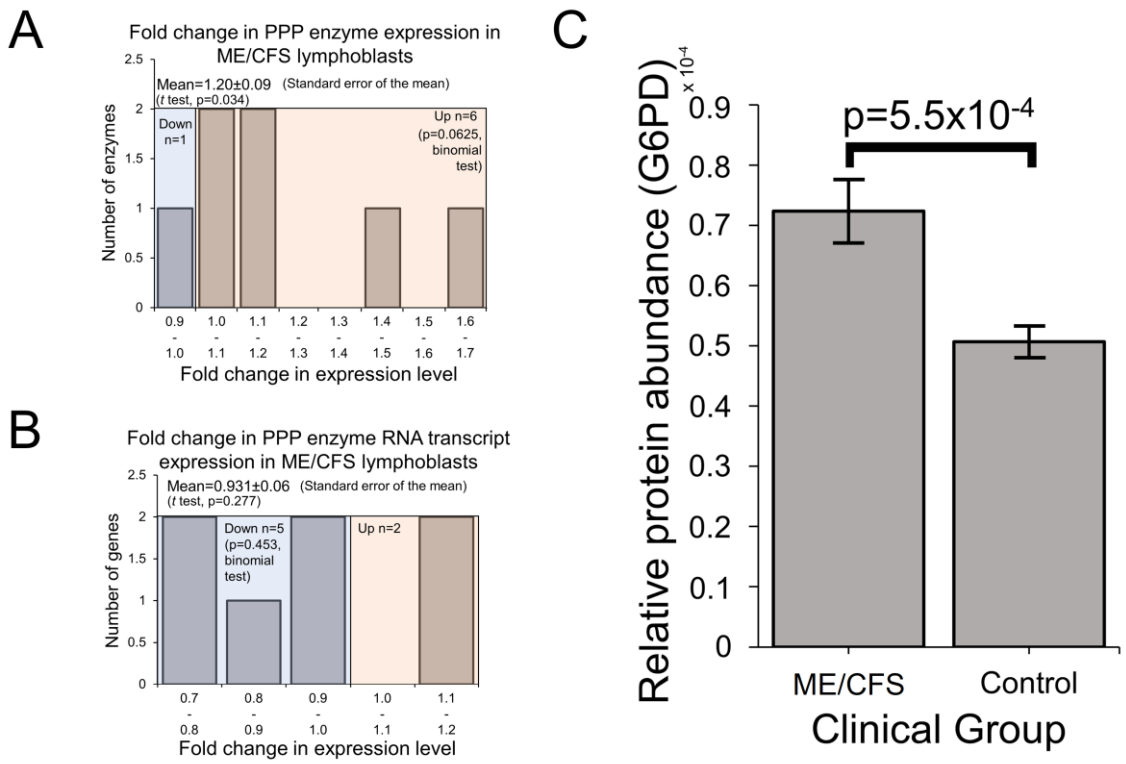

Figure 4.4: Expression of the pentose phosphate pathway (PPP) is upregulated at the protein level in ME/CFS lymphoblasts. Error bars represent standard error of the mean. (**A**) 7 PPP enzymes were detected within the whole-cell proteomes of lymphoblasts from ME/CFS and control lymphoblasts. Fold-change refers to the mean abundance of a given protein in the CFS group divided by the mean abundance in the control group. There was no significant difference in the proportion of upregulated PPP enzymes (binomial test with H_o set to 0.5), but the magnitude of upregulation was significantly elevated in ME/CFS lymphoblasts (single sample *t* test with H_o $m \leq 1$ and H_1 $m>1$, $p = 0.034$). (**B**) 7 RNA transcripts encoding PPP enzymes were detected by RNA sequencing within the whole-cell transcriptomes of ME/CFS and control lymphoblasts. Mean fold change was calculated for the ME/CFS group versus the control average for each transcript. The proportions of reduced or elevated transcripts were not significantly different (binomial test with H_o set to 0.5) nor was the average magnitude of expression (single sample *t* test with H_o $m = 1$). RNA sequencing transcriptomics experiment: ME/CFS n = 23, control n = 17. (**C**) The expression level of G6PD is significantly elevated (*t* test, $p = 5.5 \times 10^{-4}$) in whole cell mass spectrometry proteomics experiments (independent t-test).. Each cell line was sampled once, or twice for a subset of healthy controls arbitrarily selected to act as an internal control between experiments. Relative abundance was obtained from iBAQ values normalised to the control average within the respective individual experiments. Mass spectrometry proteomics experiment: ME/CFS n = 34, control n = 31.

4.2.3 Enzymes Involved in Mitochondrial and Peroxisomal β-oxidation are Elevated in their Expression

The results in Chapter 3 showed that the rate of glycolysis is unchanged in ME/CFS lymphoblasts, while the proton leak and nonmitochondrial OCR as well as the expression of mitochondrial small molecule transporters are elevated. Since these findings were consistent with an increase in mitochondrial uptake and catabolism of oxidisable substrates, it was likely that alternative substrate-providing pathways (other than glycolysis) would be utilised at higher levels in ME/CFS lymphoblasts. It was previously reported that one of these pathways, the PPP is upregulated in B cells (Waters, Ahsan et al. 2018; Weisel, Mullett et al. 2020) from which lymphoblasts are derived. The canonical preferred alternative to glycolysis is fatty acid β-oxidation and since it featured prominently in the exploratory pathway over-representation analysis described earlier, it was examined in more detail. The results showed that expression of these proteins was indeed elevated significantly in the ME/CFS group (Figure 4.5A). Sixteen of the 21 detected proteins involved in β-oxidation and transport were upregulated (binomial test, $p = 0.0133$), with mean levels 35 ± 14% higher than controls (*t* test, $p = 9.19 \times 10^{-3}$). In contrast with the elevated protein expression and in keeping with the broader transcriptional trends, the levels of mRNA transcripts encoding these enzymes were found to be slightly reduced (Figure 4.5B). 18 of the detected 25 transcripts were downregulated (binomial test, $p = 0.043$) with mean levels 9 ± 3% lower than controls (*t* test, $p = 0.014$). This suggests upregulation specifically at the translational level as was apparent with other groups of proteins such as OXPHOS Complexes I, III, IV and V (Chapter 3).

To better understand the potential functional implications of these differences in mitochondrial β-oxidation enzyme expression, the expression of these proteins was more closely examined on an individual basis. Among the detected mitochondrial β-oxidation proteins, it was found that the expression of 5 specific enzymes was significantly altered at the protein level individually, and that each of these was upregulated in the ME/CFS lymphoblasts (Figure 4.5C). Both subunits of the mitochondrial trifunctional enzyme (HADHA and HADHB) were among these 5 significantly upregulated proteins. Hydroxyacyl-CoA dehydrogenase/3-keotacyl-CoA thiolase (HADH) is an enzyme complex which catalyses multiple reactions in mitochondrial β-oxidation, exhibits specificity for long-chain fatty acids and is involved in cardiolipin synthesis – cardiolipin

being an important component of the inner mitochondrial membrane (Taylor, Mejia et al. 2012; Xia, Fu et al. 2019). Short-chain enoyl-CoA hydratase (ECHS1) was also significantly upregulated, as well as the very long-chain specific acyl-CoA dehydrogenase (ACADVL). These, together with upregulated HADH expression demonstrate the upregulation of enzymes involved in catabolising fatty acids of diverse chain-lengths, implying their complete oxidation within the mitochondria and thus their ultimate contribution towards the electron transport chain. This conclusion is reinforced by the remaining member of the 5 significantly upregulated proteins being the alpha subunit of the electron transfer flavoprotein (ETFA), which accepts electrons from the mitochondrial dehydrogenases involved in β-oxidation and passes them via Electron transfer flavoprotein-ubiquinone oxidoreductase (ETF-QO) and ubiquinone to Complex III in the electron transport chain (Salazar, Zhang et al. 1997).

Mitochondrial β-oxidation itself does not readily act upon very long-chain fatty acids (VLCFA), which are first chain-shortened by peroxisomal β-oxidation to then be utilised in either mitochondrial β-oxidation or directly in the TCA cycle as acetyl-CoA (Wanders, Waterham et al. 2015). Both mitochondrial and peroxisomal fatty acid β-oxidation, pathways which operate in tandem, are together upregulated by AMPK activity and the nuclear transcription factor peroxisome proliferator-activated receptor-α (PPAR-α) (Everett, Galli et al. 2000; Vega, Huss et al. 2000; Hardie and Pan 2002; Jager, Handschin et al. 2007). If ME/CFS lymphoblasts do switch their oxidisable substrate preference in favour of mitochondrial fatty acid β-oxidation, one would therefore also expect peroxisomal β-oxidation to be upregulated alongside it due to their shared regulatory mechanisms and entwined function. To investigate this, the expression of individual enzymes involved in peroxisomal β-oxidation was more closely investigated.

Acyl-CoA Oxidase 1 (ACOX1) is the enzyme which first initiates VLCFA β-oxidation inside the peroxisome and is the rate-controlling enzyme of this process (Zeng, Deng et al. 2017). It was found that the expression of ACOX1 was significantly upregulated in the proteomes by 91 ± 26% and unchanged in the transcriptomes of ME/CFS lymphoblasts (Figure 4.5D). Of the other enzymes involved in peroxisomal β-oxidation, most were not detected in either experiment, or were detected at low levels in only a few samples. As a result of their relatively poor detection, differences between ME/CFS and controls could not be found for these enzymes. Nonetheless, the significant upregulation of the pathway-

initiating and rate-controlling enzyme ACOX1 in addition to the functional and regulatory coupling of these pathways described earlier, suggests that peroxisomal β-oxidation is likely to be upregulated in tandem with mitochondrial β-oxidation in ME/CFS lymphoblasts.

If the rates of fatty acid β-oxidation are elevated in ME/CFS lymphoblasts in accordance with the expression of these mitochondrial and peroxisomal enzymes, this would also be consistent with the elevated steady state levels of untranslated glycolytic mRNA transcripts which I earlier observed and discussed (Ricciardi, Manfrini et al. 2018). More importantly, upregulated fatty acid β-oxidation would provide acetyl-CoA to the TCA cycle more rapidly, in turn provisioning the upregulated respiratory complexes with reducing equivalents to drive respiration – potentially offsetting the inefficiency of ATP synthesis by Complex V which was previously demonstrated in Chapter 3.

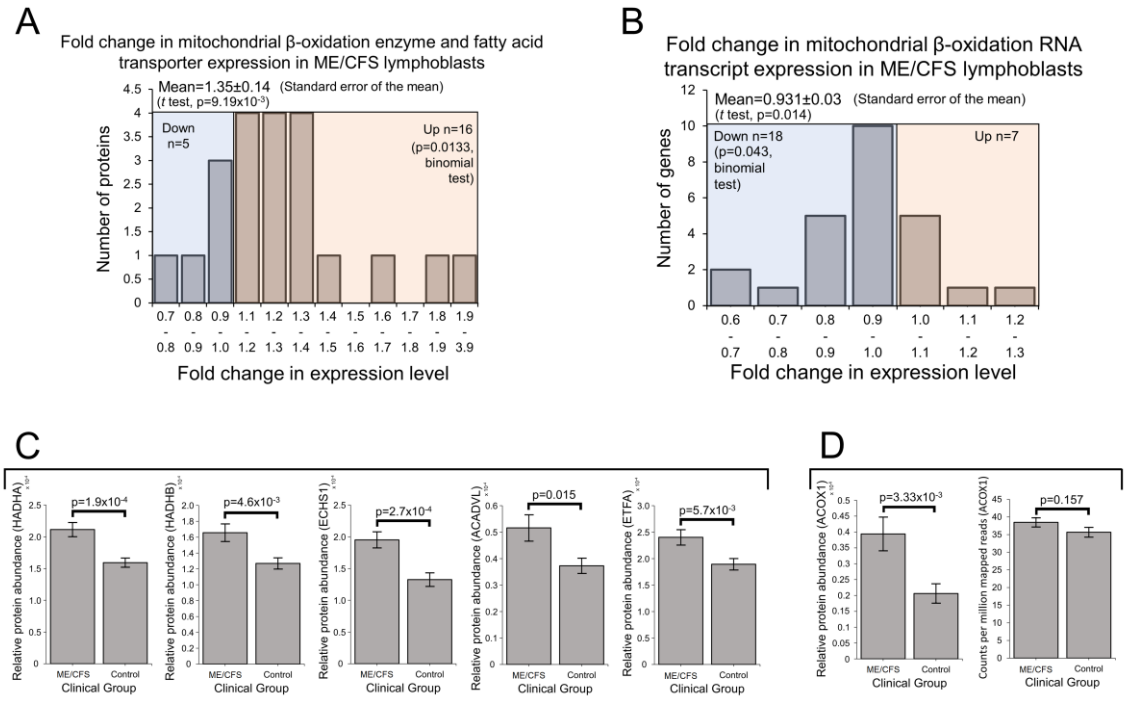

Figure 4.5: Expression of proteins involved in mitochondrial and peroxisomal fatty acid β-oxidation was elevated in ME/CFS lymphoblasts. Error bars represent standard error of the mean. (**A**) 21 proteins involved in mitochondrial fatty acid β-oxidation and transport were detected within the whole-cell proteomes of ME/CFS and control lymphoblasts. Fold-change refers to the mean abundance of a given protein in the ME/CFS group divided by the mean abundance in the control group. The proportion of detected proteins that were upregulated (binomial test with H_o set to 0.5 and H_1 being that the upregulated proportion was greater) and the average extent of the upregulation (single sample *t* test with H_o $m \leq 1$ and H_1 $m > 1$) were statistically significant. Each cell line was sampled once, or twice for a subset of healthy controls arbitrarily selected to act as an internal

control between experiments in the proteomics work. Mass spectrometry proteomics experiment: ME/CFS n = 34, control n = 31. (**B**) 25 RNA transcripts encoding proteins involved in mitochondrial fatty acid β-oxidation and transport were detected by RNA sequencing within the whole-cell transcriptomes of ME/CFS and control lymphoblasts. Fold-change refers to the mean abundance of a given transcript in the CFS group divided by the mean abundance in the control group. The proportions of reduced or elevated transcripts were not significantly different (binomial test with H_o p = 0.5) nor was the average magnitude of expression (single sample *t* test with H_o m = 1). Each cell line was sampled once. RNA sequencing transcriptomics experiment: ME/CFS n = 23, control n = 17. (**C**) The expression levels of HADHA, HADHB, ACADVL, ECHS1 and ETFA are significantly elevated in whole cell mass spectrometry proteomics experiments (independent t-test). Relative abundance was obtained from iBAQ values normalised to the control average within the respective individual experiments. (**D**) The expression of ACOX1 was significantly elevated in whole cell mass spectrometry proteomics experiments (independent t-test). Relative abundance was obtained from iBAQ values normalised to the control average within the respective individual experiments. ACOX1 expression was not altered at the transcriptional level as measured by whole-cell RNA sequencing transcriptomics. Counts per million mapped reads were calculated for each gene transcript.

Since fatty acid metabolism hinges on the controlled balance between biosynthesis and β-oxidation (Hardie and Pan 2002), it is also important to consider the pathways involved in fatty acid biosynthesis when drawing conclusions as to the favoured direction of fatty acid metabolism. Contrasting with the upregulation of β-oxidation enzymes, no significant differences were detected at either the protein level (Figure 4.6A) or the transcriptional level (Figure 4.6B) in the expression of enzymes involved in fatty acid biosynthesis as a whole.

Particularly important among the involved enzymes are acetyl-CoA carboxylase 1 (ACC1) which catalyses the synthesis of malonyl-CoA - a key, rate-limiting substrate for fatty acid synthesis, and fatty acid synthase (FASN) which in turn catalyses the conversion of malonyl-CoA to palmitate (Jayakumar, Tai et al. 1995; Kim, Moon et al. 2010). Thus, these reactions control the rate of *de novo* fatty acid biosynthesis by the cell and understanding their expression levels is important to assist with inferring functional consequences. The expression of ACC1 (ACACA) was unchanged in ME/CFS lymphoblasts compared to controls (albeit detected at low levels) in both the whole cell proteomes and transcriptomes (Figure 4.6C). This was later confirmed in a plate-based fluorescence assay (Figure 4.6D). The expression of FASN was also not significantly different at either the protein or

transcript level (Figure 4.6C). It is not surprising that the expression of these key biosynthetic enzymes in ME/CFS lymphoblasts was not changed, since fatty acid biosynthesis competes with fatty acid β-oxidation (Hardie and Pan 2002; Hue and Taegtmeyer 2009), the enzymes for which are upregulated. These observations together suggest that in ME/CFS lymphoblasts compared to controls, fatty acid metabolism is indeed operating in favour of β-oxidation rather than biosynthesis.

While mitochondrial enzymes, including those involved in fatty acid β-oxidation, are amongst those whose expression is upregulated by TORC1 activity (Cunningham, Rodgers et al. 2007; Morita, Gravel et al. 2015), their expression levels are not the only arbiters of the rates at which these pathways operate. The activity of AMPK is also important since it inactivates ACC by phosphorylation to inhibit fatty acid synthesis and promote fatty acid β-oxidation by preventing ACC from inhibiting fatty acid import into the mitochondria (Hardie and Pan 2002). To investigate this, AMPK activity was measured in ME/CFS and control lymphoblasts by assaying the phosphorylation state of ACC. The mean ACC phosphorylation state was elevated by ~17% in ME/CFS lymphoblasts, but this elevation did not reach statistical significance (Figure 4.6D). In isolation, this result could suggest that the balance between fatty acid biosynthesis and β-oxidation is not significantly altered in ME/CFS cells. However, it remains possible that the elevation of ACC inactivation is real and sufficient to contribute to tipping the balance of fatty acid metabolism in favour of β-oxidation. This merits future investigation as it would be consistent with the elevated capacity of ME/CFS mitochondria for β-oxidation as shown by the elevated levels of the enzymes involved.

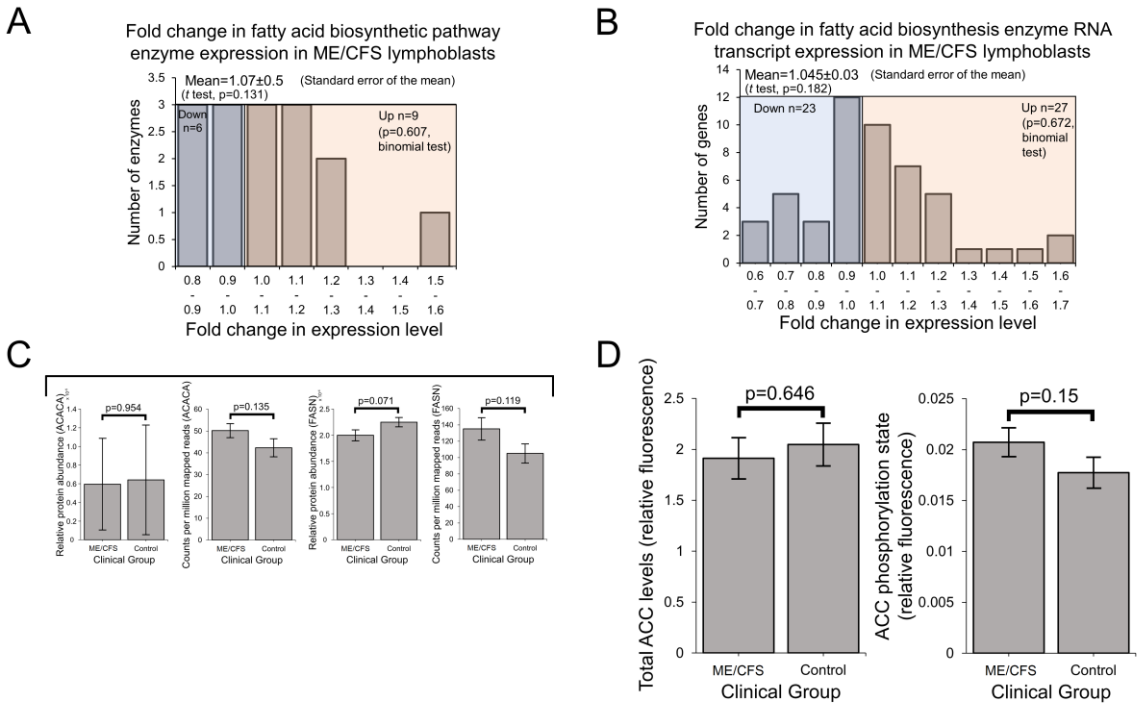

Figure 4.6: Expression of enzymes involved in mitochondrial fatty acid biosynthesis was unchanged in the whole-cell proteomes and transcriptomes of ME/CFS lymphoblasts. AMPK activity is not significantly elevated in ME/CFS lymphoblasts. Error bars represent standard error of the mean. (**A**) 15 proteins involved in fatty acid biosynthesis were detected within the whole-cell proteomes of ME/CFS and control lymphoblasts. Fold-change refers to the mean abundance of a given protein in the CFS group divided by the mean abundance in the control group. The proportion of detected proteins that were differentially expressed (binomial test with H_o set to 0.5) and the average extent of any differences (single sample *t* test with H_o m = 1) were not statistically significant. Each cell line was sampled once, or twice for a subset of healthy controls arbitrarily selected to act as an internal control between experiments in the proteomics work. Mass spectrometry proteomics experiment: ME/CFS n = 34, control n = 31. (**B**) 51 RNA transcripts encoding proteins involved in fatty acid biosynthesis were detected by RNA sequencing within the whole-cell transcriptomes of ME/CFS and control lymphoblasts. Mean fold change was calculated for the ME/CFS group versus the control average for each transcript. The proportions of reduced or elevated transcripts were not significantly different (binomial test with H_o set to 0.5) nor was the average magnitude of expression (single sample *t* test with H_o m = 1). Each cell line was sampled once. RNA sequencing transcriptomics experiment: ME/CFS n = 23, control n = 17. (**C**) The expression of ACACA and FASN, two key enzymes involved in fatty acid biosynthesis, was not significantly altered in whole cell proteomics or transcriptomics experiments (independent t-test). Relative abundance was obtained from iBAQ values normalised to the control average within the respective individual experiments. per million mapped reads were calculated for each gene transcript (**D**) AMPK activity is not significantly elevated in ME/CFS lymphoblasts. Total ACC

levels were unaltered. AMPK activity was determined by measuring the ACC phosphorylation state normalised to total ACC levels in ME/CFS lymphoblasts (n = 28) and healthy controls (n = 24). Each cell line was measured in at least three independent experiments. Fluorescence is expressed in relative terms as each experiment is normalised to an internal control cell line. AMPK activity assays were assisted with by Claire Allan.

4.2.4 Expression of Enzymes Involved in the Mitochondrial Utilisation of Glutamine, BCAAs and Essential Amino Acids is Elevated in ME/CFS Lymphoblasts

In ME/CFS, the increased utilisation of glutamine/glutamate through both the GLUD1 and GOT2 routes has been suggested by the outcomes of metabolomic studies (Armstrong, McGregor et al. 2012; Armstrong, McGregor et al. 2015; Fluge, Mella et al. 2016). If these processes are upregulated in ME/CFS, mitochondrial amino acid catabolism could be another means by which ME/CFS lymphoblasts compensate for their inefficiency in ATP synthesis. Indeed, the Electron Transfer Flavoprotein (ETF), whose expression is elevated in ME/CFS lymphoblasts (Figure 4.5C), also accepts electrons derived from the oxidation of amino acids such as lysine and tryptophan to be donated to the electron transport chain through enzymes such as glutaryl-CoA dehydrogenase (GCDH) (Besrat, Polan et al. 1969; Zhang, Frerman et al. 2006). Furthermore, TORC1, whose activity is elevated in ME/CFS lymphoblasts, is activated by glutamine catabolism (Duran and Hall 2012; Duran, Oppliger et al. 2012) and has been shown to be essential for branched-chain amino acid (BCAA) catabolism in mice (Zhen, Kitaura et al. 2016). These factors together with the observed respiratory abnormalities and elevated TCA cycle enzyme expression strongly indicate the potential importance of energy-yielding amino acid catabolism in ME/CFS lymphoblasts. Since the PANTHER analysis of upregulated proteins in ME/CFS cells revealed a significant overrepresentation of pathways involved in amino acid metabolism (Appendix Table A5.3), the expression of individual pathways and enzymes involved in these processes was more closely assessed in the whole-cell proteomes and transcriptomes.

As detailed earlier, the key enzymes involved in glutamine/glutamate degradation are 1) GLS, responsible for metabolising glutamine to glutamate, 2) GLUD1, which converts glutamate to the TCA cycle substrate α-KG and replenishes NADH, and 3) GOT2, the mitochondrial enzyme simultaneously catalysing the conversion of glutamate to aspartate and oxaloacetate to α-KG (Figure 4.1). In ME/CFS lymphoblasts, the levels of each of these

three enzymes were significantly elevated in the proteomes ($p < 0.05$ in all cases, fold increases ranging 20-27%), while the levels of the transcripts encoding them also trended upwards but did not reach statistical significance in all three cases (Figure 4.7A). Together with the absence of changes in glycolysis, this observation may confirm previous proposals that in ME/CFS, relative to glycolysis, specific amino acids and their derivatives are more heavily utilised as a mitochondrial fuel source (Armstrong, McGregor et al. 2015).

Glutamate can also be reversibly depleted or produced by the transamination activity of the branched-chain amino acid (BCAA) aminotransferases (BCATs). Like glutamate, BCAAs themselves may also be catabolised to provide the TCA cycle with substrate, the degradation of BCAAs being initiated by BCAT (Adeva-Andany, Lopez-Maside et al. 2017). BCAT catalyses the reversible conversion (by transamination) of BCAAs to their respective branched-chain ketoacids, which are precursors of TCA cycle intermediates in BCAA degradation. When the BCAT-catalysed reaction runs in the direction favouring BCAA degradation, the amino group of BCAAs is received by α-KG to generate glutamate. Since this transamination is thermodynamically reversible, BCAT-mediated synthesis of BCAAs accompanies the deamination of glutamate. This is important in metabolic regulation, since BCAAs act as signalling molecules which promote TORC1 activity when their concentrations are elevated (Neishabouri, Hutson et al. 2015; Zhenyukh, Civantos et al. 2017). Taken together with the observations of both elevated TCA cycle enzyme expression and TORC1 activity in ME/CFS lymphoblasts, these considerations highlight the importance of determining whether ME/CFS cells exhibit altered expression of enzymes involved in BCAA metabolism.

Since BCAT-catalysed transamination is reversible, changes in BCAT expression alone would not indicate the favoured steady-state direction of BCAA metabolism. However, the conversion of BCAAs to branched-chain ketoacids by BCAT is followed by the irreversible production of branched-chain Acyl-CoA derivative esters (precursors of TCA cycle intermediates) by the branched-chain ketoacid dehydrogenase (BCKDH) complex in the mitochondria (Hutson, Sweatt et al. 2005). Since this reaction is irreversible, this represents the first committed and rate-controlling step in the mitochondrial degradation of BCAAs. The expression of BCKDH complex subunits is therefore useful for inferring the favoured steady-state direction of BCAA metabolism.

To summarise: BCAT catalyses the reversible conversion (by transamination) of BCAAs to precursors of TCA cycle intermediates, also simultaneously generating glutamate. These precursors are further committed towards the TCA cycle by irreversible reactions catalysed by BCKDH.

In both the whole-cell proteomes and transcriptomes, mean expression levels of the cytosolic isoform BCAT1 were not significantly altered in ME/CFS lymphoblasts (Figure 4.7B). The transcript level of the mitochondrial isoform, BCAT2, was also unaltered (Figure 4.7B) while the protein was poorly detected in the proteomes. Thus no evidence for changes in the levels of BCAT was found in ME/CFS lymphoblasts. However, in the proteomes of ME/CFS lymphoblasts, expression levels of both BCKDH subunits were significantly elevated (BCKDHA levels by 86 ± 27%, $p = 0.028$ and BCKDHB levels by 57 ± 23%, $p = 0.031$) (Figure 4.7B). At the transcriptional level, BCKDHA showed a slight, non-significant elevation of 13 ± 6% while BCKDHB levels were significantly elevated by 30 ± 6% ($p = 0.007$) (Figure 4.7B). This upregulation of both BCKDH complex subunits strongly indicates that BCAAs are also being more heavily utilised to provide the TCA cycle with substrate. In turn this implies elevated degradation of BCAAs by mitochondrial BCAT, necessarily accompanied by increased replenishment of glutamate for utilisation by the GLUD1 or GOT2 routes, both of which are upregulated (Figure 4.7A).

Within the various pathways through which other amino acids may similarly be utilised, most of the enzymes involved were not detected, or detected at low levels in few samples. The few that were detected were present at relatively low levels compared with those present in other amino acid degradative processes such as glutaminolysis. This may be related to the reduced accessibility of these alternatives in culture medium and their less preferential metabolic utilisation compared with glutamine (Yoo, Yu et al. 2020). Of those that were detected, the expression of two was significantly altered in ME/CFS lymphoblast proteomes. While their expression was not significantly different from controls at the transcriptional level, the expression levels of GCDH and fumarylacetoacetase (FAH) were significantly elevated in ME/CFS lymphoblast proteomes, with mean levels 74 $\pm$ 21% and 61 $\pm$ 25% higher than controls, respectively (Figure 4.7C). As previously noted, GCDH catalyses the reduction of ETF as part of lysine and tryptophan degradation, thereby providing electrons towards OXPHOS (Besrat, Polan et al. 1969). On the other hand, FAH catalyses the final step of phenylalanine degradation, resulting in provision of the TCA

cycle intermediate fumarate. Together, both of these enzymes are therefore important for mediating the mitochondrial utilisation of lysine, tryptophan, and phenylalanine as alternative sources of oxidisable substrate. Thus, their elevated expression could reflect increased degradation of these amino acids to assist with driving respiration. In particular, decreased phenylalanine levels were previously reported in ME/CFS patient sera and plasma (Armstrong, McGregor et al. 2015; Germain, Barupal et al. 2020), which would be consistent with its increased degradation.

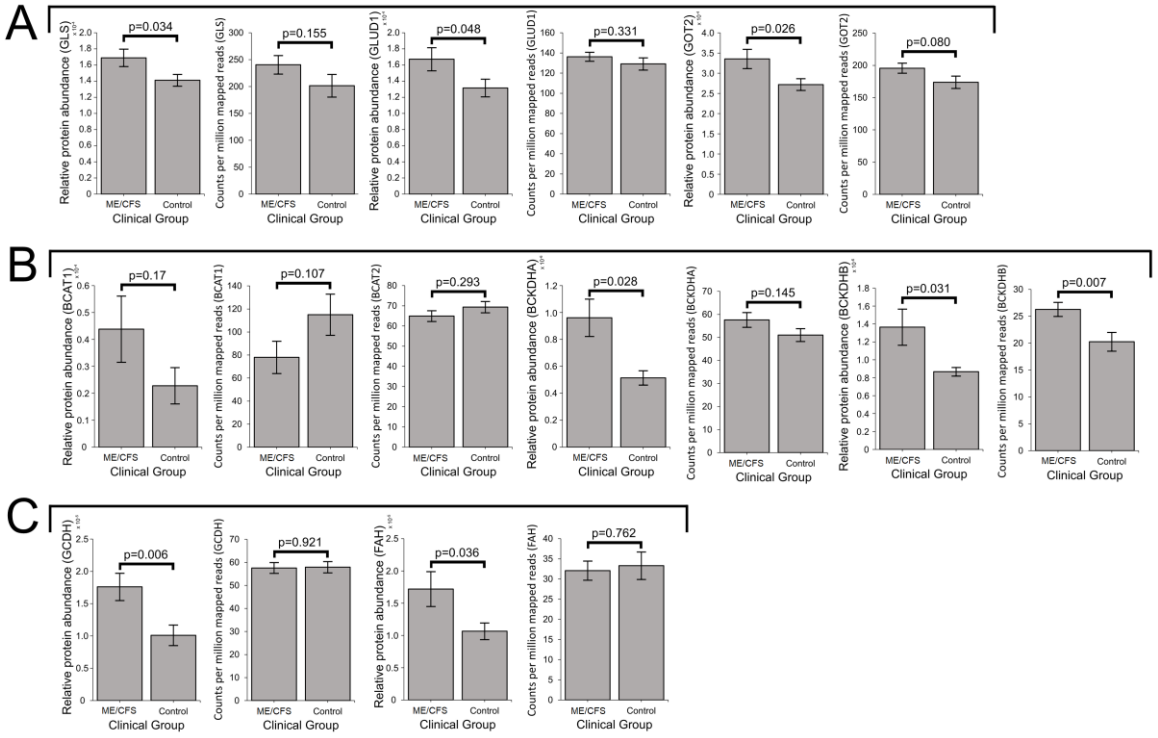

Figure 4.7: Expression of proteins involved in mitochondrial glutamine, BCAA, lysine, tryptophan and phenylalanine utilisation is elevated in ME/CFS lymphoblasts. Error bars represent standard error of the mean. RNA sequencing transcriptomics experiment: ME/CFS n = 23, control n = 17. Mass spectrometry proteomics experiment: ME/CFS n = 34, control n = 31. Each cell line was sampled once, or twice for a subset of healthy controls arbitrarily selected to act as an internal control between experiments in the mass spectrometry proteomics work. (**A**) Expression of the three enzymes mediating mitochondrial utilisation of glutamate (GLS, GLUD1 and GOT2) were elevated in the whole-cell proteomes and proteomes of ME/CFS lymphoblasts and control lymphoblasts (*t* test, $p < 0.05$ in all three cases), while each trended upwards but were not significantly elevated at the transcript level. Relative protein abundance was obtained from iBAQ values normalised to the control average within the respective individual experiments. Counts per million mapped reads were calculated for each gene transcript. (**B**) In ME/CFS lymphoblasts, the expression of BCAT1 is unchanged at the protein and transcript levels, while BCAT2 was unchanged transcriptionally and not detected at the protein level. The levels of BCKDH subunits BCKDHA and BCKDHB are both significantly elevated at the transcriptional and protein levels (*t*

test, $p < 0.05$), with the exception of BCKDHA transcripts. Relative protein abundance was obtained from iBAQ values normalised to the control average within the respective individual experiments. Counts per million mapped reads were calculated for each gene transcript (**C**) The expression levels of GCDH and FAH were unchanged at the transcriptional level but elevated at the protein level (*t* test, $p < 0.05$) in ME/CFS lymphoblasts. Relative protein abundance was obtained from iBAQ values normalised to the control average within the respective individual proteomics experiments. Counts per million mapped reads were calculated for each gene transcript.

4.2.5 Expression of Proteasome Subunits is Elevated in ME/CFS Lymphoblasts

If ME/CFS lymphoblasts do catabolise such a broad array of amino acids for energy at faster rates in accordance with the elevated expression of these various enzymes, the degradation of cellular proteins could also be affected, since it could constitute an accessible source of free amino acids. This is particularly likely given that lysine, tryptophan, and phenylalanine are all essential amino acids and cannot synthesised *de novo* in human cells. While following the trend of downregulation of many pathways at the transcriptional level, expression of the proteasome complex subunits was significantly elevated in the proteomes of ME/CFS lymphoblasts compared with controls (Figures 4.8A and 4.8B), implying the upregulation of targeted protein degradation. This was not revealed in the global PANTHER pathway analysis because proteasomal protein degradation does not feature in the reactome pathways in PANTHER, but is instead treated as a subcellular location. In any case, the upregulated expression of proteasome subunits that was observed here suggests elevated intracellular protein turnover in ME/CFS lymphoblasts. As a source of free amino acids this could act to provide the inefficient mitochondria with additional oxidisable substrate. It could also reflect elevated degradation of misfolded proteins naturally accompanying the translational upregulation of many proteins in ME/CFS lymphoblasts.

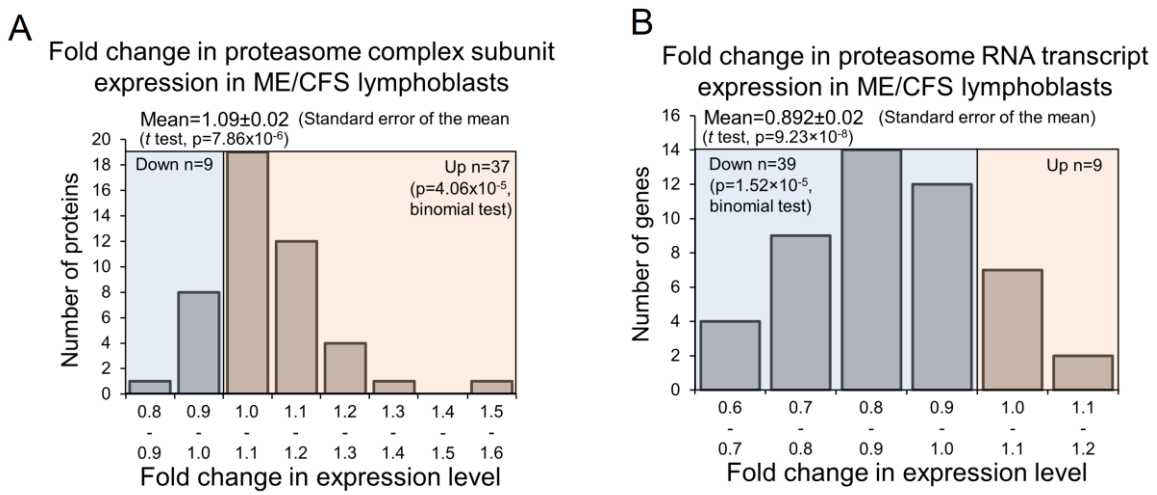

Figure 4.8: Expression of proteasome complexes in ME/CFS lymphoblasts is upregulated at the protein level but downregulated at the transcript level. Error bars represent standard error of the mean. Each cell line was sampled once, or twice for a subset of healthy controls arbitrarily selected to act as an internal control between experiments in the mass spectrometry proteomics work. (**A**) 46 proteasome complex subunits were detected within the whole-cell proteomes of ME/CFS and control lymphoblasts. Fold-change refers to the mean abundance of a given protein in the CFS group divided by the mean abundance in the control group. The fraction of detected proteins that were upregulated (binomial test with H_o set to 0.5) and the average extent of the upregulation (single sample *t* test with H_o m = 1) were statistically significant. Mass spectrometry proteomics experiment: ME/CFS n = 34, control n = 31. (**B**) 48 RNA transcripts encoding proteasome complex subunits were detected within the whole-cell transcriptomes of ME/CFS and control lymphoblasts. Fold-change refers to the mean abundance of a given transcript in the CFS group divided by the mean abundance in the control group. The fraction of detected transcripts that were downregulated (binomial test with H_o set to 0.5) and the average extent of the downregulation (single sample *t* test with H_o m = 1) were statistically significant. RNA sequencing transcriptomics experiment: ME/CFS n = 23, control n = 17.

4.3 Discussion

The results presented in this chapter demonstrate that ME/CFS cells express unchanged levels of glycolytic enzymes but elevated levels of enzymes involved in the pentose phosphate pathway, as well as protein, amino acid and fatty acid degradation. This striking pattern of dysregulated expression of catabolic enzymes provides strong support for previous metabolomics (Armstrong, McGregor et al. 2015; Fluge, Mella et al. 2016; Germain, Barupal et al. 2020), glycolytic flux (Tomas, Brown et al. 2017) and my own mitochondrial function measurements, suggesting a metabolic shift towards alternatives to

glycolytic provision of oxidisable substrates to the mitochondria. Rather than being mediated by a reduction in glycolytic function, the results presented here support that this shift is caused by an elevation of alternative catabolic pathways. The observation of an inefficiency in respiratory ATP synthesis by mitochondrial Complex V in ME/CFS cells suggests that this metabolic shift might be compensatory, while the elevated activity of TORC1 (and possibly AMPK) suggest that it is mediated by cellular stress signalling pathways.

A feature of these results is the striking difference in the pattern of expression changes at the RNA and protein levels. The proteomics revealed a broad pattern of elevated expression of proteins involved in alternatives to glycolytic provision and catabolism of oxidisable substrates for mitochondrial respiration. By contrast, the levels of transcripts encoding these proteins were, in many cases, either unchanged or decreased. This is an unexpected but important insight into the underlying cytopathological mechanisms of ME/CFS. It suggests that the overall pattern of dysregulation in ME/CFS cells is a result of a network of normally homeostatic pathways, including competing antagonistic elements like elevated TORC1 and AMPK activities, that regulate gene expression and metabolism at the transcriptional, translational and posttranslational levels (Hindupur, Gonzalez et al. 2015). The major pathways that were found to be dysregulated in this way are β-oxidation of fatty acids, glutamine metabolism, branched-chain amino acid catabolism and proteasomal protein degradation.

4.3.1 Preferential Fatty Acid β-oxidation and Dysregulated Intracellular Energy-Stress Signalling

Mitochondrial enzymes involved in the β-oxidation of fatty acids are amongst the many proteins whose expression is upregulated by PGC1α and thus indirectly by TORC1. Fatty acid β-oxidation provides acetyl-CoA to the TCA cycle, as does glycolysis, but it yields more ATP per oxidised carbon than does glycolysis. This also makes thermodynamic sense, given the more highly reduced state of the carbons in fatty acid chains compared to those in sugar molecules. It has been proposed by others that ME/CFS cells could shift their metabolism in favour of fatty acid β-oxidation because of a deficiency in glycolysis (Armstrong, McGregor et al. 2015; Mandarano, Maya et al. 2019) or PDH which partially oxidises pyruvate and supplies acetyl-CoA to the TCA cycle (Fluge, Mella et al. 2016). The

PPP is another potential alternative, which can oxidise sugars in the cytosol to generate reducing power that can be transported into the mitochondria to drive electron transport. My results support the existence of a metabolic shift, but no deficiencies in glycolysis rates, glycolytic reserve or glycolytic capacity were observed. Although there have been reports of reduced glycolytic reserve in a small sample of quiescent ME/CFS NK cells (Nguyen, Staines et al. 2018), this contrasts with reports by others (Tomas, Brown et al. 2017) and my own observations here, both of which are consistent in this regard and used larger sample sizes. Instead of impaired glycolytic capacity driving the shift in metabolism, my results suggest that the change may be driven by dysregulated energy-stress signalling and elevated usage of alternatives such as the β-oxidation of fatty acids and the PPP.

In addition to the other β-oxidation enzymes which were found to be upregulated, more highly expressed enzymes such as very long-chain specific acyl-CoA dehydrogenase (ACADVL) and acyl-CoA Oxidase 1 (ACOX1) suggest elevated VLCFA utilisation. This is consistent with the decreased sphingolipids in ME/CFS patient plasma reported by Naviaux *et al.* (Naviaux, Naviaux et al. 2016), since VLCFA are derived from these. Similarly, elevated fatty acid β-oxidation briefly suggested in metabolomics work by others (Germain, Barupal et al. 2020) is also consistent with my cellular observations here, if the rates of fatty acid β-oxidation are indeed upregulated in accordance with expression of the enzymes involved. Sweetman *et al.* observed elevated levels of enzymes involved in ketone body metabolism in the proteomes of ME/CFS PBMCs, which could indicate increased oxidation of fatty acids and their derivatives through the TCA cycle (Sweetman, Kleffmann et al. 2020). More strikingly within this same study, acyl-CoA dehydrogenases and the beta subunit of mitochondrial trifunctional enzyme (HADHB), specifically, were elevated in their expression in PBMCs (Sweetman, Kleffmann et al. 2020) – an observation shared in my own work here with lymphoblasts. This is in addition to shared observations of elevated expression of OXPHOS complex subunits - prominently Complexes I and V - and proteins in substrate-providing pathways such as the TCA cycle (Sweetman, Kleffmann et al. 2020). Since the Sweetman study examined nonimmortalised PBMCs (from which lymphoblasts are derived), this confirms that the upregulated respiratory capacity and upregulation of substrate-providing mitochondrial pathways exhibited by ME/CFS lymphoblasts is present independent of immortalisation.

Despite this broad agreement, there remain some discrepancies in the literature regarding fatty acid β-oxidation. The reduced FAD levels reported by Naviaux *et al.* and reduced carnitines reported by Nagy-Szakal *et al.* are interpreted as hindering fatty acid β-oxidation (Naviaux, Naviaux et al. 2016; Nagy-Szakal, Barupal et al. 2018). Since these and other previously mentioned studies draw inferences as to cellular function from the levels of blood metabolites, and my work here only investigated expression levels, more direct measures of fatty acid β-oxidation rates in a cellular context should continue to be pursued in the future. One previous study along these lines used Seahorse respirometry and reported unchanged fatty acid utilisation rates in permeabilised PBMCs from ME/CFS patients (Tomas, Brown et al. 2019). However, the metabolic quiescence and greater death rates of ME/CFS lymphocytes which was demonstrated in Chapter 3 may have obscured differences in this study, as may have the loss of cytoplasmic context due to permeabilisation. Respiration rates provisioned by fatty acid utilisation were also found to be unchanged in skeletal muscle cells from ME/CFS patients, contrary to the authors' expectations of elevated, compensatory β-oxidation as part of a shift away from glucose metabolism (Tomas, Elson et al. 2020). The expected increase may have been absent due the reduced exercise that ME/CFS patients can undertake, since exercise upregulates mitochondrial biogenesis and function in muscle (O'Neill, Maarbjerg et al. 2011). Another possibility is that metabolism by proliferative cells (exemplified by lymphoblasts) and non-proliferative cells (exemplified by muscle cells) in ME/CFS differ in their patterns of substrate utilisation or in their capacity to be metabolically adaptive. Direct assays of fatty acid utilisation rates in lymphoblasts and of protein expression in muscle cells are therefore needed in future studies to confirm whether the rates of fatty acid β-oxidation and expression of the involved enzymes are altered in concert with one another in both ME/CFS lymphoblasts and muscle cells.

Accompanying the upregulation of β-oxidation enzymes, a statistically non-significant ~17% increase in the level of phosphorylation of acetyl-CoA carboxylase (ACC) was observed in ME/CFS lymphoblasts. If confirmed in future work, this possible increase in AMP-activated protein kinase (AMPK) inhibition of ACC would suggest a shift towards catabolism rather than biosynthesis of fatty acids. On the other hand, mammalian target of rapamycin complex 1 (TORC1) is known to activate the transcription factor sterol regulatory element-binding protein-1 (SREBP-1) as part of the Akt signalling pathway and to thereby upregulate expression of ACC and fatty acid synthase (FASN) and fatty acid

biosynthesis (Peng, Golub et al. 2002; Brown, Stefanovic-Racic et al. 2007; Porstmann, Santos et al. 2008). Since TORC1 is chronically hyperactive in ME/CFS lymphoblasts (Missailidis, Annesley et al. 2020), elevated levels of the ACC1 and FASN transcripts were expected. It was found that both trended upwards in ME/CFS lymphoblasts but did not reach statistical significance. Nonetheless the results are consistent with the elevation of TORC1 activity and downstream activation of SREBP-1. SREBP-regulated transcription was amongst the pathways found to be upregulated in the PANTHER analysis of the transcriptomics data (Table 4.1). Despite this possible upregulation of ACC and FASN transcription, no evidence was found of elevated levels of either protein (proteomics and plate reader assays). If anything, these trended downwards (Figure 4.6) and, if confirmed in future work, this would also suggest a metabolic shift in favour of fatty acid catabolism.

4.3.2 Dysregulation of Glutamine Metabolism

The elevated expression of enzymes involved in mitochondrial glutamine degradation which I have observed here is consistent with the reductions in blood glutamine levels previously reported in ME/CFS patients (Armstrong, McGregor et al. 2012; Armstrong, McGregor et al. 2015; Fluge, Mella et al. 2016). This strongly suggests elevated usage of glutamine as a mitochondrial substrate by ME/CFS cells. Such dysregulation of glutamine metabolism would have far-reaching consequences given its importance in many cellular processes.

While also serving to replenish metabolic intermediates and reducing equivalents to aid with driving respiration, mitochondrial glutamine degradation itself activates TORC1 signalling (Duran and Hall 2012; Duran, Oppliger et al. 2012). This is thought to occur following glutamate deamination to α-KG by glutamate dehydrogenase (GLUD1) (Duran and Hall 2012), one of the enzymes whose expression was found is elevated. The α-KG is shuttled into the cytosol by the mitochondrial transporter protein SLC25A11 (Stine and Dang 2020) where it activates TORC1 via the activation of prolyl hydroxylases (Duran, MacKenzie et al. 2013). While no members of the prolyl hydroxylase family were detected in the whole-cell proteomics experiments, SLC25A11 was well detected and significantly elevated in its expression (Appendix Figure A8.1). SLC25A11 was also found to be upregulated in ME/CFS PBMCs by Sweetman *et al*. (Sweetman, Kleffmann et al. 2020).

If mitochondrial glutamine utilisation is indeed increased as suggested by the elevated expression of the enzymes involved, it could contribute to the chronic hyperactivation of TORC1 in ME/CFS lymphoblasts. This is particularly likely given the most potent amino acid activator of TORC1 (leucine) (Hara, Yonezawa et al. 1998) has been proposed to do so specifically by allosteric activation of GLUD1 and upregulation of mitochondrial glutamine catabolism (Duran, Oppliger et al. 2012). Further work should be undertaken to clarify the cause-effect relationships involved in TORC1 activation in ME/CFS lymphoblasts.

Increased glutamate flux to aspartate catalysed by GOT2 is suggested in my results by the elevation of mitochondrial aspartate aminotransferase (GOT2) expression and has been proposed in metabolomic studies by others (Armstrong, McGregor et al. 2015). As earlier described, this mechanism is an important component of the malate-aspartate shuttle (MAS) which balances cytosolic and mitochondrial redox status. In ME/CFS lymphoblasts, the cytoplasmic enzyme malate dehydrogenase (MDH1) which is critical in the MAS was also elevated in its expression (Appendix Figures A7.1A and A8.1). While the MAS is important for providing reducing equivalents for OXPHOS, its functions are also necessary to facilitate other dysregulated processes which provide ME/CFS mitochondria with oxidisable substrate, such as peroxisomal fatty acid β-oxidation. Peroxisomal β-oxidation generates NADH and is sustainable when mitochondrial shuttling mechanisms are available to oxidise NADH back to NAD^+ (Wanders, Waterham et al. 2015). Increased MAS activity in ME/CFS lymphoblasts would therefore act not only to support respiration directly by the replenishment of mitochondrial reducing equivalents, but would also indirectly assist with providing the TCA cycle with acetyl-CoA derived from alternative sources such as VLCFA.

The elevated expression of these enzymes which was observed in ME/CFS lymphoblasts adds to the accumulating body of evidence from proteomics and metabolomics supporting hypercatabolism of glutamine in ME/CFS cells, so direct assays of glutamine utilisation rates in ME/CFS lymphoblasts or other metabolically active cell types are warranted in future work to confirm this. It will be important to assess this in actively metabolising, proliferative cells given that prior work by others found no difference in glutamine-assisted respiration in metabolically quiescent, permeabilised PBMCs and a small sample of permeabilised myotubes (Tomas, Brown et al. 2019). Since conventional mammalian cell

culture medium is supplemented with glutamine in physiological abundance to satisfy proliferative cell metabolism programmes (Wise, DeBerardinis et al. 2008), it would also be useful to test the effects of varying glutamine availability in culture on ME/CFS and control lymphoblasts.

Glutamine-derived α-KG is critical for the induction of epigenetic modifications by DNA and histone demethylases (Schvartzman, Thompson et al. 2018). Because of this, increased usage of glutamine and TCA cycle intermediates to drive mitochondrial respiration could be associated with changes in the levels of DNA and histone methylation. This could be important given the large number of upregulated and even larger number of downregulated transcripts in the ME/CFS lymphoblast transcriptomes. Multiple studies examining DNA methylation in ME/CFS patients have taken place in recent years (Brenu 2014; de Vega, Vernon et al. 2014; de Vega, Herrera et al. 2017; de Vega, Erdman et al. 2018; Trivedi, Oltra et al. 2018). These studies examining differential methylation status have been recently reviewed, with the proportions of differentially hypo- or hyper-methylated sites in ME/CFS being inconsistent across studies (Almenar-Perez, Ovejero et al. 2019). More recently, Helliwell *et al* conducted the first epigenetic study to employ reduced representation bisulphite sequencing, which is capable of greater CpG site coverage than previous array based methods (Helliwell, Sweetman et al. 2020). This study found significant differences in similar numbers of both hypo- and hyper-methylated sites in the genomes of PBMCs from ME/CFS patients, suggesting that significant epigenetic dysregulation is present but does not specifically favour hypo- or hyper-methylation. This contrasts with my observation of significantly more downregulated than upregulated transcripts in ME/CFS lymphoblasts.

Within the regulatory regions of protein-coding genes investigated in the Helliwell study, it is worthwhile noting that the gene encoding the Complex 1 subunit NDUFA11 was hypomethylated (Helliwell, Sweetman et al. 2020). This is consistent with the elevated Complex 1 expression evident in my study of lymphoblasts as well as the same authors' study of PBMCs (Sweetman, Kleffmann et al. 2020). Continued epigenetic studies utilising different cell types would be valuable, since it may be possible that in proliferative cell types such as lymphoblasts, factors such as altered gene expression programmes or glutamine depletion are accentuated and thus may impact DNA methylation status to a greater degree than in PBMCs. Of course, the reverse may also be the case given that EBV

immortalisation overwrites many epigenetic alterations while others are preserved (Ghosh Roy, Robertson et al. 2016).

4.3.3 Dysregulated Branched-Chain Amino Acid and Protein Degradative Pathways

Upregulation of the branched-chain ketoacid dehydrogenase (BCKDH) complex in ME/CFS lymphoblasts strongly indicates elevated mitochondrial catabolism of branched-chain amino acids (BCAAs) as a source of oxidisable substrate and TCA cycle intermediates. It has been shown in mice that TORC1 function is essential for stimulating BCKDH degradation of BCAAs, since treatment with the TORC1 inhibitor rapamycin suppressed activation of the BCKDH complex (Zhen, Kitaura et al. 2016). Since TORC1 is hyperactive in ME/CFS lymphoblasts, it was expected and indeed observed that expression of BCKDH was elevated in the ME/CFS proteomes. However, the increased degradation and depletion of BCAA that this would produce would not contribute to activation of TORC1, since *elevated* cellular BCAA concentrations activate TORC1 (Neishabouri, Hutson et al. 2015). It seems likely that TORC1 activity upregulates BCAA degradation while TORC1 itself is activated by other phenomena in ME/CFS lymphoblasts, such as the increased mitochondrial degradation of glutamine.

BCKDH activity is also regulated by inhibitory phosphorylation by its kinase BCKDK (Harris, Hawes et al. 1997), but the levels of BCKDK in ME/CFS lymphoblasts were not significantly different from those of healthy controls (Appendix Figure A8.1). It would be valuable to directly measure the rates of BCAA utilisation in ME/CFS lymphoblasts to confirm the directional shift in mitochondrial BCAA metabolism that is indicated by elevated BCKDH expression.

A source of BCAAs and other amino acids, both as oxidisable substrates for the mitochondria and as activators of TORC1 is proteolysis. Proteolysis mediated by the ubiquitin-proteasome system results in the targeted degradation of intracellular proteins and the release of free amino acids. It is a normal response to insufficient caloric intake and is dysregulated in many diseases (Lecker, Goldberg et al. 2006). The elevated expression of proteasome subunits and assembly factors in ME/CFS lymphoblasts suggests that targeted protein degradation is upregulated. The recent proteomic study by Sweetman *et al.* (Sweetman, Kleffmann et al. 2020) also reported elevated expression of proteasome

subunits and assembly factors in ME/CFS PBMCs. Together with my results this provides compelling evidence that the ubiquitin-proteasome system is upregulated in lymphoid cells from ME/CFS patients. This would not only act to provide free amino acids, but may also be necessary to degrade the higher number of misfolded proteins which would naturally accompany the translational upregulation of many proteins in ME/CFS lymphoblasts. Since enzymes involved in the autophagic degradation of proteins were poorly detected in the whole-cell proteomes, it is uncertain whether the degradation of intracellular proteins by autophagy is also upregulated.

Autophagy is stimulated by activation of the serine/threonine-protein kinase Ulk1 by AMPK, and inhibited by TORC1, while TORC1 itself is inhibited by AMPK activity (Kim, Kundu et al. 2011). However, concurrent activation of AMPK and TORC1 can still occur and result in sustained autophagy (Narita, Young et al. 2011; Dalle Pezze, Ruf et al. 2016). This could meet the need to degrade the increased number of misfolded proteins which naturally accompany the upregulated translation of proteins that is stimulated by TORC1 (Conn and Qian 2011; Ciechanover and Kwon 2015), or to catabolically replenish metabolic intermediates used to support proliferative cell metabolism (Kaur and Debnath 2015), such as those utilised in the TCA cycle. Given that the elevation of mean AMPK activity levels did not reach statistical significance, and that this occurred alongside elevated TORC1 activity in ME/CFS lymphoblasts, it is unclear whether to expect autophagy to be increased or decreased in these cells. Autophagy in ME/CFS would therefore benefit from future study.

4.4 Conclusions

This chapter aimed to examine in detail the pathways which provide oxidisable substrate to the mitochondria in ME/CFS lymphoblasts. Unchanged levels of glycolytic enzymes are consistent with unchanged rates of glycolysis also observed in these cells. My observations also demonstrate upregulated expression of enzymes involved in the PPP and mitochondrial degradation of amino acids for energy. Together these findings strengthen the proposal that ME/CFS lymphoblasts utilise specific mitochondrial substrate-providing pathways more highly in an “attempt” to compensate for their respiratory inefficiency by Complex V. Many of the pathways or proteins upregulated in my proteomic dataset overlap with recent work by others using nonimmortalised PBMCs (Sweetman, Kleffmann et al. 2020),

strongly indicating that these changes are inherent to lymphoid cells from ME/CFS patients. Combined analysis with my transcriptomic dataset indicates the upregulated expression of many mitochondrial proteins occurs at the translational level, likely stimulated by TORC1 signalling. My early exploratory analysis of both datasets also indicated the broad activation of immunological pathways in ME/CFS lymphoblasts, which provides a basis for future hypotheses and examination. In addition, the 259 proteins and 2243 transcripts which were found to be significantly altered in expression, even after correction for multiple comparisons, highlight the possibility that diagnostic panels of differentially expressed genes may be successfully used in blood biomarker discovery work. The next chapter will focus on testing the power of these and the other key abnormalities to discriminate between ME/CFS and control PBMCs and lymphoblasts. The aim is to identify reliable cell-based blood biomarkers of disease which are informed by these new insights into the underlying cytopathology.

5.0 Identifying Cell-Based Blood Biomarkers for ME/CFS

5.1 Introduction

ME/CFS is amongst the chronic diseases which most adversely affect quality of life (Falk Hvidberg, Brinth et al. 2015). Despite this, diagnosis is often a slow process and, in the absence of a gold standard diagnostic biomarker, relies on internationally varying case criteria. The most commonly used definitions require the presence of post-exertional malaise for diagnosis, accompanied by combinations of other, variably presenting symptoms (Fukuda, Straus et al. 1994; Carruthers, Jain et al. 2003; Carruthers, van de Sande et al. 2011). Dependence on these cumbersome and varying definitions, which likely capture heterogenous patient populations, has presented a longstanding challenge for patients, clinical practice and the substantial body of ME/CFS research. The identification of robust biomarkers has consequently been one of the most recurring pursuits in the field, since it would allow for more rapid, specific and sensitive diagnoses of patients. While past and ongoing attempts at identifying such a diagnostic solution are numerous, none have yet resulted in a clinically proven biomarker of ME/CFS. It is therefore imperative that new diagnostic tools continue to be sought.

To combat the subjectivity introduced by self-reported symptom scales, more objective clinical measures have been explored previously, such as hand grip strength (Nacul, Mudie et al. 2018) or orthostatic intolerance (Richardson, Lewis et al. 2018). These physical measures have been demonstrated to have value in stratifying ME/CFS patients by disease state/severity and in aiding the separation of patients from healthy subjects. Measures of physical ability may, however, be confounded by other conditions. Such tools are therefore very useful for the clinical characterisation of patients but are not proven specific to this disease. This highlights the unmet need for specific, molecular biomarkers of ME/CFS.

Accordingly, molecular biomarkers have been pursued across multiple areas of research. For example, the role of the immune system in ME/CFS has been studied for decades, raising cytokines as potential biomarkers of disease whose clinical utility would be aided by their accessibility in blood (Brenu, van Driel et al. 2011; Hornig, Montoya et al. 2015; Landi, Broadhurst et al. 2016; Lidbury, Kita et al. 2017; Montoya, Holmes et al. 2017; Moneghetti, Skhiri et al. 2018; Lidbury, Kita et al. 2019). Other cytokine studies have utilised cerebrospinal fluid (Peterson, Brenu et al. 2015; Hornig, Gottschalk et al. 2016), the acquisition of which is more invasive than drawing blood, and so could be less amenable

to a routine diagnostic test. Despite the number of studies, these reports as a whole are largely inconsistent for individual cytokines (Mensah, Bansal et al. 2017; Yang, Yang et al. 2019), with initially promising candidates such as transforming growth factor beta 1 being subsequently refuted (Roerink, van der Schaaf et al. 2018). Therefore, the utility of cytokine measurements as such an ME/CFS diagnostic tool remains uncertain.

By contrast, studies reporting altered levels of metabolites in the blood of ME/CFS patients (Armstrong, McGregor et al. 2012; Armstrong, McGregor et al. 2014; Armstrong, McGregor et al. 2015; Fluge, Mella et al. 2016; Naviaux, Naviaux et al. 2016; Yamano, Sugimoto et al. 2016; Germain, Ruppert et al. 2017; Germain, Ruppert et al. 2018) are thought to reflect broader pathway alterations that are largely consistent, albeit with discrepancies in the specifics between studies (Germain, Ruppert et al. 2018). Such metabolite differences have been proposed as potential candidates for diagnostic blood tests (Armstrong, McGregor et al. 2012; Naviaux, Naviaux et al. 2016; Yamano, Sugimoto et al. 2016; Germain, Ruppert et al. 2017; Germain, Ruppert et al. 2018). One strength of a diagnostic test which measures multiple molecular parameters is that the likelihood of other diseases displaying the same biochemical pattern is low. However, the techniques utilised in these studies (mass spectrometry or nuclear magnetic resonance spectroscopy) may be subject to rapid fluctuations with patient diet and activity, as well as requiring strict sample acquisition and handling conditions (Ghini, Quaglio et al. 2019; Santos Ferreira, Maple et al. 2019) and expensive, specialised equipment. These requirements could introduce challenges in a broad clinical setting. Further investigation is therefore warranted, both to address the clinical suitability of blood-based metabolite measurements for diagnosing ME/CFS, and to better understand the remaining inconsistencies.

The ideal molecular biomarkers would be straightforward to sample and assess, and exhibit high sensitivity and specificity. For these reasons, the search for biomarkers has extended to investigating the utility of routine blood pathology tests, but the results are either inconsistent (Lidbury, Kita et al. 2017; Lidbury, Kita et al. 2019) or require further study (Nacul, de Barros et al. 2019). The recent development of a nanoneedle bioarray to measure the electrical impedance of ME/CFS PBMCs in plasma is highly promising, but requires identification of the underlying mechanism and proven specificity for ME/CFS (Esfandyarpour, Kashi et al. 2019). Therefore, the need for a simple blood-based biomarker remains currently unfulfilled.

It has long been suspected that mitochondrial dysfunction might play a role in the cytopathology, but the small number of direct investigations of this had produced confusing, contradictory results. In previous chapters, both specific mitochondrial dysfunction and cellular signalling dysregulation were demonstrated in ME/CFS patient blood-derived lymphoblasts, as well as an associated reduction in the viability in culture of *ex vivo*, stored lymphocytes from patients versus healthy controls. The discriminatory utility of these differences and others present in my whole-cell proteomic and transcriptomic datasets is now examined as the foundation of a potential blood-based diagnostic test. Subsets of the information contained within this chapter have been published in a research article (Missailidis, Sanislav et al. 2020).

5.2 Results

5.2.1 ME/CFS and Control Blood Samples Can be Distinguished by the Viability in Culture of Frozen Peripheral Blood Lymphocytes

It was shown in Chapter 3 that after recovery from frozen storage, lymphocytes from ME/CFS patients die markedly faster in culture than those from healthy controls. A time course revealed that the percentage of dead cells, and the difference between patients and controls, increased dramatically from 24 to 72 h of culture. To determine the utility of this difference in viability for distinguishing patient and control lymphocytes, logistic regression modelling and analysis was used (Table 5.1). To assess whether candidate biomarkers (such as the lymphocyte death rate) would be effective in correctly diagnosing ME/CFS in newly obtained samples, in this and all subsequent analysis 70% of the sample was randomly assigned for use as a training set, while the remaining 30% was used as a test data set. The results shown throughout reflect the outcomes when the resulting model was applied to the respective overall dataset.

The results of this analysis showed an overall error rate close to 20% (Table 5.1). However, the relative frequencies of false positives and false negatives were skewed in favour of a low fraction (<10%) of ME/CFS patients being incorrectly classed as “controls”, while about 40% of the controls were incorrectly classed as ME/CFS.

Clinical Group	Actual Count	Test Class		%
		ME/CFS	Control	Error
ME/CFS	57	52	5	8.8
Control	33	13	20	39.4
TOTAL	90	65	25	20.0

Table 5.1: Error matrix analysis of lymphocyte death rate after 48 h in culture medium.

The percentage of dead lymphocytes in culture at all three time points (24, 48 and 72 h) was also used in multiple logistic regression to determine if that approach would produce better discrimination between patients and controls (Table 5.2). The overall error rate was again close to 20%, although the frequency of false negatives was slightly higher and the frequency of false positives was slightly lower than when using the 48 h death rate alone. The results from this logistic regression analysis showed that the percentage of dead lymphocytes after 48 h culture performed just as well as regressing the viability against incubation time. The single time point assay would be simpler and cheaper to use for clinical purposes. These results suggest that lymphocyte isolation, frozen storage and subsequent testing for viability after 48 h in culture provides a reliable biomarker for distinguishing ME/CFS and healthy control blood samples.

Clinical Group	Actual Count	Test Class		%
		ME/CFS	Control	Error
ME/CFS	57	47	10	17.5
Control	33	8	25	24.2
TOTAL	90	65	25	20.0

Table 5.2: Error matrix for logistic regression analysis of lymphocyte death rate after 24, 48 and 72 h in culture medium.

During the course of the project, before being used for lymphoblast isolation or biochemical studies, lymphocytes were kept frozen at −80 °C for differing lengths of time ranging from a few days to almost 3.5 years. It has been previously reported that lymphocytes remain viable for long periods in frozen storage under similar conditions (Valeri and Pivacek 1996). Because biomarker stability is important in the face of varying circumstances, such as the time of frozen storage of the sample, it was verified that the death rate of lymphocytes

recovered from frozen storage and kept in culture for 48 h was not significantly altered by the time spent in storage (Figure 5.1).

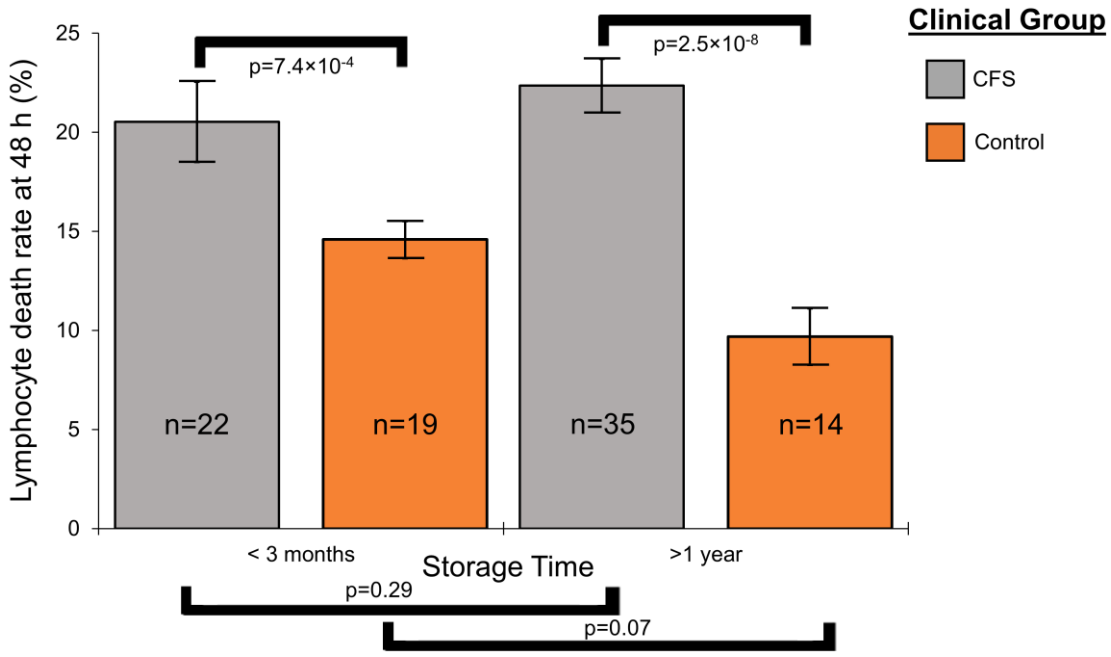

Figure 5.1: Time in frozen storage has no effect on the viability of lymphocytes after recovery and incubation in culture medium for 48 h. Some individuals were sampled on more than one occasion and some samples were tested at more than one storage time point using separately frozen aliquots. The sample sizes indicated (n) are the number of individuals shown. Since the storage time had no effect in either ME/CFS patient or control samples, multiple samples tested from the same individual were averaged for subsequent analysis. The fraction of dead cells was greater in ME/CFS lymphocytes. Significance probabilities shown are from pairwise *t* tests of the difference in means. Subsets of the lymphocyte viability counts were conducted by Oana Sanislav and Dr Sarah Annesley.

To further assess the biomarker potential of measuring the death rate of frozen lymphocytes after recovery and culture for 48 h, ROC analysis of the propensity score from the logistic regression was conducted (Figure 5.2). The results showed that using the "best" threshold (maximising the sum of the sensitivity and specificity) of 0.57 for the propensity score is effective, and this corresponded to a threshold of 16% in the 48 h lymphocyte death rate. The specificity at this threshold was 74% (26% false positives) and the sensitivity was 85% (15% false negatives). As anticipated, this ROC analysis represents a similar overall performance, but a smaller difference between sensitivity and specificity, compared to the threshold of 0.5 for the propensity score in the logistic regression analysis in Table 5.1. The area under the ROC curve (AUC), a measure of reliability, indicated that the 48 h

lymphocyte death rate could be a useful clinical test, bearing in mind that the result can be obtained from a small blood sample within a few days. For comparison with another chronic disease, clinical diagnosis of idiopathic Parkinson's disease (PD) by a neurologist is able to achieve a reliability of about 70% with high sensitivity (ca. 90%), but low specificity (ca. 60%) (relative to postmortem neuropathological diagnosis), the low specificity being partly due to confusion with similar diseases (Hughes, Daniel et al. 2002; Joutsa, Gardberg et al. 2014). More reliable diagnosis of PD can be achieved by movement disorder specialists.

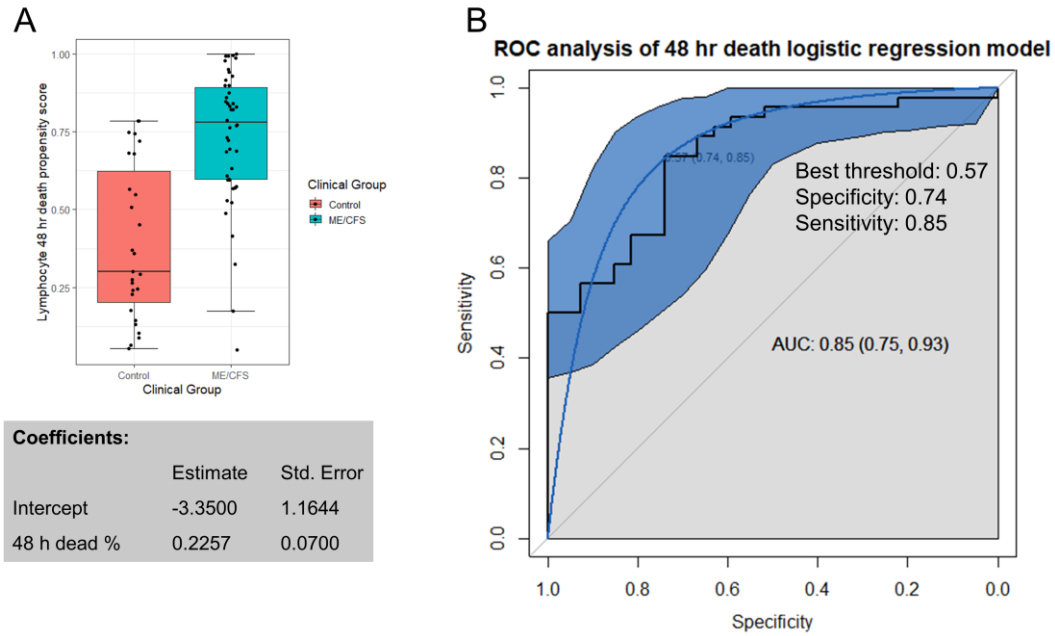

Figure 5.2: Logistic regression and ROC analysis of the percentage of dead lymphocytes after 48 h post-storage culture. (**A**) Box plot showing the distribution of the propensity score in logistic regression of the sample type against the fraction of dead lymphocytes observed after recovery from frozen storage and 48 h culture. The resulting regression coefficients are as indicated. The boxes show the median and the 25th and 75th percentiles, so that the height of the box is the interquartile range (IQR). The whiskers extend to the most extreme observations (largest and smallest) falling within ±1.5 × IQR of the box. The ME/CFS and control sample sizes were 57 and 33 individuals, respectively. Scores greater than 0.5 lead to classification of a sample as ME/CFS in the error matrix. (**B**) ROC analysis of the propensity score, plotting sensitivity (proportion of true positives) against specificity (proportion of true negatives) with 95% confidence limits (blue shading). The fractional area under the curve (AUC) is shown with 95% confidence limits. The "best" threshold for the propensity score (0.57) is shown, together with the specificity (0.74) and sensitivity (0.85) at that threshold.

5.2.2 Immortalised Lymphocytes from ME/CFS and Control Blood Samples Can be Distinguished by Mitochondrial and Cellular Respiratory Dysfunction

Although the lymphocyte death rate in culture provides a simple and potentially useful test, the diagnosis of ME/CFS would benefit from even higher sensitivity and specificity than this assay was able to provide. It was earlier shown that immortalised lymphocytes (lymphoblasts) from ME/CFS patients exhibit significant abnormalities in mitochondrial and cellular respiratory function. The key measures of mitochondrial and cellular respiratory function that were changed in patients, compared to controls, were the mitochondrial membrane potential ($\Delta\Psi_m$), the rate of O_2 consumption (OCR) by ATP synthesis and the proton leak (as fractions of the basal respiration rate), the maximum OCR by uncoupled mitochondria, the uncoupled activity of Complex I and the non-mitochondrial OCR (a surrogate measure of overall metabolic rate). These parameters were used in multiple logistic regression to determine their efficacy in distinguishing ME/CFS and control patients. Of these measures, all but $\Delta\Psi_m$ are obtained from the same respirometry experiments. For this reason, it was worthwhile to determine if $\Delta\Psi_m$ improved the discriminatory performance of the model. The results using the five respiration measures with and without $\Delta\Psi_m$ were therefore compared. The outcome (Table 5.3) showed there was a small benefit in using the assay of $\Delta\Psi_m$ in addition to the respirometry—the error matrices revealed slightly higher test specificity and sensitivity and there was an overall error rate reduction of approximately 5%.

Variables	Clinical Group	Actual Count	Test Class **ME/CFS**	**Control**	% Error
Respiratory function and $\Delta\Psi_m$	ME/CFS	44	42	2	4.5
	Control	19	6	13	31.6
	TOTAL	63	48	15	12.7
Respiratory function only	ME/CFS	44	41	3	6.8
	Control	19	8	11	42.1
	TOTAL	63	49	14	17.4

Table 5.3. Error matrix analysis of lymphoblast respiratory function and mitochondrial membrane potential ($\Delta\Psi_m$).

Figure 5.3 shows the results of ROC analysis and a box plot of the propensity scores from logistic regression of the five key respiratory parameters both with and without $\Delta\Psi_m$. At the "best" threshold of the regression propensity score without $\Delta\Psi_m$, the false positive error rate was 32% and the false negative error rate was 7%, with an AUC of 0.81. At the "best" threshold of the regression propensity score with $\Delta\Psi_m$ included in the logistic regression model, the false positive error rate was 21% and the false negative error rate was 5%, with an AUC of 0.90. However, this improvement was not statistically significant in a paired ROC comparison test ($p = 0.0685$). The ROC curve (for the ability of the lymphoblast respirometry measures to discriminate between ME/CFS patients and controls) both with and without $\Delta\Psi_m$ was not significantly different from that obtained using the 48 h lymphocyte death rate ($p = 0.563$ with $\Delta\Psi_m$, $p = 0.0963$ without $\Delta\Psi_m$). It is concluded that for diagnostic purposes, the performance of the two tests (48 h lymphocyte death rate and lymphoblast respirometry) is statistically similar and either could be used as a biomarker for ME/CFS.

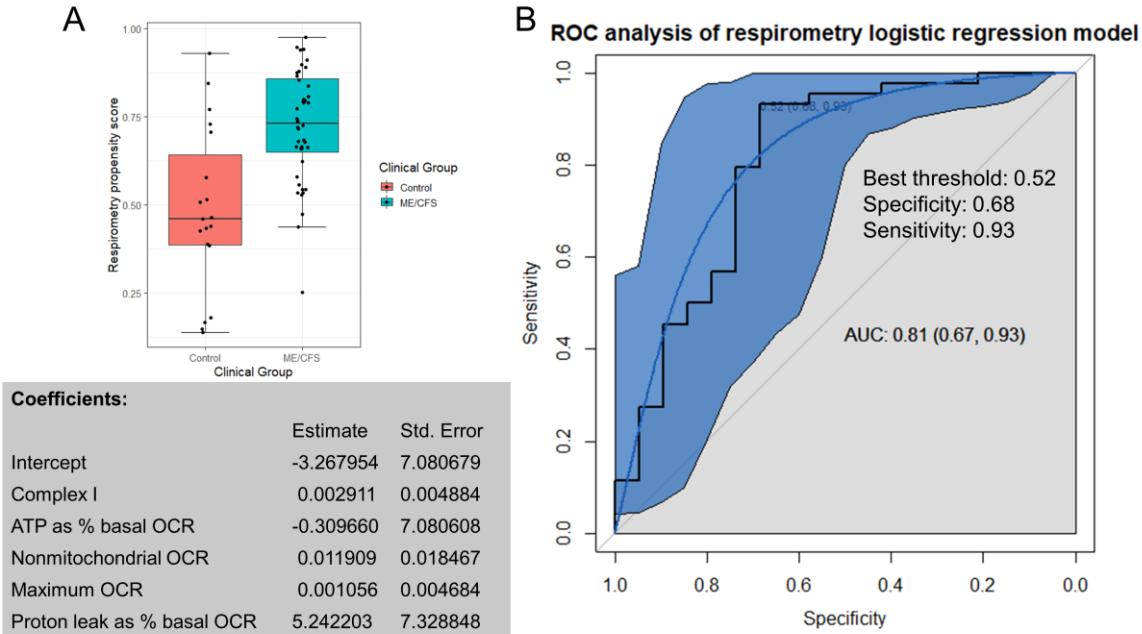

Coefficients:

	Estimate	Std. Error
Intercept	-3.267954	7.080679
Complex I	0.002911	0.004884
ATP as % basal OCR	-0.309660	7.080608
Nonmitochondrial OCR	0.011909	0.018467
Maximum OCR	0.001056	0.004684
Proton leak as % basal OCR	5.242203	7.328848

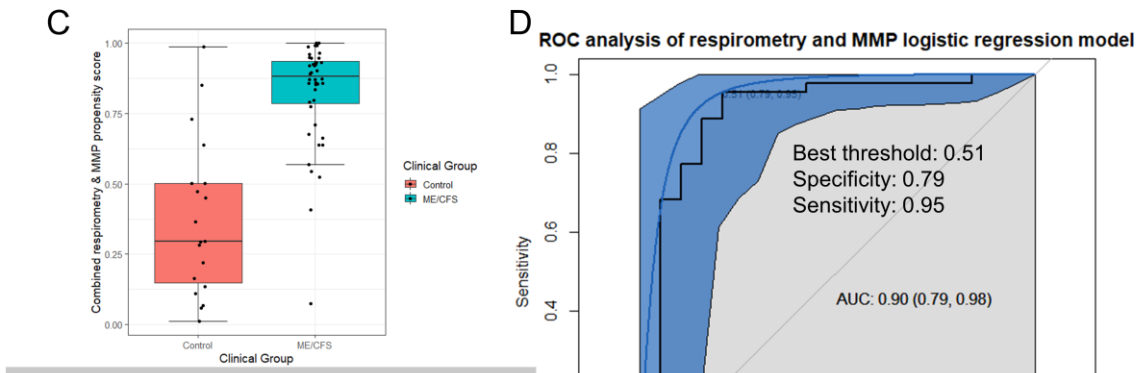

Coefficients:

	Estimate	Std. Error
Intercept	17.6005714	14.5409790
Complex I	0.0002628	0.0057151
ATP as % basal OCR	-16.1502730	13.4076860
Nonmitochondrial OCR	-0.0149765	0.0306615
Maximum OCR	0.0001247	0.0056406
Proton leak as % basal OCR	10.2265516	8.6308045
MMP	-6.7115569	3.1886148

Figure 5.3: Logistic regression and ROC analysis of lymphoblast respiration as an ME/CFS biomarker. (**A**) Box plot showing the distribution of the propensity score from logistic regression of participant type against 5 key respiratory parameters. The resulting regression coefficients are as indicated. The boxes show the median and the 25th and 75th percentiles, so that the height of the box is the interquartile range (IQR). The whiskers extend to the most extreme observations (largest and smallest) falling within ±1.5 × IQR of the box. The ME/CFS and control sample sizes were 44 and 19 individuals, respectively. Each point represents a single individual. Scores greater than 0.5 lead to classification of a sample as ME/CFS in the error matrix. (**B**) ROC analysis of the propensity score, plotting sensitivity (proportion of true positives) against specificity (proportion of true negatives) with 95% confidence limits (blue shading). The fractional area under the curve (AUC)

is shown with 95% confidence limits. The "best" threshold for the propensity score (0.52) is shown, together with the specificity (0.68) and sensitivity (0.93) at that threshold. (**C**) Box plot showing the distribution of the propensity score from logistic regression of participant type against 5 key respiratory parameters. The resulting regression coefficients are as indicated. The boxes show the median and the 25th and 75th percentiles, so that the height of the box is the interquartile range (IQR). The whiskers extend to the most extreme observations (largest and smallest) falling within ±1.5 × IQR of the box. The ME/CFS and control sample sizes were 44 and 19 individuals, respectively. Each point represents a single individual. Scores greater than 0.5 lead to classification of a sample as ME/CFS in the error matrix. (**D**) ROC analysis of the propensity score, plotting sensitivity (proportion of true positives) against specificity (proportion of true negatives) with 95% confidence limits (blue shading). The fractional area under the curve (AUC) is shown with 95% confidence limits. The "best" threshold for the propensity score (0.51) is shown, together with the specificity (0.79) and sensitivity (0.95) at that threshold.

5.2.3 Immortalised Lymphocytes from ME/CFS and Control Blood Samples Can be Distinguished by the Phosphorylation State of 4E-BP1, a TORC1 Kinase Substrate

The foregoing results showed that good biomarkers for ME/CFS are provided by both the death rates of stored lymphocytes after 48 h in culture medium and the respiratory function of cultured lymphoblasts derived from them. In both cases, the optimal thresholds were found to discriminate ME/CFS from control cells with a reliability better than 85% (AUC), with an overall error rate of less than 20%. However, in both cases, the errors at these "optimal" thresholds were not proportionately distributed between the patients and controls. Thus, although most (~80+%) of the patient samples were correctly identified as such (high sensitivity), the specificity was relatively low in that ~30-40% of the control samples were also classed incorrectly as being ME/CFS. Using ROC analysis to find the best threshold to minimise the error rates resulted in some improvement, but specificity was still lacking (0.79 using the best model). Similar analysis was therefore conducted to determine whether the elevated TORC1 activity in lymphoblasts might perform better as a biomarker of ME/CFS than the lymphocyte death rates or the lymphoblast respiratory dysfunction.

The results (Table 5.4) showed that the lymphoblast TORC1 activity assay also produced an overall error rate of about 20%. In ROC analysis (Figure 5.4) the AUC was 0.88 and at the "best" threshold of 0.43 the specificity was 0.81 and sensitivity was 0.90. This suggests that the TORC1 activity assay was no better a discriminator than the 48 h lymphocyte death rate or the lymphoblast respiratory dysfunction, which was confirmed by paired ROC curve comparisons (p = 0.673 compared with the death rate model and p = 0.837 compared with the respiratory model).

Clinical Group	Actual Count	Test Class		%
		ME/CFS	Control	Error
ME/CFS	41	32	9	22
Control	21	4	17	19
TOTAL	62	36	26	21

Table 5.4. Error matrix analysis of lymphoblast TORC1 activity.

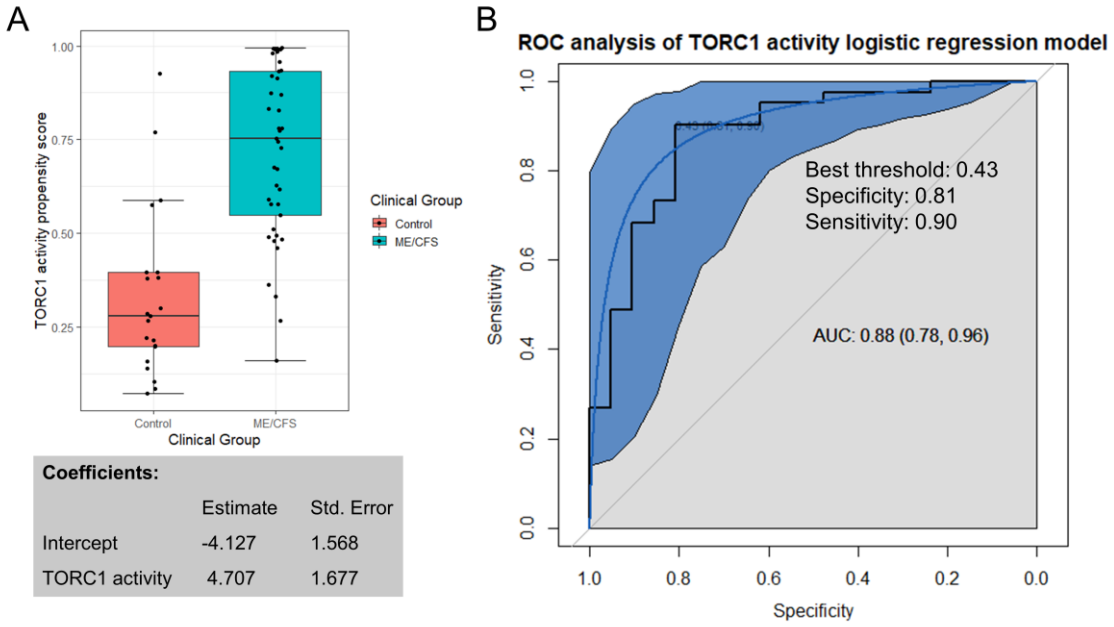

Figure 5.4: Logistic regression and ROC analysis of lymphoblast TORC1 activity. (**A**) Box plot showing the distribution of the propensity score from logistic regression of participant type against the logarithm of the relative TORC1 activity, measured as phosphorylation state of 4E-BP1 (a specific cellular target of TORC1). The resulting regression coefficients are as indicated. The boxes show the median and the 25th and 75th percentiles, so that the height of the box is the interquartile range (IQR). The whiskers extend to the most extreme observations (largest and smallest) falling within ±1.5 × IQR of the box. The ME/CFS and control sample sizes were 41 and 21 individuals, respectively. Each point represents a single individual. Scores greater than 0.5 lead to classification of a sample as ME/CFS in the error matrix. (**B**) ROC analysis of the propensity score, plotting sensitivity (proportion of true positives) against specificity (proportion of true negatives) with 95% confidence limits (blue shading). The fractional area under the curve (AUC)

is shown with 95% confidence limits. The "best" threshold for the propensity score (0.43) is shown, together with the specificity (0.81) and sensitivity (0.90) at that threshold.

5.2.4 Whole-Cell Proteomics and Transcriptomics of ME/CFS Lymphoblasts Discriminates From Controls with High Accuracy

In Chapter 4 an in-depth analysis of whole-cell proteomics and transcriptomics experiments using ME/CFS lymphoblasts was undertaken. Given that 259 proteins and 2243 transcripts were significantly altered in ME/CFS lymphoblasts even after correcting for multiple comparisons, it was likely that combinations of the most differentially-expressed gene products would have value as biomarkers.

In order to investigate this, each of the two datasets was sorted by most significantly altered (smallest Q values), and filtered by having at least a 20% mean fold change in the ME/CFS group in either direction from the healthy control mean. This produced a preliminary list of gene products from each experiment. These lists were then checked for the effects of gender and for maximum sample size coverage – no gene products in this analysis had a significant relationship with gender by ANOVA ($p > 0.05$) and all included gene products were detected in nearly every sample in the respective experiments. This process produced a working shortlist of candidate biomarkers from both the proteomics and the transcriptomics. Of the dozens of resultant gene products, discriminatory performance was relatively poor for single gene products compared with the previously analysed functional assays, often with error percentages in excess of 40%. The analysis was therefore focused on determining which *combinations* of multiple gene products yielded the best discriminatory performance.

In the proteomics, the optimal model was produced by the logistic regression model produced using the levels of the following proteins: HADHA, FARSB, G6PD, SARS, RHOG, SPTBN1, HADHB, PCMT1, RRBP1. In the error matrix this produced an overall error of 1.8% (Table 5.5). In ROC analysis of the logistic regression model, the AUC was 0.98, with the best threshold at 0.72 yielding a specificity of 0.97 and a sensitivity of 1.00 (Figure 5.5), the best performing model identified thus far.

In the transcriptomics, the optimal model was produced by logistic regression using the levels of the following transcripts: UQCC3, MGMT, SLC29A1, RMI2, ANKLE1

and PLEKHJ. In the error matrix this produced an overall error of 5% (Table 5.5). In ROC analysis of the logistic regression model, the AUC was 0.97, with the best threshold at 1.00 yielding a specificity of 1.00 and a sensitivity of 0.91 (Figure 5.5). While both tests are capable of extremely high accuracy across all parameters, this suggests that the proteomics is slightly more sensitive while the transcriptomics is slightly more specific, but neither model was significantly better than the other in paired ROC comparisons.

Variables	Clinical Group	Actual Count	Test Class		%
			ME/CFS	Control	Error
Protein levels	ME/CFS	25	25	0	0
	Control	31	1	30	3.2
	TOTAL	56	26	30	1.8
Transcript levels	ME/CFS	23	22	1	4.3
	Control	17	1	16	5.9
	TOTAL	40	23	17	5

Table 5.5. Error matrix analysis of candidate biomarkers from the whole-cell proteomics and transcriptomics datasets.

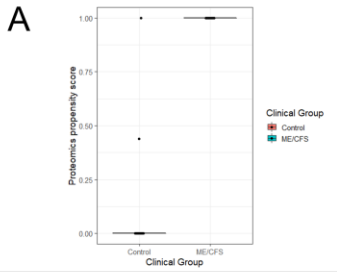

Coefficients:

	Estimate	Std. Error
Intercept	-489.5	394688.4
HADHA	2169228.3	1073259790.0
FARSB	539992.0	1975898152.6
G6PD	2230515.6	2801983686.8
SARS	1457510.2	713315020.5
RHOG	961446.2	637808301.4
SPTBN1	3279522.1	637808301.4
HADHB	-1866100.4	930502276.8
PCMT1	-2647520.9	1741515140.9
RRBP1	-5566532.7	4992071823.9

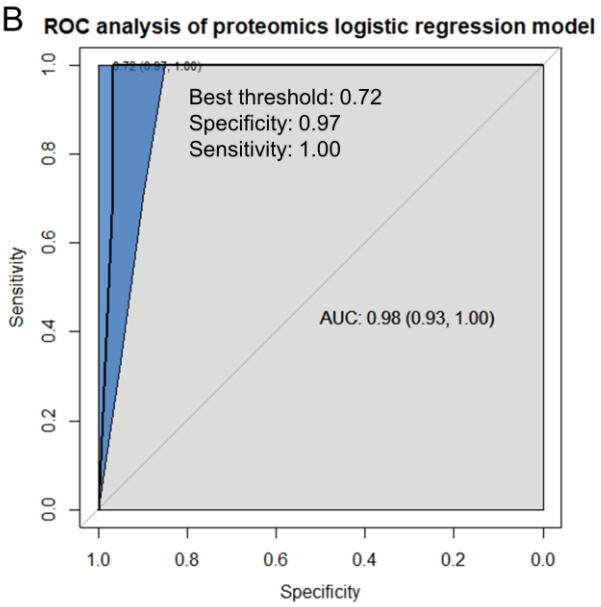

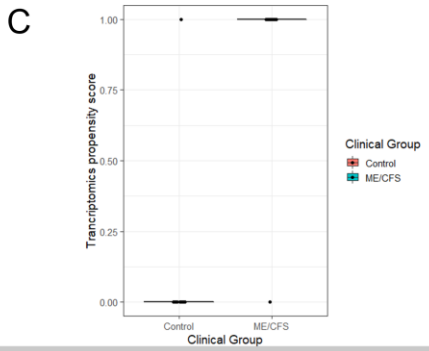

Coefficients:

	Estimate	Std. Error
Intercept	-576.472	362987.753
MGMT	-1.666	2089.053
UQCC3	-2.446	3691.933
SLC29A1	7.171	5431.699
RMI2	-8.431	5006.142
ANKLE1	10.995	9504.254

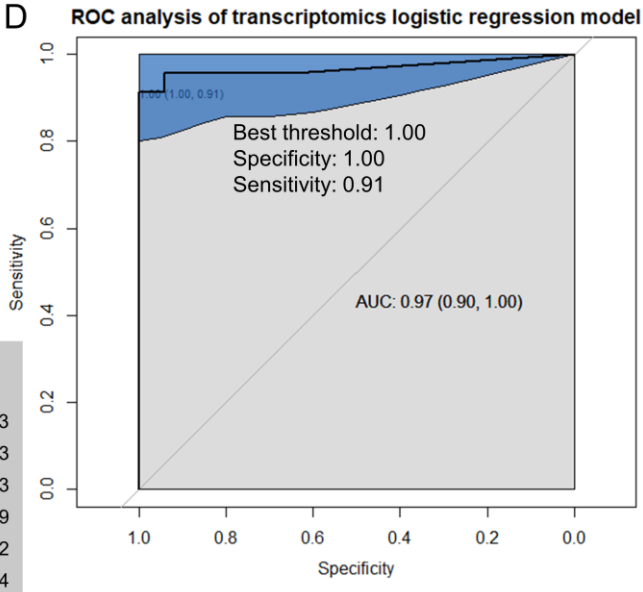

Figure 5.5: Logistic regression and ROC analysis of proteomic and transcriptomic measurements as ME/CFS biomarkers. (**A**) Box plot showing the distribution of the propensity score from logistic regression of participant type against the optimal combination of differentially-expressed proteins. The resulting regression coefficients are as indicated. The boxes show the median and the 25th and 75th percentiles, so that the height of the box is the interquartile range (IQR). The whiskers extend to the most extreme observations (largest and smallest) falling within ±1.5 × IQR of the box. The ME/CFS and control sample sizes were 25 and 31 individuals, respectively. Each point represents a single individual. Scores greater than 0.5 lead to classification of a sample as ME/CFS in the error matrix. (**B**) ROC analysis of the propensity score, plotting sensitivity (proportion of true positives) against specificity (proportion of true negatives) with 95% confidence limits (blue shading). The fractional area

under the curve (AUC) is shown with 95% confidence limits. The "best" threshold for the propensity score (0.72) is shown, together with the specificity (0.97) and sensitivity (1.00) at that threshold. (**C**) Box plot showing the distribution of the propensity score from logistic regression of participant type against the optimal combination of differentially-expressed transcripts. The resulting regression coefficients are as indicated. The boxes show the median and the 25^{th} and 75^{th} percentiles, so that the height of the box is the interquartile range (IQR). The whiskers extend to the most extreme observations (largest and smallest) falling within ±1.5 × IQR of the box. The ME/CFS and control sample sizes were 23 and 17 individuals, respectively. Each point represents a single individual. Scores greater than 0.5 lead to classification of a sample as ME/CFS in the error matrix. (**D**) ROC analysis of the propensity score, plotting sensitivity (proportion of true positives) against specificity (proportion of true negatives) with 95% confidence limits (blue shading). The fractional area under the curve (AUC) is shown with 95% confidence limits. The "best" threshold for the propensity score (1.00) is shown, together with the specificity (1.00) and sensitivity (0.91) at that threshold.

Using a combination of both datasets produced the optimal model when using the combination of HADHA, G6PD and RRBP1 protein expression and UQCC3 transcript expression. This resulted in a model producing an AUC of 0.99, with a best threshold of 0.97 yielding a specificity of 0.94 and a sensitivity of 1.00 (Figure 5.6). This was not significantly better than either experiment performed on its own. Combining protein and RNA measurements could lead to a more complex sample preparation workflow if implemented as a specific diagnostic test for ME/CFS, and so given the lack of improvement achieved by this configuration it was concluded that combined protein and RNA measurements do not constitute a preferable alternative to measurements of either only proteins or only RNA transcripts.

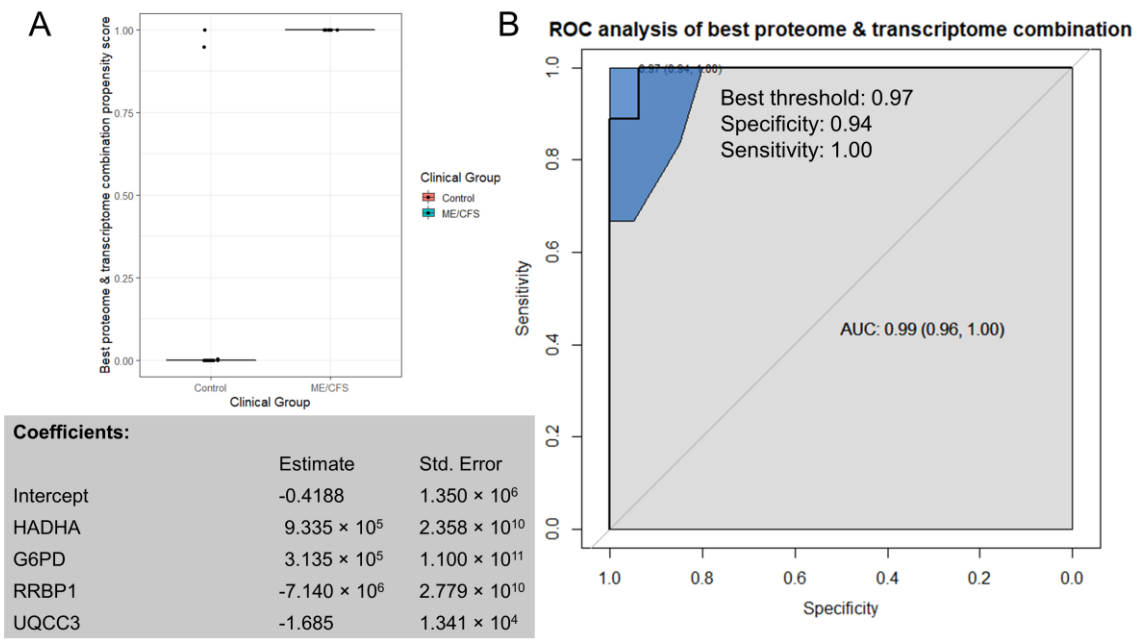

Coefficients:

	Estimate	Std. Error
Intercept	-0.4188	1.350×10^{6}
HADHA	9.335×10^{5}	2.358×10^{10}
G6PD	3.135×10^{5}	1.100×10^{11}
RRBP1	-7.140×10^{6}	2.779×10^{10}
UQCC3	-1.685	1.341×10^{4}

Figure 5.6: Logistic regression and ROC analysis of combined protein and transcript level measurements as an ME/CFS biomarker. (**A**) Box plot showing the distribution of the propensity score from logistic regression of participant type against the optimal combination of differentially-expressed proteins and transcripts. The resulting regression coefficients are as indicated. The boxes show the median and the 25th and 75th percentiles, so that the height of the box is the interquartile range (IQR). The whiskers extend to the most extreme observations (largest and smallest) falling within ±1.5 × IQR of the box. The ME/CFS and control sample sizes were 9 and 16 individuals, respectively. Each point represents a single individual. Scores greater than 0.5 lead to classification of a sample as ME/CFS in the error matrix. (**B**) ROC analysis of the propensity score, plotting sensitivity (proportion of true positives) against specificity (proportion of true negatives) with 95% confidence limits (blue shading). The fractional area under the curve (AUC) is shown with 95% confidence limits. The "best" threshold for the propensity score (0.97) is shown, together with the specificity (0.94) and sensitivity (1.00) at that threshold.

5.2.5 Combining Variables from All Measurements to Discriminate ME/CFS and Control Blood Samples with the Highest Possible Accuracy

The assays tested in the preceding sections provided good biomarkers for ME/CFS, but none were perfect discriminators between patients and controls. In pursuit of an even better discriminator, variables from all of these assays were tested in combination to identify the optimal logistic regression model (best performance with fewest assays required). This would be of extra benefit since it would involve numerous different biochemical and cellular parameters depending on the selected assay combination, likely providing greater

specificity for ME/CFS versus other conditions which may have overlapping symptoms. However, that remains to be tested in future work.

The results of this analysis (Table 5.6, Figure 5.7) showed that the best combination of variables was able to discriminate between ME/CFS patients and healthy controls with 100% accuracy in my full dataset. This accuracy was attainable with the logistic regression of as little as two measurements: the 48 h death rate of lymphocytes and the transcript levels of UQCC3 in lymphoblasts. At the "best" threshold of 0.50 in the ROC analysis, the specificity was 100% and the sensitivity was 100%. The complete absence of any detrimental overlap between the patient and control group is visible in Figure 5.7A. Various other configurations of additional transcripts performed to the same degree of "perfect" accuracy without impairing the performance of the model, suggesting that if clinically and economically practicable a simultaneous assay of multiple transcripts may be more robust than UQCC3 alone when challenged with a greater sample size and real-world variation. The combination of lymphocyte 48 h death rate and lymphoblast transcript levels may thus provide a reliable discriminator between ME/CFS and control samples. This performance exceeds that of all other known ME/CFS biomarker pursuits with the exception of the nanoneedle impedance measurement (Esfandyarpour, Kashi et al. 2019). 100% accuracy in ROC analysis was also attainable by logistic regression of a handful of protein levels (HADHA, G6PD, PCMT1, RRBP1) with the lymphocyte death rate, or by logistic regression of the respiratory abnormalities and TORC1 activity also in combination with the lymphocyte death rate (Appendix Figure A9.1). The lymphocyte death rate and lymphoblast UQCC3 transcript levels are highlighted here due to this being the simplest combination of variables and assays to achieve 100% accuracy, and therefore is the most likely combination to be clinically applicable at this stage of the analysis.

Clinical Group	Actual Count	Test Class ME/CFS	Test Class Control	% Error
ME/CFS	16	16	0	0
Control	13	0	13	0
TOTAL	29	16	13	0

Table 5.6. Error matrix analysis of combined lymphocyte 48 h death rate and lymphoblast UQCC3 transcript levels.

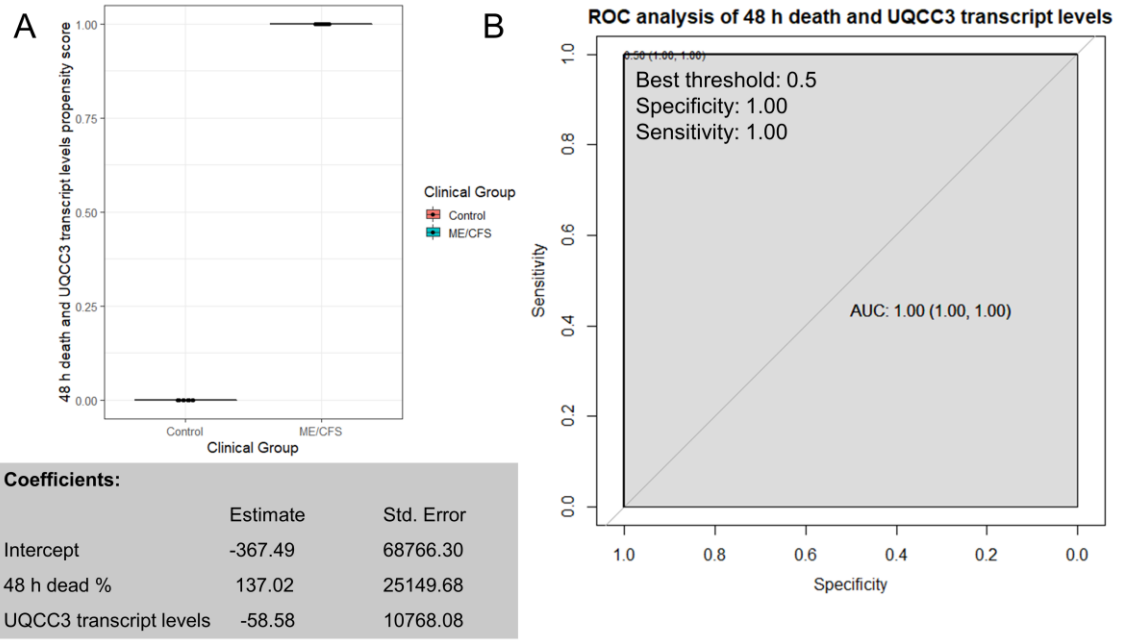

Coefficients:

	Estimate	Std. Error
Intercept	-367.49	68766.30
48 h dead %	137.02	25149.68
UQCC3 transcript levels	-58.58	10768.08

Figure 5.7: Logistic regression and ROC analysis of combined tests for lymphocyte death in culture and lymphoblast transcript levels. (**A**) Box plot showing the distribution of the propensity score from logistic regression of the percentage of dead lymphocytes after 48 h in culture and lymphoblast UQCC3 transcript levels. The resulting regression coefficients were as indicated. The boxes show the median and the 25th and 75th percentiles, so that the height of the box is the interquartile range (IQR). The whiskers extend to the most extreme observations (largest and smallest) falling within ±1.5 × IQR of the box. Each point represents a single individual. Scores greater than 0.5 lead to classification of a sample as ME/CFS in the error matrix. (**B**) ROC analysis of the propensity score, plotting sensitivity (proportion of true positives) against specificity (proportion of true negatives). The fractional area under the curve (AUC) is shown. Confidence limit calculations failed due to the complete separation between the ME/CFS and control groups (zero error to estimate). The "best" threshold for the propensity score (0.5) is shown, together with the specificity (1.0) and sensitivity (1.0) at that threshold.

5.2.6 A Protocol that Combines a Screening Test Using Lymphocyte Death Rates and the Most Effective Confirmatory Tests of Lymphoblasts

The results in the preceding sections showed that 5 different cell-based blood tests (lymphocyte death rate, lymphoblast respiratory function, lymphoblast TORC1 activity, selected protein levels and selected transcript levels) can individually provide biomarkers of ME/CFS compared to healthy controls. Of these, the lymphocyte death rate in culture could potentially provide a relatively quick test in the clinical setting, since it requires only separation and storage of the lymphocytes from a blood sample followed by incubation in

culture medium for two days. It exhibited high sensitivity but low specificity for ME/CFS and thus, would be well suited for screening purposes. These outcomes suggest a testing protocol inwhich an initial assay of lymphocyte death rate would be followed, in the case of positive results, by lymphoblast isolation and subsequent tests. In a real world setting such a staged protocol could reduce the overall time and cost of returning negative results, but has the potential downside that these could include a small percentage of true-positive ME/CFS patients. However, when combined with transcript or protein levels the 48 h death rate achieved an accuracy of 100%, a feat not achieved by any of the assays alone.

In any case, to determine the potential efficacy of such a staged protocol, I simulated it by subdividing my samples into subgroups, based on whether ME/CFS would be suspected or not from the lymphocyte death rates, using the "best" threshold from the ROC analysis of the 48 h death rate model as the cutoff criterion. Table 5.7 shows the results for these individual subgroups using the candidate confirmatory assays which earlier yielded 100% accuracy in multivariate logistic regression models alongside the 48 h death rate. The entire "suspected" or "not suspected" subsets cannot be tested in each configuration, as the analysis is only applicable to individuals for whom I have overlapping data for each tested assay (within each respective configuration).

The first configuration that was tested used UQCC3 transcript levels as the sole confirmatory test, since if successful in this application, it would be the simplest diagnostic protocol to undertake while still being 100% accurate. While each overlapping individual within the "ME/CFS suspected" subset was correctly classified by subsequent UQCC3 transcript level testing (including 2 controls which would have been misclassified by 48 h death rate alone), both ME/CFS patients incorrectly assigned to the "ME/CFS not suspected" group by the 48 h death rate assay alone were also not identified by UQCC3 transcript levels, as the sole confirmatory test. While this lead to only 2/29 individuals being misclassified (93% accuracy), improvement may be possible at a minimal practical cost to the overall protocol by the incorporation of additional transcript measurements. This test was therefore repeated with the multivariate logistic regression model of MGMT, UQCC3, SLC29A1, RMI2, ANKLE1, PLEKHJ1 as the confirmatory test. In this case, each overlapping individual in both the "ME/CFS suspected" and "ME/CFS not suspected" was correctly classified.

This staged protocol was also tested using the combination of proteins found to yield 100% accuracy when combined with 48 h death rate in multivariate logistic regression (HADHA, G6PD, PCMT1, RRBP1). These protein levels as a confirmatory test performed similarly well to the combined transcript levels with 0% error across all categories, however could not be used to follow-up false-negative ME/CFS patients from the 48 h death rate, as there was no overlap between the two assays within this subset of samples.

The results from this analysis indicate the likely success of a staged protocol as a cost- and time-saving measure, however with the downside of a 15% false negative rate from the death assay (Figure 5.2B) which in the current dataset is entirely avoidable when always followed up by confirmatory testing (Tables 5.6 & 5.7, Figure 5.7B). However, this false negative rate is likely to be minimised in clinical scenarios involving ME/CFS symptom presentation, since doctor and patient may together elect to pursue the second round of confirmatory tests in the event of a negative result.

Method	Clinical Group	Actual Count	Test Class ME/CFS	Test Class Control	% Error
"ME/CFS suspected"					
UQCC3 transcript levels	ME/CFS	14	14	0	0
	Control	2	0	2	0
	TOTAL	16	14	2	0
"ME/CFS not suspected"					
UQCC3 transcript levels	ME/CFS	2	0	2	100
	Control	11	0	11	0
	TOTAL	13	0	13	15.4
"ME/CFS suspected"					
MGMT, UQCC3, SLC29A1, RMI2, ANKLE1, PLEKHJ1 transcript levels	ME/CFS	14	14	0	0
	Control	2	0	2	0
	TOTAL	16	14	2	0
"ME/CFS not suspected"					
MGMT, UQCC3, SLC29A1, RMI2, ANKLE1, PLEKHJ1 transcript levels	ME/CFS	2	2	0	0
	Control	11	0	11	0
	TOTAL	13	2	11	0
"ME/CFS suspected"					
HADHA, G6PD, PCMT1, RRBP1 levels	ME/CFS	13	13	0	0
	Control	6	0	6	0
	TOTAL	19	13	6	0
"ME/CFS not suspected"					
	ME/CFS	0	0	0	N/A*
	Control	15	0	15	0

HADHA, G6PD, PCMT1, RRBP1 levels	TOTAL	15	0	15	0

*Indicates that there was no overlap in ME/CFS patients between the "ME/CFS not suspected" subset and the proteomics samples; thus no patients were assessed in this particular comparison.

Table 5.7. Error matrix analysis of confirmatory tests for participants whose lymphocytes had been tested for the rate of cell death in culture. On the basis of the lymphocyte death rate test, samples were classed as "ME/CFS suspected" or "ME/CFS not suspected". They were then classified on the basis of UQCC3 transcript levels (top panel), a combination by logistic regression of transcript levels for 6 different genes (middle panel) or a combination of 4 different protein levels. Note that lymphocyte death rates, transcriptomics data and proteomics data was not available for every sample, so that the sample subset sizes are different for the different combinations of experiments.

5.3. Discussion

The diagnosis of ME/CFS currently requires patients to exhibit, for at least six months, the hallmark symptoms of chronic fatigue and post-exertional malaise that cannot be explained by other conditions. For patients, physicians and the health care system, this diagnosis - that depends on exclusion of other illnesses - is a long, frustrating and potentially expensive process. Suitable diagnostic biomarkers have not yet been identified, although a recent report of an altered electrical impedance response to salt stress in patient lymphocytes looks highly promising, although requiring further validation (Esfandyarpour, Kashi et al. 2019). In previous chapters it was demonstrated that *ex vivo* lymphocytes from ME/CFS patients exhibit an elevated death rate in culture after recovery from frozen storage and that lymphoblastoid cell lines (lymphoblasts) isolated from them exhibit multiple mitochondrial and cellular stress signalling abnormalities. These abnormalities were chiefly observed in the following laboratory tests: lymphocyte death rates (viable cell staining and counting), lymphoblast mitochondrial membrane potential, lymphoblast mitochondrial respiratory function, lymphoblast TORC1 signalling activity, whole-cell proteomics and whole-cell transcriptomics. The mitochondrial respiratory dysfunction included changes in several key measures of mitochondrial activity which were applied in combination—lower efficiency of ATP synthesis, and increased "proton leak" relative to basal metabolic rate, elevated maximum rates of respiration and Complex I activity. The purpose here was to determine

if these key abnormalities in cells derived from ME/CFS patient blood samples could be used as biomarkers of disease.

5.3.1 Logistic Regression Modelling

Logistic regression modelling was used in this investigation since it is a method considered to be robust against departures of the input data from normality, equality of variances and the presence of outliers (Antonogeorgos, Panagiotakos et al. 2009). Support vector machine and neural network models were trialed and found to produce similar outcomes for all of the biomarkers tested here. To confirm that the proposed biomarkers would be effective in correctly diagnosing ME/CFS in newly obtained samples that would not be part of the original model, 70% of the sample was randomly assigned for use as a training set, while the remaining 30% was used as a test data set. Despite the fact that training the models using only 70% of the dataset inevitably makes the parameter estimates and threshold determination less powerful, the most accurate models tested with this methodology were still 100% accurate in both the training and test subsets. These results give confidence that the proposed biomarkers could be usefully deployed for diagnostic purposes.

5.3.2 Highly Accurate Biomarker Combinations

Of the biomarker tests examined here, the lymphocyte death rates are the simplest and cheapest, and would provide the quickest result in a clinical setting. It was found that the fraction of dead lymphocytes after frozen storage and culture for 48 h could distinguish between ME/CFS and control samples with a high sensitivity (85%) but with lesser specificity (74%). Although *ex vivo* lymphocyte death rates were elevated compared to controls on all three days of culture after recovery from frozen storage, assessing the proportion of dead cells in the culture at more than one time point did not improve the discriminatory value of the test.

Both the respiratory function assay and the TORC1 activity assay produced similar results to the lymphocyte death assay—high sensitivity combined with lower specificity. Additionally, the whole-cell proteomics and trancriptomics perform exceptionally well as standalone tests with respective AUC of 0.98 and 0.97, with the proteomics achieving 100% sensitivity and the transcriptomics achieving 100% specificity. Given that the frozen lymphocyte death rate has higher sensitivity than specificity, it may be more useful to

couple it with subsequent measurements of transcript rather than protein levels in a staged protocol might be more complementary than protein levels.

The best combination of the two ‘omics datasets was also capable of accurately discriminating ME/CFS patients from controls (AUC 0.99), matching the 100% sensitivity of the proteomics experiment, however with less specificity than the transcriptomics alone (94% vs 100%). Given that combining the two datasets resulted in a fewer number of samples used to construct the logistic regression model (which may have less discriminatory power when testing new samples) and in little if any improvement in overall performance, this combined ‘omics approach seems less suited for clinical implementation than either protein or transcript levels alone. This is also likely given that relying upon both protein and RNA samples in tandem may be less practicable (multiple types of sample handling, preparation and assay required).

In an attempt to find the best-performing model with the data on hand, all combinations of all 5 experiment types were tested (by logistic regression and ROC analysis), with a view to maximizing the discriminatory performance while minimizing the number of different measurements/assays required. It was found that the best-performing and simplest logistic regression model was obtained by combining the 48 h death rate with UQCC3 transcript expression. This model resulted in 100% discriminatory accuracy in the full dataset. Given this and also the relative simplicity of measuring only lymphocyte death rates and lymphoblast mRNA levels, this combination is a promising candidate for clinical application. A noteworthy alternative also achieving 100% accuracy but that is more expensive, time-consuming and expertise-requiring is the logistic regression of the respiratory abnormalities, TORC1 activity and 48 h death rate (Appendix Figure A9.1).

The best biomarker combinations identified herein achieve better accuracy and reliability (sensitivity, specificity and AUC) for discriminating ME/CFS than has been previously reported using other blood-based molecular tests (Naviaux, Naviaux et al. 2016; Yamano, Sugimoto et al. 2016; Germain, Ruppert et al. 2018) except for the recently reported lymphocyte impedance response to salt stress (Esfandyarpour, Kashi et al. 2019), the performance of which the best combinations of 48 h death rate and proteomics/transcriptomics results were able to match.

5.3.3 Practical Advantages and Considerations

Because of the time, expertise and expense associated with lymphoblast isolation and testing, it was explored whether a two-stage test would be suitable. The results suggest a test protocol which can discriminate between ME/CFS patients and healthy individuals with near-perfect accuracy. In this protocol, the frozen lymphocyte viability after 48 h in culture would be used as an initial screening test. With its high sensitivity, low cost and speed, it requires only a small blood volume allowing most of the sample to be utilised for subsequent confirmatory tests. It was also demonstrated that the test result is stable over long periods of frozen storage. These practical advantages lend great value to the protocol in a broader clinical context and set it apart from methods which would proceed directly to highly specialised testing. This in combination with subsequent lymphoblast mRNA transcript level measurements (which achieved 100% specificity on their own) could allow for the most cost-effective protocol – initial triaging based on ME/CFS lymphocyte death rate results and then confirmation by subsequent lymphoblast transcript assays. It is therefore proposed that a staged protocol combining the clinical suitability of the lymphocyte screening step and the discriminatory power of additional lymphoblast measurements provides a promising diagnostic biomarker for ME/CFS. The patient and their clinician could choose on the basis of the results from the lymphocyte death rate test, whether or not to proceed with the slower and more expensive confirmatory tests. Ultimately, the success of such a staged protocol will depend upon the real-world sensitivity of lymphocyte death rate measures or any other assay that is used as a screening step, which remains to be seen with the additional study of larger cohorts and higher throughput techniques.

It would be valuable to determine if measurements such as transcript or protein levels in ME/CFS lymphocytes are also useful for discriminatory applications as is the case with lymphoblasts. If specific transcript levels proved to be useful discriminators in lymphocytes, as they are in lymphoblasts, this would circumvent the additional cost and delay associated with immortalisation. If lymphocyte transcript or protein levels were indeed similarly useful as with the lymphoblasts, then this protocol could be further refined into an efficient single-stage test of lymphocytes only. This could form the basis of a reliable diagnostic test based solely on lymphocytes, one likely to be rapid given: a) the rapidity with which large-scale qRT-PCR testing has been successfully undertaken in Australia during the COVID-19 pandemic and b) that enzyme level measurements are

already commonplace in routine pathology work. Future work should attempt to test these possibilities and assess whether they can be successfully exploited.

One limitation of the viability assay used in this work, Trypan Blue staining, is that although it is very fast and simple in principle, it requires microscopy and cell counting by a person skilled in the art. It would be valuable in future work to determine if some of the many other cell viability assays that are commercially available might lend themselves more readily to use in a reproducible way by less skilled personnel. This would facilitate higher throughput and greater accuracy in the results in a clinical setting.

Another limitation of the tests suggested here is that it has so far been fully tested on a relatively small sample of up to 44 patients and 19 controls, which varies depending on the combination of variables applied (samples with missing variables are excluded from the multivariate logistic regression models). Because of limitations on the supply of lymphocytes and the cost of carrying out whole-cell transcriptomics and proteomics, sample sizes are reduced in assay cross-comparisons. The candidate tests identified here will need to be refined using much larger samples in order to both validate them and to refine their performance by adjusting the input and weighting variables of the logistic regression models. At this stage, it can nonetheless be concluded that the cell-based blood biomarkers used here are amongst the most promising candidates so far identified for potential use in diagnosing ME/CFS. Given that the diagnostic models proposed herein still perform so accurately despite the modest sample sizes, future work validating and refining these models appears to be promising.

A limitation of all biomarkers so far proposed for ME/CFS is that it is not yet known how specific they are versus other illnesses which cause chronic fatigue and/or post exertional malaise and with which ME/CFS may potentially be confused. It would be useful to examine the viability levels of frozen lymphocytes in similar diseases to assess how specific the elevated death rate of frozen lymphocytes is to ME/CFS patients. It has been documented previously, that frozen lymphocyte viability is also reduced in paediatric Dengue fever (Perdomo-Celis, Salgado et al. 2016). However, the strength of the frozen lymphocyte viability test is its high sensitivity as a screening step to successfully detect ME/CFS individuals and correctly triage true-positive ME/CFS samples towards subsequent confirmatory tests. It seems possible that the number and specific biological nature of these subsequent measurements means that the resulting molecular read-out is

likely to be unique to ME/CFS, particularly in combination with the patient's clinical history. To be confused with ME/CFS in subsequent confirmatory tests, other illnesses would not only need to cause reduced viability of frozen lymphocytes, they would also need to confer the same pattern of molecular abnormalities upon the derived lymphoblasts (as described in Chapters 3 & 4). It is worth noting that lymphoblasts from patients with Parkinson's disease, another complex chronic disorder, exhibit a quite different pattern of abnormalities related to mitochondrial function (Annesley, Lay et al. 2016). Of course, Parkinson's disease patients are unlikely to be confused clinically with ME/CFS patients in the first place. Thus, although the combination of cellular and molecular phenotypes reported here may well be unique to ME/CFS, it will be essential in future work to determine its specificity in relation to other, similar diseases.

5.3.4 Decreased Viability of Frozen Lymphocytes from ME/CFS Patients

Despite the clarity of the differences observed here in frozen lymphocyte viability, the underlying reason for the elevated death of ME/CFS lymphocytes after storage remains undetermined. Impaired mitochondrial respiratory function, including Complex V impairment, has long been known to result in apoptotic cell death in *ex vivo* lymphoid cells (Wolvetang, Johnson et al. 1994). In this project it has not been investigated whether the lymphocyte death observed is apoptotic or whether it is one of the other known forms of eukaryotic cell death. Whatever the specific cell death pathway involved, it may reflect an inability of ME/CFS patient cells to adequately respond to cellular damage or stress. In this case, such an insult could be introduced by freezing, which is well understood to damage biological systems by the formation of ice crystals, but has also been documented to specifically affect lymphocyte viability, function, and expression of stress response genes (Weinberg, Zhang et al. 2000; Yang, Diaz et al. 2016). While the elevated death rate of the ME/CFS lymphocytes could reflect a greater mechanical susceptibility to immediate structural damage by freezing, there remains another possibility. Compared with controls, the number of dead ME/CFS lymphocytes continued to increase at a faster rate than the controls over multiple days in culture. This suggests that underlying and ongoing cytopathological processes could be contributing towards cell death in culture of previously frozen lymphocytes.

5.4. Conclusions

In previous chapters it was shown that *ex vivo* lymphocytes from ME/CFS patients exhibit an elevated death rate in culture after recovery from frozen storage and that lymphoblastoid cell lines isolated from them exhibit multiple mitochondrial and cellular stress signalling abnormalities, and highly distinct profiles of gene expression at both the transcript and protein levels. The objective in this preliminary investigation of discriminatory power was to determine if these abnormalities could be used as blood-based biomarkers of disease. The results here demonstrate that these abnormalities are, indeed, promising candidate biomarkers, each of them able to distinguish ME/CFS patient and control samples with better than 80% reliability, and with 100% perfect accuracy possible when using the best combinations of variables available. With some tests providing very high sensitivity (correct classification of positive samples) but lower specificity (correct classification of negative samples), and other tests favouring the opposite trend (better specificity, lower sensitivity) the results suggest these tests might be most usefully deployed as synergistic components of a staged protocol depending on the practical advantages of each assay. For example, the first stage could involve a cheap, rapid and *sensitive* screening test using the frozen lymphocyte death rate. The results from this could be used by clinicians and patients to decide whether to complete the 2nd stage in which other more *specific* assays are performed in lymphoblastoid cell lines derived from the frozen lymphocytes. In any case, the candidate biomarkers tested in this chapter could evidently provide a reliable cell-based blood testing protocol to aid in ME/CFS diagnosis.

6.0 Overall Conclusions

This PhD project has both successfully fulfilled its initial aims and answered additional questions as they have arisen throughout. This iterative building of knowledge, using the same samples to address new questions, is made possible due to the phenotypic and proliferative stability of lymphoblast cell lines (Sie, Loong et al. 2009). Over the course of this project, our group's ME/CFS and counterpart control lymphoblast cohorts have been built up to a collection from 66 ME/CFs individuals and 39 healthy controls. This represents a substantial, self-renewing and, to my knowledge, internationally-unique resource from which new research can continue to answer questions arising both from this and future work. This unique capability positions the work undertaken in this PhD to blaze the trail for additional discoveries in ME/CFS without the hurdle of subject recruitment or the issue of sampling variation. This is an exciting prospect, especially given the number of new investigational avenues which have since opened and begun to be pursued following the outcomes of my initial work here.

My research successfully utilised lymphoblast cell lines created from ME/CFS patient blood to investigate mitochondrial function. related metabolic and signalling pathways, and potential biomarkers. I have shown that in ME/CFS lymphoblasts, there is an isolated inefficiency of ATP synthesis by Complex V. This is accompanied by multiple, presumably compensatory changes including increased respiratory capacity, elevated expression of a diverse array of mitochondrial proteins, elevated TORC1 activity, and non-significantly elevated AMPK activity. Extracellular acidification rate assays in conjunction with whole-cell proteomics and transcriptomics subsequently indicated that ME/CFS lymphoblasts increase the use of alternatives to glycolysis in an "attempt" to compensate for the respiratory inefficiency by Complex V. Fatty acid β-oxidation, amino acid catabolism and the pentose phosphate pathway appear to be the pathways that are utilised in this way.

Such compensatory mechanisms appear to be sufficient to meet the cell's energy requirements despite the inefficiency of ATP synthesis by Complex V. However, this may leave the cells less able to respond to additional ATP demand despite the elevated respiratory capacity, since the signalling (TORC1 and AMPK), mitochondrial and other metabolic pathways are already chronically upregulated. This seems to reflect a cellular equivalent of key clinical features of ME/CFS – in other words a "cellular chronic fatigue". If this is present in cell types or bodily tissues other than the B cells from which

lymphoblasts are derived, it may contribute to the unexplained fatigue and crippling PEM experienced by ME/CFS patients. This is suggested by the fact that the respiratory abnormalities I observed were correlated with the Weighted Standing Test measurements. My work in this area has laid the foundation for future projects to assess the cause-effect relationships between these various abnormalities, which will greatly increase our understanding of the underlying molecular mechanisms of ME/CFS.

The lack of objective, timely, and accurate diagnostic criteria or biomarkers for ME/CFS has been a major challenge facing the field, patients, and clinicians. In my work I also identified biomarkers for ME/CFS that discriminated patients from controls with 100% accuracy even when subdivided into training and test datasets (at the cost of statistical power) to simulate the testing of "new" samples. Such an outcome is remarkable. This investigation also took practical concerns of time, cost and required expertise into account and assessed the efficacy of staged diagnostic protocols utilising rapid, cheap, simple to perform and sensitive screening tests followed by more specific confirmatory tests. My results demonstrate that measures of frozen lymphocyte death rate, lymphoblast respiratory function, TORC1 activity, and levels of specific proteins or transcripts are promising biomarkers for ME/CFS. With future work to further increase the clinical practicability of the protocol (higher throughput assays with minimal required expertise, applicability of lymphocytes to speed up confirmatory tests) and to validate these tests in larger cohorts, this project may very well have laid the groundwork for the design and testing of a refined diagnostic protocol for ME/CFS.

In summation, my research has made significant strides in our mechanistic understanding of ME/CFS by identifying unique, specific defects in mitochondrial function with an accompanying array of compensatory cellular changes. This work has also highlighted multiple promising candidate diagnostic biomarkers with an impressive 100% discriminatory accuracy. This PhD project, which began with my exploratory investigation of mitochondrial function and signalling pathways, has since opened many promising new avenues of investigation for future projects to embark upon in the aims of solving the devastating disease that is Myalgic Encephalomyelitis/Chronic Fatigue Syndrome.

Appendices

Appendix 1: List of Chemicals and Suppliers

Chemical Name	Supplier
2-Deoxyglucose	Sigma
Alexa Fluor 800 goat anti-mouse IgG	Thermo Fisher
Antimycin A	Sigma
Bromophenol blue	Sigma
Carbonyl cyanide m-chlorophenyl hydrazone (CCCP)	Sigma
cOmplete™ EDTA-free Protease Inhibitor Cocktail	Roche
Corning® Matrigel® Matrigel Matrix	Sigma
Cyclosporin A	Sigma
D-Glucose	BDH
Dimethyl sulphoxide (DMSO)	Ajax
DNAzol®	MRC
Ficoll-Paque Plus	GE
GlutaMAX Supplement	Thermo Fisher
Glycerol	Ajax
HEPES sodium salt	Sigma
Hoechst 33342 Nuclear Stain	Thermo Fisher
L-Glutamine	Thermo Fisher
MitoTracker Red CMXRos	Thermo Fisher
MitoTracker™ Green FM	Thermo Fisher
NaCl	Ajax
Oligomycin	Sigma
Penicillin-Streptomycin (100X)	Thermo Fisher
Purezol RNA Isolation Reagent	Bio-Rad
Rotenone	Sigma
SDS	Ajax

Sodium hydroxide (NaOH)	Ajax
Sodium Pyruvate	Sigma
TORIN2	Sigma
Trichloroacetic acid (TCA)	Sigma
Tricine	Sigma
Tris	ICN
Trypan Blue	Sigma
Tween 20 (polyoxyethylene-sorbitan Monolaurate)	Sigma
β-mercaptoethanol	Sigma

Table A1.1: List of chemicals and suppliers.

Appendix 2: List of Media and Buffers

Name of Medium or Buffer	Composition/Supplier
Complete Medium	RPMI 1640 medium – no glutamine (Thermo Fisher) 1× GlutaMAX 1× Penicillin/Streptomycin 1× Fetal Bovine Serum (Thermo Fisher)
Growth Medium	MEM alpha medium (Thermo Fisher) 1× Penicillin/Strepomycin 1× Fetal Bovine Serum (Thermo Fisher)
Loading Buffer	63 mM Tris hydrochloride 10% glycerol 2% SDS 10% mercaptoethanol 0.0001% Bromophenol Blue 1× Protease Inhibitor Cocktail (Roche)
Phosphate Buffered Saline – endotoxin free (PBS)	Sigma
Storage Medium	Recovery™ Cell Culture Freezing Medium (Thermo Fisher)
Tris-buffered Saline (TBS) Buffer	150 mM NaCl 50 mM Tris-HCl pH 7.6

Wash Medium	RPMI 1640 medium – no glutamine (Thermo Fisher) 1× GlutaMAX 1× Penicillin/Streptomycin
XF Base Medium	Agilent
XF Calibrant	Agilent

Table A2.1: List of Media and Buffers

Appendix 3: Commercial Assays and Components

Assay Name	Manufacturer
ATP Determination Kit	Invitrogen
Fluorometric Intracellular ROS Kit	Sigma
iTaq Universal SYBR Green Supermix	Bio-Rad
Phospho-4EBP1 (Thr37/46) cellular HTRF kit	Cisbio
Phospho-ACC (Ser79) cellular HTRF kit	Cisbio
Qubit Protein Assay Kit	Thermo Fisher
RQ1 RNase-Free DNase	Promega
Seahorse XFe24 FluxPak	Agilent
Total OXPHOS Human WB Antibody Cocktail	Abcam

Table A3.1: Commerical Assays and Components

Full Company Names for Appendices 1-3:

Abcam, Cambridge, UK.

Agilent Technologies Inc., Santa Clara, California, USA.

Ajax Finechem Pty Ltd., Auburn, NSW, Australia.

BDH Chemicals Pty. Ltd., Kilysth, VIC, Australia.

Bio-Rad Laboratories Inc., Hercules, California, USA.

Cisbio Bioassays, Codolet, France.

GE Healthcare, Chicago, Illinois, USA.

ICN Biochemicals Inc., Aurora, Ohio, USA.

Invitrogen, Carlsbad, California, USA.

Molecular Research Centre Inc., Cincinnati, Ohio, USA.

Promega Corporation, Madison, Wisconsin, USA.

Roche Applied Science, Penzberg, Germany.

Sigma-Aldrich Corporation, St Louis, Missouri, USA.

Thermo Fisher Scientific, Waltham, Massachusetts, USA.

Appendix 4: Human Sample Information

Sample	Type	Gender	Age
100026	CFS	M	49
100034	CFS	M	42
100048	CFS	F	70
100073	CFS	F	38
100107	CFS	F	60
100215	CFS	F	62
100227	CFS	F	40
100250	CFS	F	48
100332	CFS	F	42
100376	CFS	F	56
100422	CFS	F	58
100527	CFS	F	67
100541	CFS	F	59
100595	CFS	F	38
100617	CFS	F	49
100685	CFS	M	61
100713	CFS	F	36
100768	CFS	F	67
100857	CFS	F	55
100877	CFS	F	28
100910	CFS	F	63
100949	CFS	F	56
101022	CFS	F	40
101030	CFS	F	62
101092	CFS	F	39
101164	CFS	F	62
101212	CFS	F	26
101238	CFS	F	52
101348	CFS	F	30
101406	CFS	M	51
101407	CFS	F	27

101468	CFS	M	55
101469	CFS	F	54
101527	CFS	F	58
101592	CFS	F	36
101610	CFS	F	57
101661	CFS	F	63
101712	CFS	F	50
101748	CFS	M	38
101869	CFS	F	40
101946	CFS	F	43
101996	CFS	F	62
101999	CFS	F	46
102002	CFS	F	48
102021	CFS	F	62
102051	CFS	F	31
102128	CFS	F	42
102233	CFS	F	42
102424	CFS	M	63
103001	CFS	M	52
103020	CFS	M	38
103041	CFS	F	41
103045	CFS	M	40
103092	CFS	F	42
103114	CFS	F	48
103129	CFS	F	50
103238	CFS	F	54
103464	CFS	F	23
103500	CFS	F	29
103527	CFS	F	61
103560	CFS	F	33
103606	CFS	F	34
103679	CFS	F	45
103690	CFS	F	22

103737	CFS	F	44
103811	CFS	M	38
103989	CFS	F	70
201532	CFS	F	53
203253	CFS	F	40
103073	CFS	F	40
SA	CFS	F	71
SA2	CFS	F	70
C0001	Control	M	21
C0002	Control	F	26
C0003	Control	M	26
C0004	Control	F	41
C0005	Control	F	45
C0006	Control	F	44
C0007	Control	M	52
C0008	Control	F	50
C0009	Control	M	43
C0010	Control	F	53
C0011	Control	M	54
C0012	Control	F	36
C0013	Control	M	36
C0014	Control	F	58
C0015	Control	F	37
C0016	Control	F	28
C0017	Control	M	30
C0018	Control	F	27
C0019	Control	M	21
C0020	Control	F	26
C0021	Control	F	33
C0022	Control	M	21
C0023	Control	F	54
C0024	Control	F	25
C0025	Control	M	30

C0026	Control	M	22
C0027	Control	F	54
C0028	Control	M	24
C0029	Control	M	34
C0030	Control	M	21
C0031	Control	M	19
C0032	Control	M	55
C0033	Control	F	44
C0034	Control	F	49
C0035	Control	F	24
C0036	Control	M	24
C0037	Control	M	29
C101	Internal	M	83
C105	Internal	M	64

Table A4.1: Human sample information.

Appendix 5: Pathway Over-Representation Analysis of Differentially Expressed Transcripts and Proteins in ME/CFS Lymphoblasts

Table A5.1. Pathways overrepresented amongst downregulated transcripts in ME/CFS lymphoblasts.

Reactome pathway	Number of genes: In entire experiment	Number of genes: In downregulated fraction (Q<0.05)	Expected	Fold enrichment	Binomial test P-value	False discovery rate (FDR)
Formation of a pool of free 40S subunits (R-HSA-72689)	97	63	9.92	6.35	5.54×10^{-30}	1.20×10^{-26}
GTP hydrolysis and joining of the 60S ribosomal subunit (R-HSA-72706)	107	65	10.94	5.94	2.68×10^{-29}	1.45×10^{-26}
Cap-dependent Translation Initiation (R-HSA-72737)	114	67	11.66	5.75	2.35×10^{-29}	1.69×10^{-26}
Eukaryotic Translation Initiation (R-HSA-72613)	114	67	11.66	5.75	2.35×10^{-29}	2.54×10^{-26}
L13a-mediated translational silencing of Ceruloplasmin expression (R-HSA-156827)	106	64	10.84	5.9	1.01×10^{-28}	3.63×10^{-26}
Viral mRNA Translation (R-HSA-192823)	85	58	8.69	6.67	9.12×10^{-29}	3.94×10^{-26}

Translation (R-HSA-72766)	286	105	29.24	3.59	1.94×10^{-28}	5.98×10^{-26}
Peptide chain elongation (R-HSA-156902)	85	57	8.69	6.56	6.35×10^{-28}	1.71×10^{-25}
Selenocysteine synthesis (R-HSA-2408557)	89	58	9.1	6.37	8.94×10^{-28}	1.93×10^{-25}
Eukaryotic Translation Elongation (R-HSA-156842)	89	58	9.1	6.37	8.94×10^{-28}	2.14×10^{-25}
Regulation of expression of SLITs and ROBOs (R-HSA-9010553)	155	75	15.85	4.73	1.57×10^{-27}	3.08×10^{-25}
Eukaryotic Translation Termination (R-HSA-72764)	89	57	9.1	6.26	5.95×10^{-27}	1.07×10^{-24}
Nonsense Mediated Decay (NMD) independent of the Exon Junction Complex (EJC) (R-HSA-975956)	91	57	9.31	6.13	1.74×10^{-26}	2.89×10^{-24}
Nonsense Mediated Decay (NMD) enhanced by the Exon Junction Complex (EJC) (R-HSA-975957)	111	62	11.35	5.46	4.10×10^{-26}	5.89×10^{-24}

Nonsense-Mediated Decay (NMD) (R-HSA-927802)	111	62	11.35	5.46	4.10×10^{-26}	6.31×10^{-24}
Response of EIF2AK4 (GCN2) to amino acid deficiency (R-HSA-9633012)	97	58	9.92	5.85	6.10×10^{-26}	8.22×10^{-24}
SRP-dependent cotranslational protein targeting to membrane (R-HSA-1799339)	108	60	11.04	5.43	3.39×10^{-25}	4.31×10^{-23}
Selenoamino acid metabolism (R-HSA-2408522)	106	59	10.84	5.44	7.75×10^{-25}	9.29×10^{-23}
Metabolism of RNA (R-HSA-8953854)	635	159	64.93	2.45	1.11×10^{-24}	1.26×10^{-22}
rRNA processing (R-HSA-72312)	194	79	19.84	3.98	2.67×10^{-24}	2.88×10^{-22}
Influenza Viral RNA Transcription and Replication (R-HSA-168273)	127	63	12.99	4.85	7.32×10^{-24}	7.52×10^{-22}
rRNA processing in the nucleus and cytosol (R-HSA-8868773)	185	76	18.92	4.02	1.22×10^{-23}	1.19×10^{-21}
Major pathway of rRNA processing in the nucleolus	175	73	17.89	4.08	3.99×10^{-23}	3.74×10^{-21}

and cytosol (R-HSA-6791226)						
Signalling by ROBO receptors (R-HSA-376176)	191	76	19.53	3.89	7.74×10^{-23}	6.96×10^{-21}
Influenza Life Cycle (R-HSA-168255)	136	63	13.91	4.53	2.30×10^{-22}	1.99×10^{-20}
Influenza Infection (R-HSA-168254)	146	64	14.93	4.29	1.71×10^{-21}	1.42×10^{-19}
Metabolism of amino acids and derivatives (R-HSA-71291)	278	89	28.43	3.13	2.06×10^{-20}	1.65×10^{-18}
Infectious disease (R-HSA-5663205)	411	103	42.03	2.45	3.24×10^{-16}	2.50×10^{-14}
Formation of the ternary complex, and subsequentl y, the 43S complex (R-HSA-72695)	49	31	5.01	6.19	3.65×10^{-15}	2.71×10^{-13}
Translation initiation complex formation (R-HSA-72649)	55	31	5.62	5.51	7.34×10^{-14}	5.11×10^{-12}
Ribosomal scanning and start codon recognition (R-HSA-72702)	55	31	5.62	5.51	7.34×10^{-14}	5.28×10^{-12}
Activation of the mRNA upon binding of the cap-	56	31	5.73	5.41	1.17×10^{-13}	7.86×10^{-12}

binding complex and eIFs, and subsequent binding to 43S (R-HSA-72662)						
Cellular responses to external stimuli (R-HSA-8953897)	486	106	49.7	2.13	7.00×10^{-13}	4.58×10^{-11}
Cellular responses to stress (R-HSA-2262752)	481	105	49.18	2.13	8.61×10^{-13}	5.46×10^{-11}
Axon guidance (R-HSA-422475)	402	91	41.11	2.21	4.76×10^{-12}	2.93×10^{-10}
Respiratory electron transport, ATP synthesis by chemiosmotic coupling, and heat production by uncoupling proteins. (R-HSA-163200)	109	40	11.15	3.59	1.33×10^{-11}	7.95×10^{-10}
Respiratory electron transport (R-HSA-611105)	90	34	9.2	3.69	2.14×10^{-10}	1.25×10^{-8}
The citric acid (TCA) cycle and respiratory electron transport (R-HSA-1428517)	152	44	15.54	2.83	1.95×10^{-9}	1.11×10^{-7}
Mitochondrial	87	31	8.9	3.48	5.03×10^{-9}	2.78×10^{-7}

translation elongation (R-HSA-5389840)						
Metabolism of proteins (R-HSA-392499)	1533	226	156.76	1.44	1.21×10^{-8}	6.54×10^{-7}
Mitochondrial translation initiation (R-HSA-5368286)	87	30	8.9	3.37	1.80×10^{-8}	9.27×10^{-7}
Mitochondrial translation termination (R-HSA-5419276)	87	30	8.9	3.37	1.80×10^{-8}	9.50×10^{-7}
Mitochondrial translation (R-HSA-5368287)	93	31	9.51	3.26	2.23×10^{-8}	1.12×10^{-6}
Metabolism (R-HSA-1430728)	1513	221	154.71	1.43	3.80×10^{-8}	1.86×10^{-6}
Complex I biogenesis (R-HSA-6799198)	49	21	5.01	4.19	7.59×10^{-8}	3.64×10^{-6}
Developmental Biology (R-HSA-1266738)	616	105	62.99	1.67	3.82×10^{-7}	1.79×10^{-5}
Disease (R-HSA-1643685)	863	136	88.25	1.54	5.25×10^{-7}	2.41×10^{-5}
Regulation of mRNA stability by proteins that bind AU-rich elements (R-HSA-450531)	84	25	8.59	2.91	3.57×10^{-6}	1.60×10^{-4}
Protein localization (R-HSA-9609507)	145	34	14.83	2.29	1.19×10^{-5}	5.23×10^{-4}
Vif-mediated	51	17	5.21	3.26	3.16×10^{-5}	0.0014

degradation of APOBEC3G (R-HSA-180585)						
Negative regulation of NOTCH4 signalling (R-HSA-9604323)	52	17	5.32	3.2	4.00×10^{-5}	0.0017
Metabolism of polyamines (R-HSA-351202)	55	17	5.62	3.02	7.83×10^{-5}	0.0033
mRNA Splicing (R-HSA-72172)	183	37	18.71	1.98	1.07×10^{-4}	0.0042
Autodegradation of Cdh1 by Cdh1:APC/C (R-HSA-174084)	62	18	6.34	2.84	1.06×10^{-4}	0.0042
Oxygen-dependent proline hydroxylation of Hypoxia-inducible Factor Alpha (R-HSA-1234176)	62	18	6.34	2.84	1.06×10^{-4}	0.0043
FBXL7 down-regulates AURKA during mitotic entry and in early mitosis (R-HSA-8854050)	52	16	5.32	3.01	1.32×10^{-4}	0.0050
HIV Infection (R-HSA-162906)	213	41	21.78	1.88	1.31×10^{-4}	0.0051
Regulation of activated	48	15	4.91	3.06	1.79×10^{-4}	0.0067

PAK-2p34 by proteasome mediated degradation (R-HSA-211733)						
APC/C:Cdc20 mediated degradation of Securin (R-HSA-174154)	65	18	6.65	2.71	1.88×10^{-4}	0.0069
Degradation of DVL (R-HSA-4641258)	54	16	5.52	2.9	2.00×10^{-4}	0.0071
mRNA Splicing - Major Pathway (R-HSA-72163)	175	35	17.89	1.96	1.98×10^{-4}	0.0071
Assembly of the pre-replicative complex (R-HSA-68867)	66	18	6.75	2.67	2.25×10^{-4}	0.0077
Regulation of ornithine decarboxylase (ODC) (R-HSA-350562)	49	15	5.01	2.99	2.23×10^{-4}	0.0078
Ubiquitin-dependent degradation of Cyclin D (R-HSA-75815)	50	15	5.11	2.93	2.75×10^{-4}	0.0085
Autodegradation of the E3 ubiquitin ligase COP1 (R-HSA-349425)	50	15	5.11	2.93	2.75×10^{-4}	0.0086
Vpu mediated degradation of CD4 (R-	50	15	5.11	2.93	2.75×10^{-4}	0.0087

HSA-180534)						
Regulation of RAS by GAPs (R-HSA-5658442)	61	17	6.24	2.73	2.60×10^{-4}	0.0088
Ubiquitin Mediated Degradation of Phosphorylated Cdc25A (R-HSA-69601)	50	15	5.11	2.93	2.75×10^{-4}	0.0089
Degradation of GLI2 by the proteasome (R-HSA-5610783)	56	16	5.73	2.79	2.98×10^{-4}	0.0089
p53-Independent DNA Damage Response (R-HSA-69610)	50	15	5.11	2.93	2.75×10^{-4}	0.0090
GLI3 is processed to GLI3R by the proteasome (R-HSA-5610785)	56	16	5.73	2.79	2.98×10^{-4}	0.0090
p53-Independent G1/S DNA damage checkpoint (R-HSA-69613)	50	15	5.11	2.93	2.75×10^{-4}	0.0091
Regulation of RUNX2 expression and activity (R-HSA-8939902)	62	17	6.34	2.68	3.12×10^{-4}	0.0092
Orc1 removal from chromatin	68	18	6.95	2.59	3.19×10^{-4}	0.0093

(R-HSA-68949)						
Regulation of Apoptosis (R-HSA-169911)	51	15	5.21	2.88	3.37×10^{-4}	0.0097
Degradation of GLI1 by the proteasome (R-HSA-5610780)	57	16	5.83	2.75	3.60×10^{-4}	0.010
Cdc20:Phospho-APC/C mediated degradation of Cyclin A (R-HSA-174184)	69	18	7.06	2.55	3.78×10^{-4}	0.010
Cellular response to hypoxia (R-HSA-1234174)	69	18	7.06	2.55	3.78×10^{-4}	0.010
Switching of origins to a post-replicative state (R-HSA-69052)	87	21	8.9	2.36	3.58×10^{-4}	0.010
Mitochondrial protein import (R-HSA-1268020)	63	17	6.44	2.64	3.73×10^{-4}	0.010
CDK-mediated phosphorylation and removal of Cdc6 (R-HSA-69017)	69	18	7.06	2.55	3.78×10^{-4}	0.010
AUF1 (hnRNP D0) binds and destabilizes mRNA (R-HSA-450408)	52	15	5.32	2.82	4.11×10^{-4}	0.011

APC:Cdc20 mediated degradation of cell cycle proteins prior to satisfation of the cell cycle checkpoint (R-HSA-179419)	70	18	7.16	2.51	4.46×10^{-4}	0.012
APC/C:Cdh1 mediated degradation of Cdc20 and other APC/C:Cdh1 targeted proteins in late mitosis/early G1 (R-HSA-174178)	70	18	7.16	2.51	4.46×10^{-4}	0.011
Degradation of AXIN (R-HSA-4641257)	53	15	5.42	2.77	4.98×10^{-4}	0.012
Hh mutants that don't undergo autocatalytic processing are degraded by ERAD (R-HSA-5362768)	53	15	5.42	2.77	4.98×10^{-4}	0.012
SCF-beta-TrCP mediated degradation of Emi1 (R-HSA-174113)	53	15	5.42	2.77	4.98×10^{-4}	0.013
Regulation of RUNX3 expression and activity (R-HSA-8941858)	53	15	5.42	2.77	4.98×10^{-4}	0.013

Synthesis of DNA (R-HSA-69239)	116	25	11.86	2.11	5.45×10^{-4}	0.013
Processing of Capped Intron-Containing Pre-mRNA (R-HSA-72203)	229	41	23.42	1.75	5.50×10^{-4}	0.013
DNA Replication (R-HSA-69306)	123	26	12.58	2.07	5.65×10^{-4}	0.013
Hh mutants abrogate ligand secretion (R-HSA-5387390)	54	15	5.52	2.72	6.01×10^{-4}	0.014
Stabilization of p53 (R-HSA-69541)	54	15	5.52	2.72	6.01×10^{-4}	0.014
Regulation of PTEN stability and activity (R-HSA-8948751)	66	17	6.75	2.52	6.22×10^{-4}	0.014
APC/C:Cdc20 mediated degradation of mitotic proteins (R-HSA-176409)	72	18	7.36	2.44	6.15×10^{-4}	0.014
Degradation of beta-catenin by the destruction complex (R-HSA-195253)	79	19	8.08	2.35	6.94×10^{-4}	0.015
ER-Phagosome pathway (R-HSA-1236974)	79	19	8.08	2.35	6.94×10^{-4}	0.015
Activation of APC/C and	73	18	7.46	2.41	7.18×10^{-4}	0.016

APC/C:Cdc20 mediated degradation of mitotic proteins (R-HSA-176814)						
Cross-presentation of soluble exogenous antigens (endosomes) (R-HSA-1236978)	44	13	4.5	2.89	7.82×10^{-4}	0.017
NIK-->noncanonical NF-kB signalling (R-HSA-5676590)	57	15	5.83	2.57	0.0010	0.021
The role of GTSE1 in G2/M progression after G2 checkpoint (R-HSA-8852276)	69	17	7.06	2.41	0.0010	0.021
Hedgehog ligand biogenesis (R-HSA-5358346)	57	15	5.83	2.57	0.0010	0.021
CDT1 association with the CDC6:ORC:origin complex (R-HSA-68827)	57	15	5.83	2.57	0.0010	0.022
DNA Replication Pre-Initiation (R-HSA-69002)	82	19	8.38	2.27	0.0011	0.022
UCH proteinases (R-HSA-5689603)	89	20	9.1	2.2	0.0012	0.023
Antigen processing-	89	20	9.1	2.2	0.0012	0.023

Cross presentation (R-HSA-1236975)						
SCF(Skp2)-mediated degradation of p27/p21 (R-HSA-187577)	58	15	5.93	2.53	0.0012	0.023
Dectin-1 mediated noncanonical NF-kB signalling (R-HSA-5607761)	58	15	5.93	2.53	0.0012	0.024
mRNA Splicing - Minor Pathway (R-HSA-72165)	52	14	5.32	2.63	0.0012	0.024
Defective CFTR causes cystic fibrosis (R-HSA-5678895)	58	15	5.93	2.53	0.0012	0.024
Regulation of APC/C activators between G1/S and early anaphase (R-HSA-176408)	77	18	7.87	2.29	0.0013	0.025
tRNA modification in the nucleus and cytosol (R-HSA-6782315)	41	12	4.19	2.86	0.0013	0.025
Asymmetric localization of PCP proteins (R-HSA-4608870)	60	15	6.14	2.44	0.0017	0.031
RAF/MAP kinase	162	30	16.57	1.81	0.0018	0.032

cascade (R-HSA-5673001)						
RUNX1 regulates transcription of genes involved in differentiation of HSCs (R-HSA-8939236)	80	18	8.18	2.2	0.0019	0.035
KSRP (KHSRP) binds and destabilizes mRNA (R-HSA-450604)	17	7	1.74	4.03	0.0021	0.038
p53-Dependent G1 DNA Damage Response (R-HSA-69563)	62	15	6.34	2.37	0.0023	0.040
p53-Dependent G1/S DNA damage checkpoint (R-HSA-69580)	62	15	6.34	2.37	0.0023	0.041
Signalling by NOTCH4 (R-HSA-9013694)	75	17	7.67	2.22	0.0024	0.041
MAPK1/MAPK3 signalling (R-HSA-5684996)	167	30	17.08	1.76	0.0027	0.047
Regulation of mitotic cell cycle (R-HSA-453276)	83	18	8.49	2.12	0.0029	0.048
APC/C-mediated degradation of cell cycle proteins (R-	83	18	8.49	2.12	0.0029	0.049

HSA-174143) PCP/CE pathway (R-HSA-4086400)	83	18	8.49	2.12	0.0029	0.049

Table A5.1: Pathway over-representation analysis of downregulated transcripts in the whole-cell transcriptome using PANTHER gene expression analysis. "Reactome Pathway" was set as the level of biological granularity. Genes were included in the "downregulated fraction" on the basis of possessing a mean log fold change < 0 in the ME/CFS group versus the control mean, and a Q value < 0.05 according to the Benjamini-Hochberg method applied to P values from the F test. The PANTHER analysis was then applied to the list, testing for over-representation of particular pathways in the list using the binomial test, followed by calculation of the False Discovery Rate (FDR, using the Benjamini-Hochberg method). Output was sorted by statistical significance.

Table A5.2. Pathways overrepresented amongst upregulated transcripts in ME/CFS lymphoblasts.

Reactome pathway	Number of genes: In entire experiment	Number of genes: In upregulated fraction (Q<0.05)	Expected	Fold enrichment	Binomial test P-value
RNA Polymerase II Transcription (R-HSA-73857)	1116	105	74.65	1.41	2.74×10^{-4}
Gene expression (Transcription) (R-HSA-74160)	1234	113	82.55	1.37	4.30×10^{-4}
Generic Transcription Pathway (R-HSA-212436)	997	93	66.69	1.39	8.18×10^{-4}
ZBP1(DAI) mediated induction of type I IFNs (R-HSA-1606322)	20	6	1.34	4.48	0.0025
Cytosolic sensors of pathogen-associated DNA (R-HSA-1834949)	61	11	4.08	2.7	0.0032
RIP-mediated NFkB activation via ZBP1 (R-HSA-1810476)	16	5	1.07	4.67	0.0048
Signalling by MET (R-HSA-6806834)	56	10	3.75	2.67	0.0052
Cargo recognition for clathrin-mediated endocytosis (R-HSA-8856825)	70	11	4.68	2.35	0.0086
Transport of vitamins, nucleosides, and related	27	6	1.81	3.32	0.010

molecules (R-HSA-425397)					
HATs acetylate histones (R-HSA-3214847)	93	13	6.22	2.09	0.011
Antiviral mechanism by IFN-stimulated genes (R-HSA-1169410)	75	11	5.02	2.19	0.014
Netrin-1 signalling (R-HSA-373752)	29	6	1.94	3.09	0.014
Interferon Signalling (R-HSA-913531)	162	19	10.84	1.75	0.015
p75NTR signals via NF-kB (R-HSA-193639)	14	4	0.94	4.27	0.015
Netrin mediated repulsion signals (R-HSA-418886)	3	2	0.2	9.97	0.018
Metabolism of ingested H2SeO4 and H2SeO3 into H2Se (R-HSA-2408550)	3	2	0.2	9.97	0.018
Transport of nucleotide sugars (R-HSA-727802)	9	3	0.6	4.98	0.023
OAS antiviral response (R-HSA-8983711)	9	3	0.6	4.98	0.023
STING mediated induction of host immune responses (R-HSA-1834941)	16	4	1.07	3.74	0.024
Signalling by Hippo (R-HSA-2028269)	16	4	1.07	3.74	0.024

Regulation of cholesterol biosynthesis by SREBP (SREBF) (R-HSA-1655829)	52	8	3.48	2.3	0.026
Downstream signal transduction (R-HSA-186763)	25	5	1.67	2.99	0.028
PPARA activates gene expression (R-HSA-1989781)	95	12	6.35	1.89	0.029
Clathrin-mediated endocytosis (R-HSA-8856828)	106	13	7.09	1.83	0.029
NR1H2 & NR1H3 regulate gene expression linked to triglyceride lipolysis in adipose (R-HSA-9031528)	4	2	0.27	7.47	0.030
Transport of organic anions (R-HSA-879518)	4	2	0.27	7.47	0.030
RHO GTPases activate KTN1 (R-HSA-5625970)	10	3	0.67	4.48	0.030
Regulation of lipid metabolism by PPARalpha (R-HSA-400206)	96	12	6.42	1.87	0.031
Toll Like Receptor 9 (TLR9) Cascade (R-HSA-168138)	86	11	5.75	1.91	0.033
CREB1 phosphorylation through NMDA	18	4	1.2	3.32	0.034

receptor-mediated activation of RAS signalling (R-HSA-442742)					
Nuclear Receptor transcription pathway (R-HSA-383280)	27	5	1.81	2.77	0.037
Transport of small molecules (R-HSA-382551)	443	40	29.63	1.35	0.037
N-Glycan antennae elongation (R-HSA-975577)	11	3	0.74	4.08	0.039
p75NTR recruits signalling complexes (R-HSA-209543)	11	3	0.74	4.08	0.039
PECAM1 interactions (R-HSA-210990)	11	3	0.74	4.08	0.039
TRIF(TICAM1)-mediated TLR4 signalling (R-HSA-937061)	89	11	5.95	1.85	0.040
MyD88-independent TLR4 cascade (R-HSA-166166)	89	11	5.95	1.85	0.040
Retrograde transport at the Trans-Golgi-Network (R-HSA-6811440)	47	7	3.14	2.23	0.041
Membrane Trafficking (R-HSA-199991)	526	46	35.19	1.31	0.042
Transport to the Golgi and subsequent modification (R-HSA-948021)	159	17	10.64	1.6	0.043

Vesicle-mediated transport (R-HSA-5653656)	540	47	36.12	1.3	0.043
NR1H2 & NR1H3 regulate gene expression to limit cholesterol uptake (R-HSA-9031525)	5	2	0.33	5.98	0.045
Signalling by Receptor Tyrosine Kinases (R-HSA-9006934)	334	31	22.34	1.39	0.045
Signalling by NTRKs (R-HSA-166520)	80	10	5.35	1.87	0.046
Diseases of Immune System (R-HSA-5260271)	20	4	1.34	2.99	0.047
Diseases associated with the TLR signalling cascade (R-HSA-5602358)	20	4	1.34	2.99	0.047
SLC transporter disorders (R-HSA-5619102)	59	8	3.95	2.03	0.048
Gastrin-CREB signalling pathway via PKC and MAPK (R-HSA-881907)	12	3	0.8	3.74	0.048
Ion channel transport (R-HSA-983712)	103	12	6.89	1.74	0.048
TRAF6 mediated induction of NFkB and MAP kinases upon TLR7/8	81	10	5.42	1.85	0.049

or 9 activation (R-HSA-975138)					
Activation of gene expression by SREBF (SREBP) (R-HSA-2426168)	39	6	2.61	2.3	0.049

Table A5.2: Pathway over-representation analysis of upregulated transcripts in whole-cell transcriptome data using PANTHER gene expression analysis. "Reactome Pathway" was set as the level of biological granularity. Genes were included in the "upregulated fraction" on the basis of possessing a mean log fold change > 0 in the ME/CFS group versus the control mean, and a Q value < 0.05 according to the Benjamini-Hochberg method applied to P values from the F test. Output was sorted according to statistical significance. The PANTHER analysis was then applied to the list testing for over-representation of particular pathways in the list using the binomial test. The FDR correction was not applied to the PANTHER analysis. Output was sorted by statistical significance.

Table A5.3. Pathways over-represented amongst upregulated proteins in ME/CFS lymphoblasts.

Reactome pathway	Number of proteins: In entire dataset	Number of proteins: In significantly upregulated fraction (Q<0.05)	Expected	Fold enrichment	Binomial test P value
Metabolism (R-HSA-1430728)	789	66	43.61	1.51	2.12×10^{-4}
Mitochondrial Fatty Acid Beta-Oxidation (R-HSA-77289)	23	7	1.27	5.51	3.32×10^{-4}
Interferon gamma signalling (R-HSA-877300)	49	10	2.71	3.69	4.60×10^{-4}
Beta oxidation of palmitoyl-CoA to myristoyl-CoA (R-HSA-77305)	3	3	0.17	18.09	6.64×10^{-4}
Mitochondrial fatty acid beta-oxidation of saturated fatty acids (R-HSA-77286)	7	4	0.39	10.34	6.72×10^{-4}
Phosphorylation of CD3 and TCR zeta chains (R-HSA-202427)	13	5	0.72	6.96	8.53×10^{-4}
Mitochondrial calcium ion transport (R-HSA-8949215)	13	5	0.72	6.96	8.53×10^{-4}
Beta oxidation of lauroyl-CoA to decanoyl-CoA-CoA (R-HSA-77310)	4	3	0.22	13.57	0.0015
Glutamate Neurotransmitter Release Cycle (R-HSA-210500)	4	3	0.22	13.57	0.0015
Interleukin-2 family signalling (R-HSA-451927)	15	5	0.83	6.03	0.0016
PD-1 signalling (R-HSA-389948)	15	5	0.83	6.03	0.0016
Cytokine Signalling in Immune system (R-HSA-1280215)	327	31	18.08	1.72	0.0023
Interleukin-9 signalling (R-HSA-8985947)	5	3	0.28	10.85	0.0028
Beta oxidation of hexanoyl-CoA to	5	3	0.28	10.85	0.0028

butanoyl-CoA (R-HSA-77350)					
Beta oxidation of octanoyl-CoA to hexanoyl-CoA (R-HSA-77348)	5	3	0.28	10.85	0.0028
Beta oxidation of decanoyl-CoA to octanoyl-CoA-CoA (R-HSA-77346)	5	3	0.28	10.85	0.0028
Interleukin-21 signalling (R-HSA-9020958)	5	3	0.28	10.85	0.0028
Mitochondrial fatty acid beta-oxidation of unsaturated fatty acids (R-HSA-77288)	5	3	0.28	10.85	0.0028
Fatty acid metabolism (R-HSA-8978868)	63	10	3.48	2.87	0.0029
Translocation of ZAP-70 to Immunological synapse (R-HSA-202430)	11	4	0.61	6.58	0.0035
Generation of second messenger molecules (R-HSA-202433)	18	5	0.99	5.03	0.0035
Cell-Cell communication (R-HSA-1500931)	27	6	1.49	4.02	0.0042
Interleukin-2 signalling (R-HSA-9020558)	6	3	0.33	9.05	0.0047
Acyl chain remodeling of CL (R-HSA-1482798)	2	2	0.11	18.09	0.0057
Adenylate cyclase inhibitory pathway (R-HSA-170670)	2	2	0.11	18.09	0.0057
Beta oxidation of myristoyl-CoA to lauroyl-CoA (R-HSA-77285)	2	2	0.11	18.09	0.0057
Signalling by PDGF (R-HSA-186797)	13	4	0.72	5.57	0.0062
Downstream signal transduction (R-HSA-186763)	13	4	0.72	5.57	0.0062
Nephrin family interactions (R-HSA-373753)	7	3	0.39	7.75	0.0072

Signalling by cytosolic FGFR1 fusion mutants (R-HSA-1839117)	8	3	0.44	6.78	0.010
Processing of SMDT1 (R-HSA-8949664)	8	3	0.44	6.78	0.010
Interleukin-20 family signalling (R-HSA-8854691)	8	3	0.44	6.78	0.010
Erythropoietin activates STAT5 (R-HSA-9027283)	3	2	0.17	12.06	0.012
Release of apoptotic factors from the mitochondria (R-HSA-111457)	3	2	0.17	12.06	0.012
STAT5 Activation (R-HSA-9645135)	3	2	0.17	12.06	0.012
Mitochondrial biogenesis (R-HSA-1592230)	45	7	2.49	2.81	0.013
Organelle biogenesis and maintenance (R-HSA-1852241)	104	12	5.75	2.09	0.014
FGFR1 mutant receptor activation (R-HSA-1839124)	9	3	0.5	6.03	0.014
Neurotransmitter release cycle (R-HSA-112310)	9	3	0.5	6.03	0.014
Growth hormone receptor signalling (R-HSA-982772)	9	3	0.5	6.03	0.014
TCR signalling (R-HSA-202403)	80	10	4.42	2.26	0.014
Immune System (R-HSA-168256)	805	58	44.5	1.3	0.017
Transmission across Chemical Synapses (R-HSA-112315)	60	8	3.32	2.41	0.019
Metabolism of amino acids and derivatives (R-HSA-71291)	220	20	12.16	1.64	0.021
Signalling by Leptin (R-HSA-2586552)	4	2	0.22	9.05	0.021
Gluconeogenesis (R-HSA-70263)	19	4	1.05	3.81	0.022
Signalling by FGFR1 in disease (R-HSA-5655302)	11	3	0.61	4.93	0.024

EPH-Ephrin signalling (R-HSA-2682334)	40	6	2.21	2.71	0.025
The citric acid (TCA) cycle and respiratory electron transport (R-HSA-1428517)	115	12	6.36	1.89	0.027
Formation of ATP by chemiosmotic coupling (R-HSA-163210)	12	3	0.66	4.52	0.030
Pentose phosphate pathway (R-HSA-71336)	12	3	0.66	4.52	0.030
RAB geranylgeranylation (R-HSA-8873719)	31	5	1.71	2.92	0.030
Transcriptional activation of mitochondrial biogenesis (R-HSA-2151201)	21	4	1.16	3.45	0.030
Activation of GABAB receptors (R-HSA-991365)	5	2	0.28	7.24	0.032
VxPx cargo-targeting to cilium (R-HSA-5620916)	5	2	0.28	7.24	0.032
Interleukin-15 signalling (R-HSA-8983432)	5	2	0.28	7.24	0.032
ADP signalling through P2Y purinoceptor 12 (R-HSA-392170)	5	2	0.28	7.24	0.032
Sulphide oxidation to sulphate (R-HSA-1614517)	5	2	0.28	7.24	0.032
G-protein activation (R-HSA-202040)	5	2	0.28	7.24	0.032
Interaction between L1 and Ankyrins (R-HSA-445095)	5	2	0.28	7.24	0.032
Aspartate and asparagine metabolism (R-HSA-8963693)	5	2	0.28	7.24	0.032
Phenylalanine and tyrosine metabolism (R-HSA-8963691)	5	2	0.28	7.24	0.032
GABA B receptor activation (R-HSA-977444)	5	2	0.28	7.24	0.032

GABA receptor activation (R-HSA-977443)	5	2	0.28	7.24	0.032
Interferon Signalling (R-HSA-913531)	121	12	6.69	1.79	0.038
Detoxification of Reactive Oxygen Species (R-HSA-3299685)	23	4	1.27	3.15	0.040
Costimulation by the CD28 family (R-HSA-388841)	34	5	1.88	2.66	0.042
FLT3 Signalling (R-HSA-9607240)	96	10	5.31	1.88	0.042
Cargo trafficking to the periciliary membrane (R-HSA-5620920)	14	3	0.77	3.88	0.043
Signalling by SCF-KIT (R-HSA-1433557)	14	3	0.77	3.88	0.043
Prolactin receptor signalling (R-HSA-1170546)	6	2	0.33	6.03	0.044
Nef Mediated CD8 Down-regulation (R-HSA-182218)	6	2	0.33	6.03	0.044
Lysine catabolism (R-HSA-71064)	6	2	0.33	6.03	0.044
Clathrin-mediated endocytosis (R-HSA-8856828)	71	8	3.92	2.04	0.045
Downstream TCR signalling (R-HSA-202424)	71	8	3.92	2.04	0.045
Neuronal System (R-HSA-112316)	71	8	3.92	2.04	0.045
Diseases of metabolism (R-HSA-5668914)	24	4	1.33	3.02	0.045

Table A5.3: Pathway over-representation analysis of upregulated whole-cell proteome data using PANTHER gene expression analysis. "Reactome Pathway" was set as the level of biological granularity. Proteins were included in the "upregulated fraction" on the basis of possessing a mean fold change > 1 in the ME/CFS group versus the control mean, and a Q value < 0.05 according to the Benjamini-Hochberg method applied to P-values from the t test. The PANTHER analysis was then applied to the list testing for over-representation of particular pathways in the list using the binomial test. The FDR correction was not applied to the PANTHER analysis as it obscured true positives confirmed by alternative investigation of concerned functional groups, including respirometry, western blotting and closer proteome analysis. Output was sorted by statistical significance.

Table A5.4. Pathways over-represented amongst downregulated proteins in ME/CFS lymphoblasts.

Reactome pathway	Number of proteins: In entire dataset	Number of proteins: In significantly downregulated fraction (Q<0.05)	Expected	Fold enrichment	Binomial test P-value
Vitamin B1 (thiamin) metabolism (R-HSA-196819)	1	1	0.01	> 100	0.0097
Defective PMM2 causes PMM2-CDG (CDG-1a) (R-HSA-4043911)	1	1	0.01	> 100	0.0097
Regulation of gene expression by Hypoxia-inducible Factor (R-HSA-1234158)	2	1	0.02	51.26	0.019
Protein repair (R-HSA-5676934)	2	1	0.02	51.26	0.019
RHO GTPases activate PKNs (R-HSA-5625740)	27	2	0.26	7.59	0.029
NOTCH4 Activation and Transmission of Signal to the Nucleus (R-HSA-9013700)	3	1	0.03	34.17	0.029
ALKBH3 mediated reversal of alkylation damage (R-HSA-112126)	3	1	0.03	34.17	0.029
GP1b-IX-V activation signalling (R-HSA-430116)	3	1	0.03	34.17	0.029
Meiosis (R-HSA-1500620)	29	2	0.28	7.07	0.033
Synthesis of GDP-mannose (R-HSA-446205)	4	1	0.04	25.63	0.038
Reproduction (R-HSA-1474165)	32	2	0.31	6.41	0.039
Reversal of alkylation damage by DNA dioxygenases (R-HSA-73943)	5	1	0.05	20.5	0.048

Table A5.4: Pathway over-representation analysis of downregulated whole-cell proteome data using PANTHER gene expression analysis. "Reactome Pathway" was set as the level of biological granularity. Proteins were included in the "downregulated fraction" on the basis of possessing a mean fold change < 1 in the ME/CFS group versus the control mean, and a Q value < 0.05 according to the Benjamini-Hochberg method applied to P-values from the t test. The PANTHER analysis was then applied to the list, testing for over-representation of particular pathways in the list using binomial test. The FDR correction was not applied to the PANTHER analysis as it obscured true positives confirmed by alternative investigation of concerned functional groups, including respirometry, western blotting and closer proteome analysis. Output was sorted by statistical significance.

Appendix 6: Levels of CD Cell Markers and Sirtuins Detected in Whole-Cell Proteomes and Transcriptomes of ME/CFS and Control Lymphoblasts

Table A6.1. Transcript levels of CD cell markers and Sirtuins detected in whole cell transcriptomes of ME/CFS and control lymphoblasts.

Gene Name	LogFC	P-value	Q-value
CD151	-0.13	0.51	1.71
CD164	0.28	0.028	0.032
CD180	-0.007	0.98	95.21
CD19	-0.42	0.0007	0.00074
CD200	-0.085	0.80	6.79
CD22	0.051	0.80	6.72
CD226	0.24	0.38	0.94
CD24	0.38	0.31	0.68
CD27	-0.33	0.22	0.40
CD274	0.16	0.51	1.70
CD2AP	0.11	0.24	0.45
CD300A	0.31	0.13	0.19
CD320	-0.37	0.052	0.065
CD37	-0.12	0.33	0.73
CD38	-0.15	0.55	1.96
CD40	0.079	0.52	1.79
CD44	-0.053	0.75	5.08
CD46	0.19	0.21	0.38
CD47	-0.33	0.031	0.035
CD48	0.10	0.56	2.13
CD52	-0.39	0.030	0.035
CD53	0.24	0.057	0.072
CD55	0.30	0.17	0.27
CD58	0.026	0.85	9.64
CD59	-0.13	0.27	0.54
CD63	-0.33	0.056	0.070
CD69	0.20	0.32	0.71
CD70	-0.00068	1.00	341.15
CD72	0.020	0.94	25.35

CD74	0.069	0.67	3.41
CD79A	-0.34	0.040	0.048
CD79B	-0.25	0.16	0.26
CD80	0.047	0.82	7.79
CD81	-0.15	0.22	0.39
CD82	0.17	0.29	0.61
CD83	0.23	0.22	0.40
CD84	0.053	0.82	7.99
CD86	-0.15	0.41	1.07
CD99	0.045	0.79	6.66
CD99L2	-0.23	0.14	0.21
SIRT1	0.29	0.091	0.13
SIRT2	0.23	0.0058	0.0060
SIRT3	-0.22	0.011	0.012
SIRT4	0.042	0.86	10.50
SIRT5	-0.11	0.18	0.31
SIRT6	-0.30	0.012	0.013
SIRT7	-0.080	0.31	0.68

Table A6.1: Transcript levels of CD cell markers and Sirtuins detected in whole cell transcriptomics of ME/CFS and control lymphoblasts. LogFC represents the log fold change in the ME/CFS group relative to the control group. Q values were assigned according to the Benjamini-Hochberg method.

Table A6.2. Protein levels of CD cell markers detected in whole cell proteomes of ME/CFS and control lymphoblasts.

Protein Name	Fold change	P-value	Q-value
CD226	4.06	0.038	0.041
CD2AP	0.95	0.67	2.48
CD37	1.62	0.12	0.15
CD38	1.42	0.11	0.13
CD40	1.22	0.31	0.52
CD44	1.18	0.17	0.23
CD48	1.30	0.016	0.016
CD59	1.04	0.82	5.66
CD70	1.83	0.0010	0.0010
CD74	1.12	0.29	0.45
CD79A	0.56	0.39	0.75
CD81	1.11	0.68	2.62
CD97	1.20	0.39	0.74

Table A6.2: Protein levels of CD cell markers detected in whole cell proteomics of ME/CFS and control lymphoblasts. Fold change represents the mean fold change in the ME/CFS group relative to the control group. Q values were assigned according to the Benjamini-Hochberg method.

Appendix 7: Confirmatory Tests Verifying the Proteomics and Transcriptomics Experiments

Figure A7.1. Verification of proteomics and transcriptomics data.

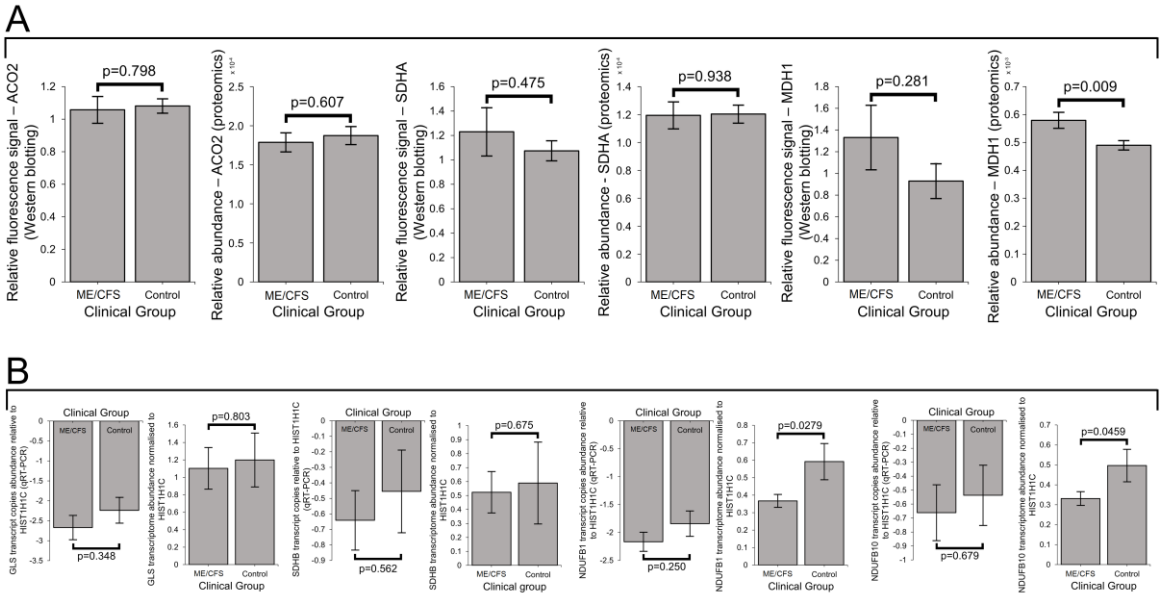

Figure A7.1: Western blots and qRT-PCR results verifying whole-cell proteome and transcriptome observations, respectively. (A) ACO2, SDHA and MDH1 expression as measured by semiquantitative Western blotting are consistent with expression as measured by whole-cell proteomics. In each pair of charts, the left panel is the result of semiquantitative western blotting and the right panel is the relative abundance of the same protein in the proteomics. Western blot sample sizes are as follows. ACO2: ME/CFS n = 21, Control = 22. SdhA: ME/CFS n = 17, Control = 19. MDH1: ME/CFS n = 6, Control = 7. Whole-cell proteomics experiment: ME/CFS n = 34, Control = 31. Western blots were assisted with by Oana Sanislav. **(B)** GLS, SdhB, NDUFB1 and NDUFB10 transcript levels relative to HIST1H1C were consistent in direction between qRT-PCR experiments and the whole-cell transcriptomes. In each pair of charts, the left panel is the result of semiquantitative qRT-PCR and the right panel is the relative abundance of the same transcript in the transcriptomics. GLS qRT-PCR: ME/CFS n = 23, Control = 16. SdhB qRT-PCR: ME/CFS n = 23, Control = 16. NDUFB1 and NDUFB10 GLS qRT-PCR: ME/CFS n = 22, Control = 16. Whole-cell transcriptomics experiment: ME/CFS n = 23, Control = 17.

Figure A7.2. Example semi-quantitative Western blot and loading control images as part of confirmatory experiments verifying the whole-cell proteomics data

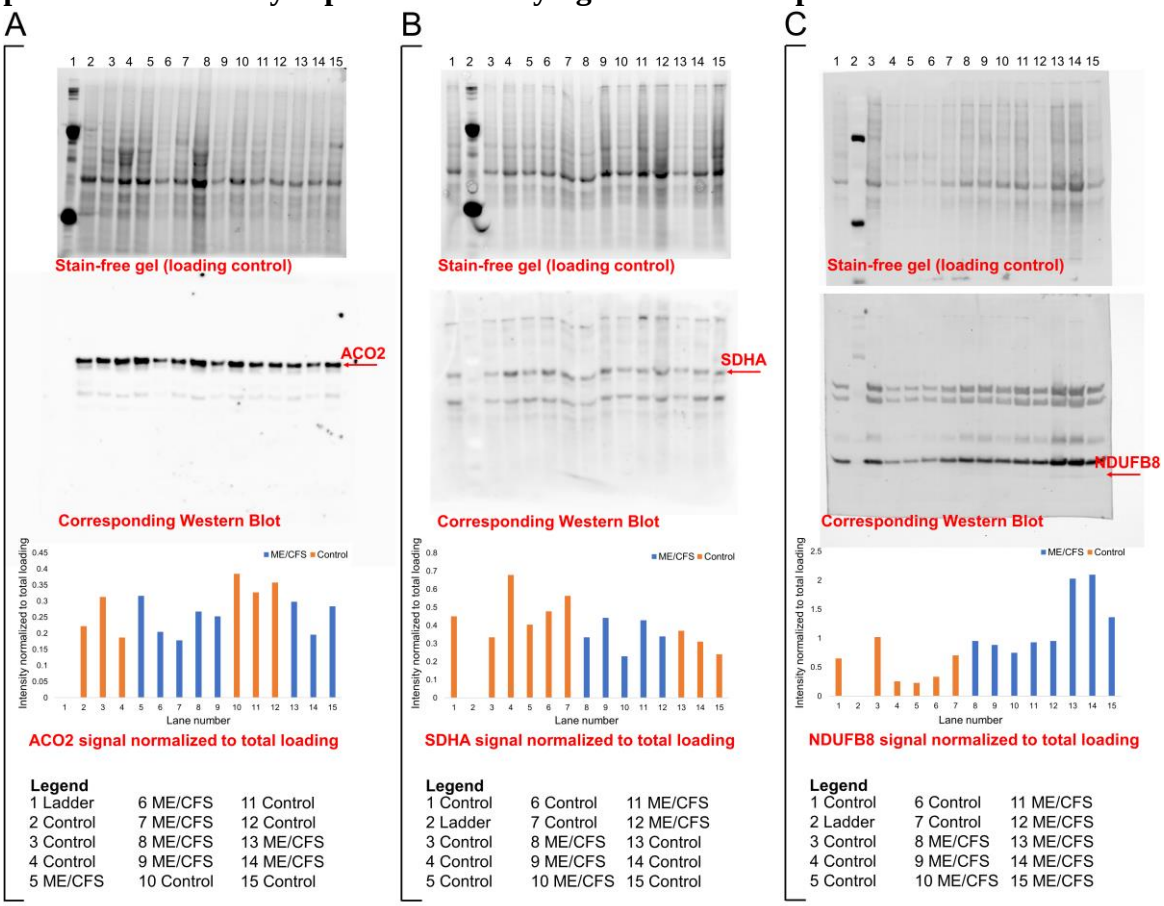

Figure A7.2: Example images of confirmatory semi-quantitative Western blots and loading controls (stain-free gels). (A) Example Western blot undertaken as part of the experiments verifying ACO2 levels in the whole-cell proteomes. The intensity of individual bands was digitally quantified and normalised to internal control cell lines included in every experiment. Protein ladder was visible in the stain-free gel but not in this particular corresponding blot. The chart below the blot shows the signal from the band of interest normalised to total protein loading. Western blots were assisted with by Oana Sanislav. **(B)** Example Western blot undertaken as part of the experiments verifying SDHA levels in the whole-cell proteomes. The intensity of individual bands was digitally quantified and normalised to internal control cell lines included in every experiment. The chart below the blot shows the signal from the band of interest normalised to total protein loading. **(C)** Example Western blot undertaken as part of the experiments verifying NDUFB8 levels in the whole-cell proteomes. The intensity of individual bands was digitally quantified and normalised to internal control cell lines included in every experiment. The chart below the blot shows the signal from the band of interest normalised to total protein loading. Mean NDUFB8 levels in the whole-cell proteomes of ME/CFS lymphoblasts were increased by 25% compared with controls, consistent with the NDUFB8 signal normalised to total loading as seen in this representative blot.

Appendix 8: Enzyme Levels of SLC25A11, MDH1 and BCKDK in the Whole-Cell Proteomes

Figure A8.1. SLC25A11 and MDH1 expression are elevated, while that of BCKDK is unaltered in ME/CFS lymphoblasts.

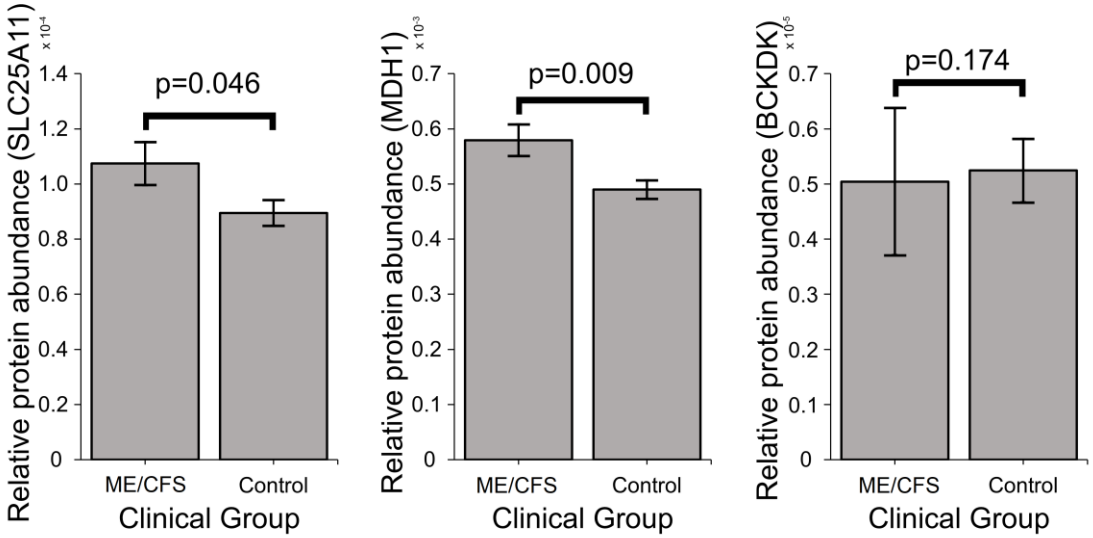

Figure A8.1: Expression of SLC25A11 and MDH1 is elevated in the whole-cell proteomes of ME/CFS lymphoblasts, while that of BCKDK is unaltered (two-tailed *t* tests in each case). Error bars represent standard error of the mean. Relative protein abundance was obtained from iBAQ values normalised to the control average within the respective individual experiments.

Appendix 9: Combined Measures of Lymphocyte Death Rate, Lymphoblast TORC1 Activity and Respiratory Abnormalities as an ME/CFS Biomarker

Figure A9.1. The combination of lymphocyte death rate, lymphoblast TORC1 signalling and lymphoblast respiratory abnormalities accurately distinguishes ME/CFS from healthy control lymphoblasts.

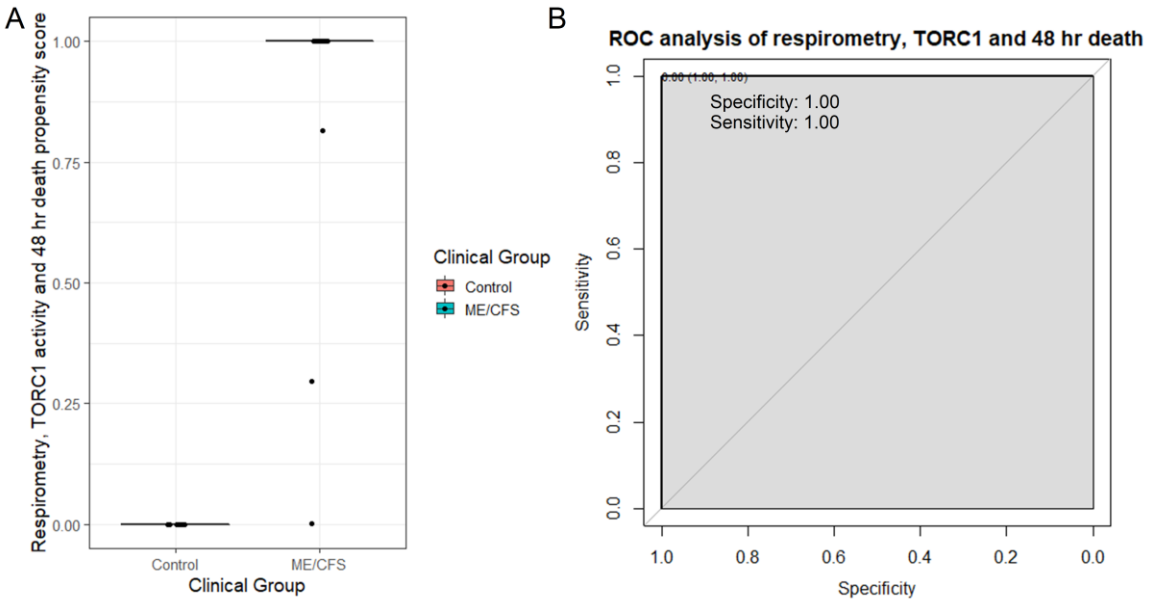

Figure A9.1: Logistic regression and ROC analysis of the combination of lymphocyte death rate, TORC1 activity and respiratory abnormalities. (**A**) Box plot showing the distribution of the propensity score in logistic regression resulting from analysis of the combined variables. The resulting regression coefficients are as indicated. The boxes show the median and the 25th and 75th percentiles, so that the height of the box is the interquartile range (IQR). The whiskers extend to the most extreme observations (largest and smallest) falling within ±1.5 × IQR of the box. Scores greater than 0.0 lead to classification of a sample as ME/CFS in the error matrix. (**B**) ROC analysis of the propensity score, plotting sensitivity (proportion of true positives) against specificity (proportion of true negatives) with 95% confidence limits (blue shading, N/A). The fractional area under the curve (AUC) is shown with 95% confidence limits. The "best" threshold for the propensity score (0.00) is shown, together with the specificity (1.00) and sensitivity (1.00) at that threshold.

References

Aaron, L. A., M. M. Burke and D. Buchwald (2000). "Overlapping conditions among patients with chronic fatigue syndrome, fibromyalgia, and temporomandibular disorder." Arch Intern Med **160**(2): 221-227.

Abrego, J., V. Gunda, E. Vernucci, S. K. Shukla, R. J. King, A. Dasgupta, G. Goode, D. Murthy, F. Yu and P. K. Singh (2017). "GOT1-mediated anaplerotic glutamine metabolism regulates chronic acidosis stress in pancreatic cancer cells." Cancer Lett **400**: 37-46.

Abuaita, B. H., T. L. Schultz and M. X. O'Riordan (2018). "Mitochondria-Derived Vesicles Deliver Antimicrobial Reactive Oxygen Species to Control Phagosome-Localized Staphylococcus aureus." Cell Host Microbe **24**(5): 625-636 e625.

Adeva-Andany, M. M., L. Lopez-Maside, C. Donapetry-Garcia, C. Fernandez-Fernandez and C. Sixto-Leal (2017). "Enzymes involved in branched-chain amino acid metabolism in humans." Amino Acids **49**(6): 1005-1028.

Afari, N. and D. Buchwald (2003). "Chronic fatigue syndrome: a review." Am J Psychiatry **160**(2): 221-236.

Allman, D. and S. Pillai (2008). "Peripheral B cell subsets." Curr Opin Immunol **20**(2): 149-157.

Almenar-Perez, E., T. Ovejero, T. Sanchez-Fito, J. A. Espejo, L. Nathanson and E. Oltra (2019). "Epigenetic Components of Myalgic Encephalomyelitis/Chronic Fatigue Syndrome Uncover Potential Transposable Element Activation." Clin Ther **41**(4): 675-698.

Almenar-Perez, E., T. Sanchez-Fito, T. Ovejero, L. Nathanson and E. Oltra (2019). "Impact of Polypharmacy on Candidate Biomarker miRNomes for the Diagnosis of Fibromyalgia and Myalgic Encephalomyelitis/Chronic Fatigue Syndrome: Striking Back on Treatments." Pharmaceutics **11**(3).

Almenar-Perez, E., L. Sarria, L. Nathanson and E. Oltra (2020). "Assessing diagnostic value of microRNAs from peripheral blood mononuclear cells and extracellular vesicles in Myalgic Encephalomyelitis/Chronic Fatigue Syndrome." Sci Rep **10**(1): 2064.

Anand, S. K. and S. K. Tikoo (2013). "Viruses as modulators of mitochondrial functions." Adv Virol **2013**: 738794.

Annesley, S. J., S. T. Lay, S. W. De Piazza, O. Sanislav, E. Hammersley, C. Y. Allan, L. M. Francione, M. Q. Bui, Z. P. Chen, K. R. Ngoei, F. Tassone, B. E. Kemp, E. Storey, A. Evans, D. Z. Loesch and P. R. Fisher (2016). "Immortalized Parkinson's disease lymphocytes have enhanced mitochondrial respiratory activity." Dis Model Mech **9**(11): 1295-1305.

Antonogeorgos, G., D. B. Panagiotakos, K. N. Priftis and A. Tzonou (2009). "Logistic Regression and Linear Discriminant Analyses in Evaluating Factors Associated with Asthma Prevalence among 10- to 12-Years-Old Children: Divergence and Similarity of the Two Statistical Methods." Int J Pediatr **2009**: 952042.

Armstrong, C. W., N. R. McGregor, H. L. Butt and P. R. Gooley (2014). "Metabolism in chronic fatigue syndrome." Adv Clin Chem **66**: 121-172.

Armstrong, C. W., N. R. McGregor, D. Lewis, H. Butt and P. R. Gooley (2015). "Metabolic profiling reveals anomalous energy metabolism and oxidative stress pathways in chronic fatigue syndrome patients." Metabolomics **11**(6): 1626–1639.

Armstrong, C. W., N. R. McGregor, D. P. Lewis, H. L. Butt and P. R. Gooley (2017). "The association of fecal microbiota and fecal, blood serum and urine metabolites in myalgic encephalomyelitis/chronic fatigue syndrome." Metabolomics **13**(8).

Armstrong, C. W., N. R. McGregor, J. R. Sheedy, I. Buttfield, H. L. Butt and P. R. Gooley (2012). "NMR metabolic profiling of serum identifies amino acid disturbances in chronic fatigue syndrome." Clin Chim Acta **413**(19-20): 1525-1531.

Barker, E., S. F. Fujimura, M. B. Fadem, A. L. Landay and J. A. Levy (1994). "Immunologic abnormalities associated with chronic fatigue syndrome." Clin Infect Dis **18 Suppl 1**: S136-141.

Barnes, P. R., D. J. Taylor, G. J. Kemp and G. K. Radda (1993). "Skeletal muscle bioenergetics in the chronic fatigue syndrome." J Neurol Neurosurg Psychiatry **56**(6): 679-683.

Bartlett, K. and S. Eaton (2004). "Mitochondrial beta-oxidation." Eur J Biochem **271**(3): 462-469.

Behan, W. M., I. A. More and P. O. Behan (1991). "Mitochondrial abnormalities in the postviral fatigue syndrome." Acta Neuropathol **83**(1): 61-65.

Benatti, U., A. Morelli, M. Frascio, E. Melloni, F. Salamino, B. Sparatore, S. Pontremoli and A. De Flora (1978). "Glucose 6-phosphate dehydrogenase activity in membranes of erythrocytes from normal individuals and subjects with Mediterranean G6PD deficiency." Biochem Biophys Res Commun **85**(4): 1318-1324.

Benjamini, Y., Hochberg, Y. (1995). "Controlling the False Discovery Rate: A Practical and Powerful Approach to Multiple Testing." Journal of the Royal Statistical Society. Series B (Methodological) **57**(1): 289-300.

Bereiter-Hahn, J. and M. Voth (1994). "Dynamics of mitochondria in living cells: shape changes, dislocations, fusion, and fission of mitochondria." Microsc Res Tech **27**(3): 198-219.

Besrat, A., C. E. Polan and L. M. Henderson (1969). "Mammalian metabolism of glutaric acid." J Biol Chem **244**(6): 1461-1467.

Bigot, A., V. Jacquemin, F. Debacq-Chainiaux, G. S. Butler-Browne, O. Toussaint, D. Furling and V. Mouly (2008). "Replicative aging down-regulates the myogenic regulatory factors in human myoblasts." Biol Cell **100**(3): 189-199.

Billing-Ross, P., A. Germain, K. Ye, A. Keinan, Z. Gu and M. R. Hanson (2016). "Mitochondrial DNA variants correlate with symptoms in myalgic encephalomyelitis/chronic fatigue syndrome." J Transl Med **14**: 19.

Blundell, S., K. K. Ray, M. Buckland and P. D. White (2015). "Chronic fatigue syndrome and circulating cytokines: A systematic review." Brain Behav Immun **50**: 186-195.

Bokko, P. B., L. Francione, E. Bandala-Sanchez, A. U. Ahmed, S. J. Annesley, X. Huang, T. Khurana, A. R. Kimmel and P. R. Fisher (2007). "Diverse cytopathologies in mitochondrial disease are caused by AMP-activated protein kinase signaling." Mol Biol Cell **18**(5): 1874-1886.

Booth, N. E., S. Myhill and J. McLaren-Howard (2012). "Mitochondrial dysfunction and the pathophysiology of Myalgic Encephalomyelitis/Chronic Fatigue Syndrome (ME/CFS)." Int J Clin Exp Med **5**(3): 208-220.

Bradley, A. S., B. Ford and A. S. Bansal (2013). "Altered functional B cell subset populations in patients with chronic fatigue syndrome compared to healthy controls." Clin Exp Immunol **172**(1): 73-80.

Brenu, E. (2014). "Methylation Profile of CD4+ T Cells in Chronic Fatigue Syndrome/Myalgic Encephalomyelitis." Journal of Clinical & Cellular Immunology **05**(03).

Brenu, E. W., M. L. van Driel, D. R. Staines, K. J. Ashton, S. B. Ramos, J. Keane, N. G. Klimas and S. M. Marshall-Gradisnik (2011). "Immunological abnormalities as

potential biomarkers in Chronic Fatigue Syndrome/Myalgic Encephalomyelitis." J Transl Med **9**: 81.

Bretin, A., A. T. Gewirtz and B. Chassaing (2018). "Microbiota and metabolism: what's new in 2018?" Am J Physiol Endocrinol Metab **315**(1): E1-E6.

Brown, A. E., B. Dibnah, E. Fisher, J. L. Newton and M. Walker (2018). "Pharmacological activation of AMPK and glucose uptake in cultured human skeletal muscle cells from patients with ME/CFS." Biosci Rep **38**(3).

Brown, A. E., D. E. Jones, M. Walker and J. L. Newton (2015). "Abnormalities of AMPK activation and glucose uptake in cultured skeletal muscle cells from individuals with chronic fatigue syndrome." PLoS One **10**(4): e0122982.

Brown, N. F., M. Stefanovic-Racic, I. J. Sipula and G. Perdomo (2007). "The mammalian target of rapamycin regulates lipid metabolism in primary cultures of rat hepatocytes." Metabolism **56**(11): 1500-1507.

Brown, R. L. and T. B. Clarke (2017). "The regulation of host defences to infection by the microbiota." Immunology **150**(1): 1-6.

Buchwald, D., R. L. Ashley, T. Pearlman, P. Kith and A. L. Komaroff (1996). "Viral serologies in patients with chronic fatigue and chronic fatigue syndrome." J Med Virol **50**(1): 25-30.

Burnet, R. B. and B. E. Chatterton (2004). "Gastric emptying is slow in chronic fatigue syndrome." BMC Gastroenterol **4**: 32.

Butt, H. L., R. Dunstan, N. R. McGregor and T. K. Roberts (2001). "Bacterial colonosis in patients with persistent fatigue. ." Proceedings of the AHMF international clinical and scientific conference. Sydney, Australia.

Cabanas, H., K. Muraki, C. Balinas, N. Eaton-Fitch, D. Staines and S. Marshall-Gradisnik (2019). "Validation of impaired Transient Receptor Potential Melastatin 3 ion channel activity in natural killer cells from Chronic Fatigue Syndrome/ Myalgic Encephalomyelitis patients." Mol Med **25**(1): 14.

Cabanas, H., K. Muraki, N. Eaton, C. Balinas, D. Staines and S. Marshall-Gradisnik (2018). "Loss of Transient Receptor Potential Melastatin 3 ion channel function in natural killer cells from Chronic Fatigue Syndrome/Myalgic Encephalomyelitis patients." Mol Med **24**(1): 44.

Cadenas, E. and K. J. Davies (2000). "Mitochondrial free radical generation, oxidative stress, and aging." Free Radic Biol Med **29**(3-4): 222-230.

Campanella, M., A. Seraphim, R. Abeti, E. Casswell, P. Echave and M. R. Duchen (2009). "IF1, the endogenous regulator of the F(1)F(o)-ATPsynthase, defines mitochondrial volume fraction in HeLa cells by regulating autophagy." Biochim Biophys Acta **1787**(5): 393-401.

Carling, D., F. V. Mayer, M. J. Sanders and S. J. Gamblin (2011). "AMP-activated protein kinase: nature's energy sensor." Nat Chem Biol **7**(8): 512-518.

Carruthers, B. M., A. K. Jain, K. L. De Meirleir, D. L. Peterson, N. G. Klimas, A. M. Lerner, A. C. Bested, P. Flor-Henry, P. Joshi, A. C. Powles, J. A. Sherkey and M. I. Van de Sande (2003). "Myalgic Encephalomyelitis/Chronic Fatigue Syndrome: Clinical Working Case Definition, Diagnostic and Treatment Protocols." Journal of Chronic Fatigue Syndrome, **11**(1): 7-36.

Carruthers, B. M., M. I. van de Sande, K. L. De Meirleir, N. G. Klimas, G. Broderick, T. Mitchell, D. Staines, A. C. Powles, N. Speight, R. Vallings, L. Bateman, B. Baumgarten-Austrheim, D. S. Bell, N. Carlo-Stella, J. Chia, A. Darragh, D. Jo, D. Lewis, A. R. Light, S. Marshall-Gradisbik, I. Mena, J. A. Mikovits, K. Miwa, M. Murovska, M. L. Pall and S. Stevens (2011). "Myalgic encephalomyelitis: International Consensus Criteria." J Intern Med **270**(4): 327-338.

Castro-Marrero, J., M. D. Cordero, N. Saez-Francas, C. Jimenez-Gutierrez, F. J. Aguilar-Montilla, L. Aliste and J. Alegre-Martin (2013). "Could mitochondrial dysfunction be a differentiating marker between chronic fatigue syndrome and fibromyalgia?" Antioxid Redox Signal **19**(15): 1855-1860.

Chambers, E. S., T. Preston, G. Frost and D. J. Morrison (2018). "Role of Gut Microbiota-Generated Short-Chain Fatty Acids in Metabolic and Cardiovascular Health." Curr Nutr Rep **7**(4): 198-206.

Ciechanover, A. and Y. T. Kwon (2015). "Degradation of misfolded proteins in neurodegenerative diseases: therapeutic targets and strategies." Exp Mol Med **47**: e147.

Ciregia, F., L. Kollipara, L. Giusti, R. P. Zahedi, C. Giacomelli, M. R. Mazzoni, G. Giannaccini, P. Scarpellini, A. Urbani, A. Sickmann, A. Lucacchini and L. Bazzichi (2016). "Bottom-up proteomics suggests an association between differential expression of mitochondrial proteins and chronic fatigue syndrome." Transl Psychiatry **6**(9): e904.

Clark, A. and N. Mach (2017). "The Crosstalk between the Gut Microbiota and Mitochondria during Exercise." Front Physiol **8**: 319.

Cliff, J. M., E. C. King, J. S. Lee, N. Sepulveda, A. S. Wolf, C. Kingdon, E. Bowman, H. M. Dockrell, L. Nacul, E. Lacerda and E. M. Riley (2019). "Cellular Immune Function in Myalgic Encephalomyelitis/Chronic Fatigue Syndrome (ME/CFS)." Front Immunol **10**: 796.

Close, S., S. Marshall-Gradisnik, J. Byrnes, P. Smith, S. Nghiem and D. Staines (2020). "The Economic Impacts of Myalgic Encephalomyelitis/Chronic Fatigue Syndrome in an Australian Cohort." Front Public Health **8**: 420.

Conn, C. S. and S. B. Qian (2011). "mTOR signaling in protein homeostasis: less is more?" Cell Cycle **10**(12): 1940-1947.

Cortes Rivera, M., C. Mastronardi, C. T. Silva-Aldana, M. Arcos-Burgos and B. A. Lidbury (2019). "Myalgic Encephalomyelitis/Chronic Fatigue Syndrome: A Comprehensive Review." Diagnostics (Basel) **9**(3).

Cost, N. G. and M. F. Czyzyk-Krzeska (2015). "Regulation of autophagy by two products of one gene: TRPM3 and miR-204." Mol Cell Oncol **2**(4): e1002712.

Craddock, T. J., P. Fritsch, M. A. Rice, Jr., R. M. del Rosario, D. B. Miller, M. A. Fletcher, N. G. Klimas and G. Broderick (2014). "A role for homeostatic drive in the perpetuation of complex chronic illness: Gulf War Illness and chronic fatigue syndrome." PLoS One **9**(1): e84839.

Cunningham, J. T., J. T. Rodgers, D. H. Arlow, F. Vazquez, V. K. Mootha and P. Puigserver (2007). "mTOR controls mitochondrial oxidative function through a YY1-PGC-1alpha transcriptional complex." Nature **450**(7170): 736-740.

Curriu, M., J. Carrillo, M. Massanella, J. Rigau, J. Alegre, J. Puig, A. M. Garcia-Quintana, J. Castro-Marrero, E. Negredo, B. Clotet, C. Cabrera and J. Blanco (2013). "Screening NK-, B- and T-cell phenotype and function in patients suffering from Chronic Fatigue Syndrome." J Transl Med **11**: 68.

Dalle Pezze, P., S. Ruf, A. G. Sonntag, M. Langelaar-Makkinje, P. Hall, A. M. Heberle, P. Razquin Navas, K. van Eunen, R. C. Tolle, J. J. Schwarz, H. Wiese, B. Warscheid, J. Deitersen, B. Stork, E. Fassler, S. Schauble, U. Hahn, P. Horvatovich, D. P. Shanley and K. Thedieck (2016). "A systems study reveals concurrent activation of AMPK and mTOR by amino acids." Nat Commun **7**: 13254.

de Vega, W. C., L. Erdman, S. D. Vernon, A. Goldenberg and P. O. McGowan (2018). "Integration of DNA methylation & health scores identifies subtypes in myalgic encephalomyelitis/chronic fatigue syndrome." Epigenomics **10**(5): 539-557.

de Vega, W. C., S. Herrera, S. D. Vernon and P. O. McGowan (2017). "Epigenetic modifications and glucocorticoid sensitivity in Myalgic Encephalomyelitis/Chronic Fatigue Syndrome (ME/CFS)." BMC Med Genomics **10**(1): 11.

de Vega, W. C., S. D. Vernon and P. O. McGowan (2014). "DNA methylation modifications associated with chronic fatigue syndrome." PLoS One **9**(8): e104757.

Dowling, R. J., I. Topisirovic, T. Alain, M. Bidinosti, B. D. Fonseca, E. Petroulakis, X. Wang, O. Larsson, A. Selvaraj, Y. Liu, S. C. Kozma, G. Thomas and N. Sonenberg (2010). "mTORC1-mediated cell proliferation, but not cell growth, controlled by the 4E-BPs." Science **328**(5982): 1172-1176.

Du Preez, S., M. Corbitt, H. Cabanas, N. Eaton, D. Staines and S. Marshall-Gradisnik (2018). "A systematic review of enteric dysbiosis in chronic fatigue syndrome/myalgic encephalomyelitis." Syst Rev **7**(1): 241.

Duran, R. V. and M. N. Hall (2012). "Glutaminolysis feeds mTORC1." Cell Cycle **11**(22): 4107-4108.

Duran, R. V., E. D. MacKenzie, H. Boulahbel, C. Frezza, L. Heiserich, S. Tardito, O. Bussolati, S. Rocha, M. N. Hall and E. Gottlieb (2013). "HIF-independent role of prolyl hydroxylases in the cellular response to amino acids." Oncogene **32**(38): 4549-4556.

Duran, R. V., W. Oppliger, A. M. Robitaille, L. Heiserich, R. Skendaj, E. Gottlieb and M. N. Hall (2012). "Glutaminolysis activates Rag-mTORC1 signaling." Mol Cell **47**(3): 349-358.

Elfaitouri, A., B. Herrmann, A. Bolin-Wiener, Y. Wang, C. G. Gottfries, O. Zachrisson, R. Pipkorn, L. Ronnblom and J. Blomberg (2013). "Epitopes of microbial and human heat shock protein 60 and their recognition in myalgic encephalomyelitis." PLoS One **8**(11): e81155.

Esfandyarpour, R., A. Kashi, M. Nemat-Gorgani, J. Wilhelmy and R. W. Davis (2019). "A nanoelectronics-blood-based diagnostic biomarker for myalgic encephalomyelitis/chronic fatigue syndrome (ME/CFS)." Proc Natl Acad Sci U S A.

Everett, L., A. Galli and D. Crabb (2000). "The role of hepatic peroxisome proliferator-activated receptors (PPARs) in health and disease." Liver **20**(3): 191-199.

Falk Hvidberg, M., L. S. Brinth, A. V. Olesen, K. D. Petersen and L. Ehlers (2015). "The Health-Related Quality of Life for Patients with Myalgic Encephalomyelitis / Chronic Fatigue Syndrome (ME/CFS)." PLoS One **10**(7): e0132421.

Fletcher, M. A., X. R. Zeng, Z. Barnes, S. Levis and N. G. Klimas (2009). "Plasma cytokines in women with chronic fatigue syndrome." J Transl Med **7**: 96.

Fletcher, M. A., X. R. Zeng, K. Maher, S. Levis, B. Hurwitz, M. Antoni, G. Broderick and N. G. Klimas (2010). "Biomarkers in chronic fatigue syndrome: evaluation of natural killer cell function and dipeptidyl peptidase IV/CD26." PLoS One **5**(5): e10817.

Fluge, O. and O. Mella (2009). "Clinical impact of B-cell depletion with the anti-CD20 antibody rituximab in chronic fatigue syndrome: a preliminary case series." BMC Neurol **9**: 28.

Fluge, O., O. Mella, O. Bruland, K. Risa, S. E. Dyrstad, K. Alme, I. G. Rekeland, D. Sapkota, G. V. Rosland, A. Fossa, I. Ktoridou-Valen, S. Lunde, K. Sorland, K. Lien, I. Herder, H. Thurmer, M. E. Gotaas, K. A. Baranowska, L. M. Bohnen, C. Schafer, A. McCann, K. Sommerfelt, L. Helgeland, P. M. Ueland, O. Dahl and K. J. Tronstad (2016). "Metabolic profiling indicates impaired pyruvate dehydrogenase function in myalgic encephalopathy/chronic fatigue syndrome." JCI Insight **1**(21): e89376.

Fluge, O., I. G. Rekeland, K. Lien, H. Thurmer, P. C. Borchgrevink, C. Schafer, K. Sorland, J. Assmus, I. Ktoridou-Valen, I. Herder, M. E. Gotaas, O. Kvammen, K. A. Baranowska, L. Bohnen, S. S. Martinsen, A. E. Lonar, A. H. Solvang, A. E. S. Gya, O. Bruland, K. Risa, K. Alme, O. Dahl and O. Mella (2019). "B-Lymphocyte Depletion in Patients With Myalgic Encephalomyelitis/Chronic Fatigue Syndrome: A Randomized, Double-Blind, Placebo-Controlled Trial." Ann Intern Med.

Fluge, O., K. Risa, S. Lunde, K. Alme, I. G. Rekeland, D. Sapkota, E. K. Kristoffersen, K. Sorland, O. Bruland, O. Dahl and O. Mella (2015). "B-Lymphocyte Depletion in Myalgic Encephalopathy/ Chronic Fatigue Syndrome. An Open-Label Phase II Study with Rituximab Maintenance Treatment." PLoS One **10**(7): e0129898.

Fox, J. (2005). "The R commander: a basic-statistics graphical user interface to R." J. Stat. Software **14**: 1-42.

Fremont, M., D. Coomans, S. Massart and K. De Meirleir (2013). "High-throughput 16S rRNA gene sequencing reveals alterations of intestinal microbiota in myalgic encephalomyelitis/chronic fatigue syndrome patients." Anaerobe **22**: 50-56.

Fukuda, K., S. E. Straus, I. Hickie, M. C. Sharpe, J. G. Dobbins and A. Komaroff (1994). "The chronic fatigue syndrome: a comprehensive approach to its definition and study. International Chronic Fatigue Syndrome Study Group." Ann Intern Med **121**(12): 953-959.

Garcia-Bermudez, J. and J. M. Cuezva (2016). "The ATPase Inhibitory Factor 1 (IF1): A master regulator of energy metabolism and of cell survival." Biochim Biophys Acta **1857**(8): 1167-1182.

Gardiner, C. M. and D. K. Finlay (2017). "What Fuels Natural Killers? Metabolism and NK Cell Responses." Front Immunol **8**: 367.

Genomes Project, C., A. Auton, L. D. Brooks, R. M. Durbin, E. P. Garrison, H. M. Kang, J. O. Korbel, J. L. Marchini, S. McCarthy, G. A. McVean and G. R. Abecasis (2015). "A global reference for human genetic variation." Nature **526**(7571): 68-74.

Germain, A., D. K. Barupal, S. M. Levine and M. R. Hanson (2020). "Comprehensive Circulatory Metabolomics in ME/CFS Reveals Disrupted Metabolism of Acyl Lipids and Steroids." Metabolites **10**(1).

Germain, A., D. Ruppert, S. M. Levine and M. R. Hanson (2017). "Metabolic profiling of a myalgic encephalomyelitis/chronic fatigue syndrome discovery cohort reveals disturbances in fatty acid and lipid metabolism." Mol Biosyst **13**(2): 371-379.

Germain, A., D. Ruppert, S. M. Levine and M. R. Hanson (2018). "Prospective Biomarkers from Plasma Metabolomics of Myalgic Encephalomyelitis/Chronic Fatigue Syndrome Implicate Redox Imbalance in Disease Symptomatology." Metabolites **8**(4).

Ghini, V., D. Quaglio, C. Luchinat and P. Turano (2019). "NMR for sample quality assessment in metabolomics." N Biotechnol **52**: 25-34.

Ghosh Roy, S., E. S. Robertson and A. Saha (2016). "Epigenetic Impact on EBV Associated B-Cell Lymphomagenesis." Biomolecules **6**(4).

Ghosh, S., C. Dai, K. Brown, E. Rajendiran, S. Makarenko, J. Baker, C. Ma, S. Halder, M. Montero, V. A. Ionescu, A. Klegeris, B. A. Vallance and D. L. Gibson (2011). "Colonic microbiota alters host susceptibility to infectious colitis by modulating inflammation, redox status, and ion transporter gene expression." Am J Physiol Gastrointest Liver Physiol **301**(1): G39-49.

Gilardini Montani, M. S., R. Santarelli, M. Granato, R. Gonnella, M. R. Torrisi, A. Faggioni and M. Cirone (2019). "EBV reduces autophagy, intracellular ROS and mitochondria to impair monocyte survival and differentiation." Autophagy **15**(4): 652-667.

Giloteaux, L., J. K. Goodrich, W. A. Walters, S. M. Levine, R. E. Ley and M. R. Hanson (2016). "Reduced diversity and altered composition of the gut microbiome in individuals with myalgic encephalomyelitis/chronic fatigue syndrome." Microbiome **4**(1): 30.

Grainger, J., R. Daw and K. Wemyss (2018). "Systemic instruction of cell-mediated immunity by the intestinal microbiome." F1000Res **7**.

Grimm, C., R. Kraft, S. Sauerbruch, G. Schultz and C. Harteneck (2003). "Molecular and functional characterization of the melastatin-related cation channel TRPM3." J Biol Chem **278**(24): 21493-21501.

Haigis, M. C., R. Mostoslavsky, K. M. Haigis, K. Fahie, D. C. Christodoulou, A. J. Murphy, D. M. Valenzuela, G. D. Yancopoulos, M. Karow, G. Blander, C. Wolberger, T. A. Prolla, R. Weindruch, F. W. Alt and L. Guarente (2006). "SIRT4 inhibits glutamate dehydrogenase and opposes the effects of calorie restriction in pancreatic beta cells." Cell **126**(5): 941-954.

Halpin, P., M. V. Williams, N. G. Klimas, M. A. Fletcher, Z. Barnes and M. E. Ariza (2017). "Myalgic encephalomyelitis/chronic fatigue syndrome and gulf war illness patients exhibit increased humoral responses to the herpesviruses-encoded dUTPase: Implications in disease pathophysiology." J Med Virol **89**(9): 1636-1645.

Hara, K., K. Yonezawa, Q. P. Weng, M. T. Kozlowski, C. Belham and J. Avruch (1998). "Amino acid sufficiency and mTOR regulate p70 S6 kinase and eIF-4E BP1 through a common effector mechanism." J Biol Chem **273**(23): 14484-14494.

Hardcastle, S. L., E. W. Brenu, S. Johnston, T. Nguyen, T. Huth, N. Wong, S. Ramos, D. Staines and S. Marshall-Gradisnik (2015). "Characterisation of cell functions and receptors in Chronic Fatigue Syndrome/Myalgic Encephalomyelitis (CFS/ME)." BMC Immunol **16**: 35.

Hardie, D. G. (2011). "Adenosine monophosphate-activated protein kinase: a central regulator of metabolism with roles in diabetes, cancer, and viral infection." Cold Spring Harb Symp Quant Biol **76**: 155-164.

Hardie, D. G. and D. Carling (1997). "The AMP-activated protein kinase--fuel gauge of the mammalian cell?" Eur J Biochem **246**(2): 259-273.

Hardie, D. G. and D. A. Pan (2002). "Regulation of fatty acid synthesis and oxidation by the AMP-activated protein kinase." Biochem Soc Trans **30**(Pt 6): 1064-1070.

Harris, M. A., J. Clark, A. Ireland, J. Lomax, M. Ashburner, R. Foulger, K. Eilbeck, S. Lewis, B. Marshall, C. Mungall, J. Richter, G. M. Rubin, J. A. Blake, C. Bult, M. Dolan, H. Drabkin, J. T. Eppig, D. P. Hill, L. Ni, M. Ringwald, R. Balakrishnan, J. M. Cherry, K. R. Christie, M. C. Costanzo, S. S. Dwight, S. Engel, D. G. Fisk, J. E. Hirschman, E. L. Hong, R. S. Nash, A. Sethuraman, C. L. Theesfeld, D. Botstein, K. Dolinski, B. Feierbach, T. Berardini, S. Mundodi, S. Y. Rhee, R. Apweiler, D. Barrell, E. Camon, E. Dimmer, V. Lee, R. Chisholm, P. Gaudet, W. Kibbe, R. Kishore, E. M. Schwarz, P. Sternberg, M. Gwinn, L. Hannick, J. Wortman, M. Berriman, V. Wood, N. de la Cruz, P. Tonellato, P. Jaiswal, T. Seigfried, R. White and C. Gene Ontology (2004). "The Gene Ontology (GO) database and informatics resource." Nucleic Acids Res **32**(Database issue): D258-261.

Harris, R. A., J. W. Hawes, K. M. Popov, Y. Zhao, Y. Shimomura, J. Sato, J. Jaskiewicz and T. D. Hurley (1997). "Studies on the regulation of the mitochondrial alpha-ketoacid dehydrogenase complexes and their kinases." Adv Enzyme Regul **37**: 271-293.

Hawley, S. A., D. A. Pan, K. J. Mustard, L. Ross, J. Bain, A. M. Edelman, B. G. Frenguelli and D. G. Hardie (2005). "Calmodulin-dependent protein kinase kinase-beta is an

alternative upstream kinase for AMP-activated protein kinase." Cell Metab **2**(1): 9-19.

Helbig, K., R. Harris, J. Ayres, H. Dunckley, A. Lloyd, J. Robson and B. P. Marmion (2005). "Immune response genes in the post-Q-fever fatigue syndrome, Q fever endocarditis and uncomplicated acute primary Q fever." QJM **98**(8): 565-574.

Helbig, K. J., S. L. Heatley, R. J. Harris, C. G. Mullighan, P. G. Bardy and B. P. Marmion (2003). "Variation in immune response genes and chronic Q fever. Concepts: preliminary test with post-Q fever fatigue syndrome." Genes Immun **4**(1): 82-85.

Helliwell, A. M., E. C. Sweetman, P. A. Stockwell, C. D. Edgar, A. Chatterjee and W. P. Tate (2020). "Changes in DNA methylation profiles of myalgic encephalomyelitis/chronic fatigue syndrome patients reflect systemic dysfunctions." Clin Epigenetics **12**(1): 167.

Henriksson, A. E., C. Tagesson, A. Uribe, K. Uvnas-Moberg, C. E. Nord, R. Gullberg and C. Johansson (1988). "Effects of prostaglandin E2 on disease activity, gastric secretion and intestinal permeability, and morphology in patients with rheumatoid arthritis." Ann Rheum Dis **47**(8): 620-627.

Hernando, H., C. Shannon-Lowe, A. B. Islam, F. Al-Shahrour, J. Rodriguez-Ubreva, V. C. Rodriguez-Cortez, B. M. Javierre, C. Mangas, A. F. Fernandez, M. Parra, H. J. Delecluse, M. Esteller, E. Lopez-Granados, M. F. Fraga, N. Lopez-Bigas and E. Ballestar (2013). "The B cell transcription program mediates hypomethylation and overexpression of key genes in Epstein-Barr virus-associated proliferative conversion." Genome Biol **14**(1): R3.

Hindupur, S. K., A. Gonzalez and M. N. Hall (2015). "The opposing actions of target of rapamycin and AMP-activated protein kinase in cell growth control." Cold Spring Harb Perspect Biol **7**(8): a019141.

Holmes, G. P., J. E. Kaplan, N. M. Gantz, A. L. Komaroff, L. B. Schonberger, S. E. Straus, J. F. Jones, R. E. Dubois, C. Cunningham-Rundles, S. Pahwa and et al. (1988). "Chronic fatigue syndrome: a working case definition." Ann Intern Med **108**(3): 387-389.

Horecker, B. L. (2002). "The pentose phosphate pathway." J Biol Chem **277**(50): 47965-47971.

Hornig, M., G. Gottschalk, D. L. Peterson, K. K. Knox, A. F. Schultz, M. L. Eddy, X. Che and W. I. Lipkin (2016). "Cytokine network analysis of cerebrospinal fluid in myalgic encephalomyelitis/chronic fatigue syndrome." Mol Psychiatry **21**(2): 261-269.

Hornig, M., J. G. Montoya, N. G. Klimas, S. Levine, D. Felsenstein, L. Bateman, D. L. Peterson, C. G. Gottschalk, A. F. Schultz, X. Che, M. L. Eddy, A. L. Komaroff and W. I. Lipkin (2015). "Distinct plasma immune signatures in ME/CFS are present early in the course of illness." Sci Adv **1**(1).

Horton, J. D., N. A. Shah, J. A. Warrington, N. N. Anderson, S. W. Park, M. S. Brown and J. L. Goldstein (2003). "Combined analysis of oligonucleotide microarray data from transgenic and knockout mice identifies direct SREBP target genes." Proc Natl Acad Sci U S A **100**(21): 12027-12032.

Hsieh, A. C., M. Costa, O. Zollo, C. Davis, M. E. Feldman, J. R. Testa, O. Meyuhas, K. M. Shokat and D. Ruggero (2010). "Genetic dissection of the oncogenic mTOR pathway reveals druggable addiction to translational control via 4EBP-eIF4E." Cancer Cell **17**(3): 249-261.

Hue, L. and H. Taegtmeyer (2009). "The Randle cycle revisited: a new head for an old hat." Am J Physiol Endocrinol Metab **297**(3): E578-591.

Hughes, A. J., S. E. Daniel, Y. Ben-Shlomo and A. J. Lees (2002). "The accuracy of diagnosis of parkinsonian syndromes in a specialist movement disorder service." Brain **125**(Pt 4): 861-870.

Hurst, J. K. and S. V. Lymar (1997). "Toxicity of peroxynitrite and related reactive nitrogen species toward Escherichia coli." Chem Res Toxicol **10**(7): 802-810.

Hussain, T. and R. Mulherkar (2012). "Lymphoblastoid Cell lines: a Continuous in Vitro Source of Cells to Study Carcinogen Sensitivity and DNA Repair." Int J Mol Cell Med **1**(2): 75-87.

Hutson, S. M., A. J. Sweatt and K. F. Lanoue (2005). "Branched-chain [corrected] amino acid metabolism: implications for establishing safe intakes." J Nutr **135**(6 Suppl): 1557S-1564S.

Huttenlocher, A., M. Lakonishok, M. Kinder, S. Wu, T. Truong, K. A. Knudsen and A. F. Horwitz (1998). "Integrin and cadherin synergy regulates contact inhibition of migration and motile activity." J Cell Biol **141**(2): 515-526.

Israel, B. F., M. Gulley, S. Elmore, S. Ferrini, W. H. Feng and S. C. Kenney (2005). "Anti-CD70 antibodies: a potential treatment for EBV+ CD70-expressing lymphomas." Mol Cancer Ther **4**(12): 2037-2044.

Jackson, M. L., H. Butt, M. Ball, D. P. Lewis and D. Bruck (2015). "Sleep quality and the treatment of intestinal microbiota imbalance in Chronic Fatigue Syndrome: A pilot study." Sleep Sci **8**(3): 124-133.

Jager, S., C. Handschin, J. St-Pierre and B. M. Spiegelman (2007). "AMP-activated protein kinase (AMPK) action in skeletal muscle via direct phosphorylation of PGC-1alpha." Proc Natl Acad Sci U S A **104**(29): 12017-12022.

Janssen, A. W. and S. Kersten (2015). "The role of the gut microbiota in metabolic health." FASEB J **29**(8): 3111-3123.

Jason, L. A., A. Boulton, N. S. Porter, T. Jessen, M. G. Njoku and F. Friedberg (2010). "Classification of myalgic encephalomyelitis/chronic fatigue syndrome by types of fatigue." Behav Med **36**(1): 24-31.

Jason, L. A., K. Corradi, S. Torres-Harding, R. R. Taylor and C. King (2005). "Chronic fatigue syndrome: the need for subtypes." Neuropsychol Rev **15**(1): 29-58.

Jayakumar, A., M. H. Tai, W. Y. Huang, W. al-Feel, M. Hsu, L. Abu-Elheiga, S. S. Chirala and S. J. Wakil (1995). "Human fatty acid synthase: properties and molecular cloning." Proc Natl Acad Sci U S A **92**(19): 8695-8699.

Johnston, S., E. W. Brenu, D. Staines and S. Marshall-Gradisnik (2013). "The prevalence of chronic fatigue syndrome/ myalgic encephalomyelitis: a meta-analysis." Clin Epidemiol **5**: 105-110.

Johnston, S. C., D. R. Staines and S. M. Marshall-Gradisnik (2016). "Epidemiological characteristics of chronic fatigue syndrome/myalgic encephalomyelitis in Australian patients." Clin Epidemiol **8**: 97-107.

Joutsa, J., M. Gardberg, M. Roytta and V. Kaasinen (2014). "Diagnostic accuracy of parkinsonism syndromes by general neurologists." Parkinsonism Relat Disord **20**(8): 840-844.

Kaliannan, K., B. Wang, X. Y. Li, K. J. Kim and J. X. Kang (2015). "A host-microbiome interaction mediates the opposing effects of omega-6 and omega-3 fatty acids on metabolic endotoxemia." Sci Rep **5**: 11276.

Kanda, Y. (2013). "Investigation of the freely available easy-to-use software 'EZR' for medical statistics." Bone Marrow Transplant **48**(3): 452-458.

Kashi, A. A., R. W. Davis and R. D. Phair (2019). "The IDO Metabolic Trap Hypothesis for the Etiology of ME/CFS." Diagnostics (Basel) **9**(3).

Kaur, J. and J. Debnath (2015). "Autophagy at the crossroads of catabolism and anabolism." Nat Rev Mol Cell Biol **16**(8): 461-472.

Kaushik, N., D. Fear, S. C. Richards, C. R. McDermott, E. F. Nuwaysir, P. Kellam, T. J. Harrison, R. J. Wilkinson, D. A. Tyrrell, S. T. Holgate and J. R. Kerr (2005). "Gene expression in peripheral blood mononuclear cells from patients with chronic fatigue syndrome." J Clin Pathol **58**(8): 826-832.

Kawasaki, A., Y. Shinkai, Y. Kuwana, A. Furuya, Y. Iigo, N. Hanai, S. Itoh, H. Yagita and K. Okumura (1990). "Perforin, a pore-forming protein detectable by monoclonal antibodies, is a functional marker for killer cells." Int Immunol **2**(7): 677-684.

Kerr, J. R., B. Burke, R. Petty, J. Gough, D. Fear, D. L. Mattey, J. S. Axford, A. G. Dalgleish and D. J. Nutt (2008). "Seven genomic subtypes of chronic fatigue syndrome/myalgic encephalomyelitis: a detailed analysis of gene networks and clinical phenotypes." J Clin Pathol **61**(6): 730-739.

Kerr, J. R., R. Petty, B. Burke, J. Gough, D. Fear, L. I. Sinclair, D. L. Mattey, S. C. Richards, J. Montgomery, D. A. Baldwin, P. Kellam, T. J. Harrison, G. E. Griffin, J. Main, D. Enlander, D. J. Nutt and S. T. Holgate (2008). "Gene expression subtypes in patients with chronic fatigue syndrome/myalgic encephalomyelitis." J Infect Dis **197**(8): 1171-1184.

Kim, C. W., Y. A. Moon, S. W. Park, D. Cheng, H. J. Kwon and J. D. Horton (2010). "Induced polymerization of mammalian acetyl-CoA carboxylase by MIG12 provides a tertiary level of regulation of fatty acid synthesis." Proc Natl Acad Sci U S A **107**(21): 9626-9631.

Kim, J., M. Kundu, B. Viollet and K. L. Guan (2011). "AMPK and mTOR regulate autophagy through direct phosphorylation of Ulk1." Nat Cell Biol **13**(2): 132-141.

Klimas, N. G., F. R. Salvato, R. Morgan and M. A. Fletcher (1990). "Immunologic abnormalities in chronic fatigue syndrome." J Clin Microbiol **28**(6): 1403-1410.

Komaroff, A. L. and D. Buchwald (1991). "Symptoms and signs of chronic fatigue syndrome." Rev Infect Dis **13 Suppl 1**: S8-11.

Krebs, H. A. (1935). "Metabolism of amino-acids: The synthesis of glutamine from glutamic acid and ammonia, and the enzymic hydrolysis of glutamine in animal tissues." Biochem J **29**(8): 1951-1969.

Landi, A., D. Broadhurst, S. D. Vernon, D. L. Tyrrell and M. Houghton (2016). "Reductions in circulating levels of IL-16, IL-7 and VEGF-A in myalgic encephalomyelitis/chronic fatigue syndrome." Cytokine **78**: 27-36.

Laplante, M. and D. M. Sabatini (2009). "An emerging role of mTOR in lipid biosynthesis." Curr Biol **19**(22): R1046-1052.

Lawson, N., C. H. Hsieh, D. March and X. Wang (2016). "Elevated Energy Production in Chronic Fatigue Syndrome Patients." J Nat Sci **2**(10).

Lecker, S. H., A. L. Goldberg and W. E. Mitch (2006). "Protein degradation by the ubiquitin-proteasome pathway in normal and disease states." J Am Soc Nephrol **17**(7): 1807-1819.

Lidbury, B. A., B. Kita, D. P. Lewis, S. Hayward, H. Ludlow, M. P. Hedger and D. M. de Kretser (2017). "Activin B is a novel biomarker for chronic fatigue syndrome/myalgic encephalomyelitis (CFS/ME) diagnosis: a cross sectional study." J Transl Med **15**(1): 60.

Lidbury, B. A., B. Kita, A. M. Richardson, D. P. Lewis, E. Privitera, S. Hayward, D. de Kretser and M. Hedger (2019). "Rethinking ME/CFS Diagnostic Reference Intervals via Machine Learning, and the Utility of Activin B for Defining Symptom Severity." Diagnostics (Basel) **9**(3).

Light, K. C., N. Agarwal, E. Iacob, A. T. White, A. Y. Kinney, T. A. VanHaitsma, H. Aizad, R. W. Hughen, L. Bateman and A. R. Light (2013). "Differing leukocyte gene expression profiles associated with fatigue in patients with prostate cancer versus chronic fatigue syndrome." Psychoneuroendocrinology **38**(12): 2983-2995.

Loebel, M., P. Grabowski, H. Heidecke, S. Bauer, L. G. Hanitsch, K. Wittke, C. Meisel, P. Reinke, H. D. Volk, O. Fluge, O. Mella and C. Scheibenbogen (2016). "Antibodies to beta adrenergic and muscarinic cholinergic receptors in patients with Chronic Fatigue Syndrome." Brain Behav Immun **52**: 32-39.

Loesch, D. Z., S. J. Annesley, N. Trost, M. Q. Bui, S. T. Lay, E. Storey, S. W. De Piazza, O. Sanislav, L. M. Francione, E. M. Hammersley, F. Tassone, D. Francis and P. R. Fisher (2017). "Novel Blood Biomarkers Are Associated with White Matter Lesions in Fragile X- Associated Tremor/Ataxia Syndrome." Neurodegener Dis **17**(1): 22-30.

Loewith, R. and M. N. Hall (2011). "Target of rapamycin (TOR) in nutrient signaling and growth control." Genetics **189**(4): 1177-1201.

Lorusso, L., S. V. Mikhaylova, E. Capelli, D. Ferrari, G. K. Ngonga and G. Ricevuti (2009). "Immunological aspects of chronic fatigue syndrome." Autoimmun Rev **8**(4): 287-291.

Ma, X. M. and J. Blenis (2009). "Molecular mechanisms of mTOR-mediated translational control." Nat Rev Mol Cell Biol **10**(5): 307-318.

Maclachlan, L., S. Watson, P. Gallagher, A. Finkelmeyer, L. A. Jason, M. Sunnquist and J. L. Newton (2017). "Are current chronic fatigue syndrome criteria diagnosing different disease phenotypes?" PLoS One **12**(10): e0186885.

Maes, M., F. Coucke and J. C. Leunis (2007). "Normalization of the increased translocation of endotoxin from gram negative enterobacteria (leaky gut) is accompanied by a remission of chronic fatigue syndrome." Neuro Endocrinol Lett **28**(6): 739-744.

Maes, M. and J. C. Leunis (2008). "Normalization of leaky gut in chronic fatigue syndrome (CFS) is accompanied by a clinical improvement: effects of age, duration of illness and the translocation of LPS from gram-negative bacteria." Neuro Endocrinol Lett **29**(6): 902-910.

Maes, M., J. C. Leunis, M. Geffard and M. Berk (2014). "Evidence for the existence of Myalgic Encephalomyelitis/Chronic Fatigue Syndrome (ME/CFS) with and without abdominal discomfort (irritable bowel) syndrome." Neuro Endocrinol Lett **35**(6): 445-453.

Maes, M., I. Mihaylova and J. C. Leunis (2007). "Increased serum IgM antibodies directed against phosphatidyl inositol (Pi) in chronic fatigue syndrome (CFS) and major depression: evidence that an IgM-mediated immune response against Pi is one factor underpinning the comorbidity between both CFS and depression." Neuro Endocrinol Lett **28**(6): 861-867.

Maes, M., F. N. Twisk, M. Kubera and K. Ringel (2012). "Evidence for inflammation and activation of cell-mediated immunity in Myalgic Encephalomyelitis/Chronic Fatigue Syndrome (ME/CFS): increased interleukin-1, tumor necrosis factor-alpha, PMN-elastase, lysozyme and neopterin." J Affect Disord **136**(3): 933-939.

Maes, M., F. N. Twisk, M. Kubera, K. Ringel, J. C. Leunis and M. Geffard (2012). "Increased IgA responses to the LPS of commensal bacteria is associated with inflammation and activation of cell-mediated immunity in chronic fatigue syndrome." J Affect Disord **136**(3): 909-917.

Maher, K. J., N. G. Klimas and M. A. Fletcher (2005). "Chronic fatigue syndrome is associated with diminished intracellular perforin." Clin Exp Immunol **142**(3): 505-511.

Mandarano, A. H., J. Maya, L. Giloteaux, D. L. Peterson, M. Maynard, C. G. Gottschalk and M. R. Hanson (2019). "Myalgic encephalomyelitis/chronic fatigue syndrome patients exhibit altered T cell metabolism and cytokine associations." J Clin Invest.

Marshall-Gradisnik, S., T. Huth, A. Chacko, S. Johnston, P. Smith and D. Staines (2016). "Natural killer cells and single nucleotide polymorphisms of specific ion channels and receptor genes in myalgic encephalomyelitis/chronic fatigue syndrome." Appl Clin Genet **9**: 39-47.

Mastorodemos, V., I. Zaganas, C. Spanaki, M. Bessa and A. Plaitakis (2005). "Molecular basis of human glutamate dehydrogenase regulation under changing energy demands." J Neurosci Res **79**(1-2): 65-73.

Mathew, S. J., X. Mao, K. A. Keegan, S. M. Levine, E. L. Smith, L. A. Heier, V. Otcheretko, J. D. Coplan and D. C. Shungu (2009). "Ventricular cerebrospinal fluid lactate is increased in chronic fatigue syndrome compared with generalized anxiety disorder: an in vivo 3.0 T (1)H MRS imaging study." NMR Biomed **22**(3): 251-258.

McCarthy, D. J., Y. Chen and G. K. Smyth (2012). "Differential expression analysis of multifactor RNA-Seq experiments with respect to biological variation." Nucleic Acids Res **40**(10): 4288-4297.

McCully, K. K., B. H. Natelson, S. Iotti, S. Sisto and J. S. Leigh, Jr. (1996). "Reduced oxidative muscle metabolism in chronic fatigue syndrome." Muscle Nerve **19**(5): 621-625.

Mejia, E. M., S. Chau, G. C. Sparagna, S. Sipione and G. M. Hatch (2016). "Reduced Mitochondrial Function in Human Huntington Disease Lymphoblasts is Not Due to Alterations in Cardiolipin Metabolism or Mitochondrial Supercomplex Assembly." Lipids **51**(5): 561-569.

Mensah, F. F. K., C. W. Armstrong, V. Reddy, A. S. Bansal, S. Berkovitz, M. J. Leandro and G. Cambridge (2018). "CD24 Expression and B Cell Maturation Shows a Novel Link With Energy Metabolism: Potential Implications for Patients With Myalgic Encephalomyelitis/Chronic Fatigue Syndrome." Front Immunol **9**: 2421.

Mensah, F. K. F., A. S. Bansal, B. Ford and G. Cambridge (2017). "Chronic fatigue syndrome and the immune system: Where are we now?" Neurophysiol Clin **47**(2): 131-138.

Mi, H., Q. Dong, A. Muruganujan, P. Gaudet, S. Lewis and P. D. Thomas (2010). "PANTHER version 7: improved phylogenetic trees, orthologs and collaboration with the Gene Ontology Consortium." Nucleic Acids Res **38**(Database issue): D204-210.

Milrad, S. F., D. L. Hall, D. R. Jutagir, E. G. Lattie, G. H. Ironson, W. Wohlgemuth, M. V. Nunez, L. Garcia, S. J. Czaja, D. M. Perdomo, M. A. Fletcher, N. Klimas and M. H. Antoni (2017). "Poor sleep quality is associated with greater circulating pro-inflammatory cytokines and severity and frequency of chronic fatigue syndrome/myalgic encephalomyelitis (CFS/ME) symptoms in women." J Neuroimmunol **303**: 43-50.

Missailidis, D., S. J. Annesley, C. Y. Allan, O. Sanislav, B. A. Lidbury, D. P. Lewis and P. R. Fisher (2020). "An isolated Complex V inefficiency and dysregulated mitochondrial function in immortalized lymphocytes from ME/CFS patients." Int. J. Mol. Sci. **21**(3): 1074.

Missailidis, D., O. Sanislav, C. Y. Allan, S. J. Annesley and P. R. Fisher (2020). "Cell-Based Blood Biomarkers for Myalgic Encephalomyelitis/Chronic Fatigue Syndrome." Int J Mol Sci **21**(3).

Missailidis, D., O. Sanislav, C. Y. Allan, P. K. Smith, S. J. Annesley and P. R. Fisher (2021). "Dysregulated Provision of Oxidisable Substrates to the Mitochondria in ME/CFS Lymphoblasts." Int J Mol Sci **22**(4).

Moneghetti, K. J., M. Skhiri, K. Contrepois, Y. Kobayashi, H. Maecker, M. Davis, M. Snyder, F. Haddad and J. G. Montoya (2018). "Value of Circulating Cytokine Profiling During Submaximal Exercise Testing in Myalgic Encephalomyelitis/Chronic Fatigue Syndrome." Sci Rep **8**(1): 2779.

Montoya, J. G., T. H. Holmes, J. N. Anderson, H. T. Maecker, Y. Rosenberg-Hasson, I. J. Valencia, L. Chu, J. W. Younger, C. M. Tato and M. M. Davis (2017). "Cytokine signature associated with disease severity in chronic fatigue syndrome patients." Proc Natl Acad Sci U S A **114**(34): E7150-E7158.

Morissette, M. R., V. P. Sah, C. C. Glembotski and J. H. Brown (2000). "The Rho effector, PKN, regulates ANF gene transcription in cardiomyocytes through a serum response element." Am J Physiol Heart Circ Physiol **278**(6): H1769-1774.

Morita, M., S. P. Gravel, L. Hulea, O. Larsson, M. Pollak, J. St-Pierre and I. Topisirovic (2015). "mTOR coordinates protein synthesis, mitochondrial activity and proliferation." Cell Cycle **14**(4): 473-480.

Murrough, J. W., X. Mao, K. A. Collins, C. Kelly, G. Andrade, P. Nestadt, S. M. Levine, S. J. Mathew and D. C. Shungu (2010). "Increased ventricular lactate in chronic fatigue syndrome measured by 1H MRS imaging at 3.0 T. II: comparison with major depressive disorder." NMR Biomed **23**(6): 643-650.

Myhill, S., N. E. Booth and J. McLaren-Howard (2009). "Chronic fatigue syndrome and mitochondrial dysfunction." Int J Clin Exp Med **2**(1): 1-16.

Myhill, S., N. E. Booth and J. McLaren-Howard (2013). "Targeting mitochondrial dysfunction in the treatment of Myalgic Encephalomyelitis/Chronic Fatigue Syndrome (ME/CFS) - a clinical audit." Int J Clin Exp Med **6**(1): 1-15.

Nacul, L., B. de Barros, C. C. Kingdon, J. M. Cliff, T. G. Clark, K. Mudie, H. M. Dockrell and E. M. Lacerda (2019). "Evidence of Clinical Pathology Abnormalities in People with Myalgic Encephalomyelitis/Chronic Fatigue Syndrome (ME/CFS) from an Analytic Cross-Sectional Study." Diagnostics (Basel) **9**(2).

Nacul, L. C., K. Mudie, C. C. Kingdon, T. G. Clark and E. M. Lacerda (2018). "Hand Grip Strength as a Clinical Biomarker for ME/CFS and Disease Severity." Front Neurol **9**: 992.

Nagy-Szakal, D., D. K. Barupal, B. Lee, X. Che, B. L. Williams, E. J. R. Kahn, J. E. Ukaigwe, L. Bateman, N. G. Klimas, A. L. Komaroff, S. Levine, J. G. Montoya, D. L. Peterson, B. Levin, M. Hornig, O. Fiehn and W. I. Lipkin (2018). "Insights into myalgic encephalomyelitis/chronic fatigue syndrome phenotypes through comprehensive metabolomics." Sci Rep **8**(1): 10056.

Nakajima, A., A. Vogelzang, M. Maruya, M. Miyajima, M. Murata, A. Son, T. Kuwahara, T. Tsuruyama, S. Yamada, M. Matsuura, H. Nakase, D. A. Peterson, S. Fagarasan and K. Suzuki (2018). "IgA regulates the composition and metabolic function of gut microbiota by promoting symbiosis between bacteria." J Exp Med **215**(8): 2019-2034.

Narita, M., A. R. Young, S. Arakawa, S. A. Samarajiwa, T. Nakashima, S. Yoshida, S. Hong, L. S. Berry, S. Reichelt, M. Ferreira, S. Tavare, K. Inoki, S. Shimizu and M. Narita (2011). "Spatial coupling of mTOR and autophagy augments secretory phenotypes." Science **332**(6032): 966-970.

Naviaux, R. K. (2012). "Oxidative shielding or oxidative stress?" J Pharmacol Exp Ther **342**(3): 608-618.

Naviaux, R. K. (2014). "Metabolic features of the cell danger response." Mitochondrion **16**: 7-17.

Naviaux, R. K., J. C. Naviaux, K. Li, A. T. Bright, W. A. Alaynick, L. Wang, A. Baxter, N. Nathan, W. Anderson and E. Gordon (2016). "Metabolic features of chronic fatigue syndrome." Proc Natl Acad Sci U S A **113**(37): E5472-5480.

Neishabouri, S. H., S. M. Hutson and J. Davoodi (2015). "Chronic activation of mTOR complex 1 by branched chain amino acids and organ hypertrophy." Amino Acids **47**(6): 1167-1182.

Nelson, C., V. Ambros and E. H. Baehrecke (2014). "miR-14 regulates autophagy during developmental cell death by targeting ip3-kinase 2." Mol Cell **56**(3): 376-388.

Neumann, C., J. Blume, U. Roy, P. P. Teh, A. Vasanthakumar, A. Beller, Y. Liao, F. Heinrich, T. L. Arenzana, J. A. Hackney, C. Eidenschenk, E. J. C. Galvez, C. Stehle, G. A. Heinz, P. Maschmeyer, T. Sidwell, Y. Hu, D. Amsen, C. Romagnani, H. D. Chang, A. Kruglov, M. F. Mashreghi, W. Shi, T. Strowig, S. Rutz, A. Kallies and A. Scheffold (2019). "c-Maf-dependent Treg cell control of intestinal TH17 cells and IgA establishes host-microbiota homeostasis." Nat Immunol **20**(4): 471-481.

Nguyen, T., S. Johnston, L. Clarke, P. Smith, D. Staines and S. Marshall-Gradisnik (2017). "Impaired calcium mobilization in natural killer cells from chronic fatigue syndrome/myalgic encephalomyelitis patients is associated with transient receptor potential melastatin 3 ion channels." Clin Exp Immunol **187**(2): 284-293.

Nguyen, T., D. Staines, S. Johnston and S. Marshall-Gradisnik (2018). "Reduced glycolytic reserve in isolated natural killer cells from Myalgic encephalomyelitis/chronic fatigue syndrome patients: A preliminary investigation." Asian Pac J Allergy Immunol.

O'Neill, H. M., S. J. Maarbjerg, J. D. Crane, J. Jeppesen, S. B. Jorgensen, J. D. Schertzer, O. Shyroka, B. Kiens, B. J. van Denderen, M. A. Tarnopolsky, B. E. Kemp, E. A. Richter and G. R. Steinberg (2011). "AMP-activated protein kinase (AMPK) beta1beta2 muscle null mice reveal an essential role for AMPK in maintaining mitochondrial content and glucose uptake during exercise." Proc Natl Acad Sci U S A **108**(38): 16092-16097.

Osinska, I., K. Popko and U. Demkow (2014). "Perforin: an important player in immune response." Cent Eur J Immunol **39**(1): 109-115.

Owen, O. E., S. C. Kalhan and R. W. Hanson (2002). "The key role of anaplerosis and cataplerosis for citric acid cycle function." J Biol Chem **277**(34): 30409-30412.

Pansarasa, O., M. Bordoni, L. Drufuca, L. Diamanti, D. Sproviero, R. Trotti, S. Bernuzzi, S. La Salvia, S. Gagliardi, M. Ceroni and C. Cereda (2018). "Lymphoblastoid cell lines as a model to understand amyotrophic lateral sclerosis disease mechanisms." Dis Model Mech **11**(3).

Pendergrass, W., N. Wolf and M. Poot (2004). "Efficacy of MitoTracker Green and CMXrosamine to measure changes in mitochondrial membrane potentials in living cells and tissues." Cytometry A **61**(2): 162-169.

Peng, T., T. R. Golub and D. M. Sabatini (2002). "The immunosuppressant rapamycin mimics a starvation-like signal distinct from amino acid and glucose deprivation." Mol Cell Biol **22**(15): 5575-5584.

Perdomo-Celis, F., D. M. Salgado, D. M. Castaneda and C. F. Narvaez (2016). "Viability and Functionality of Cryopreserved Peripheral Blood Mononuclear Cells in Pediatric Dengue." Clin Vaccine Immunol **23**(5): 417-426.

Peterson, D., E. W. Brenu, G. Gottschalk, S. Ramos, T. Nguyen, D. Staines and S. Marshall-Gradisnik (2015). "Cytokines in the cerebrospinal fluids of patients with chronic fatigue syndrome/myalgic encephalomyelitis." Mediators Inflamm **2015**: 929720.

Porstmann, T., C. R. Santos, B. Griffiths, M. Cully, M. Wu, S. Leevers, J. R. Griffiths, Y. L. Chung and A. Schulze (2008). "SREBP activity is regulated by mTORC1 and contributes to Akt-dependent cell growth." Cell Metab **8**(3): 224-236.

Proal, A. and T. Marshall (2018). "Myalgic Encephalomyelitis/Chronic Fatigue Syndrome in the Era of the Human Microbiome: Persistent Pathogens Drive Chronic Symptoms by Interfering With Host Metabolism, Gene Expression, and Immunity." Front Pediatr **6**: 373.

Qin, X., B. Jiang and Y. Zhang (2016). "4E-BP1, a multifactor regulated multifunctional protein." Cell Cycle **15**(6): 781-786.

Ransohoff, R. M., D. Schafer, A. Vincent, N. E. Blachere and A. Bar-Or (2015). "Neuroinflammation: Ways in Which the Immune System Affects the Brain." Neurotherapeutics **12**(4): 896-909.

Rasa, S., Z. Nora-Krukle, N. Henning, E. Eliassen, E. Shikova, T. Harrer, C. Scheibenbogen, M. Murovska, B. K. Prusty and M. C. European Network on (2018). "Chronic viral infections in myalgic encephalomyelitis/chronic fatigue syndrome (ME/CFS)." J Transl Med **16**(1): 268.

Rekeland, I. G., O. Fluge, K. Alme, K. Risa, K. Sorland, O. Mella, A. de Vries and J. Schjott (2018). "Rituximab Serum Concentrations and Anti-Rituximab Antibodies During B-Cell Depletion Therapy for Myalgic Encephalopathy/Chronic Fatigue Syndrome." Clin Ther.

Reznick, R. M. and G. I. Shulman (2006). "The role of AMP-activated protein kinase in mitochondrial biogenesis." J Physiol **574**(Pt 1): 33-39.

Ricciardi, S., N. Manfrini, R. Alfieri, P. Calamita, M. C. Crosti, S. Gallo, R. Muller, M. Pagani, S. Abrignani and S. Biffo (2018). "The Translational Machinery of Human CD4(+) T Cells Is Poised for Activation and Controls the Switch from Quiescence to Metabolic Remodeling." Cell Metab **28**(6): 895-906 e895.

Richardson, A. M., D. P. Lewis, B. Kita, H. Ludlow, N. P. Groome, M. P. Hedger, D. M. de Kretser and B. A. Lidbury (2018). "Weighting of orthostatic intolerance time measurements with standing difficulty score stratifies ME/CFS symptom severity and analyte detection." J Transl Med **16**(1): 97.

Robin, X., N. Turck, A. Hainard, N. Tiberti, F. Lisacek, J. C. Sanchez and M. Muller (2011). "pROC: an open-source package for R and S+ to analyze and compare ROC curves." BMC Bioinformatics **12**: 77.

Robinson, M. D., D. J. McCarthy and G. K. Smyth (2010). "edgeR: a Bioconductor package for differential expression analysis of digital gene expression data." Bioinformatics **26**(1): 139-140.

Roerink, M. E., M. E. van der Schaaf, L. Hawinkels, R. P. H. Raijmakers, H. Knoop, L. A. B. Joosten and J. W. M. van der Meer (2018). "Pitfalls in cytokine measurements - Plasma TGF-beta1 in chronic fatigue syndrome." Neth J Med **76**(7): 310-313.

Ruprecht, J. J. and E. R. S. Kunji (2020). "The SLC25 Mitochondrial Carrier Family: Structure and Mechanism." Trends Biochem Sci **45**(3): 244-258.

Russell, L., G. Broderick, R. Taylor, H. Fernandes, J. Harvey, Z. Barnes, A. Smylie, F. Collado, E. G. Balbin, B. Z. Katz, N. G. Klimas and M. A. Fletcher (2016). "Illness progression in chronic fatigue syndrome: a shifting immune baseline." BMC Immunol **17**: 3.

Rutherford, G., P. Manning and J. L. Newton (2016). "Understanding Muscle Dysfunction in Chronic Fatigue Syndrome." J Aging Res **2016**: 2497348.

Rutter, J., D. R. Winge and J. D. Schiffman (2010). "Succinate dehydrogenase - Assembly, regulation and role in human disease." Mitochondrion **10**(4): 393-401.

Saint-Georges-Chaumet, Y. and M. Edeas (2016). "Microbiota-mitochondria inter-talk: consequence for microbiota-host interaction." Pathog Dis **74**(1): ftv096.

Salazar, D., L. Zhang, G. D. deGala and F. E. Frerman (1997). "Expression and characterization of two pathogenic mutations in human electron transfer flavoprotein." J Biol Chem **272**(42): 26425-26433.

Santos Ferreira, D. L., H. J. Maple, M. Goodwin, J. S. Brand, V. Yip, J. L. Min, A. Groom, D. A. Lawlor and S. Ring (2019). "The Effect of Pre-Analytical Conditions on Blood Metabolomics in Epidemiological Studies." Metabolites **9**(4).

Scheibenbogen, C., M. Loebel, H. Freitag, A. Krueger, S. Bauer, M. Antelmann, W. Doehner, N. Scherbakov, H. Heidecke, P. Reinke, H. D. Volk and P. Grabowski (2018). "Immunoadsorption to remove ss2 adrenergic receptor antibodies in Chronic Fatigue Syndrome CFS/ME." PLoS One **13**(3): e0193672.

Schlauch, K. A., S. F. Khaiboullina, K. L. De Meirleir, S. Rawat, J. Petereit, A. A. Rizvanov, N. Blatt, T. Mijatovic, D. Kulick, A. Palotas and V. C. Lombardi (2016). "Genome-wide association analysis identifies genetic variations in subjects with myalgic encephalomyelitis/chronic fatigue syndrome." Transl Psychiatry **6**: e730.

Schvartzman, J. M., C. B. Thompson and L. W. S. Finley (2018). "Metabolic regulation of chromatin modifications and gene expression." J Cell Biol **217**(7): 2247-2259.

Sharpe, M. C., L. C. Archard, J. E. Banatvala, L. K. Borysiewicz, A. W. Clare, A. David, R. H. Edwards, K. E. Hawton, H. P. Lambert, R. J. Lane and et al. (1991). "A report--chronic fatigue syndrome: guidelines for research." J R Soc Med **84**(2): 118-121.

She, Q. B., E. Halilovic, Q. Ye, W. Zhen, S. Shirasawa, T. Sasazuki, D. B. Solit and N. Rosen (2010). "4E-BP1 is a key effector of the oncogenic activation of the AKT and ERK signaling pathways that integrates their function in tumors." Cancer Cell **18**(1): 39-51.

Sheedy, J. R., R. E. Wettenhall, D. Scanlon, P. R. Gooley, D. P. Lewis, N. McGregor, D. I. Stapleton, H. L. Butt and D. E. M. KL (2009). "Increased d-lactic Acid intestinal bacteria in patients with chronic fatigue syndrome." In Vivo **23**(4): 621-628.

Shikova, E., V. Reshkova, C. Kumanova capital A, S. Raleva, D. Alexandrova, N. Capo, M. Murovska and M. C. European Network on (2020). "Cytomegalovirus, Epstein-Barr virus, and human herpesvirus-6 infections in patients with myalgic small ie, Cyrillicncephalomyelitis/chronic fatigue syndrome." J Med Virol.

Shukla, S. K., D. Cook, J. Meyer, S. D. Vernon, T. Le, D. Clevidence, C. E. Robertson, S. J. Schrodi, S. Yale and D. N. Frank (2015). "Changes in Gut and Plasma Microbiome following Exercise Challenge in Myalgic Encephalomyelitis/Chronic Fatigue Syndrome (ME/CFS)." PLoS One **10**(12): e0145453.

Shungu, D. C., N. Weiduschat, J. W. Murrough, X. Mao, S. Pillemer, J. P. Dyke, M. S. Medow, B. H. Natelson, J. M. Stewart and S. J. Mathew (2012). "Increased ventricular lactate in chronic fatigue syndrome. III. Relationships to cortical glutathione and clinical symptoms implicate oxidative stress in disorder pathophysiology." NMR Biomed **25**(9): 1073-1087.

Sie, L., S. Loong and E. K. Tan (2009). "Utility of lymphoblastoid cell lines." J Neurosci Res **87**(9): 1953-1959.

Smits, B., L. van den Heuvel, H. Knoop, B. Kusters, A. Janssen, G. Borm, G. Bleijenberg, R. Rodenburg and B. van Engelen (2011). "Mitochondrial enzymes discriminate between mitochondrial disorders and chronic fatigue syndrome." Mitochondrion **11**(5): 735-738.

Stine, Z. E. and C. V. Dang (2020). "Glutamine Skipping the Q into Mitochondria." Trends Mol Med **26**(1): 6-7.

Straus, S. E., G. Tosato, G. Armstrong, T. Lawley, O. T. Preble, W. Henle, R. Davey, G. Pearson, J. Epstein, I. Brus and et al. (1985). "Persisting illness and fatigue in adults with evidence of Epstein-Barr virus infection." Ann Intern Med **102**(1): 7-16.

Sweetman, E., T. Kleffmann, C. Edgar, M. de Lange, R. Vallings and W. Tate (2020). "A SWATH-MS analysis of Myalgic Encephalomyelitis/Chronic Fatigue Syndrome peripheral blood mononuclear cell proteomes reveals mitochondrial dysfunction." J Transl Med **18**(1): 365.

Tapiero, H., G. Mathe, P. Couvreur and K. D. Tew (2002). "II. Glutamine and glutamate." Biomed Pharmacother **56**(9): 446-457.

Taylor, W. A., E. M. Mejia, R. W. Mitchell, P. C. Choy, G. C. Sparagna and G. M. Hatch (2012). "Human trifunctional protein alpha links cardiolipin remodeling to beta-oxidation." PLoS One **7**(11): e48628.

Theorell, T., V. Blomkvist, G. Lindh and B. Evengard (1999). "Critical life events, infections, and symptoms during the year preceding chronic fatigue syndrome (CFS): an examination of CFS patients and subjects with a nonspecific life crisis." Psychosom Med **61**(3): 304-310.

Thomas, P. D., M. J. Campbell, A. Kejariwal, H. Mi, B. Karlak, R. Daverman, K. Diemer, A. Muruganujan and A. Narechania (2003). "PANTHER: a library of protein families and subfamilies indexed by function." Genome Res **13**(9): 2129-2141.

Thomas, P. D., A. Kejariwal, N. Guo, H. Mi, M. J. Campbell, A. Muruganujan and B. Lazareva-Ulitsky (2006). "Applications for protein sequence-function evolution data: mRNA/protein expression analysis and coding SNP scoring tools." Nucleic Acids Res **34**(Web Server issue): W645-650.

Tirelli, U., G. Marotta, S. Improta and A. Pinto (1994). "Immunological abnormalities in patients with chronic fatigue syndrome." Scand J Immunol **40**(6): 601-608.

Tomas, C., A. Brown, V. Strassheim, J. L. Elson, J. Newton and P. Manning (2017). "Cellular bioenergetics is impaired in patients with chronic fatigue syndrome." PLoS One **12**(10): e0186802.

Tomas, C., A. E. Brown, J. L. Newton and J. L. Elson (2019). "Mitochondrial complex activity in permeabilised cells of chronic fatigue syndrome patients using two cell types." PeerJ **7**: e6500.

Tomas, C., J. L. Elson, J. L. Newton and M. Walker (2020). "Substrate utilisation of cultured skeletal muscle cells in patients with CFS." Sci Rep **10**(1): 18232.

Tomas, C., T. A. Lodge, M. Potter, J. L. Elson, J. L. Newton and K. J. Morten (2019). "Assessing cellular energy dysfunction in CFS/ME using a commercially available laboratory test." Sci Rep **9**(1): 11464.

Tomoda, A., T. Joudoi, M. Rabab el, T. Matsumoto, T. H. Park and T. Miike (2005). "Cytokine production and modulation: comparison of patients with chronic fatigue syndrome and normal controls." Psychiatry Res **134**(1): 101-104.

Trivedi, M. S., E. Oltra, L. Sarria, N. Rose, V. Beljanski, M. A. Fletcher, N. G. Klimas and L. Nathanson (2018). "Identification of Myalgic Encephalomyelitis/Chronic Fatigue Syndrome-associated DNA methylation patterns." PLoS One **13**(7): e0201066.

Tsai, S. Y., H. J. Chen, C. F. Lio, C. F. Kuo, A. C. Kao, W. S. Wang, W. C. Yao, C. Chen and T. Y. Yang (2019). "Increased risk of chronic fatigue syndrome in patients with inflammatory bowel disease: a population-based retrospective cohort study." J Transl Med **17**(1): 55.

Valeri, C. R. and L. E. Pivacek (1996). "Effects of the temperature, the duration of frozen storage, and the freezing container on in vitro measurements in human peripheral blood mononuclear cells." Transfusion **36**(4): 303-308.

Vega, R. B., J. M. Huss and D. P. Kelly (2000). "The coactivator PGC-1 cooperates with peroxisome proliferator-activated receptor alpha in transcriptional control of nuclear genes encoding mitochondrial fatty acid oxidation enzymes." Mol Cell Biol **20**(5): 1868-1876.

Vermeulen, R. C., R. M. Kurk, F. C. Visser, W. Sluiter and H. R. Scholte (2010). "Patients with chronic fatigue syndrome performed worse than controls in a controlled repeated exercise study despite a normal oxidative phosphorylation capacity." J Transl Med **8**: 93.

Vermeulen, R. C. and I. W. Vermeulen van Eck (2014). "Decreased oxygen extraction during cardiopulmonary exercise test in patients with chronic fatigue syndrome." J Transl Med **12**: 20.

Vernon, S. D., T. Whistler, B. Cameron, I. B. Hickie, W. C. Reeves and A. Lloyd (2006). "Preliminary evidence of mitochondrial dysfunction associated with post-infective fatigue after acute infection with Epstein Barr virus." BMC Infect Dis **6**: 15.

Wanders, R. J., H. R. Waterham and S. Ferdinandusse (2015). "Metabolic Interplay between Peroxisomes and Other Subcellular Organelles Including Mitochondria and the Endoplasmic Reticulum." Front Cell Dev Biol **3**: 83.

Waters, L. R., F. M. Ahsan, D. M. Wolf, O. Shirihai and M. A. Teitell (2018). "Initial B Cell Activation Induces Metabolic Reprogramming and Mitochondrial Remodeling." iScience **5**: 99-109.

Weinberg, A., L. Zhang, D. Brown, A. Erice, B. Polsky, M. S. Hirsch, S. Owens and K. Lamb (2000). "Viability and functional activity of cryopreserved mononuclear cells." Clin Diagn Lab Immunol **7**(4): 714-716.

Weisel, F. J., S. J. Mullett, R. A. Elsner, A. V. Menk, N. Trivedi, W. Luo, D. Wikenheiser, W. F. Hawse, M. Chikina, S. Smita, L. J. Conter, S. M. Joachim, S. G. Wendell, M. J. Jurczak, T. H. Winkler, G. M. Delgoffe and M. J. Shlomchik (2020). "Germinal center B cells selectively oxidize fatty acids for energy while conducting minimal glycolysis." Nat Immunol **21**(3): 331-342.

Whitehead, S. J. and S. Ali (2010). "Health outcomes in economic evaluation: the QALY and utilities." Br Med Bull **96**: 5-21.

Williams, G. J. (2011). "Data Mining with Rattle and R." Use R!, Springer.

Winder, W. W. and D. G. Hardie (1996). "Inactivation of acetyl-CoA carboxylase and activation of AMP-activated protein kinase in muscle during exercise." Am J Physiol **270**(2 Pt 1): E299-304.

Wise, D. R., R. J. DeBerardinis, A. Mancuso, N. Sayed, X. Y. Zhang, H. K. Pfeiffer, I. Nissim, E. Daikhin, M. Yudkoff, S. B. McMahon and C. B. Thompson (2008). "Myc regulates a transcriptional program that stimulates mitochondrial glutaminolysis and leads to glutamine addiction." Proc Natl Acad Sci U S A **105**(48): 18782-18787.

Wolvetang, E. J., K. L. Johnson, K. Krauer, S. J. Ralph and A. W. Linnane (1994). "Mitochondrial respiratory chain inhibitors induce apoptosis." FEBS Lett **339**(1-2): 40-44.

Woods, A., K. Dickerson, R. Heath, S. P. Hong, M. Momcilovic, S. R. Johnstone, M. Carlson and D. Carling (2005). "Ca2+/calmodulin-dependent protein kinase kinase-beta acts upstream of AMP-activated protein kinase in mammalian cells." Cell Metab **2**(1): 21-33.

Xia, C., Z. Fu, K. P. Battaile and J. P. Kim (2019). "Crystal structure of human mitochondrial trifunctional protein, a fatty acid beta-oxidation metabolon." Proc Natl Acad Sci U S A **116**(13): 6069-6074.

Yamano, E., M. Sugimoto, A. Hirayama, S. Kume, M. Yamato, G. Jin, S. Tajima, N. Goda, K. Iwai, S. Fukuda, K. Yamaguti, H. Kuratsune, T. Soga, Y. Watanabe and Y. Kataoka (2016). "Index markers of chronic fatigue syndrome with dysfunction of TCA and urea cycles." Sci Rep **6**: 34990.

Yang, J., N. Diaz, J. Adelsberger, X. Zhou, R. Stevens, A. Rupert, J. A. Metcalf, M. Baseler, C. Barbon, T. Imamichi, R. Lempicki and L. M. Cosentino (2016). "The effects of storage temperature on PBMC gene expression." BMC Immunol **17**: 6.

Yang, T., Y. Yang, D. Wang, C. Li, Y. Qu, J. Guo, T. Shi, W. Bo, Z. Sun and T. Asakawa (2019). "The clinical value of cytokines in chronic fatigue syndrome." J Transl Med **17**(1): 213.

Yoo, H. C., Y. C. Yu, Y. Sung and J. M. Han (2020). "Glutamine reliance in cell metabolism." Exp Mol Med.

Zeng, J., S. Deng, Y. Wang, P. Li, L. Tang and Y. Pang (2017). "Specific Inhibition of Acyl-CoA Oxidase-1 by an Acetylenic Acid Improves Hepatic Lipid and Reactive Oxygen Species (ROS) Metabolism in Rats Fed a High Fat Diet." J Biol Chem **292**(9): 3800-3809.

Zhang, J., F. E. Frerman and J. J. Kim (2006). "Structure of electron transfer flavoprotein-ubiquinone oxidoreductase and electron transfer to the mitochondrial ubiquinone pool." Proc Natl Acad Sci U S A **103**(44): 16212-16217.

Zhang, L., J. Gough, D. Christmas, D. L. Mattey, S. C. Richards, J. Main, D. Enlander, D. Honeybourne, J. G. Ayres, D. J. Nutt and J. R. Kerr (2010). "Microbial infections in eight genomic subtypes of chronic fatigue syndrome/myalgic encephalomyelitis." J Clin Pathol **63**(2): 156-164.

Zhen, H., Y. Kitaura, Y. Kadota, T. Ishikawa, Y. Kondo, M. Xu, Y. Morishita, M. Ota, T. Ito and Y. Shimomura (2016). "mTORC1 is involved in the regulation of branched-chain amino acid catabolism in mouse heart." FEBS Open Bio **6**(1): 43-49.

Zhenyukh, O., E. Civantos, M. Ruiz-Ortega, M. S. Sanchez, C. Vazquez, C. Peiro, J. Egido and S. Mas (2017). "High concentration of branched-chain amino acids promotes oxidative stress, inflammation and migration of human peripheral blood mononuclear cells via mTORC1 activation." Free Radic Biol Med **104**: 165-177.

Zong, H., J. M. Ren, L. H. Young, M. Pypaert, J. Mu, M. J. Birnbaum and G. I. Shulman (2002). "AMP kinase is required for mitochondrial biogenesis in skeletal muscle in response to chronic energy deprivation." Proc Natl Acad Sci U S A **99**(25): 15983-15987.